Investigation of the Intrinsic Mechanism of Drug Resistance in Multiple Myeloma

A thesis submitted for the degree of Ph.D

Melissa G. Ooi, MB BCh.

The experimental work described in this thesis was carried out under the supervision of
Prof. Martin Clynes and Dr. Robert O'Connor,
NICB and School of Nursing, Dublin City University
And
Prof. Ken Anderson and Dr. Constantine S. Mitsiades,
LeBow Myeloma Center, Dana Farber Cancer Institute,
Boston, USA

August 2011

The experimental work described in this thesis was carried out in two institutions, the National Institute for Cellular Biotechnology, Dublin City University, Dublin, Ireland and in the LeBow Myeloma Center, Dana Farber Cancer Institute, Boston, USA over a period of 3.5 years.

In the National Institute for Cellular Biotechnology, School of Nursing, Dublin City University, the work was done under the supervision of Prof. Martin Clynes and Dr. Robert O'Connor.

In the LeBow Myeloma Center, Dana Farber Cancer Institute, Boston, USA, the work was supervised by Prof. Ken Anderson and Dr. Constantine S. Mitsiades.

Dr. Peter O'Gorman from the Mater Misericordiae Hospital, Dublin, Ireland was instrumental in setting up the partnership between DCU and DFCI and the initial funding for this project.

I hereby certify that this material, which I now submit for assessment on the programme of study leading to the award of Ph.D. is entirely my own work, that I have exercised reasonable care to ensure that the work is original, and does not to the best of my knowledge breach any law of copyright, and has not been taken from the work of others save and to the extent that such work has been cited and acknowledged within the text of my work.

Signed:

ID No.:

Date:

ACKNOWLEDGEMENT

My journey to do a PhD was not a straight forward one and I would like to thank Dr. Peter O'Gorman who first gave me the idea and opportunity to study for a PhD. I would also like to thank my other supervisors, Dr. Robert O'Connor and Prof. Martin Clynes here in NICB, DCU, Ireland and also Prof. Ken Anderson and Dr. Constantine Mitsiades in DFCI, Boston, USA for giving me the opportunity to do a PhD, for always being there and for all the insight, support and encouragement over the past three years, especially towards the end. Doing an external PhD in USA had its own challenges and without the support from all these great men, it would have been a near impossibility.

Thanks to all the great researchers who have helped, encouraged and supported me over the years and who have made research enjoyable for a doc! On both sides of the Altantic, this past three years has been a great learning opportunity and also a time of friendship that I will treasure always. A special mention to Dr. Jana Jakubikova for all her help with flow cytometry as well as coffee break chats. Dr. Steffen Klippel for help with *in vivo* work and board games, Joe Negri and Jake Delmore who started me on the path of cell culture and MTT viability assays and Friday night brainstorming sessions in the pub and finally Dr. Doug McMillin who allowed me to help out with his project as a way to learn laboratory techniques. A big thank you to Mayer 555 and to Jeff Sorrell, a Mayer 555 adoptee who was always helpful with orders and always had a joke or kind work in times of stress. I would also like to pay homage to the researchers over in NICB who helped me out a lot in the process of obtaining this PhD. Justine Meiller who helped out with Pgp work and sharing baby stories, Raj Rajpal for his coffee (especially in the afternoons) and Paul Dowling for his great and indispensable help with the proteomics part of my PhD. To the other researchers in Mayer 5 and in NICB a big thank you!

Finally on a personal note, an important thanks goes to my parents, sisters, husband and my little girl Siobhan. My parents for their encouragement and especially my mother who helped me out with the baby in the middle of my thesis writeup. To my husband, Tee who was so understanding about my needing time away from the baby to write up the thesis. He also had to put up with the bad days and endless complaints

about experiments not working. I would also like to acknowledge my little girl for brightening up my life and giving me meaning beyond work and academics.

.

Melissa Ooi

ABSTRACT

The focus of this thesis was to evaluate the mechanisms whereby myeloma cells develop intrinsic resistance with a focus on resistance in the context of bortezomib treatment. The aims of this thesis were to examine multidrug resistance pumps as a mechanism of resistance in MM, to investigate the contribution of p53 signalling perturbations in resistance mechanism in MM, to study the AMPK pathway as an alternative target to overcome MM resistance and finally to characterise myeloma resistance to bortezomib treatment using 2D-DIGE analysis.

Focussing on bortezomib resistance models, we found that that overexpression of P-gp attenuates bortezomib activity. Bortezomib is a P-gp substrate and a combination of P-gp inhibitor and bortezomib is able to overcome resistance. Bortezomib is also able to downregulate the expression and function of P-gp. Our findings therefore suggest that combination of a P-gp inhibitor and bortezomib in P-gp positive myeloma would be a reasonable treatment combination to extend use of the drug.

We have shown that p53 apoptotic signalling pathways can be accentuated when bortezomib is combined with a Mdm2 inhibitor. In p53 WT cells, nutlin-3 in combination with bortezomib generates additive toxicity in MM cells but is highly synergistic in epithelial models and p53-mutated cell lines. This synergy persists in the presence of BMSCs. This observation has implications more so in epithelial cancers and p53 mutated cancers where single agent bortezomib activity is mild. We have also shown that bortezomib-treated patients who had high expression of nutlin-3-suppressed genes had significantly shorter progression-free ($p=0.001$, log-rank test) and overall survival ($p=0.002$, log-rank test) compared to those with low expression levels.

AMPK activation is promising as an anticancer pathway and may also be a chemoprevention target. Metformin and AICAR, which activate this pathway, both have demonstrated useful preclinical anticancer properties and have a good therapeutic index in patients. We explored mechanism of cell death and showed that AICAR was able to activate the apoptotic pathway. These agents also synergise with glycolysis inhibitors to further increase cytotoxicity in cancer cells.

Identification of proteins whose expression is altered in differing states of sensitivity and resistance provides candidates for better understanding of resistance mechanisms so we also investigated bortezomib resistance in cellular models using proteomic techniques and isolated and identified several novel proteins which may play a role in this phenomenon. Our findings are mechanistically consistent since two of the identified proteins Hsp70 and caspase-3 are known in the literature to be affected by bortezomib treatment.

Table of Contents

Chapter 1
Introduction

1.1. Multiple Myeloma

1.1.1. Pathogenesis

Cancer is a major cause of human morbidity and mortality. It is caused by a group of cells demonstrating abnormal growth, invasion and metastasis. Cancers are caused by abnormalities in the genetic material of the abnormal cells. Genetic changes can occur at many levels, from gain or loss of entire chromosomes to a mutation affecting a single DNA nucleotide. There are two broad categories of genes which are affected by these changes. Oncogenes may be normal genes which are expressed at inappropriately high levels, or altered genes which have novel properties due to aberrant expression or mutation. In either case, expression of these genes promotes the malignant phenotype of cancer cells. Tumour suppressor genes are genes which inhibit cell division, survival, or other properties of cancer cells. Tumour suppressor genes are often disabled by cancer-promoting genetic changes. Typically, changes in several genes are required to transform a normal cell into a cancer cell [1]. Cancer can arise from virtually any tissue in the body and is typically referred to as a "solid" malignancy if originating from epithelial or connective tissue or haematological if originating from haematopoietic cells. Multiple Myeloma (MM) is one of a number of malignancies originating from haematological cells.

MM is a plasma cell disorder that is characterized by an excess of plasma cells, monoclonal gammopathy (M-protein) and immunodeficiency. The diagnostic hallmarks of this disease are the development of hypercalcaemia, renal disease, anaemia and osteolytic bone disease (CRAB).

A recent study by Landgren *et al*. [2], showed that monoclonal gammopathy of unknown significance (MGUS) precedes virtually all cases of MM. This is a key finding that helps to fill a gap in our understanding of myelomagenesis. The events that trigger progression of MGUS to MM is are currently still unknown. However, one has to keep in mind that the vast majority of MGUS cases will never develop MM or other lymphoproliferative disorders [2]. MGUS patients presenting with an abnormal serum kappa-lambda free light chain (FLC) -ratio, non-IgG MGUS, and a high serum M-protein level (>1.5 g/dL) have been found to have a 58% absolute risk of developing MM over 20 years of follow up, whereas, in sharp contrast, MGUS cases with none of these risk factors have only a 5% absolute risk of MM progression (when accounting

for death as a competing risk, the corresponding absolute risk estimates were 27% and 2%, respectively) [3]. These findings suggest that the well-documented 1% annual average risk of MM progression among MGUS patients [4] is highly heterogeneous and emphasize the fact that the risk of developing MM varies greatly among patients diagnosed with MGUS.

Serum M-protein concentration may show a year by year increase prior to MM diagnosis or remain stable up to the diagnosis of MM [2]. As a result of this finding, the current recommendation for clinicians is to follow patients presenting with MGUS indefinitely as stable M-protein levels do not exclude the underlying development of MM. Until better molecular markers for progression to MM are available, clinicians will continue to use clinical measures in combination with routine blood test (including renal function, haemoglobin, and serum calcium) and serum and urine M-protein markers in their monitoring of MGUS cases to aid early detection of progression to MM.

1.1.2. Epidemiology

Globally, MM is a common haematological malignancy particularly increasing in prevalence as individuals' age with a median age at diagnosis of 62 years for men and 61 years for women (range 20–92); only 2% of patients are younger than 40 years. In the USA, MM is the second most frequent malignancy of the blood after non-Hodgkin's lymphoma - the disease accounts for approximately 20 percent of deaths from haematological malignancy and two percent of deaths from all cancers [5]. About 20,000 cases occur every year in the USA; the incidence adjusted for age and ethnic group is 7.1 per 100,000 in men and 4.6 per 100,000 in women. Occurrence of the disease is more common in men than women, and is twice as high in African American than in Caucasian American people [6, 7]. The reason for the uneven racial and gender distribution is unknown.

The median survival for patients diagnosed with multiple myeloma ranges from about 3 to 5 years, with variation largely dictated by genetic heterogeneity [8]. With the advent of autologous stem cell transplantation, the median survival has extended to 5 to 7 years in patients eligible for this procedure [8]. The treatment landscape has changed in the last several years due to the introduction of novel therapies. These new approach to treatment have resulted in higher response rates and increases in both

progression-free survival and OS rates in the context of randomized, controlled trials [9].

1.1.3. Genetics

Conventional cytogenetics and fluorescent in-situ hybridization (FISH) have shown that numeric abnormalities occur in the genes of MM cells in both a non-hyperdiploid (NHRD; <48 or >75 chromosomes) and a hyperdiploid (HRD; 48–75 chromosomes) pattern. Non-hyperdiploid abnormalities are associated with reduced life-span because of high-risk translocations of immunoglobulin heavy chain variable region (IGHR) (t[4;14] or t[14;16]), partial (q14) or complete loss of chromosome 13, and partial loss of chromosome 17(p13). By comparison, hyperdiploid abnormalities caused by multiple trisomies, and low frequency of monosomy or deletion of chromosome 13 and translocation of *IGHR* (t[11;14]) are associated with improved survival statistics[10]. This difference in clinical outcome suggests that different molecular genetic pathways are involved in pathogenesis of the 2 subgroups.

Primary early onset reciprocal choromosomal translocations occur at IGHR locus on chromosome 14q32 in about 50% to 70% of myeloma cases [11]. The most common 5 translocations, accounting for 40% of all cases with IgH translocation are summarized in Table 1.1.3. The genes and their function are mostly related to cell cycle regulation.

Numerical aberrations are also common in MM. Trisomy most frequently involves chromosomes 3, 5, 7, 9, 11, 15, 19, and 21, whereas monosomy and partial deletions affect mainly chromosomes 6, 13, 16, and 22. Gains of 1q are the most common chromosomal aberrations in myeloma, detectable in up to 40% of those with an abnormal karyotype [11]. Monosomy 13 or interstitial deletion of 13 (q14) is detectable in 15% to 20% of newly diagnosed MM by conventional cytogenetics and 50% of cases by interphase FISH [11]. Deletion 13 can also be found in MGUS.

Secondary late onset translocations and gene mutations that have been implicated in disease progression are MYC rearrangement, activation of N or K-RAS mutations, FGFR3 mutations, inactivation or mutation of TP53, RB1 and PTEN; and inactivation of cyclin-dependent kinase inhibitors *CDKN2A* and *CDKN2C*. Recent studies found that

mutations of the nuclear factor-kappa B (NF-kB) pathway components, such as TRAF3, cIAP1/2, CYLD, and NIK, also contribute to pathogenesis of myeloma [12, 13].

Chromosome	Gene	Frequency (%)	Functions
11q13	CCND1	15 – 20	Cell cycle regulator
4p16	FGFR-3 & MMSET	15	Growth factor receptor tyrosine kinase Transcription factor
16q23	C-MAF	5	Transcription factor
6p21	CCND3	3	Cell cycle regulator
20q11	MAFB	2	Transcription factor

Table 1.1.3. Most common partner genes involved in translocation of immunoglobulin heavy chain gene in MM [11]

1.2. Treatment options for Multiple Myeloma

1.2.1. Conventional agents

The conventional treatment agents employed in MM have historically been alkylating agents, anthracyclines and glucocorticoids. In 1962, the use of melphalan was first reported by Bergsagel *et al.* [14] to show a significant improvement in 8 out of 24 MM patients treated with the drug. Mass *et al.* [15] first tested corticosteroids and showed that in a placebo-controlled double-blind trial that prednisolone as a single agent produced haematological response and a reduction in serum globulin but no difference in survival. The classic regimen of melphalan plus prednisone (MP) was established in a randomized trial of 183 myeloma patients led by Alexanian *et al*., in which survival was 6 months longer with MP compared with melphalan alone [16]. This was the treatment for MM until the 1980's when vincristine, doxorubicin, and dexamethasone (VAD) followed by autologous transplant (ASCT) became regarded as the standard of care for eligible patients [17, 18]. Patients ineligible for ASCT continue to receive MP. Although this approach possesses proven efficacy and robust experience, its cumbersome nature and ultimate inferiority in terms of response rates and OS in comparison to novel agents has resulted in the diminished utility of VAD.

1.2.2. Stem cell transplantation

Substantial improvement in progression-free and overall survival has been achieved by the introduction of high dose drug treatment followed by stem-cell transplantation. Barlogie *et al.* [19] established an intense treatment program using melphalan 140mg/m^2 followed by autologous transplantation that is still a protocol in current use. In 1996, a randomised trial by Intergroupe Francophone du Myelome showed that stem-cell transplantation resulted in significantly more disease-free individuals and better overall survival (OS) than did conventional chemotherapy (5-year OS 52% *vs* 12%; mortality 3% for both treatments)[20]. This study group was the first to show better 7-year event-free survival (EFS) from tandem stem-cell transplantation (two sequential transplants) than from one transplantation, at least for patients who had not achieved complete response, broadly defined as no disease activity detectable, after the first transplantation [21]. Barlogie and colleagues [22] using a total therapy approach, in which all available methods of treatment were incorporated into front-line

treatment, showed similar results to the French study using tandem stem cell transplantation.

The results for allogeneic transplantation have been controversial. Although this treatment is curative for 10 to 20% of patients with chemotherapy-resistant, refractory disease and is able to maintain a durable remission, there is a high transplant-related mortality of 25 to 50% that offsets the advantage with this approach. Much of the high response and curative potential of allografts is attributed to a 'graft-versus tumour' effect [23-25], which is not seen in autologous transplantation.

A large European Bone Marrow Transplant (EBMT) registry trial found equivalent OS but inferior progression-free survival (PFS) when reduced-intensity allografts were compared with ablative allografts [26]. Reduced-intensity allogeneic transplant regimens result in reliable donor engraftment with a relatively low mortality compared with ablative regimens; however, the immunologic effect of the allograft treatment is modest, resulting in reduced rate of complete response and a higher rate of progression. Thus far, allogeniec transplant remains a tool used as a last line treatment.

1.2.3. Novel agents

In the last decade, there has been great advancement in the treatment options for MM. Three new therapies have been recently approved by the FDA for use in MM (thalidomide, bortezomib and lenalidomide). These agents have been able to overcome drug resistant disease in preclinical models and in clinical trials. They have not only exhibited direct anti-MM affect but are also capable of overcoming the protective effects of the bone marrow microenvironment [27-29]. Each drug will be discussed separately.

1.2.3.1. Thalidomide

The antiangiogenic properties of thalidomide [30] initially led to the consideration of its use in MM based on the premise that myeloma is associated with both elevated levels of circulating angiogenic cytokines, such as vascular endothelial growth factor, and

increased bone marrow vascularization [31, 32]. Barlogie *et al.*[33] conducted a landmark trial that enrolled 84 patients and 32% of patients responded, making it the first new drug with single-agent activity for myeloma in more than 3 decades. This initial result with single agent thalidomide was confirmed by other centres. The 2-year EFS and OS were 20 and 48%, respectively [33], with 10-year EFS and OS rates of 6 and 10%[34].

Response rates in relapsed disease are approximately 55% with the combination of thalidomide and steroids, with comparable activity among patients resistant to previous dexamethasone based therapy [35]. Thalidomide has also been used in combination with other chemotherapeutic agents in the management of relapse and refractory MM. Several trials with different combination of thalidomide and chemotherapeutics produced a response rate of 32% to 76% [36, 37].

1.2.3.2. Bortezomib

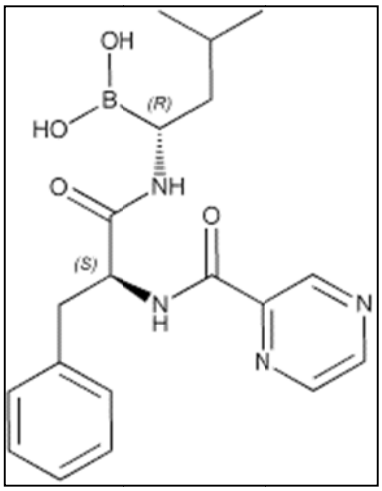

Figure 1.2.3.2 Bortezomib

The proteasome functions as the ‘garbage disposal’ for a cell. Its role is to remove excess proteins to ensure maintenance of key cellular functions. The 26S proteasome consists of a core 20S catalytic complex and a 19S regulatory complex. Ubiquitin-tagged proteins are recognized by the 19S regulatory complex where the ubiquitin tags are removed. Proteins then move into the 20S proteasome cylinder for hydrolysis into

small polypeptides. Inhibition of the proteasome causes endoplasmic reticulum stress leading to cellular apoptosis, with malignant, transformed, and proliferating cells being more susceptible [38, 39].

Two phase II trials, the Study of Uncontrolled Myeloma Management with proteasome Inhibition Therapy (SUMMIT) and Clinical Response and the Efficacy Study of bortezomib in the Treatment of refractory myeloma (CREST) trials demonstrated a response rate of 35% to 38% and a median survival of 16 months (SUMMIT). A subset analysis of SUMMIT and CREST underscored the ability of bortezomib to overcome poor prognosis conferred in MM by chromosome 13 deletion [40, 41]. These results were confirmed in the international, multicenter phase III Assessment of Proteasome Inhibition for EXtending remissions (APEX) trial, in the response rate among individuals in the bortezomib group was 38%, with a CR rate of 6%, whereas the OR and CR rates in the dexamethasone group were 18% and 1%, respectively. Superior median time to progression (TTP) (6.22 versus 3.49 months) and 1-year survival (80 versus 66%) were observed in the bortezomib as compared with dexamethasone-treated patients [42]. In an updated analysis, the OR and CR rates in the bortezomib arm were 43 and 9%, respectively [43].

Preclinical studies [44] have showed the potent sensitizing effect of bortezomib in combination with other classes of drugs including alkylating agents and anthracyclines and provided rationale for additional bortezomib-containing combinations in the treatment of relapsed and/or refractory MM. Trials evaluating bortezomib combination with liposomal doxorubicin demonstrated that 36% of patients achieved a response [45, 46]. The combination of bortezomib, doxorubicin and dexamethasone (PAD) has been evaluated in a study involving 64 patients with relapsed and/or refractory MM [47]. In this heavily pre-treated group, PAD produced a response in more than 67% of patients.

1.2.3.3. Lenalidomide

Several analogs of thalidomide were synthesized in an attempt to increase efficacy and minimize toxicity associated with the parental compound. Lenalidomide, a 4-amino substituted analog of thalidomide, formerly called CC-5013, belongs to a class of thalidomide analogs termed immunomodulatory drugs.

The MM-009 North American trial and the MM-010 European/Israeli/Australian trial showed a longer TTP in the lenalidomide/dexamethasone combination (MM-009: 11.1 months; MM-010: 11.3 months) compared with placebo/dexamethasone (4.7 months in both trials) [48, 49]. The combination of lenalidomide, doxorubicin and dexamethasone was evaluated in a recently published study with relapsed and refractory MM [50]. This regimen produced an OR rate of 73%. The median TTP in the study was 45 weeks.

1.2.3.4. Emerging therapies

New therapies such as heat shock protein (HSP) 90 inhibitors, Akt inhibitors, histone deacytelase (HDAC) inhibitors, BCL2 inhibitors, pro-apoptotic peptides and other proteasome inhibitors are in preclinical studies to provide the framework for phase I and II clinical trials [51]. These new agents are tested singly or more commonly, in combination with other MM therapies.

Microarray profiling showed that bortezomib induces HSP90 gene transcripts in MM cells[52]. The combination of Hsp90 inhibitor, 17AAG and bortezomib can block this stress response and increase cytotoxicity [53]. An ongoing clinical trial combining bortezomib and 17AAG is currently ongoing to see if the combination can overcome bortezomib resistance.

Bortezomib downregulates ERK, Jak/STAT and PKC signalling pathways but activates the Akt survival pathway *in vitro* [27]. Hideshima *et al*. demonstrated that perifosine, an Akt inhibitor, when combined with bortezomib, is able to abrogate this response and induce synergistic MM cytotoxicity *in vitro* [51], A phase II clinical trial is currently evaluating this combination.

Other important new combinations are the HDAC inhibitors SAHA or LBH589 with bortezomib. The HDAC inhibitors are able to block protein degradation through the aggresome autophagy pathway and upregulate proteasomal degradation; conversely, blockade of the proteasome with bortezomib upregulates aggresome activity [54, 55]. Preclinical studies have shown that combinations that block both pathways of protein degradation induce synergistic cytotoxicity in MM. A phase II trial of LBH589 is now ongoing in MM, with a combination LBH589 and bortezomib trial to follow. Richardson *et al.* [56] had reported modest single agent activity of SAHA in a phase I trial in

advanced MM patients and we are currently awaiting results of a combination trial involving SAHA and bortezomib.

1.3. The impact of the bone marrow microenvironment on drug resistance in Multiple Myeloma

The role of the local microenvironment in cancer cell growth, proliferation and survival has been recognized lately. Several studies in haematological malignancies and solid tumours [57-60] have provided evidence supporting the idea that the non-malignant cells that surround the neoplasia can affect the cancer cell growth, survival and drug resistance.

In this context, MM is the prototypical disease model that best characterizes these tumour-microenvironmental interactions. Indeed, it is now well established that MM-induced disruption of the bone marrow (BM) homeostasis between the highly organized cellular and extracellular compartments supports MM cell proliferation, survival, migration and drug resistance through activation of various signalling pathways (as reviewed in [60, 61]). For instance, it has been demonstrated that the response of MM to conventional therapies, such as glucocorticoids or cytotoxic chemotherapeutics is attenuated by the presence of bone marrow stromal cells (BMSCs) [27, 62-64]. As discussed above, the three novel agents that are FDA approved for use in MM (bortezomib, thalidomide and lenalidomide) not only exhibit direct anti-MM affect but are also capable of overcoming the protective effects of the BMSCs. This new understanding of the interplay between the microenvironment and malignant cells will serve as a model for identifying and validating new targeted therapeutics, not only in MM but also in other haematological malignancies and solid tumours.

The BM milieu consists of two parts; organized cellular and non-cellular components which include the liquid component. The cellular component of the BM is composed of haematopoietic stem cells; progenitor and precursor cells; immune cells (including T cells, macrophages, and natural killer cells); erythrocytes; bone marrow stromal cells (BMSCs); BM endothelial cells (BMECs); and cells involved in bone homeostasis (including osteoclasts and osteoblasts). The non-cellular component comprises extracellular matrix (ECM) proteins (fibronectin, collagen, laminin and osteopontin) and

the liquid component consists of growth factors and cytokines such as interleukins (IL)-6, IL-1β, IL-3, IL-10, IL-15, IL-21, insulin-like growth factor-1 (IGF-1), vascular endothelial growth factor (VEGF), B-cell activating factor (BAFF), CD-40, transforming growth factor (TGF)-β, macrophage inflammatory protein (MIP)-1α, hepatocyte growth factor (HGF), fibroblast growth factors (FGFs), stromal cell–derived factor (SDF)–1a, tumour necrosis factor (TNF)–α and matrix metalloproteinases, for example, MMP-2 and MMP-9.

1.3.1. Role of growth factors/cytokines in drug resistance in Multiple Myeloma

The liquid milieu of the BM microenvironment directly and indirectly plays a role in MM pathogenesis, MM cell growth, survival, migration and drug resistance. Cytokines and growth factors are produced and secreted by MM and other cells within the BM compartment and regulated by both autocrine and paracrine loops. The direct contact of MM cells to ECM proteins, BMSCs, BMECs, osteoclast, osteoblast and other cells in the BM milieu triggers in MM cells a pleiotropic spectrum of proliferative, antiapoptotic signalling pathways including PI3K/Akt/mTOR, IKK-α/NF-κB, Ras/Raf/MAPK, Wnt and JAK/STAT3 (as reviewed in [60, 61]). These signalling pathways can also be activated by binding of growth factors and cytokines to their receptors. Some of the more important growth factors/cytokines will be discussed in detail below.

1.3.1.1. IL-6-induced signalling pathway

IL-6 has historically been viewed as a major player in MM pathogenesis by inducing growth and survival. It is predominantly produced and secreted by BMSCs and osteoblasts [64, 65]**.** IL-6 also induces expression of Xbp-1 which is a transcription factor involved in plasma cell/MM cell differentiation [66-68].

Several prosurvival, antiapoptotic pathways are stimulated by IL-6. MEK/MAPK, JAK/STAT3 and PI3K/Alt/mTOR pathways are the major survival pathways in cancer stimulated by IL-6. Conversely, blockade of IL-6 induces upregulation of BH3-only

protein Bim coupled with Mcl-1 downregulation and activation of Bax, the sum of which induces MM cell apoptosis [69].

Besides MM cell proliferation, IL-6 also triggers drug resistance to dexamethasone and other conventional therapeutics by inducing PI-3K/Akt, MAPK, and JAK/STAT3 cascades [70-72]. IL-6 also stimulates osteoclastogenesis [73], linking the increase in MM tumour burden in the BM with bone resorption.

There have been anecdotal reports on the use of anti-IL-6 neutralising antibodies in MM [74, 75]. Based on the preclinical hypothesis and *in vitro* work, it was disappointing that major clinical responses were not observed. A likely explanation for the lack of response may be reasons related to the pharmacodynamics of the drug. It may not be possible to neutralise all the IL-6 present in a MM patient with a single anti-IL-6 Ab [76, 77]. However, the more likely explanation is that IL-6 is crucial but not the sole factor in MM pathogenesis. It has been noted *in vitro* that only a subset of MM cell lines responds to IL-6 stimulation (and usually at a level many times higher than present in blood samples of MM patients) and even fewer cell lines depend on IL-6 for sustained growth.

Several other compounds targeting IL-6 signalling pathways, including antibodies against IL-6 and IL-6 receptor, for example, CNTO328, IL-6 antisense oligonucleotides and IL-6 super antagonist Sant7, have been described. CNTO328 is the only anti-IL-6 monoclonal antibody that is currently in clinical trials as a single agent or in combination with other anti-myeloma therapeutics (http://clinicaltrials.gov/).

1.3.1.2. IGF-1-induced signalling pathway

Another growth factor that plays a major role in MM growth, survival and migration is IGF-1. In solid tumours, IGFs and IGF-1R have been implicated in cancer pathogenesis and increased levels of circulating IGF-1 have been associated with higher risk of carcinogenesis [78-80]. A review by Mitsiades *et al.* [81] on IGF-1 reported that many studies have reported increased proliferation of neoplastic cell lines, including MM cell lines with IGF-1 stimulation.

Although there is extensive preclinical data and strong epidemiological evidence for the inhibition of IGFs, there has been reluctance by myeloma clinicians and researches to utilize IGF-1 as a target for small molecule inhibitors. The extensive homology of the IGF-1 receptor (IGF-1R) to the insulin receptor and the fact that IGF-1R is expressed in normal tissues and at levels comparable to those present in their malignant counterparts, suggest perhaps that IGF-1R small molecule inhibitors might prove too toxic for clinical use [52]. These potential pitfalls were addressed in part by studies initially focused in MM models. NVP-AEW541, a selective IGF-1R kinase inhibitor, demonstrated *in vitro* antitumour activity against a broad spectrum of MM cell lines as well as primary MM cells and tumour cells from other neoplasias [82]. The same study reported anti-MM activity *in vivo* with no significant hyperglycaemia observed. An IGF-1R monoclonal antibody, IMC-A12, and small molecule inhibitor, XL-228, (active against IGF-1R, Src, FGFR, and BCR-Abl) are currently in clinical trials to assess their safety and efficacy.

IGF-1R functions as a key regulator of many pathways critical for the malignant phenotype. IGF-1R stimulates telomerase and proteasome activity, upregulates anti-apoptotic caspase inhibitors, enhances the ability of MM cells to respond to other cytokines (e.g. IL-6) and stimulates the production of proangiogenic cytokines (e.g. VEGF) [52]. This translates into conferring resistance against conventional chemotherapeutics and in part, proteasome inhibitors.

1.3.1.3. VEGF-induced signalling pathway

Tumour-associated angiogenesis has been shown to be as important in MM as in solid tumours. A review by Rajkumar [83], reported there is increased BM microvascular density (MVD) in MM compared with MGUS or normal BM. The authors also highlighted the finding of higher MVD in advanced disease or plasma cell leukaemia as compared to early stage disease and there is a correlation of higher MVD with adverse clinical outcome. This neovascularization in MM contributes to increased proliferation, survival and drug resistance through paracrine and cell adhesion-mediated interactions.

VEGF, one of the major growth factors associated with neoangiogenesis, is linked to tumour cell development, progression, metastatic osteolysis and drug resistance. The

role of VEGF in MM is exhibited by a high expression of VEGF receptor-1 (VEGFR-1) expressed on MM cells and it has been shown that several MM cell lines secrete VEGF and that VEGF is present in MM patient BM plasma [84]. The expression of VEGFR-1 is consistent with autocrine signalling. Antiapoptotic and prosurvival pathways activated by VEGF include caveolin-1/PI3K/PKCα-dependent cascade mediating MM migration on fibronectin, MEK/ERK pathways mediating MM cell proliferation and upregulation of Mcl-1 and survivin leading to increase survival [84, 85]. VEGF also affects other BM cellular components such as osteoblasts, NK cells, monocytes and endothelial progenitors [86].

In various solid tumours, a humanized monoclonal antibody against VEGF, bevacizumab (Avastin, Genentech Inc., CA, USA), has been used especially in combination with conventional chemotherapeutics with success. There are ongoing clinical trials in MM testing this agent in combination with other anti-MM novel agents. In addition to bevacizumab, there are other VEGF-targeting compounds under preclinical and clinical investigation in MM including pazopanib, sorafenib and sunitinib. Thalidomide, lenalidomide and bortezomib have been shown to indirectly target VEGF-signalling sequelae.

1.3.1.4. TNF-α superfamily-induced signalling pathway

The TNF-α superfamily includes SDF-1α, CD40, BAFF and APRIL. SDF-1α and its G-protein-linked cognate receptor CXCR4 are discussed in 1.3.2.1.

CD40 is expressed by antigen-presenting cells, T cells and B cells. Its presence has been demonstrated on the majority of MM cell lines and MM patients' cells, as well as BMSCs. CD40 is important in increasing MM growth via p53, PI3K/Akt/NF-κB dependent MM migration and triggers VEGF secretion [87]. CD40 activated MM cells adhere to fibronectin and are protected against apoptosis triggered by irradiation and doxorubicin [87]. A clinical phase 1 trial using SGN, the humanized anti-CD40 monoclonal antibody, in patients with refractory and relapsed MM has now been completed [88] and based on preclinical work by Tai *et al.* [89], a combination trial with lenalidomide, which augments antibody-dependent cellular cytotoxicity, is ongoing.

Circulating TNF-α levels are higher in MM patients with overt bone disease, whose osteoblasts constitutively overexpress Fas, DR4/DR5 complex as receptors for TNF-related apoptosis-inducing ligand, intercellular adhesion molecule-1 (ICAM-1), and monocyte chemotactic protein-1 (MCP-1) [90]. TNF-α, mainly secreted by macrophages and MM cells, does not induce significant growth or drug resistance in tumour cells. However, TNF-α is a more potent stimulus of IL-6 secretion (around 5 fold) in BMSCs than VEGF or TGFβ, via nuclear factor-kappa B (NF-κB) activation [91]. Most MM cell lines and patient samples show evidence of constitutive NF-κB activation. NF-κB is a transcriptional factor that promotes transcription of a number of cytokines, chemokines, cell adhesion molecules, as well as anti-apoptotic and cellular growth control proteins [62]. After stimulation by TNF-α, κBα protein is phosphorylated by inhibition of kappaB kinase complex beta (IKKβ) and subsequently ubiquitinated and degraded by the 26S proteasome, thereby inducing p50/p65 NF-κB nuclear translocation to modulate gene transcription. NFκB also regulates expression of adhesion molecules (i.e. ICAM-1 and VCAM-1): TNFα further upregulates these adhesion molecules on both MM cells and BMSCs, thereby increasing binding of MM cells and the resultant induction of IL-6 transcription and secretion in BMSCs, as well as cell adhesion-mediated drug resistance (CAM-DR) [92]. Agents that target TNF-α, such as bortezomib, thalidomide and lenalidomide, in part abrogate the paracrine growth and survival advantage conferred by MM cell adhesion to the BM microenvironment.

B-cell activation factor (BAFF) is normally expressed by monocytes, macrophages, dendritic cells, T cells and BMSCs. Osteoclasts produce both BAFF and a proliferation-inducing ligand (APRIL), in high levels. This is also true of MM patients where both the tumour cells and their stromal counterparts express receptors and secrete high levels of BAFF and APRIL [93]. Functionally, BAFF and APRIL protect MM cells from apoptosis and promote growth by activating NF-κB, PI-3K/AKT, and MAPK pathways. Furthermore, BAFF and APRIL are able to upregulate antiapoptotic proteins such as Mcl-1 and Bcl-2, as well as regulate TACI and c-Maf-dependent expression of both cyclin D2 and integrin β7 [93, 94].

1.3.2. Bone marrow non-malignant accessory cells

The interaction of MM cells with the BM microenvironment activates a pleiotropic cascade of proliferative/antiapoptotic signalling pathways. Importantly, this growth factor circuit between MM cells and BMSCs in the BM milieu promotes MM cell growth, survival, and migration, contributing to both MM progression and resistance to conventional drug treatment.

1.3.2.1. Homing and adhesion of Multiple Myeloma cells to the bone marrow

The homing of MM cells to the BM is mediated by certain chemokines, SDF-1α being one with a prominent role. SDF-1α interacts with its receptor CXCR4 on MM cells to trigger motility, internalization of CXCR4 and cytoskeletal rearrangement in MM cells [95]. SDF-1α is primarily produced by BMSCs but also by MM cells. Other factors that are known to stimulate MM cell migration *in vitro* and are considered to contribute to MM cell homing to the BM *in vivo* include VEGF [86, 96], HGF [97], MIP-1α [95], and IGF-1 [98, 99].

Both homotypic and heterotypic adhesion of MM cells to either ECM proteins or BMSCs are mediated through adhesion molecules. For instance, CD44, VLA-4 (very late antigen-4, CD49d), VLA-5 (CD49e), LFA-1 (leukocyte function-associated antigen-1, CD11a), NCAM (neuronal adhesion molecule, CD56), ICAM-1 (intercellular adhesion molecule, CD54), syndecan-1 (CD138), and MPC-1 (CD49e) all contribute to MM cell adhesion to the ECM or BMSCs [60]. VLA-4 is expressed on MM cells and binds fibronectin and VCAM-1 (CD106) of ECM and BMSCs, respectively. The binding to fibronectin upregulates p27Kip1 and induces NF-κB activation in MM [92], which confers cell adhesion–mediated resistance to conventional chemotherapy [100, 101]. Furthermore, MM cell adhesion to BMSCs results in bone resorption and tumour invasion, triggered by release of MMP-1 resulting from the binding of syndecan-1 to type 1 collagen [102].

The CXCR4 inhibitor AMD3100 reversibly blocks SDF-1α binding to CXCR4 and inhibits stem cell homing. MM patients scheduled to undergo autologous stem cell transplantation have been treated with AMD3100 to facilitate stem cell mobilisation. It

has been shown that AMD3100 can be safely administered in these patients and can increase the number of mobilized CD34+ cells. This observation will facilitate prompt and durable engraftment of mobilized cells without mobilizing tumour cells from the BM [103].

1.3.2.2. Bone marrow stromal cells and Multiple Myeloma

Of all the cellular components in the BM microenvironment, BMSCs are considered to have a key role in localizing MM cells to the microenvironment via cell adhesion but also to have important additional functional sequelae. In the context of normal BM physiology, BMSCs are believed to function as an accessory cell population that supports the survival, cell division, and differentiation of normal hematopoietic stem cells and progenitors [104]. MM cell adhesion to BMSCs triggers the NF-κB-dependent transcription and secretion of cytokines such as IL-6 in BMSCs, which further stimulate MM growth, survival and drug resistance [62]. In turn, activation of NF-κB by cell adhesion and cytokines augments the binding of MM cells to BMSCs which further induces IL-6 secretion [91]. Furthermore, MM cells secrete other cytokines such as TNF-α, TGFβ and VEGF which further upregulate IL-6 secretion from BMSCs [84, 91, 105]. Within the BM, interaction of CD40 on MM cells with its ligand CD40L on BMSCs upregulate adhesion molecules (such as VLA4 and LFA1) and augments MM cell adhesion, thereby increasing IL-6 and VEGF secretion in BMSCs [106].

Besides integrins and CD40/CD40L, BMSC-MM interaction is also mediated through Notch. Upon Notch-notch ligand interaction, Notch signalling pathways are activated both in MM cells and BMSCs, with induction of IL-6, VEGF and IGF-1 secretion with associated MM proliferation and survival [107-109]. Activation of Notch-1, but not Notch-2, results in protection of tumour cells from alkylating agent-induced apoptosis [107]. The Notch ligand, Jagged2, was found to be overexpressed and is able to induce BMSCs to secrete IL-6, VEGF and IGF-1. Notch activation can interact with NF-κB and C-myc to promote proliferation and inhibit apoptosis of MM cells, conferring drug resistance [110].

Interactions of MM cell with the BM microenvironment – either directly through cell adhesion molecule-mediated interactions between MM cells and BMSCs, or indirectly by the effect of growth factors and cytokines released – activate a pleiotropic

proliferative and antiapoptotic cascade. In addition to NF-κB, other signalling pathways involved in this response are PI3K/Akt, Ras/Raf/MAPK and JAK/STAT3 pathway. Downstream sequelae of activation of this pathway include upregulation of cell cycle regulatory proteins and antiapoptotic proteins (such as Bcl-xl, Mcl-1 and caspase inhibitors). These events results in MM growth, survival, migration and contribute to drug resistance.

An unanswered question about the role of BMSCs is whether there exists MM-specific abnormal BMSCs. A recent study by Zdzisinka *et al.* [111], reported that MMP-1, MMP-2 and TIMP-2 is significantly increased in the BMSCs of MM patients versus healthy controls. Further studies are needed to verify this finding and to identify specific targets.

1.3.2.3. Bone marrow endothelial cells and Multiple Myeloma

Tumour associated angiogenesis has been shown to be as important in MM as in solid tumours. Rajkumar *et al.* [83] reported an increase in BM MVD in MM, especially in advanced disease, compared with MGUS or normal BM. The authors also reported a correlation of higher MVD with adverse clinical outcome. This neovascularization in MM contributes to increased proliferation, survival and drug resistance through paracrine and cell adhesion mediated interactions.

MM cells constitutively produce growth factors such as VEGF, bFGF and MMPs that stimulate BM angiogenesis. In the meantime, BMECs secrete VEGF, IL-6 and IGF-1, which promote MM cell growth in the BM milieu [84]. Importantly, VEGF and IL-8 allow MM cells to recruit new blood vessels in the BM [112]. The BMECs in these new MM associated vessels further support tumoural cell survival through cytokines and direct adhesion interactions. In addition to VEGF and bFGF, BMECs also express other pro-angiogenic factors such as angiopontin 1, TGFβ, HGF and IL-1. MM progression is supported through these autocrine and/or paracrine loops present in the BM milieu

The anti-MM activity exhibited by thalidomide [30] (a known antiangiogenic agent) is able to inhibit BMECs-mediated secretion of VEGF, bFGF, and HGF, BMEC proliferation and capillarogenesis in patients who have MM [113]. Evidence is also accumulating of the antiangiogenic properties of bortezomib [114]. The antiangiogenic properties of these novel agents make them more effective in treating MM patients.

1.3.2.4. Osteoclast and Multiple Myeloma

Normal bone is being continuously remodelled whereby osteoclasts (OCs) resorb old bone, which is replaced by deposition of new bone by osteoblasts (OBs). Bone remodelling should normally create no major net change in bone mass, because new bone deposition by OBs is regulated to equal the quantity of bone resorbed by OCs. In MM, bone resorption by OCs is uncoupled from new bone formation by OBs [115]. This uncoupling involves upregulated activity of OCs without corresponding increases in new bone deposition by OBs leading to the hallmark of MM; lytic lesions, also diffuse osteopenia, pathological fractures and bone pain. A variety of OC activating factors, produced by both tumour and BMSCs include MIP1α, MIP1β, RANKL (receptor activator of nuclear factor κB ligand), osteoprotegerin ligand, VEGF, TNFα, TNFβ, IL-1α, IL-1β, IL-11, parathyroid hormone-related protein, HGF and IL-6. OC activity in turn modulates MM growth and survival [116, 117].

One of the more important OC regulators is RANKL. RANKL expression is associated with differentiation and is induced from immature OB. RANKL stimulates osteoclast differentiation and activity whereas osteoprotegerin (OPG) functions as a decoy receptor by binding to RANKL and thereby inhibiting its ability to stimulate osteoclastogenesis [118]. It has been proposed that MM cells can trigger increased RANK signalling in OCs by stimulating RANKL expression by BMSCs and suppressing production (by BMSCs) of OPG thereby promoting lytic lesions [116].

Among these mediators of MM osteoclastogenesis, there has been considerable interest in MIP-1α, which potently stimulates OC formation independently of RANKL and increases RANKL- and IL-6–stimulated formation of OCs [119]. MIP-1α levels in plasma from BM aspirates of MM patients are higher compared with healthy controls and correlate with the degree of osteolytic lesions [120]. MIP-1α binds to CCR1 on OCs and CCR5 on MM cells. It has been shown that blocking CCR1 and CCR5 inhibits OC formation and MM cell adhesion to BMSCs respectively [121]. The functional significance of MIP-1α has been further demonstrated by studies in which antisense oligonucleotide against MIP-1α decreases bone destruction *in vivo*, and by MM cell adherence to BMSCs *in vitro* via decreased expression of the α5β1 integrin [119], suggesting a MIP-1α–mediated link between bone resorption and BMSC-mediated MM cell proliferation/survival.

Other cytokines involved in osteoclastogenesis include IL-6 which is secreted by BMSCs, and TGF-β. TGF-β produced by MM cells augments IL-6 secretion from BMSCs [105, 122], further triggering increased OC activity. p38MAPK in BMSCs upregulates the production of IL11, RANKL and MIP-1α, inducing OC formation and activity. Conversely, a p38MAPK inhibitor can suppress these cytokines resulting in decreased MM proliferation, adhesion and decreased osteoclastogenesis [123].

The main therapy for bone disease in MM is the amino bisphosphonates which inhibit osteoclastogenensis and thus reduce the bone resorption seen in MM. Newer agents, such as bortezomib, have been shown to increase OB activity [117] and lenalidomide has been shown to have inhibitory effects on osteoclastogenesis [124]. Moreover, *in vivo* studies have demonstrated both a decrease in osteolysis, as well as an indirect anti-MM effect using RANKL-Fc or OPG-Fc [65, 116, 117]. Based on signalling pathways in OCs and OBs, several additional compounds have been tested preclinically and shown to have antibone resorptive activity including: the MEK inhibitor AZD6244 [125], CCR1 inhibitor MLN3897 [126], the HDAC inhibitor PXD101 [127], Resveratrol [128] and cox inhibitor SDX-308 [129].

1.3.2.5. Osteoblast and Multiple Myeloma

Lytic lesions in MM are not only caused by increased OC activity but also by decreased OB activity. The differentiation of mesenchymal stem cells to osteoblastic cells requires the activity and function of transcriptional factor Runx2/Cbfa1 [130]. The direct cell-to-cell contact of osteoprogenitor cells with MM cells inhibits Runx2/Cbfa1 activity in osteoprogenitor cells via binding of VLA4 on MM cells to VCAM-1 on osteoblast progenitors [65]. Furthermore, soluble factors released by MM cells, such as Dickkopf 1 (DKK1) and IL-3 also contribute to decreased Runx2/Cbfa1 activity and OB differentiation.

DKK1 is an inhibitor of the Wnt pathway which is overexpressed at the transcriptional level in MM cells of approximately one third of patients (compared with normal plasma cells) and is detected in the serum of approximately one fourth of patients who have extensive osteolytic bone lesions [131]. As DKK1 inhibits the canonical Wnt pathway, which mediates differentiation of osteoblast progenitor cells, DKK1 expression by MM cells could inhibit osteoblastogenesis. Importantly, recombinant human DKK1 or serum

of BM aspirates containing high concentrations of DKK1 inhibited the *in vitro* differentiation of osteoblast precursor cells [131]. In addition, a subset of MM cell lines and primary MM tumour cells constitutively secrete a soluble Wnt inhibitor, Frizzled-related protein 2 (sFRP-2), which also suppresses OB differentiation [132]. Conversely, DKK1 may have a key role in mediating osteolytic process as the expression of OPG and RANKL is also regulated by gWnt signalling [133].

IL-3 has been shown to stimulate the activity of OCs, but recent reports indicate that it also inhibits bone morphogenic protein-2 (BMP-2)–stimulated osteoblast formation [134]. TGFβ from MM cells augments IL6 secretion from BMSCs [105] and OBs [122], thus further stimulating OC activity and bone resorption. HGF directly inhibits osteoblastogenesis *in vitro* and its serum levels in MM patients are increased and correlated inversely with bone-specific alkaline phosphatase, a marker of osteoblast activity [135]. The imbalance in the functional interaction of OCs versus OBs in MM is not mediated by a single cascade, and instead is due to multiple cytokine/growth factor networks.

Unfortunately, reduction of tumour burden in MM does not lead to significant improvement in bone homeostasis; in many cases, patients who achieve complete remission after treatment with conventional therapies may still find that their pre-existing osteolytic lesions not healed. This finding suggests that in MM, the relationship of disease activity in tumour cell burden versus bone homeostasis is complex and significant suppression of the MM cell population may not be sufficient to allow for resolution of bone lesions. From a therapeutic standpoint, identifying treatment strategies that not only abrogate bone resorption but also stimulate new bone formation will be useful toward improving the long-term outcome of patients who have MM. Bortezomib is an example of such an agent as it not only has anti-MM activity, but can also activate OB activity.

1.4. Intrinsic mechanisms conferring drug resistance in Multiple Myeloma

1.4.1. Drug efflux pumps

Clinical drug resistance has always been a major obstacle in the treatment of all types of cancer. There is primary (intrinsic) resistance where the drug insensitivity is present from first diagnosis and unresponsive to first line chemotherapy or secondary (acquired) resistance where tumour cells develop resistance during chemotherapy. There are myriad mechanisms of resistance described in cancer and all forms of resistance fall into one of two categories, pharmacokinetic resistance (PK), e.g. overexpression of drug efflux pumps and pharmacodynamic resistance, e.g. apoptosis resistance or altered survival pathways, where the agent reaches an appropriate concentration but this fails to propagate an appropriate cell death response. Both forms of resistance have been characterised as being important for MM cell survival.

The cell membrane is the major determinant of cancer drug penetration to sub-cellular targets. Cells have evolved complex chemical defence mechanisms to regulate the entry of foreign substances into and out of the cell. Of the known pump mechanisms, p-glycoprotein (P-gp; MDR-1; ABCB1), multidrug resistant protein-1 (MRP-1; ABCC1) and breast cancer resistance protein (BCRP; MXR; ABCG2), have the broadest substrate specificity and a strong correlation with drug resistance *in vitro* and *in vivo* in many models and forms of cancer [136]. Of all these drug efflux transporters, P-gp is the best studied, and considered to be the most important in contributing to drug resistance.

1.4.1.1. P-glycoprotein (MDR-1; ABCB1)

P-glycoprotein, called classical MDR, results from the overexpression of P-gp, a transmembrane protein with a mass of 170 kDa. P-gp is coded by the mdr-1 gene on chromosome 7q21 and belongs to the ATP binding cassette (ABC) transporter family. According to the human gene nomenclature proposed in 1999, P-gp is called ABCB1 (http://www.gene.ucl.ac.uk/users/hester/abc.html). ABC transporters are a large superfamily of integral membrane proteins involved in ATP- dependent transport of chemotherapeutic drugs across biological membranes. Most ABC transporters consist of four domains, two membrane-spanning domains and two cytoplasmic domains. The

latter contain conserved nucleotide-binding motifs. Chemoresistance caused by the overexpression of P-gp exhibits a typical resistance pattern towards many drug classes (Table 1.4.1.1) [137].

Drug resistance resulting from ABC multidrug transporters can be prevented by another group of compounds, known variously as MDR modulators, reversers, inhibitors or chemosensitizers. In cellular models of resistance, the combination of a modulator with a drug to which cells are resistant will restore its cytotoxicity by shifting the LD_{50} to a much lower value. Modulators show the same diversity of chemical structure as substrates, and appear to act in several different ways. The mechanism of action of modulators has been explored in detail for P-gp. Some P-gp modulators compete with transport substrates for the drug-binding pocket of the transporter. Many of these compounds are transported by the efflux pump (e.g. cyclosporin A or verapamil) and can be viewed as competitive inhibitors. These first generation P-gp inhibitors, such as verapamil and cyclosporin A, have displayed useful MDR reversal activities *in vitro* and in murine models. The concentrations required, however, were high and often accompanied by increased side effects of toxicity [138]. Second generation inhibitors comprise newer analogues of the first generation agents like dexverapamil (less cardiotoxic r-enantiomer of verapamil) and PSC 833 (valspodar), the non-immunosuppressive analogue of cyclosporin A. These compounds were less cytotoxic and in some cases more potent P-gp modulators but still required micromolar concentrations to be effective. Third generation P-gp modulators have been developed based on structure-activity relationships that exhibit effective MDR reversal concentrations in the nanomolar range. These include GF120918 (Elacridar) [139], LY335979 (Zosuquidar) [140], XR9051 [141] and OC144-093-Ontogen (ONT-093) [142]. Other than competitive inhibition, there are other mechanisms of action of these modulators. The high-affinity modulator XR9576 (Tariquidar) [143] appears to interact with Pgp at a location distinct from the site of interaction of transport substrates, which may serve a modulatory function. Overall, the different mechanisms by which modulators exert their action at the molecular level are not well understood, making the rational design of new templates a challenging task.

In normal physiology, P-gp is expressed at high levels in the apical membranes of epithelial cells lining the colon, small intestine, pancreatic and bile ductules, and the kidney proximal tubule. It is also found in the endothelial cells lining capillaries in the

brain, testis and inner ear. The pregnant endometrium, the placenta and the adrenal gland also express high levels of P-gp. The location of P-gp suggests that its primary physiological role is to protect sensitive organs and the fetus from toxic xenobiotics [144]. In the intestine, P-gp extrudes many drugs into the lumen, thus reducing their absorption and oral bioavailability. It may export endogenous steroid hormones from the adrenal gland. The presence of P-gp in hematopoietic progenitor cells protects the bone marrow from the toxicity of chemotherapeutic drugs [145].

The role of ABC transport proteins in drug-resistant cancers is still a topic that is being examined. A high incidence of P-gp overexpression has been observed prior to chemotherapy treatment in many different poorly responsive tumour types, including kidney, colon, liver, breast and ovarian cancers. In haematological malignancies, such as leukaemias, lymphomas and MMs, the low levels of P-gp expression observed initially are often markedly increased after chemotherapy treatment and relapse. Grogan *et al.* [146] have shown that previous treatments with anthracyclines and vinca alkaloids can induce expression of P-gp in MM patients. However, clinical trials that used a combination of VAD with P-gp inhibitors such as cyclosporine [147], verapamil [148] or PS-833 [149] showed no clinical benefit in terms of increased OS or PFS. The failure of these trials can be related to poor inhibition of P-gp function by the P-gp inhibitors; additionally, generalized inhibition of P-gp can reduce the elimination of cytotoxic agents and in some trials this necessitated dose reduction to compensate for increases in toxicity evident in the P-gp treated patients. There are efforts under way to find more effective and less cytotoxic MDR modulators but another answer to the question may be to pair these modulators to drugs that are not chemotherapeutics in the traditional sense, such as bortezomib.

Bortezomib, as described earlier, is a novel treatment for MM. The mechanism of resistance to bortezomib is multifactorial and while little is known about the interaction of bortezomib with P-gp, there are indications that overexpression of this pump may contribute to resistance to this agent. Rumpold *et al* .[150] showed that knockdown of P-gp resensitises P-gp-expressing cells to proteasome inhibitors. Another strategy to overcome P-gp-induced resistance is to prevent P-gp from reaching the cell surface after synthesis in the endoplasmic reticulum. Proteasome inhibitors, lactacystin and MG-132 have been shown to inhibit the maturation of P-gp [151]. Bortezomib may be able to do the same if this is a class effect. Hence, better characterization of the

interactions of this drug with classical resistance mechanisms should identify improved treatment applications.

Anticancer drugs	*Vinca* alkaloids (vinblastine and vincristine) Anthracyclines (doxorubicin and daunorubicin) Taxanes (paclitaxel and docetaxel) Epipodophyllotoxins (etoposide and teniposide) Camptothecins (topotecan) Anthracenes (bisantrene and mitoxantrone)
HIV protease inhibitors	Ritonavir Saquinavir Nelfinavir
Analgesics	Morphine
Antihistamines	Terfenadine Fexofenadine
H_2-receptor antagonists	Cimetidine
Immunosuppressive agents	Cyclosporine A Tacrolimus (FK506)
Antiarrhythmics	Quinidine Amiodarone
HMG-CoA reductase inhibitors	Lovastatin Simvastatin
Antiemetics	Ondansetron
Tyrosine kinase inhibitors	Imatinib mesylate Gefitinib
Cardiac glycosides	Digoxin
Antihelminthics	Ivermectin

Calcium-channel blockers	Verapamil Nifedipine Azidopine Diltiazem
Antihypertensives	Reserpine Propanolol
Antibiotics	Erythromycin Gramicidin A
Steroids	Corticosterone Dexamethasone Aldosterone Cortisol

Table 1.4.1.1 Drugs and other compounds that interact with P-gp, taken from [137]

1.4.1.2. Multidrug resistant protein-1 (MRP-1; ABCC1)

MRP-1 is a drug transporter located in the plasma membrane, where it engages in active efflux of many drugs and drug conjugates. MRP-1 is a 190 kDa protein consisting of two NBDs and three transmembrane domains, a feature it shares with the MRP-2 (ABCC2), MRP-3 (ABCC3), MRP-6 (ABCC6) and MRP-7 (ABCC10). Other members of the MRP family (MRP-4, MRP-5, MRP-8 and MRP-9) contain two NBDs and two transmembrane domains similar to P-gp [152].

In contrast to P-gp and BCRP, MRP1 is expressed at the basolateral membrane of polarized epithelial cells. It protects tissues such as the bone marrow, kidney collecting tubules and oropharyngeal and intestinal mucosa from toxicants and is also involved in drug clearance from the cerebrospinal fluid, testicular tubules and peritoneum [153]. MRP1 plays a central role in glutathione homeostasis *in vivo* and exports LTC_4 from mast cells. It may also be involved in protecting cells from the toxicity of bilirubin.

Less is known about the significance of MRP1 in tumours and its role in drug resistance remains controversial. MRP1 is expressed in many different tumour types, including solid tumours (non-small-cell lung cancer, gastrointestinal carcinoma, melanoma, neuroblastoma and cancers of the breast, ovary and prostate) and haematological malignancies including leukaemias [154]. Some studies have linked the presence of MRP1 to poor treatment outcome, but no comprehensive picture of its role in clinical MDR has emerged as yet.

MRP1 transports a variety of endogenous molecules of physiological significance, including free glutathione, glutathione-conjugated leukotrienes and prostaglandins (LTC_4, LTD_4, LTE_4, prostaglandin A_2-SG, hydroxynonenal-SG), glucuronide conjugates (β-estradiol-β-D-glucuronide and glucuronosyl-bilirubin) and sulfate conjugates (dehydroepiandrosterone-3-sulfate and sulfatolithocholyl-taurine) (see Table 1.4.1.2) [137]. Similarly to P-gp, MRP1 also confers resistance to a variety of anti-cancer agents, although not taxanes.

In contrast, only a few modulators have been described for MRP1 [155], including VX-710 (biricodar), MK571 (a leukotriene D_4-receptor antagonist), sulindac (an NSAID) flavonoids, raloxifene analogs, isoxazole-based compounds and glutathione derivatives.

Anticancer drugs	*Vinca* alkaloids (vinblastine and vincristine) Anthracyclines (doxorubicin and daunorubicin) Epipodophyllotoxins (etoposide and teniposide) Camptothecins (topotecan and irinotecan) Methotrexate
Metalloids	Sodium arsenate Sodium arsenite Potassium antimonite

Peptides	Glutathione (GSH, GSSG)
Glutathione conjugates	Leukotrienes C_4, D_4 and E_4 Prostaglandin A_2-SG Hydroxynonenal-SG Aflatoxin B_1-epoxide-SG Melphalan-SG Cyclophosphamide-SG Doxorubicin-SG
Sulfate conjugates	Estrone-3-sulfate Dehydroepiandrosterone-3-sulfate Sulfatolithocholyl taurine
Pesticides	Fenitrothion Methoxychlor
Glucuronide conjugates	Glucuronosylbilirubin Estradiol-17-β-D-glucuronide Etoposide-glucuronide NS-38-glucuronide
HIV protease inhibitors	Ritonavir Saquinavir
Tyrosine kinase inhibitors	Imatinib mesylate Gefitinib
Antibiotics	Difloxacin Grepafloxicin

Table 1.4.1.2 Drugs and other compounds that interact with MRP-1, taken from [137]

1.4.1.3. Breast cancer resistance protein (BCRP; MXR; ABCG2)

BCRP is a 72 kDa half-transporter, and likely functions as a homodimeric complex. It is also referred to as MXR (mitoxantrone resistance associated protein), ABCP (Placenta-specific ABC gene) and ABCG2. Identification of the molecule in the anthracycline-selected breast cancer cell line MCF-7/AdrVp led to it being named BCRP [156]. The BCRP gene has been mapped to chromosome 4q22 [157].

BCRP is expressed in a variety of normal tissues, including intestine, kidney and placenta, as well as brain endothelial cells and hematopoietic stem cells. Its expression is strongly induced in the mammary gland during pregnancy and lactation. Similarly to P-gp, it is assumed to function in protecting tissues from toxicants and it likely plays a role in intestinal absorption, brain penetration and transplacental passage of drugs. The transporter is also expressed in certain stem cells, where it acts as a marker of pluripotent stem cells (the side population). In these cells, BCRP appears to interact with heme and prevent accumulation of porphyrins, enhancing cell survival under hypoxic conditions [158].

BCRP is a broad specificity drug transporter like P-gp; however, it appears to transport both positively and negatively charged drugs, including sulfate conjugates (Table 1.4.1.3). BCRP cannot transport taxanes, cisplatin and verapamil (P-gp substrates), calcein (an MRP1 substrate) or *Vinca* alkaloids or anthracyclines (substrates for both P-gp and MRP1), indicating that its substrate specificity partially overlaps with that of the other two transporters.

Since its discovery in 1998, high levels of BCRP expression have been found on a variety of drug-resistant cell lines that do not express either P-gp or MRP1. Since then, BCRP expression has been reported in many solid tumours [159], especially those from the GI tract, endometrium, lung and melanoma. However, a case has been made for the likely involvement of BCRP in resistance of both adult and childhood acute myeloid leukaemia to anticancer drugs [160] .

BCRP inhibitors have only recently been investigated, and include VX-710, GF120918 (elacridar), XR9576 (tariquidar), fumitremorgin C (a mycotoxin) and its derivative

Ko143, pantoprazole, flavonoids, estrogens and antiestrogens [161].

Anticancer drugs	Mitoxantrone Bisantrene (R482T mutant form) Epipodophyllotoxins (etoposide and teniposide) Camptothecins (topotecan and irinotecan) Anthracyclines (doxorubicin and daunorubicin; R482T mutant form) Flavopiridol
Antifolates	Methotrexate
Porphyrins	Pheophorbide a Protoporphyrin IX Hematoporphyrin
Flavanoids	Genestein Quercetin
Carcinogens	Aflatoxin B PhiP
Fungal toxins	Fumitremorgin C Ko143
Antihypertensive	Reserpine
HMG CoA reductase inhibitors	Rosuvastatin Pravastatin Cerivastatin
Antiviral drugs	Zidovudine Lamivudine

Drug & metabolite conjugates	Acetominaphen sulfate Estrone-3-sulfate Dehydroepiandrosterone sulphate Estradiol-17-β-D-glucuronide
Tyrosine kinase inhibitors	Imatinib mesylate Gefitinib
Antibiotics	Ciprofloxacin Norfloxacin

Table 1.4.1.3 Drugs and other compounds that interact with BCRP, taken from [137]

1.4.2. p53 signalling perturbations

Mammalian p53 family proteins – p53, p63 and p73, are descendents of an evolutionarily ancient family of transcription factors. Of the three mammalian p53 family proteins, p53 is unique in its pre-eminence as a tumour suppressor. In fact, it is thought to be the 'guardian of the genome' and hailed as the 'molecule of the year' in 1993 [162]. p53 is a transcription factor with multiple regulatory roles in stress and damage response such as DNA repair, cell cycle and apoptosis. It also plays a part in various physiological processes, including fertility, cell metabolism and mitochondrial respiration, autophagy, cell adhesion, stem cell maintenance and development [163]. In normal unstressed cells, p53 activity is maintained at a low level through a combination of p53 degradation and direct transcriptional repression, principally mediated by Mdm2 and Mdm4 (also known as MDMX in humans) [164].

p53 and Mdm2 interact with each other through an autoregulatory feedback loop. When p53 is activated, it transcribes the Mdm2 gene and in turn, the Mdm2 protein inhibits p53 activity by binding to the p53 transactivation domain and inhibiting its transcriptional activity [165]. Mdm2 is also responsible for exporting p53 out of the nucleus, promoting its degradation via the ubiquitin/proteasome pathway [166] and rendering it inaccessible to the target genes. The importance of the balance between Mdm2 and p53 protein is underscored by genetic studies, which have demonstrated that the genetic deletion of Mdm2 is embryonic lethal and that Mdm2 -/- mice can be successfully rescued only by a concomitant deletion of the TP53 gene [167, 168]. Another player in the regulation of p53 is Mdm4 which shows a high degree of homology to Mdm2. Mdm4 binds to p53 and inhibits its transactivation properties. The only difference between the two is that Mdm4 does not ubiquitinate and degrade p53 [169, 170].

As p53 has such an important role in tumour suppression, it is perhaps surprising that p53 is not functionally inactivated in more tumours – only about 50% of solid tumours have a mutation or deletion of the TP53 gene [171], while only about 15% of all haematological malignancies show deletion/mutation of p53, at least in the early stages of the disease [172]. In MM, this is the case as well with p53 mutation/deletion occurring at later stages of the disease. The significance of p53 mutation/deletion in MM was unknown in the context of novel therapies until a recent study by the IFM

group showed that bortezomib was able to overcome some poor prognostic markers [i.e. t(4;14)] but not Del 17p [173].

It would seem that direct inactivation of p53 would be an effective means of inactivating the whole tumour suppressor pathway, however, tumours are seldom optimized for growth, as evident by their high apoptotic indices, necrotic cores, hypoxia and abundant cytopathologies [163]. There can be tumour growth even if p53-mediated apoptosis proceeds unchecked provided that cell proliferation is more rapid. There is a theory that partial loss-of-function p53 mutations that retain p53 attributes are advantageous to tumour cells: such mutant p53 forms would have gain-of-function properties when activated by upstream oncogenic and stress signals. Clearly, the inopportune shunting of rogue cells into repair and survival modes by such mutant forms of p53 has substantial potential to promote tumourigenesis [174, 175]. That might explain the paradox of why p53-inactivating mutations confer a selective advantage only relatively late in the oncogenicity of many tumour types. In the remaining human cancers, p53 retains wild-type (p53WT) status but its function is inhibited by Mdm2. Mdm2 was initially discovered as the product of an oncogene found overexpressed by amplification in a spontaneously transformed mouse cell line [176]. Mdm2 has been found to be overexpressed in many human tumours [172] as its deregulated expression provides growth advantage to cells.

Small molecule inhibitors of Mdm2 have been developed as therapeutic anticancer agents. Compounds that bind to Mdm2 and inhibit its ability to bind to or regulate p53 can stabilize p53, increase its protein levels, and activate the p53 apoptotic pathway in a nongenotoxic manner. Nutlins, benzodiazepines, spiro-oxindoles and quinolinols bind to Mdm2 and inhibit its p53 association.

1.4.2.1. Nutlin-3

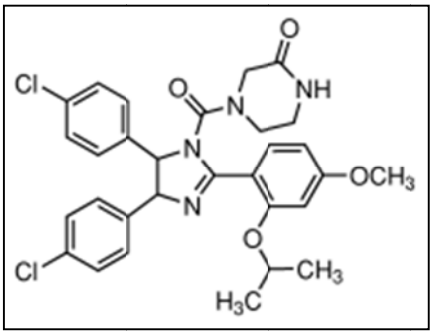

Figure 1.4.2.1 Nutlin-3

Nutlin-3 is a *cis*-imidazoline small molecule with affinity for the p53-binding pocket of Mdm2. The nutlins were first identified by Vassilev and colleagues [177]. They have the ability to displace p53 from Mdm2 *in vitro* with nanomolar potency (IC50 = 90 nM for nutlin-3a, the active enantiomer of nutlin-3). It is capable of disrupting the p53-Mdm2 interaction, thus protecting p53 from proteasomal degradation and activating the p53 pathway, leading to apoptosis in various malignancies, including MM [177-180]. In the original study by Vassilev *et al.* [177], they demonstrated that nutlin-3a can be administrated orally to nude mice that bear established human solid tumour xenografts for up to 3 weeks without systemic toxic effects.

There appears to be an exception to the general rule of nutlins being able to activate exclusively the p53 pathway. It has been demonstrated that in p53-deleted or p53-mutated cells, nutlins are able to activate alternative transcription factors, in particular E2F1 [181, 182]. E2F1 can induce proliferation or apoptosis depending on the cell context and depending on the simultaneous activation of the Akt-prosurvival pathway [183]. Another study has demonstrated that nutlins are able to induce apoptosis in p53-null cells through activation of p73 [184]. p73 is a homolog of p53 and is able to transactivate proapoptotic genes and induce cell death. It is also regulated by Mdm2. These two targets make nutlin a viable therapeutic option even when p53 is deleted or mutated.

1.4.2.1.1. Combination therapies with Nutlin

Experiments in patient samples retaining wild-type p53 show that nutlin-3 synergizes with doxorubicin, chlorambucil and fludarabine in CLL [178, 185, 186]; with doxorubicin and 1-h-Darabinofuranosylcytosine (Ara-C) in acute myeloid leukemia [187, 188]; and with doxorubicin in Hodgkin and Reed-Sternberg cells [189] in inducing apoptosis. In these studies, nutlin-3 was non-toxic toward normal haematopoietic cells. Another strategy is to combine Mdm2 inhibitor with tumour necrosis factor-related apoptosis-inducing ligand (TRAIL). TRAIL is known to bind to TRAIL-R2, a cell surface receptor, and transduces an apoptosis signal. It was shown that in p53WT acute myeloid leukaemia cells, nutlin-3 induces p53-dependent production of TRAIL-R2, leading to synergistic cell death when used in combination with TRAIL [187].

Mitsiades *et al.,* have previously reported the *in vitro* synergistic activity of the combination between bortezomib and DNA-damaging, p53-activating, chemotherapeutic agents, such as doxorubicin and melphalan [44]. This concept has been validated in the clinical setting by trials demonstrating the superiority of combined pegylated liposomal doxorubicin plus bortezomib compared with bortezomib monotherapy for the treatment of patients with relapsed or refractory MM [46], as well as the superiority of combined bortezomib plus melphalan and prednisolone compared with only melphalan plus prednisolone to treat newly diagnosed MM patients [190]. These findings support the role of combining p53-activating chemotherapeutics with proteasome inhibitors as a promising novel therapeutic approach in MM.

The ubiquitin/proteasome pathway is responsible for the degradation of many tumour-suppressing and pro-apoptotic proteins that are important for survival and proliferation of cancer cells, including p53. The hypothesis that nongenotoxic stabilization of p53, caused by nutlin-3 through suppression of Mdm2-mediated p53 ubiquitination, may synergize with accumulation of p53 caused by bortezomib through proteasome inhibition, thereby leading to increased antitumour activity.

1.4.3. AMP-activated protein kinase pathway

AMP-activated protein kinase (AMPK) is a serine/threonine protein kinase and serves as an energy sensor in all eukaryotic cells. AMPK is a heterotrimeric complex comprising of a catalytic α subunit and regulatory β and γ subunits [191]. AMPK is activated under conditions that deplete cellular ATP and elevate AMP levels such as glucose deprivation, hypoxia, ischaemia and heat shock which are associated with an increased AMP/ATP ratio [192]. As a result of the activation, AMP binds to the γ subunit causing phosphorylation of threonine 172 in the activation loop of the α catalytic subunit by upstream kinases such as LKB1 and CaMKK.

LKB1 is a serine/threonine protein kinase and is the product of the gene *lkb1.* In patients with Peutz-Jeghers syndrome (PJS), this gene is mutated. Mutations in PJS patients were shown to be loss of function mutations of LKB1 ([193, 194]. PJS is characterized by mucocutaneous melanin pigmentation, gastrointestinal polyposis and markedly increased risk of cancer. LKB1 mutants that are inactive failed to suppress cell growth indicating that LKB1 has antiproliferative function and hence anti-tumour effect. LKB1 also induce p53 and p21 upregulation resulting in cell cycle arrest in melanoma cells [195] providing further evidence that it can function as a tumour suppressor. Several studies from different groups have shown a clear connection between LKB1 and AMPK-induced cell cycle arrest [196, 197].

Several groups have reported that activation of AMPK suppresses mTOR signalling by growth factors and amino acids [198-200]. When AMPK is activated, TSC2 is phosphorylated at Thr-1227 and Ser-1345 and increases the activity of TSC1–TSC2 complex to inhibit mammalian target of rapamycin (mTOR) [201]. In addition, AMPK reportedly phosphorylates mTOR at Thr-2446 to reduce S6K1 phosphorylation by insulin, suggesting the inhibition of mTOR action [202]. Thus, AMPK directly and indirectly (via TSC2) suppresses mTOR activity to limit protein synthesis through the inhibition of translation elongation factor 2 (EF2). Therefore, AMPK activation regulates cellular proliferation in response to energy status or nutrient availability by limiting cell growth and proliferation when there is a lack thereof.

mTOR is an evolutionarily conserved serine/threonine kinase and a key regulator of protein translation/synthesis and cell growth [203, 204]. The mTOR pathway is activated by amino acids and by growth factors (e.g. PDGF, epidermal growth factor

(EGF) and insulin. This stimulates protein synthesis, cell growth and proliferation. mTOR increases translation initiation of 5′-terminal oligopyrimidine tract-containing mRNAs, which encode components of the protein synthesis machinery. The downstream effectors of mTOR ribosomal protein S6 kinase 1 ($p70^{S6K1}$ or S6K1) and the eukaryotic translation initiation factor 4E (eIF4E)-binding protein 1 (4E-BP1) stimulates the initiation step of translation [205].

Constitutive activation of PI3K-Akt signalling has been reported in many cancers including glioblastoma, melanoma, prostate cancer and haematological malignancies, including MM. Previous studies have demonstrated that IL-6 stimulates growth and survival of MM cells in part via the PI3K-Akt pathway [70]. Other studies have shown that IGF-1, another growth factor for MM also activates the PI3K pathway [206, 207]. One of the most important targets of PI3K is activation of Akt which mediates survival, proliferation and growth of tumour cells [208, 209]. Akt also regulates cell cycle by modulating cyclin D1. Through phosphorylation and inhibition of cyclin D1, Akt prevents its degradation and leads to its accumulation in the cell [210]. Hideshima *et al.* [211], has demonstrated that perifosine, an Akt inhibitor, has significant anti-MM activity and this drug is currently in clinical trials. mTOR, a downstream target of Akt has shown significant antiapoptotic activity in MM [212-214]. AMPK activation is a feasible therapeutic strategy for these cancers since AMPK inhibits mTOR signalling downstream of Akt, and inhibition of mTOR pathway has been reported to inhibit tumour growth and metastasis in experimental animal models as well as in cultured cells.

Activation of AMPK by metformin, AICAR or thiazolidinediones or expression of constitutively active mutants have been shown to cause apoptosis or cell cycle arrest of various cancer cells (to be discussed below). On the other hand, activation of this pathway has been shown to be protective on non-neoplastic tissues such as injured cells in cardiac ischemia and reperfusion injury models [215, 216]. AMPK activation protects human umbilical vein endothelial cells from hyperglycaemia by inhibition of caspase 3 and Akt activation [217] and by a similar mechanism in thymocytes [218]. These and other studies have suggested that AMPK activation confers protection against cell death. The underlying mechanism for these apparently opposing effects of AMPK activation is unknown at this time, but it can be postulated that in actively dividing cancer cells, the inhibition of ATP-consuming processes by AMPK may be less

compatible with their survival, whereas in non-dividing (non-neoplastic) cells, where the protective effects of AMPK have been observed under acute stress, the shutdown of ATP-consuming pathways may not alter the balance for survival and may be beneficial [219].

1.4.3.1. Metformin

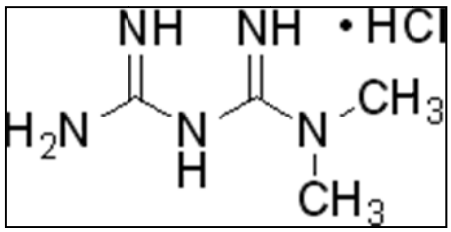

Figure 1.4.3.1 Metformin

Metformin (1,1-dimethylbiguanide hydrochloride) is a biguanide commonly used in the treatment of type 2 diabetes mellitus. It has a beneficial effect on hyperglycaemia without causing hypoglycaemia or weight gain. It has been used since 1957 in Europe and other countries, although in the US it was only introduced in 1995. The metabolic effects of metformin are mediated by indirect activation of AMPK, which leads to suppression of liver gluconeogenesis; decreased expression of lipogenic enzymes; increased fatty acid oxidation; and stimulation of glucose plasma membrane transport in skeletal muscle. The primary site of action for metformin is currently considered to be a direct inhibitory effect on complex 1 of the respiratory chain. The resulting high cellular ratio of AMP:ATP functions as an allosteric signal that sensitizes AMPK to phosphorylation at Thr172 by LKB1. Metformin is positively charged and accumulates (~1000 fold) within the mitochondrial matrix in a slow, membrane-potential-driven fashion, that is also self-limiting, because progressive inhibition of the respiratory chain leads to a drop in membrane potential, which will prevent further accumulation of the drug. This may explain why lactic acidosis is extremely rare with metformin, in contrast to phenformin, another biguanide.

A pilot case-control study and a population-based cohort study have demonstrated decreased incidence of cancer and decreased cancer mortality in metformin users compared to controls, sulfonylurea monotherapy users, or subjects who used insulin [220, 221]. Furthermore, metformin use has been associated with a 44% risk reduction for prostate cancer diagnosis among Caucasian men [222] and a 56% risk reduction for breast cancer diagnosis among women long-term users [223]. Concurrent metformin use in diabetic women with breast cancer receiving neoadjuvant chemotherapy increased the rate of pathologic complete response, suggesting that metformin can enhance the cytotoxic activity of conventional chemotherapy [224]. It is possible that the anticancer activity of metformin is exerted indirectly via the beneficial effects of metformin on the endocrine and metabolic milieu, such as improvement of hyperinsulinemia and suppression of systemic IGF-I levels. Alternatively, there could be a direct effect of metformin on the cancer cell. Direct anticancer activity of metformin has recently been demonstrated in *in vitro* studies using breast, prostate, colon, pancreatic, endometrial and ovarian carcinoma cell lines [225-230]. Such a direct effect may be mediated via increased phosphorylation of AMPK, decreased mTOR, p70S6K, ribosomal protein S6 and eIF4E-binding protein 1 activation and phosphorylation, and inhibition of translation initiation.

1.4.3.2. AICAR

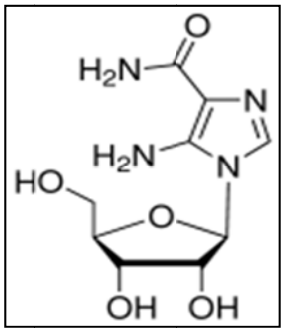

Figure 1.4.3.2 AICAR

5-aminoimidazole-4-carboxamide ribonucleoside (AICAR) is a cell permeable activator of AMPK, a metabolic master regulator that is activated in times of reduced energy availability (high cellular AMP:ATP ratios) and serves to inhibit anabolic processes. *In vivo*, pharmacologic activation of AMPK with AICAR mimics exercise and triggers insulin-independent glucose uptake by skeletal muscle. The drug is converted to its triphosphorylated form, ZMP, inside the cell, by an adenosine kinase, which acts as an AMP analogue and activates AMPK and its upstream kinase *LKB* without affecting the ATP:AMP ratio in the cell [231].

Cell division is an energetically demanding process that can be executed only if cells have sufficient metabolic resources to support a doubling of cell mass. It is postulated that proliferating mammalian cells have a cell-cycle checkpoint that responds to glucose availability. The glucose-dependent checkpoint occurs at the G(1)/S boundary and is regulated by AMPK. Recent studies have shown that AICAR has been shown to cause cell cycle arrest in hepatoma HepG2 cells [232], mouse embryonic fibroblasts [233], human aortic smooth muscle cells (SMCs) and rabbit aortic strips [234]. These reports also supported the hypothesis that the mechanism of cell cycle arrest by AMPK activation involves accumulation of the tumour suppressor protein p53 by phosphorylation of its Ser-15 residue (Ser-18 in mice), and the accumulated p53 protein upregulates one of the CDKIs, $p21^{CIP}$protein by a transcriptional mechanism.

Whether phosphorylation of Ser-15 on p53 is mediated by AMPK itself or by another protein kinase, which is co-immunoprecipitated with AMPK, has not been elucidated.

AMPK activation by AICAR has also been recently reported to inhibit proliferation of various cancer cell lines *in vitro* and *in vivo* by causing cell cycle arrest with an increase in $p21^{CIP}$, $p27^{KIP}$ and p53. The authors of this study also demonstrated that AICAR seems to affect the PI3K-Akt proliferation pathway, because AICAR inhibited PI3K activity and Akt phosphorylation [219]. AICAR has also been shown to have an anti-tumour role in myeloma [235] and to cause a proliferation block and cell death by inhibiting fatty acid and protein synthesis pathways and increasing p21 expression in prostate cells [236]. Other studies have shown that AMPK activation is able to cause apoptosis in gastric cancer cells [237] and pancreatic cells by inducing JNK pathway [238]. Similarly, AMPK induced JNK and caspase 3 activity resulting in apoptosis in liver cells [239]. AMPK activation was also demonstrated to enhance H2O2-mediated apoptosis in neuroblastoma cells by inducing NF-κB activation along with activation of p38 MAPK and c-Jun [240]. These studies suggest that AMPK is an efficient growth inhibitor and apoptosis inducer. Thus, AMPK can be considered as a negative regulator of proliferation and can modulate protein expression to this effect, classifying it as a tumour suppressor pathway system that can be exploited for attenuation of cancer growth.

1.5. Use of proteomics to investigate drug resistance in Multiple Myeloma

The success of the human genome project highlights how far science has advanced our understanding of the human body and cellular interactions. However, limitations of information on DNA sequence must be acknowledged. Although the DNA code provides the instructions for the amino-acid sequence, there are an estimated 1.5 million proteins, or roughly 50 proteins for every gene [241]. As the human body is made up mostly of proteins, being able to assess protein-protein interaction is important in understanding normal physiology as well as disease states.

The correlation between genotype and phenotype is low as many other processes affect protein synthesis such as chemical modification of amino acids (glycosylation, acetylation, glucuronidation, phosphorylation, deaminations and methylations). In addition, multiple products can arise from a single gene through alternate transcription

and post-transcriptional modification of the gene product through alternative splicing, translation of more than one polypeptide from a single mRNA, or modification of an amino acid before or after release from a polysome [242].

Proteomics is the study of proteins in a cell. Proteomics represents a powerful tool to discover protein locations, protein modifications, changes in protein abundance and to interrogate protein-protein interaction. Disease states arise when any part of this system is perturbed.

1.5.1. 2D-DIGE MALDI-TOF MS

The traditional method to measure protein expression is two-dimensional gel electrophoresis (2-DE) and it remains the gold standard to this day. 2-DE is a protein separation method that separates proteins in a first dimension by isoelectric focusing, which separates proteins by charge and then by molecular weight in the second dimension. Among proteomic techniques, differential in-gel electrophoresis (DIGE) circumvents many of the issues associated with traditional 2DE, such as reproducibility and limited dynamic range, and allows more accurate and sensitive quantitative proteomics studies. This innovative technology relies on pre-electrophoretic labelling of samples with one of three CyDye fluors (Cy2, Cy3, Cy5), each with a unique fluorescent wavelength, allowing for two experimental samples and an internal standard to be simultaneously separated on the same gel. The internal standard is a pool of an equal amount of all the experimental samples and facilitates accurate data normalization among gels, increasing statistical confidence in quantitative comparative analysis. Under optimal condition, several thousand proteins' expression levels can be defined simultaneously on a single 2D gel. The proteins can then be compared using computer software, e.g. DeCyder biological variation analysis (BVA), to identify proteins that are differentially expressed.

2D-DIGE is a descriptive technique and must be coupled with an analytical method such as mass spectrometry (MS) to identify the proteins. MS provides structural information, such as peptide mass and amino acid sequence, which is then used to identify the protein by searching against nucleotide and protein databases [243]. Proteins that are identified to be of interest are then picked from preparatory gels and subsequently digested using trypsin to extract the proteins. These specific

proteolytically-derived peptides are then characterized for protein identification. Mass spectrometers are capable of forming, separating, and detecting molecular ions on the basis of the mass-to charge ratio (m/z). This requires that the peptides are ionized. Ionization techniques transfer biomolecules from the solid or liquid phase to the gas phase, making them amenable to MS measurement. A method of peptide ionization for MS analysis is matrix-assisted laser desorption/ionization (MALDI). Ionization ensues as a result of the addition of 1 or more protons. Thus, a peptide of molecular weight 1000 Da will have an m/z value of 1001 after ionization by the addition of a single proton and 501 with the addition of 2 protons (M+2H/2). The time-of-flight (TOF) analyser separates ions according to their m/z ratios by measuring the time it takes for ions to travel through a field free region known as the flight or drift tube. The smaller ions possess higher velocity relative to larger/heavier ions. Separated ion fractions arriving at the end of the drift tube are detected by an appropriate recorder that produces a signal upon impact of each ion group. The TOF mass spectrum is a recording of the detector signal as a function of time.

After the unknown protein of interest is cleaved into smaller peptides and the absolute masses accurately measured with a mass spectrometer, these masses are then compared to either a database containing known protein sequences or even the genome. This is achieved by using computer programs that translate the known genome of the organism into proteins, then theoretically cut the proteins into peptides and calculate the absolute masses of the peptides from each protein. They then compare the masses of the peptides of the unknown protein to the theoretical peptide masses of each protein encoded in the genome. The results are statistically analyzed to find the best match. This method of protein analysis is also known as peptide mass fingerprint (PMF) [244, 245]. Unfortunately, a single peptide is rarely unique to 1 protein, thus several peptides (>3) that are derived from the same protein are typically required for identification. Accurate identification can be problematic in some scenarios, for example a simple rearrangement of the constitutive amino acids can have the same mass or that the peptides from post-translationally-modified proteins will not match the masses of the peptides from the unmodified protein in the database. Any contamination by keratin and peptides from the autolysis of trypsin may also be problematic. Moreover, not all proteins are amenable to identification by PMF alone as a large percentage of human proteins are not represented in databases. In addition,

small proteins may not yield a sufficient number of peptides from the tryptic digest for unambiguous identification. However, 2-DIGE MALDI-TOF MS is still a robust method to measure protein expression and protein identification.

1.5.2. Bioinformatics

Bioinformatics is the application of information technology and computer science to the field of molecular biology. The term *bioinformatics* was coined by Paulien Hogeweg in 1979 for the study of informatics processes in biological systems. Its primary use since at least the late 1980s has been in genomics and genetics, particularly in those areas of genomics involving large-scale DNA sequencing. In proteomics, bioinformatics can determine proteomic signatures responsible for the important clinico-pathological features and identify key proteins that may be candidates for disease markers and therapeutic targets. Bioinformatics now entails the creation and advancement of databases, algorithms, computational and statistical techniques and theory to solve formal and practical problems arising from the management and analysis of biological data.

Information about proteins can be obtained using large international databases such as SWISS-PROT and NCBI, primarily. Secondary proteomic databases, such as Bioinfomatic harvester, Open proteomics and Pubmed, are also informative in searching all that is known about a protein's interactions and its related gene. Software packages are available to analyse proteomic data e.g. PathwayStudio and Gene Ontology (GO STAT). PathwayStudio is a product aimed at the visualisation and analysis of biological pathways, gene regulation networks and protein interaction maps. It comes with a comprehensive database that gives a snapshot of all information available in PubMed, with the focus on pathways and cell signalling networks. This product allows visualisation of results in the context of automatically created pathways, gene regulation networks and protein interaction maps. The GO STAT consortium provides structural description of protein function that is used as a common language for gene annotation in many organisms. Large-scale techniques have generated many valuable protein-protein interaction datasets that are useful for the study of protein function [246].

The combination between 2D-DIGE, mass spectrometry and bioinformatics gives us a powerful tool in understanding disease. The efforts to understand the overall features of the proteome by using a bioinformatics approach to analyse 2D-DIGE data, together with the integrated information of the individual proteins identified by 2D-DIGE, will enable us to probe further the action of any drug as well as resistance mechanisms that can arise.

1.5.3. Proteomics and drug resistance biomarkers in Multiple Myeloma

Gottesman and colleagues [247], were one of the first groups to study protein profiles in drug resistant human KB carcinoma cells. However, it was years later before the first systematic comparative proteomic profiling and analysis of the drug-selected cancer cell lines were performed with the advancement of MS technology [248]. Currently, advances in the use of proteomic technologies (specifically the comparative proteomic approach) provide a robust approach to study multiple signalling pathways simultaneously and mechanism of resistance to anticancer therapy (Table 1.5.5). The altered proteins identified by proteomic approach can be further characterized as potential drug targets and the global analysis of the protein alterations can result in valuable information to understand the drug resistance mechanisms [249-251].

Proteomics has also been utilized to investigate mechanism of drug activity in MM. Ge *et al.,* has shown that 14-3-3ζ may play a vital role in mediating arsenic trioxide-induced apoptosis [252]. 14-3-3 proteins are a family of multifunctional phosphoserine binding molecules that can serve as effectors of survival signalling. They are involved in a variety of important cellular processes that include cell cycle progression, growth, differentiation as well as apoptosis. The authors also demonstrated that arsenic trioxide increased the expression levels of heat shock proteins (HSPs) but suppressed ubiquitin proteasome system (UPS) in myeloma cells. HSPs and UPS are participants in keeping proteins folded correctly and are essential for cellular functions and survival in many tissues. Another study demonstrating that proteomics is a valuable tool to examine resistance markers in MM implicated FKBP5, which was noted to be increased in MM cells following dexamethasone treatment [253]. The FKPB5 protein plays a role in immunoregulation and basic cellular processes involving protein folding and trafficking. It is also a member of the Hsp90 steroid receptor complex [254].

Resistance to the novel agent bortezomib has been described in MM and other cancers. The mechanism of resistance is still unclear. One study by Weinkauf *et al.,* has used 2-DE technology to investigate the proteins that are up- or downregulated with this drug to try to determine potential resistance mechanisms [255]. In colon cancer, aldo-keto reductase ARK1B10 has been shown to be upregulated after bortezomib treatment in HRT-18 cell line [256]. HRT-18 which was previously less sensitive to bortezomib, was sensitized when siRNA was used to knockdown this protein.

Tumour	Drug	Proteins Altered in Resistant Cells		Reference
		Up-regulated	Down-regulated	
Gastric cancer	Daunorubicin Mitoxantrone	Annexin I Annexin I Thioredoxin		[248]
Pancreatic Cancer	Daunorubicin Mitoxantrone	Cofilin Cofilin Epidermal Fatty Acid Binding Protein Stratifin (14-3-3-σ)		[257]
Fibrosarcoma	Mitoxantrone	Rho-Guanine Dinucleotide Phosphate (Rho-GDP) Dissociation Inhibitor		[258]
Colon cancer	Mitoxantrone	Adenine Phosphoribosyl Transferase Breast Cancer Specific Gene 1		[258]
Colon cancer	5-fluorouracil	Metabotropic Glutamate Receptor 4		[259]
Colon cancer	5-fluorouracil		F1F0-ATP Synthase	[260]
Melanoma	Vindesine Cisplatin Fotemustine Etoposide	Translationally Controlled Tumour Protein Human Elongation Factor 1-δ Tetratricopeptide Repeat Protein 14-3-3-γ		[261]

Neuro- blastoma	Etoposide	Peroxiredoxin I β-Galactoside Soluble Lectin Binding Protein Vimentin Heat Shock Protein 27 Heterogeneous Nuclear Ribonucleoprotein K	dUTP Pyrophosphatase	[262]
Gastric cancer	Cisplatin		Pyruvate Kinase M2	[263]
Breast cancer	Melphalan	Retinoic Acid Binding Protein II Macrophage Migration Inhibition Factor	Calreticulin Cyclophin A Heat Shock Protein 27	[264]
Breast cancer	Doxorubicin	Annexin I Neuronal Ubiquitin Carboxyl Hydrolase Isoenzyme L1 Glutathione-S-Transferase pi Nicotinamide N-Methyltransferase Interleukin-18 Precursor	Catechol-O- Methyltransferase	[265]

Table 1.5.5 Summary of studies using 2DE/MS to investigate chemotherapy resistance using cell lines [266]

1.6 Aims of the thesis

The focus of this research project was to evaluate the mechanisms whereby myeloma cells develop intrinsic resistance with a focus on resistance in the context of bortezomib treatment. The aims of this thesis are as follows:

- Examine multidrug resistance pumps as a mechanism of resistance in MM.
- Characterise the interaction of bortezomib with multidrug resistance pumps.

- Investigate the role of p53 signalling perturbations in resistance mechanism in MM using nutlin-3 (Mdm2 inhibitor)
- Assess the activity of nutlin-3 in MM cell lines
- Toxicologically characterise the effect of nutlin-3 combinations with bortezomib in MM cell models.

- Examine the AMPK pathway as an alternative therapeutic target in drug-resistant MM
- Explore the activity of AICAR and Metformin on MM cell lines, patient samples and non-neoplastic cells.
- Define the *in vivo* anti-cancer activity of AICAR and Metformin.

- Examining myeloma resistance to bortezomib treatment using 2D-DIGE analysis.

Chapter 2
Materials and Methods

2.1. Ultrapure Water

Ultrapure water, (UHP) was used for the preparation of all media and solutions. This water was purified to a standard of 12-18 MΩ/cm resistance by a reverse osmosis system (Millipore Milli-RO 10 Plus, Elgastat UHP). A conductivity meter in the system continuously monitored the quality of the UHP.

2.2. Glassware

Some of the solutions utilized in the various stages of cell culture were stored in sterile glass bottles. These sterile bottles and other glassware required for cell culture-related applications were prepared as follows: glassware and lids were soaked in a 2% solution of RBS-25 (AGB Scientific) for 1 hour. After this time, they were cleaned and rinsed in tap water. The glassware was then washed in an industrial dishwasher, using Neodisher detergent and rinsed twice with UHP. The materials were finally sterilized by autoclaving as described in Section 2.3.

2.3. Sterilisation Procedures

All thermostable solutions, water and glassware were sterilized by autoclaving at 121^{o}C for 20 minutes (mins) at 15 p.s.i.. Thermolabile solutions were filtered through 0.22µm sterile filters (Millipore, Millex-GV SLGV025BS).

2.4. Preparation of Cell Culture Media

Cell culture media Roswell Park Memorial Institute medium (RPMI)-1640, Dubelcco's Modified Eagle Medium (DMEM) and *Minimum Essential Medium* Eagle, *Alpha* Modification (*MEM Alpha*) were purchased from Cellgro, Mediatech, Manassas, VA, USA. Complete media was prepared as follows: 5-10% foetal calf serum (FCS) (GIBCO/BRL, Gaithersburg, MD, USA), 100U/L of penicillin and 100ug/ml streptomycin were added to volumes of 50ml basal media as required. Complete media were maintained at 4^{o}C for up to a maximum of 1 week.

2.5. Cells and Cell Culture

All cell culture work was carried out in a class II laminar air-flow cabinet. Before and after use, the laminar air-flow cabinet was cleaned with 70% industrial methylated spirits (IMS). Any items brought into the cabinet were also cleaned with IMS. At any time, only one cell line was used in the laminar air-flow cabinet and upon completion of work with the cell line, the laminar air-flow cabinet was allowed to clear for at least 15 mins so as to eliminate any possibility of cross-contamination between the various cell lines. Details pertaining to the cell lines used for the experiments in this thesis are provided in table 2.5.1. All cells are incubated at 37^{o}C and in an atmosphere of 5% CO_2. Cells were fed with fresh media or subcultured every 3 days in order to maintain active cell growth.

2.5.1. Subculturing of cell lines

For adherent cell lines

1. The waste cell culture medium was removed from the tissue culture flask and discarded into a waste bottle containing bleach. The flask was then rinsed out with 1ml of PBS to ensure the removal of any residual media.

2. 5ml of trypsin (Cellgro) was then added to the flask, which was then incubated at 37^{o}C, 5% CO_2 for approximately 5 mins, until all of the cells detached from the inside surface of the flask.

3. The trypsin was deactivated by adding an equal volume of complete media to the flask.

4. The cell suspension was removed from the flask and placed in a sterile tube (Falcon, BD, Franklin Lakes, NJ, USA) and centrifuged at 1000 xg for 5 minutes.

5. The supernatant was then discarded from the tube and the pellet suspended in 5ml of complete medium. A cell count was performed and an aliquot of cells was used to reseed a new flask at the required density.

For suspension or semi-adherent cell lines

1. A cell scraper (Corning, Lowell, MA, USA) was used to remove any attached cells on the inside surface of the flask.

2. The cell suspension was removed from the flask and placed in a sterile tube (Falcon) and centrifuged at 1000 xg for 5 mins.

3. The supernatant was then discarded from the tube and the pellet suspended in 5ml of complete medium. A cell count was performed and an aliquot of cells was used to reseed a new flask at the required density.

Cell Line	Media	Source
Myeloma Cell Line (MM)	RPMI-1640 with 100 U/ml penicillin, 100 µg/ml streptomycin and 10% FCS	Dana Farber Cancer Institute
OCIMy5		
OPM2		
OPM1		
RPMI8226 and its sublines		
Dox40		
MR20		
INA6 (plus IL-6 10ng.ml)		
KMS11		
KMS34		
U266		
L363		
MM.1S and its subline		
MM.1R		
NCIH929		
SKMM1		
S6B45		
JJN3		
ARK		
ANBL6 and its subline (plus IL-6 10ng/ml)		
ANBL6-VR5		

Thyroid Cancer cell line	DMEM with 100 U/ml penicillin, 100 µg/ml streptomycin and 10% FCS	Dana Farber Cancer Institute
KAT18		
WRO		
FRO		
TT		
SW579		
DRO-81-1		
HRO-85-1		
Other Cancer Cell Line	DMEM with 100 U/ml penicillin, 100 µg/ml streptomycin and 10% FCS	Dana Farber Cancer Institute
MDA-MB-231 (breast)		
PC3 (prostate)		
DU145 (prostate)		
DLKP and its sublines (lung)	DMEM with 10% FCS	NICB
DLKP-A		
DLKP-SQ -Mitox		
A549 and its subline (lung)	RPMI-1640 with 5% FCS	NICB
A549-taxol		
NCI/Adr-res (ovarian)	RPMI-1640 with 10% FCS	NICB
Non Malignant Cell Line	DMEM with 100 U/ml penicillin, 100 µg/ml streptomycin and 10% FCS	Dana Farber Cancer Institute
HS-5		
THLE3		

Table 2.5.1 Source description and media requirements of cell lines used in experiments described in this thesis.

2.5.2. Assessment of cell number and viability

1. Cells were trypsinised, pelleted and resuspended in 5ml media. An aliquot of the cell suspension was then added to trypan blue at a ratio of 1:10.

2. The mixture was incubated for 3 mins at room temperature. A 10µl aliquot of the mixture was then applied to the chamber of a glass coverslip-enclosed haemocytometer.

3. Cells in the 16 squares of the four grids of the chamber were counted. The average cell number per 16 squares was multiplied by 10^5 to determine the number of cells per ml in the original cell suspension.

4. Non-viable cells stained blue, while viable cells excluded the trypan blue dye as their membrane remained intact and thus unstained. On this basis, % viability could be calculated and only viable cells were counted.

2.5.3. Cryopreservation of cells

1. Cells for cryopreservation were harvested in the log phase of growth and counted as described in Section 2.5.2.

2. Cell pellets were resuspended in a suitable volume of serum. An equal volume of 10% (final concentration) DMSO/serum solution was added dropwise to the cell suspension. This is done quickly to minimize the duration of exposure of the cells to DMSO toxicity.

3. A total volume of 2ml (usually 2 x 10^5 to 5 x 10^6 cells/1 ml vial) of this suspension was then placed in cryovials (Nunc, Rochester, NY, USA). These vials were then placed in a isopropanol bath container (Nalgene, Cat#5100-0001, Rochester, NY, USA) that is subsequently cooled in a -80^{o}C freezer. The container provided cooling at a rate of 1^{o}C/minute.

4. The next day, the frozen vials were then removed from the -80^{o}C freezer and transferred to the liquid nitrogen-fill storage (-196^{o}C).

2.5.4. Thawing of cryopreserved cells

1. A volume of 9ml of fresh complete medium was added to a sterile 15ml tube (Falcon). The cryopreserved vials were removed from the liquid nitrogen and kept in dry ice until all of the apparatus for thawing cells were readied. The vials were then thawed rapidly in a water bath at 37^{o}C. The cells were removed from the vials and transferred to the aliquoted media.

2. The resulting cell suspension was centrifuged at 1000 xg for 5 mins. The supernatant was removed and the pellet resuspended in fresh culture medium.

3. An assessment of cell viability on thawing was then carried out (Section 2.5.2).

4. Thawed cells were then added to an appropriately sized tissue culture flask with a suitable volume of growth medium that contained twice the amount of FCS that the cells would normally need.

2.5.5. Selection of primary myeloma cells using CD138 tagged micro-beads (Miltenyi Biotec; Bergisch Gladbach, Germany) as per manufacturer's instructions.

1. In brief, following consent, myeloma patient samples were collected in Lithium heparin tubes, the bone marrow sample was then Ficoll gradient separated. The bone marrow was layered over the Ficoll and centrifuged for 800 xg for 30 mins. The interface was removed and washed twice with PBS before resuspended in medium and cells counted.

2. The cells were pelleted again and resuspended in buffer (PBS, 0.1%BSA, EDTA). There should be 10^{7} cells/80µl Buffer. 20µl of beads/80µl buffer was added and incubated at 4^{o}C for 20 minutes.

3. After the incubation period, 5ml of buffer was added to the bead suspension and centrifuged at 1000 xg for 5 mins. Cells were resuspended in 1ml of buffer.

4. The columns were placed in the magnet and primed with 3ml of buffer. The cells were passed through each column and then washed with 3ml of buffer. The cells collected in the first pass were the CD138- cells.

5. The columns were removed from the magnet and washed with 3ml of buffer. These cells collected were the CD138+ cells. The cells were then counted and plated at a density of 10^4 cells/well and cultured in RPMI-1640 U/ml penicillin, 100 µg/ml streptomycin, 10ng/ml IL6 (R&D systems, Minneapolis, MN) and 20% FBS.

2.5.6. *Mycoplasma* analysis of cell lines using PlasmoTest Mycoplasma Detection test (InvivoGen, San Diego, CA, USA) as per manufacturer's instructions.

1. In brief, cells of interest were cultured without antibiotics two days prior to running the test. 500µL of cell culture was collected and transferred to a 1.5mL microtube. Sample was then heated at 100^{o}C for 15 mins and allowed to cool to room temperature before addition to a 96 well plate.

2. HEK-Blue 2 cells were prepared by removing the medium and washing the cells with PBS. The HEK-Blue 2 cells were removed from the flask by tapping it gently. The cells were diluted with HEK-Blue detection media to a concentration of 250,000 cells/mL.

3. 50µl of each sample and 200µl of HEK-Blue 2 cells were added to each well of a 96 well plate. A 1X dilution of a positive and negative control were added. The plate was incubated overnight and read on a spectrophotometer at 620-655nm.

4. All cell lines used in this thesis were screened for *mycoplasma* contamination as above and were determined to be *mycoplasma*-free.

2.5.7. Osteoclast differentiation as described by [125]

In brief, peripheral blood mononuclear (PBMCs) were isolated as described in section 2.5.5 using Ficoll gradient separation. The PBMCs were cultured in alpha-MEM media containing 10% FBS and Pen/Strep for 16 hrs to allow attachment. The non-adherent cells were removed, fresh media supplemented with macrophage colony stimulating factor (MCSF) (25 ng/mL; R&D Systems # 216-MC-005) and receptor activator of NF-kappaB ligand (RANKL) (50 ng/mL; Peprotech #310-01), and cells were cultured for 3-4 weeks to differentiate into mature osteoclasts. The culture medium was replaced twice weekly with alpha-MEM containing fresh MCSF and RANKL. At 3-4 weeks, cells were trypsinized, replated, and stained using the Acid Phosphatase, Leukocyte (TRAP) Kit (Sigma-Aldrich, St Louis, MO) to determine differentiation of osteoclasts.

2.6. Reagents

Reagent	MW (g/mol)	Source	Solubility
2-deoxyglucose	164.16	Sigma-Aldrich	Molecular grade H_2O
3-Bromopyruvate	166.96	Sigma-Aldrich	Molecular grade H_2O
AICAR	258.23	Toronto Research Chemicals	Molecular grade H_2O/ PBS*
Bortezomib	384.24	Millenium Pharmaceuticals	DMSO
Compound C	399.5	Calbiochem/Merck	DMSO
Doxorubicin	543.52	Sigma-Aldrich	PBS
Elacridar	563.64	Sequoia Research	DMSO
Metformin	165.62	Sigma-Aldrich	Molecular grade H_2O
Nutlin-3	581.5	Cayman Chemical Company	DMSO
Phytohemagglutinin		Sigma-Aldrich	PBS
SN38	392.4	Sequoia Research	DMSO
Sulindac Sulphide	340.41	Sigma-Aldrich	DMSO
Verapamil	464.6	Sigma-Aldrich	Molecular grade H_2O
ZVAD-FMK	467.5	Calbiochem	DMSO

Table 2.6 The reagents used in this thesis

All reagents are kept at -20^{o}C until use.

* AICAR was reconstituted with molecular grade H2O for *in vitro* experiments and PBS for *in vivo* experiments

2.7. *In vitro* Toxicity Assays

2.7.1. *In vitro* assay experimental procedure

1. Cells in the exponential phase of growth were harvested as described in Section 2.5.1.

2. Cell suspension containing 1-x10^4 cells/ml was prepared in complete medium. Volumes of 100µl/well of this cell suspension were added to 96-well plates (Falcon) using a multichannel pipette. Plates were agitated gently in order to ensure even dispersion of cells over a given well. Cells were then incubated overnight at 37^{o}C in 5% CO_2.

3. Drug dilutions were prepared at 2X their final concentration for single agent treatment or 4X their final concentration for combination treatment in cell culture medium. Volumes of the drug dilutions (50µl or 100µl) were added to each well using a multichannel pipette. Plates were then mixed gently as above.

4. Cells were incubated for a further 2 to 5 days (indicated in experiment) at 37^{o}C in 5% CO_2. After this incubation period, control wells would have reached approximately 80-90% confluency.

5. Assessment of cell survival in the presence of drug was determined by the acid phosphatase assay (Section 2.7.2), 3-(4,5-dimethylthiazol-2-yl)-2,5-diphenyl tetrasodium bromide (MTT;Chemicon International, Temecula, CA) colorimetric survival assay (Section 2.7.3) or Cell Titre Glo assay (Promega, Madison, WI, USA) (Section 2.7.4). The concentration of the drug which caused 50% cell kill (IC_{50} of the drug) was determined from a plot of the % survival (relative to the control cells) versus cytotoxic drug concentration.

2.7.2. Acid phosphatase assay as described by [267]

1. Following the incubation period of 5 days, medium was removed from the plates.

2. Each well on the plate was washed twice with 100µl of PBS. This was then removed and 100µl of freshly prepared phosphatase substrate (10mM p-

nitrophenol phosphate (Sigma,104-0) in 0.1M sodium acetate (Sigma, S8625), 0.1% triton X-100 (BDH, 30632), pH 5.5) was added to each well.

3. The plates were then incubated in the dark at 37^{o}C for 2 hours.
4. The enzymatic reaction was stopped by the addition of 50µl of 1M NaOH.
5. The plate was read in a dual beam plate reader at 405nm with a reference wavelength of 620nm.

2.7.3. 3-(4,5-dimethylthiazol-2-yl)-2,5-diphenyl tetrasodium bromide (MTT) colorimetric survival assay

1. Following the incubation period of 2-3 days, MTT 5mg/ml at a ratio of 1:10 to total volume in wells was added. The plate were then incubated the dark at 37^{o}C for 4 hours. After incubation period, the plates were centrifuged at 1000 xg for 5 mins and medium was removed from the plates.
2. 100µl of DMSO was added to each well. The plates were then shaken to dissolve the crystals.
3. The plate was read in a dual beam plate reader at 540nm with a reference wavelength of 690nm.

2.7.4. Cell Titre Glo assay (Promega, Madison, WI, USA).

The Cell Titer-Glo reagent was prepared as per manufacturer's instructions. The prepared reagent was stored as aliquots in -20^{o}C. CTG at a ratio of 1:10 to total volume in wells was added. The plates were then agitated briefly and incubated in the dark at 37^{o}C for 30 mins. The plates were read using a Luminoskan luminometer (Labsystems, Franklin, MA).

2.7.5. Stromal cell and osteoclast coculture as described by [212]

1. The luciferase (luc)-expressing cell line MM.1S-GFP/luc, NCI-H929-GFP/luc and JJN3-GFP/luc was generated by retroviral transduction with the pGC-*gfp/luc* vector (kind gift of C.G. Fathman, Stanford University). RPMI-Dox40-MCherry/luc was generated by retroviral transduction with the pFUW-Luc-Ch-puro vector. All these cell lines were used for co-culture experiments with the luc-negative human stromal line HS-5 and generated osteoclasts.

2. Briefly, 50µl of $4x10^4$/ml HS-5 stromal cells or $8x10^4$/ml osteoclasts were plated in 96-well plates and allowed to attach overnight. 50µl of $1x10^4$/ml MM cells were then plated and treated for at the doses indicated.

3. Following incubation, 2.5mg/ml of luciferin substrate (Xenogen Corp, Alameda, CA) at a ratio of 1:10 to total volume in wells was added. The plates were then incubated in the dark at 37°C for 30 mins and the resulting bioluminescence signal was measured using a Luminoskan luminometer (Labsystems).

2.8. Western Blotting

2.8.1. Lysate preparation

1. Cells were seeded at a density of 10^7 cells per 30mm tissue culture dish (Falcon). Treatment of cells and duration of exposure of cells to treatment were carried out as shown in the example below:

   All cells were plated at the same time using the same media. The longest time point was treated first and each subsequent treatment was carried out counting down to the shortest time point (see timeline). After the incubation period for the longest time point, all the cells were collected at the same time. This was to ensure that all the cells had the same environmental exposure for the same amount of time to reduce variability.

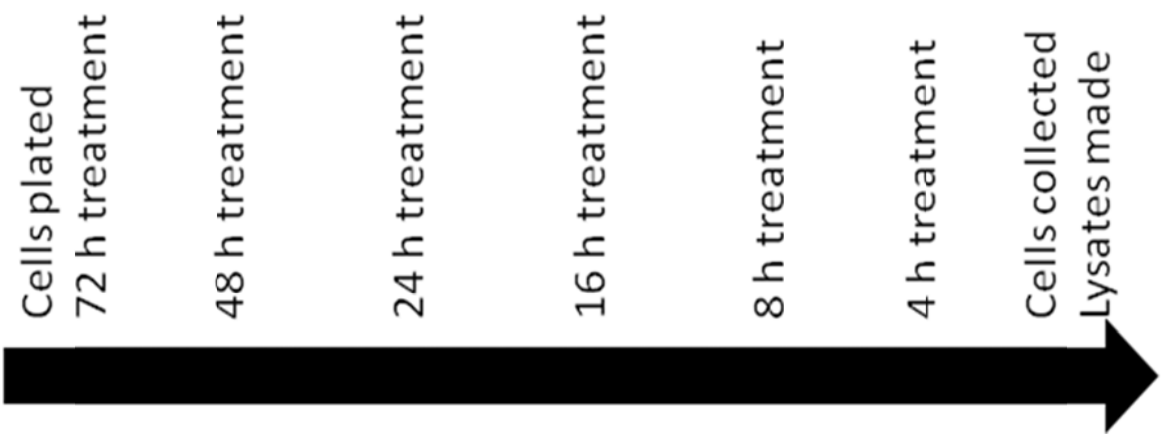

Figure 2.8.1 Timeline for plating cells for Western blotting

2. After an appropriate incubation period, media was removed and cells trypsinised (for adherent cells) or pelleted (for suspension cells).

3. Cells were washed twice with ice cold PBS. All procedures from this point forward were performed on ice.

4. Cells were resuspended in 1ml of NP-40 lysis buffer in 1.5ml eppendorf tubes and placed on a rotator for 30 mins in the cold room. Table 2.8.1 below provides the recipe for the lysis buffer.

5. Lysed cells were pelleted at 14,000 rpm for 20 mins in the cold room.

6. Supernatant was removed and transferred to new eppendorf tubes. Protein concentration was quantified as detailed in section 2.8.2. Samples were then stored in aliquots at -80^{o}C.

NP-40 lysis buffer
50mM Tris-HCl pH=8.0 120mM NaCl 5mM EDTA 1% Igepal (NP40) Complete TM Proteinase inhibitors (1 tablet in 50 ml) Phosphatase inhibitors from Calbiochem

Table 2.8.1 NP-40 lysis buffer

2.8.2. Protein quantification

Protein levels were determined using the Bio-Rad protein assay kit (Bio-Rad, 500-0122) as follows:

1. A 2mg/ml bovine serum albumin (BSA) solution (Bio-Rad, 500-0122) was prepared freshly in lysis buffer.
2. A protein standard curve was prepared from the BSA stock with dilutions made in lysis buffer.
3. The Bio-Rad reagent was diluted 1:5 in UHP water and filtered through Whatman paper before use.
4. A 20µl volume of protein standard dilution or sample was added to 980µl of diluted dye reagent and the mixture vortexed.
5. After 5 mins incubation, absorbance was assessed at 595nm.
6. The concentration of the protein samples was determined from the plot of the absorbance at 595nm versus concentration of the protein standard.

2.8.3. Gel electrophoresis

Proteins for analysis by Western blotting were resolved using precast 4-12% Bis Tris SDS-polyacrylamide gel electrophoresis (SDS-PAGE) (Invitrogen, Carlsbad, CA, USA).

1. 20µg of protein was prepared for electrophoresis by mixing with high grade molecular water, sample buffer (Invitrogen) and reducing agent (Invitrogen) to a volume of 26µl. The samples were heated for 10 mins at 70^{o}C and then loaded into the wells.

2. 1X MOPS (Invitrogen, NuPage) running buffer and 500 µl of Antioxidant (Invitrogen) was added to gel apparatus.

3. Gel was run at 200V until dye reached the bottom of the gel.

2.8.4. Gel transfer

1. PVDF membrane was activated with 100% methanol (MeOH) prior to transfer. Two pieces of thick blotting pads were soaked in transfer buffer (Boston Scientific, MA, USA) with 20% MeOH.

2. A sandwich of blotting pad, membrane, gel and blotting pad was assembled on the semi-dry transfer apparatus. The gel was transferred at 0.4 amps for 1 hour.

2.8.5. Membrane probing

1. Membrane was blocked for 1 hour with 5% non fat milk in TBS-T. Primary antibody (Table 2.8) made at a dilution that had been optimally predetermined, was incubated with the membrane overnight at 4^{o}C.

2. The membrane was washed 3 times (5 mins each) with TBS-T and then incubated with the respective secondary horseradish peroxidase (HRP)-labelled antibody (Jackson ImmunoResearch (West Grove, PA) was added at 1:10,000 dilution for 1 hour at room temperature. The membrane was then washed 5 times with TBS-T.

3. The protein was visualized using chemiluminescence (SuperSignal West Pico, Pierce, Rockford, IL). If enhanced signal was required, then SuperSignal West Femto IPierce, Rockford, IL) was used. The film used was from Kodak Scientific Imaging.

2.8.6. Image acquisition

The developed films with the protein bands were digitized using a flatbed scanner (HP scanjet 5500c, Hewlett-Packard, USA). The scanner operates in reflection mode and the films scanned at a resolution of 600 dpi (equals maximal physical, noninterpolated resolution). Adobe Photoshop software was used to crop the scanned films and all files were saved as TIFF files.

2.8.7. Densitometry reading

1. For analysis of the Western blot images, ImageJ 1.38 (Windows version of NIH Image, http://rsb.info.nih.gov/nih-image/), allows the measurement of density profiles and peak intensity (average OD of the band). Using ImageJ, the background correction was performed by measuring a rectangle (same size as the rectangle used to define the band) of developed film without any bands. To define the profiles, a rectangular box was defined in which the band was fitted as tight as possible. All bands were quantified using the same size rectangular box.

2. The background OD was subtracted from all quantified bands. The bands of interest were expressed as a ratio to their individual loading control (usually GAPDH).

Antibody	Molecular Weight (kDa)	Company Name	Catalogue Number	1^0 Ab dilution	2^0 Antibody
AMPKá	62	Cell Signaling	2793	1:1000	mouse
AMPKá (phos Thr 172)	62	Cell Signaling	2535	1:1000	rabbit
AMPKâ ½	38, 34	Cell Signaling	4150	1:1000	rabbit
Annexin A2	38	Abcam	ab55771	1:5000	mouse
A+U-rich element RNA binding factor	46	Abcam		1:2000	rabbit
Caspase 3	17, 19, 35	Cell Signaling	9662	1:1000	rabbit
cdc2 (cdk1)	34	Santa Cruz	8395	1:1000	mouse
cdk4	30	Cell Signaling	2906	1:1000	mouse
cdk6	36	Cell Signaling	3136	1:1000	mouse
cyclin B1	60	Santa Cruz	245	1:1000	mouse
cyclin D1	38	Santa Cruz	8396	1:500	mouse
Endoplasmic reticulum protein 29	29	Abcam	ab83073	1:1000	mouse
FSCN1	55	Milipore	MAB3582	1:1000	mouse
Ferritin light chain	20	Abcam	ab80617	1:10,000	mouse
FUBP1	68	Abcam	ab29732	1:1000	rabbit
GAPDH - HRP conjugate	40	Abcam	ab9482	1:10,000	none
GSK3 (phos Ser21/9)	46, 51	Cell Signaling	9331S	1:1000	rabbit
GSK3 á/â	47, 51	Santa Cruz	7291	1:1000	mouse
hnRNP A1	39	Abcam	ab4791	1:5000	rabbit
hnRNP A2/B1	36	Cell Signaling	9304	1:1000	mouse
hnRNP K	51	Abcam	ab23644	1:1000	mouse
Hsp70	72, 73	Cell Signaling	4872	1:1000	rabbit
KHSRP	73	Abcam	83291	1:1000	rabbit
MDM2	60, 90	Santa Cruz	965	1:1000	mouse
Noxa	10	IMGENEX	349A	1:1000	mouse
p53	53	Upstate Biotechnology	05-224	1:1000	mouse
p70S6 Kinase	70, 85	Cell Signaling	9202	1:1000	rabbit
p70S6K (phos Thr389)	70, 85	Cell Signaling	9205	1:1000	rabbit
P-glycoprotein	170	Alexis Biochemicals	801-002	1:250	mouse
PARP	24, 89, 116	Cell Signaling	9542	1:1000	rabbit
Puma	18, 23	Cell Signaling	4976	1:1000	rabbit
S6 ribosomal protein	32	Cell Signaling	2217	1:1000	rabbit
S6 ribosomal protein (phos ser235/236)	32	Cell Signaling	2211	1:1000	rabbit

Table 2.8 List of primary antibodies used

2.9. Two dimensional difference gel electrophoresis (2D-DIGE)

2.9.1. Lysate preparation

Lysate was prepared as detailed in Section 2.8.1.

2.9.2. Sample preparation for 2-D Electrophoreses

Cell lysates were subsequently precipitated prior to labelling using a 2-D Cleanup Kit (Biorad, Cat #163-2130) as per manufacturer's instructions.

1. In brief, 500µg of protein was mixed with 300µl of precipitating agent 1 in a 1.5ml eppendorf tube and incubated on ice for 15 mins. 300µl of precipitating agent 2 was then added, sample mixed well and centrifuged at (> 12,000 x g) for 5 minutes to form a pellet. The supernatant was discarded and 40 µl of wash reagent 1 was added on top of the pellet.

2. The tube was centrifuged as before for 5 mins. After centrifugation, the wash was discarded and 25 µl of ultrapure water was added on top of the pellet.

3. 1 ml of wash reagent 2 (which was prechilled at -20°C for at least 1 hr) and 5 µl of wash 2 additive was added to the tube. The tube was then incubated at -20°C for 30 mins.

4. After the incubation period, the tube was centrifuged at (> 12,000 x g) for 5 mins and the supernatant discarded. The pellet was air-dried briefly before being resuspended in ice-cold DIGE-lysis buffer. See Table 2.9.2 for recipe.

5. Protein quantification was performed using the Quick Start Bradford Protein Assay as described in Section 2.8.3.

DIGE-lysis buffer
20mM Tris 7 M Urea 2 M Thiourea 4% CHAPS pH 8.5

Table 2.9.2 DIGE-lysis buffer

2.9.3. 2-D DIGE labelling:

1. Samples were labelled with N-hydroxy succinimidyl ester-derivatives of the cyanine dyes Cy2, Cy3, and Cy5 following standard protocol.

2. The CyDye DIGE Fluor minimal dye was reconstituted as follows. The dye was allowed to warm to room temperature before dimethylformamide (DMF) was added to give a stock concentration of 1 mM.

3. Typically, 50 µg of lysate was minimally labelled with 200 pmol of either Cy3 or Cy5 for comparison on the same 2D gel. Labelling reactions were performed on ice in the dark for 30 minutes and then quenched with a 50-fold molar excess of free lysine to dye for 10 minutes on ice. A pool of all samples was also prepared and labelled with Cy2 to be used as a standard on all gels to aid image matching and cross-gel statistical analysis. The Cy3 and Cy5 labelling reactions (50 µg of each) from each lysate were mixed and run on the same gels with an equal amount (50 µg) of Cy2-labelled standard.

2.9.4. Casting 12.5% homogeneous polyacrylamide gels

1. Low fluorescence glass plates without scratches were used to cast high quality gels.

2. Displacing solution (see Table 2.9.4a) and acrylamide gel stock solution (see Table 2.9.4b) was prepared. The gel caster was assembled as described in the Ettan DALT electrophoresis user manual.

3. Gels were poured and allowed to set before use. They were then used on the same day for 2D gel electrophoresis.

Reagents	**Final concentration**
1.5mM Tris pH 8.8	375mM
Glycerol	50% (v/v)
1% Bromophenol blue stock solution	0.002% (w/v)
Make up to 100ml with distilled water	

Table 2.9.4A Displacing solution

Reagents	**Quantity for 900ml**
Acrylamide/PAGE 40% (w/v)	281.25ml
PlusOne Methylenebisacrylamide 2% (w/v)	150.3ml
Tris (1.5 M, pH 8.8)	225ml
10% (w/v) SDS	9ml
10% (v/v) TEMED	1.24ml
10% (w/v) APS	9ml
Make up to 900 ml with distilled water	

Table 2.9.4B Acrylamide gel stock solution (12.5%)

2.9.5. Protein separation by 2D gel electrophoresis

1. Immobilized 24cm linear pH gradient (IPG) strips, pH 3-11NL, were rehydrated in rehydration buffer (see Table 2.9.5) overnight, according to the manufacturer's guidelines.

2. Isoelectric focusing was performed using an IPGphor apparatus (GE Healthcare) for a total of 40 kV/hs at 20°C, 50 mA. Strips were equilibrated for 20 minutes in 50 mM Tris-HCl, pH 8.8, 6 M Urea, 30% (v/v) Glycerol, 1% (w/v) SDS containing 65 mM DTT and then for 20 minutes in the same buffer containing 240 mM iodoacetamide.

3. Equilibrated IPG strips were transferred onto 18x20-cm 12.5% uniform polyacrylamide gels (Section 2.9.4). Strips were overlaid with 0.5% (w/v) low melting point agarose in running buffer containing bromphenol blue.

4. Gels were run using the Ettan Dalt 12 apparatus (GE Healthcare) at 2 Watt/gel for 45 minutes, then 15W/gel at 10°C until the dye front had run off the bottom of the gels.

2.9.6. Image acquisition and data analysis

All of the gels were scanned using the Typhoon 9400 Variable Mode Imager (GE Healthcare) to generate gel images at the appropriate excitation and emission wavelengths from the Cy2-, Cy3- and Cy5-labeled samples. All gels were scanned at a 100µm pixel resolution to generate a target maximum pixel value of 50,000 to 80,000. The resultant gel images were cropped using the Image Quant software tool and imported into Decyder 6.5 software. The biological variation analysis (BVA) module of Decyder 6.5 was used to compare the sensitive cells lines from the resistance cell lines before and after treatment to generate lists of differentially expressed proteins.

2.9.7. Spot digestion

1 Preparative gels containing 400 µg of protein were fixed and then post stained with colloidal CBB stain (Sigma).

2 The subsequent gels were scanned using the Typhoon 9400 Variable Mode Imager (GE Heatlhcare) to generate gel images at the appropriate excitation and emission wavelengths for the colloidal CBB stain. Preparative gel images were then matched to the Master gel image generated from the DIGE experiment. Spots of interest were selected and a pick list was generated and imported into the software of the Ettan Spot Picker robot (GE Healthcare).

3 Gel plugs were placed into presiliconised microtitre plate and stored at 4°C until digestion. Tryptic digestions were performed using the Ettan Digestor robot (GE Healthcare).

4 Excess liquid was removed from each plug, and washed for three cycles of 20 min using 50 mM NH4HCO3 in 50% methanol solution.

5 The plugs were then washed for two cycles of 15 min using 70% ACN and left to air dry for 1 hour. Lyophilised sequencing grade trypsin (Promega) was reconstituted with 50 mM acetic acid as a stock solution and then diluted to a working solution with 40 mM NH4HCO3 in 10% ACN solution, to a concentration of 12.5 ng trypsin per mL.

6 Samples were digested at 37°C overnight and were then extracted twice with 50% ACN and 0.1% TFA solution for 20 min each. All extracts were pooled and concentrated by SpeedVac (Thermo Scientific) for 50 min. Subsequently, dried peptides were resuspended in 20 µl of 0.1% TFA.

2.9.8. Protein identification using MALDI ToF/ToF Mass spectrometry

1 Dried peptides were resuspended in 10 µl of 0.1% TFA, desalted and concentrated using µ-C18 ZipTips. Samples were eluted form the µ-C18 ZipTips using 0.5 µl of 50% acetonitrile/0.1% TFA and supplemented with 0.5 µl of a 5 mg/ml solution of recrystalised α-cyano-4-hydroxy-trans-cinnamic acid matrix (Laser Biolabs) in 50% acetonitrile/0.1% TFA prior to analysis.

2 Samples were subsequently spotted onto a 384 spot MALDI sample plate (Applied Biosystems).

3 MALDI mass spectra were generated using a 4800 TOF/TOF Proteomics Analyzer instrument (Applied Biosystems). An internal sample mix, Pep4 (Laser Biolabs) was also spotted onto target slides and used as an internal calibrant. All MS and MS/MS experiments were carried out in positive reflectron mode. Ten precursor ions for MS/MS were selected automatically on the basis of intensity from the MS spectra. The MS and MS/MS data were combined and searched against a number of databases using GPS Explorer software (Applied Biosystems) and a local MASCOT (Matrix Science) search engine for protein identification. A mass window of 20 ppm was set for database searching on all precursors.

4 Full scan mass spectra were recorded in profile mode and tandem mass spectra in centroid mode. The peptides were identified using the information in the tandem mass spectra by searching against the SWISS PROT database using SEQUEST.

2.9.9. Statistical analysis

DIGE gels were exported into image analysis using BVA module of Decyder software (GE Healthcare) statistics and quantitation of protein expression was carried out. Following confirmation of appropriate spot detection, matching, normalisation and spot statistics were reviewed. Averages for each spot were compared by their normalised volume using one-way analysis of variance between groups (ANOVA) test. The normalised volume of a spot was compared in all the gels between each group. Spots that were found to be statistically significant (t-test ≤ 0.01) were isolated for further analysis.

2.10. Flow cytometry

For all these assays, cells were passed through a flow cytometer (BD, FACS Canto II) and analyzed using FlowJo analysis software (Treestar; Ashland, OR). A minimum of 10,000 events were collected for each sample for all flow cytometry experiments.

2.10.1. Cell Cycle

$1x10^5$ cells/ml was incubated in 12 well plates and treated for the time points indicated. After incubation, the cells were harvested and washed twice with PBS. The cells were incubated with 300µl of 0.2% Triton X-l00 and 1µl of 1mg/ml RNAse for 30 mins in the dark at 37^oC to lyse the cells. Finally, the cells were stained with 20µl of 1mg/ml propodium iodide (PI) for 10 mins, according to published methods [268]. After staining period, the cells were place on ice and PI uptake was analyzed by flow cytometry.

2.10.2. Annexin V-PI apoptosis assay

For evaluation of apoptosis, cells were processed using an Annexin V-FITC / PI kit as per manufacturer's instructions (Becton Dickinson Biosciences, San Jose, CA). Briefly, cell suspension of $1x10^5$ cells/ml was treated at doses and time points indicated. After treatment period, cells were washed twice with ice-cold PBS and then resuspended in 100µl 1X binding buffer. 5µl each of Annexin V and PI were added to the binding buffer and the mixture incubated for 15 mins in the dark at room temperature. After incubation, an additional 100µl of binding buffer was added to the mixture and analysed by flow cytometry as soon as possible.

2.10.3. Mitochondrial membrane depolarization as described by [268]

To evaluate the mitochondrial membrane potential ($\Delta\Psi$), JC-1 dye was used to measure red/green fluorescence ratio. Briefly, cell suspension of $1x10^5$ cells/ml was treated at doses and time points indicated. After treatment period, cells were washed twice with PBS and incubated with 400µl of PBS/0.2% BSA containing a final concentration of 2µM JC-1 (Molecular Probes, Eugene, OR, USA) at 37^oC for 30 min. After incubation period, cells were passed through a flow cytometer with 488nm

excitation using emission filters appropriate for Alexa Fluor 488 dye and R-phycoerythrin.

2.10.4. Cell Vue Claret for membrane labelling

MM cell proliferation, both in the presence vs. absence of BMSCs, was evaluated using flow cytometry, by labelling MM cells with the CellVue® cell linker kit (Molecular Targeting Technologies, West Chester, PA, USA) as per manufacturer's instructions.

1. 2 X10^7/ml of cells in Diluent C was stained with 4µl/ml of CellVue® dye in a final staining volume of 2 ml. The cells were incubated for 2 minutes with periodic mixing.

2. After incubation, an equal volume (2 ml) of serum was added to the sample followed by 1 min incubation.

3. Cells were then washed three times in complete medium to ensure removal of unbound dye. MM cells were analysed for viability (>95%) before using in coculture experiment.

4. Stained MM cells were plated on BMSCs (which were plated the day before) and treated at concentrations indicated.

5. After incubation period, cells were analyzed on a flow cytometry at 655nm excitation.

2.10.5. Functional drug accumulation assay

1. The P-glycoprotein activity was determined by means of Rhodamine (Rho) 123 (Sigma) efflux, as this fluorescent dye is a substrate for P-gp. HS-5 cells were seeded in 6-well plates at 1x10^4 cells and allowed to attach overnight. Then, RPMI-Dox40 cells were seeded in the 6-well plates in the presence or absence of HS-5 cells at a density of 1x10^4 cells and treated with various concentrations of bortezomib as described for 72 hours.

2. After the incubation period, the cells were washed and incubated with 200 ng/ml of Rho 123 dye in the presence or absence of the P-gp inhibitor, verapamil (VP) (Sigma) at a concentration of 10 μM for 30 min at 37˚C in 5% CO_2.

3. After washing, cells were incubated at 37˚C in 5% CO_2 in a Rho 123-free medium supplemented with 10% FCS, in the presence or absence of VP. Aliquots were removed for analysis at 30, 60 and 90 min respectively.

4. Prior to analysis, cells were centrifuged and washed twice in PBS before incubation for 20 mins at room temperature with P-gp monoclonal Ab (CD243/PE, Beckman Coulter, Cat# IM2370U) and 7AAD (Becton Dickinson, CA).

5. Cells were used for the analysis of antigen expression and for studies of P-gp activity. Data acquisition and analysis were performed using a FACS Canto equipped with a 488-nm argon laser. To investigate dye efflux in RPMI-Dox40 cells, this cell subset was prelabelled with Cellvue dye (Section 2.10.4) to distinguish from stroma cells. The relative values were identified by dividing the median fluorescence intensity of each measurement by that of control cells. Rho 123 efflux was calculated based on the percentage of dye-effluxing cells in the VP-free experiment, compared with cells treated with VP.

2.11. Relative quantification of selected transcripts in Multiple Myeloma cells

MM1.S-GFP/luc cells were cultured for 24 hrs in the presence or absence of the BMSC line HS-5 and then sorted by FACS cell sorter (BD FACSAria™ cell sorter, Becton Dickinson, San Jose, CA). RNA was extracted with TRIZOL-LS (Invitrogen), further treated with DNase I, and purified with the RNeasy MinElute Cleanup Kit (Qiagen, Valencia, CA). Reverse transcription was accomplished with random hexamers and Superscript II, followed by incubation with RNase H (Invitrogen). Amplification reactions (25 μl, 100 ng cDNA/reaction) with Taqman FAM/MGB probes were performed in a 7500 Real-Time PCR System (Applied Biosystems) for select p53-regulated transcripts. Relative quantification for each target vs a reference gene transcript (glucuronidase beta, GUSB) was assessed with the SDS v1.3 software (Applied Biosystems). For all assessments, the evaluation threshold was set at 0.3. The

treatment and FACS sorting of cells as well as the collection of RNA were done in Dana Farber Cancer Institute but the PCR and relative quantification of transctipts analysis were done in a collabotor laboratory in the Department of Pathology, School of Medicine, Aristotle University of Thessaloniki, Thessaloniki, Greece.

2.12. *In vivo* Study

2.12.1. *In vivo* Study protocol

1. The *in vivo* anti-MM activity of AICAR was evaluated in both subcutaneous xenograft model in which male (7-week old) SCID/CB17 mice (Jackson laboratories, Bar Harbor, ME) were housed and monitored in the Animal Research Facility of the Dana-Farber Cancer Institute.

2. Mice were gamma-irradiated (150 rads) using Cs137 γ-irradiator source and (24 hrs post-irradiation) injected subcutaneously in between the shoulder blades with MM cells ($1x10^6$ / mouse) suspended in PBS.

3. Subcutaneous MM tumours were documented within 7 days of injection by biphotonic imaging (Section 2.12.2). The reason to stratify the mice using biphotonic imaging rather than the traditional calliper measurement was because at this stage, the tumours were barely palpable and thus a more accurate measurement of tumour load could be made by biphotonic imaging rather than calliper measurement.

4. Tumour bearing mice were then randomly assigned to two cohorts: group 1: control (PBS) administered by intraperitoneal (i.p.) injection; and group 2: (treatment) AICAR 600mg/kg i.p. The two groups started out with similar tumour burden (average). Treatment was given every day.

5. Tumour burden was monitored by calliper measurement. Tumour volume was calculated using this formula - $1/2(\text{length} \times \text{width}^2)$.

6. Mice were also followed for changes in body weight, potential toxicity and signs of infection or paralysis. In accordance with institutional guidelines, mice were sacrificed by CO_2 inhalation in the event of tumour size >2cm, paralysis or

major compromise in their quality of life. All experimental procedures and protocols had been approved by the Animal Care and Use Committee of the Dana-Farber Cancer Institute. OS (defined as time between initiation of treatment and sacrifice or death) was compared in control vs. AICAR-treated mice by Kaplan-Meier method.

2.12.2. Biphotonic imaging

Mice were injected with a ketamine (5mg/ml), xylazine (1.5mg/ml) and D-luciferin potassium salt (6mg/ml) mixture. The ketamine and xylazine acted as an anaesthetic for the mice. Mice were imaged using a Xenogen IVIS 100 series system. Briefly, each animal was serially imaged after i.p. injection of luciferin mixture (10 µl per 1g of mice). Photons were quantified using the software Living Image (Xenogen, Alameda, CA).

2.13. Transcriptional signature of stroma-responsive genes and relationship with clinical outcome in bortezomib-treated Multiple Myeloma patients

A transcriptional index of tumour cell response to nutlin-3 was identified, based on previously published studies of transcripts selectively downregulated by nutlin-3 treatment in responsive but not in unresponsive, tumour lines [180]. The probes of that signature for U133plus2.0 oligonucleotide microarray chips were utilized to filter the log2-transformed and median centered gene expression dataset of tumour cells from bortezomib-treated MM patients enrolled in phase II and III clinical trials of this agent [40, 42, 269]. After the filtering, the transcriptional index of nutlin-3-suppressed genes was calculated as the average of the log2-transformed and median centered values for each probe of the signature. Patients were then classified as having low (bottom tertile of expression) vs. high (top 2 tertiles) expression of nutlin-3-suppressed genes and Kaplan-Meier survival analyses for progression-free and OS of bortezomib-treated patients were performed using SPSS 17.0. This analysis was kindly done by Dr Constantine Mitsiades, Dana Farber Cancer Institute.

2.14. Statistical Analysis

In the cell viability assays, each experimental point was set up in triplicate wells and each assay was repeated identically and independently at least once. The final data were expressed as a percentage of the proliferation that took place in control wells where cells were not exposed to any drugs. IC_{50} values were determined for each experiment. To evaluate the differences across various experimental conditions, one-way analysis of variance was performed, and post-hoc tests (Students t-test) served to evaluate differences between individual pairs of experimental conditions.

The additive, synergistic or antagonistic nature of the interaction between two drug combinations was evaluated using the combination index method of Chou and Talalay [270, 271]. Calcusyn software (version 1.1, Biosoft, Cambridge, UK), which is based on this method and takes into account both potency [median dose (Dm) or IC_{50}] and the shape of the dose-effect curve (the *m* value), was used to calculate the combination index (CI). With the use of the combination index, synergism is defined as a more-than-expected additive effect and antagonism is defined as a less-than-expected additive effect. Thus, by this method, a combination index equal to 1 indicates an additive effect, a combination index less than 1 indicates synergy, and a combination index greater than 1 indicates antagonism. It has been proposed by the creators of CalcuSyn software that CIN values be interpreted as follows: antagonistic effect when CIN > 1.1, additive effect when CIN = 0.9–1.1, slight synergism when CIN = 0.7–0.9, synergism when CIN = 0.3–0.7, strong synergism when CIN = 0.1–0.3 and very strong synergism when CIN < 0.1. The combination index value can be calculated at different “effect levels” or “fraction affected” levels (e.g. at LC_{50} or LC_{99} [i.e. concentration lethal to 50% or 99% of the cells]) and may vary depending on the fractional effect level at which it is calculated. The mutually nonexclusive assumption was used in these analyses because agents tested in combinations were assumed to have different mechanisms of action. For combination index plots, the combination index is plotted as the $\log_{10}$ (CIN) versus fraction affected (defined as 1 − survival fraction), and the 95% confidence intervals (CIs) are shown where calculable, with the use of the algebraic approximation method of the CalcuSyn program. On these plots, additivity is defined as $\log_{10}$ (CIN) = 0; very strong synergy is defined as $\log_{10}$ (CIN) = −1; and antagonism is defined as $\log_{10}$ (CIN) > 0. Although synergism and cytotoxicity may be related, a combination

index that indicates strong synergy does not necessarily imply a high degree of absolute cytotoxicity (i.e. a small survival fraction); conversely, a combination index that indicates antagonism need not exclude a high degree of cytotoxicity.

In the *in vivo* models, the OS of mice was evaluated with Kaplan-Meier survival analyses, and differences between the various cohorts of each experiment were assessed by log-rank tests. All values are expressed as mean plus or minus the standard deviation (SD) or standard error (SE) (where indicated). The statistical significance of differences between treatments was analyzed using the Student *t* test; differences were considered significant when *P* was less than or equal to .05.

Chapter 3
Results

3.1. MDR associated protein expression as a mechanism of resistance

3.1.1. Introduction

MDR proteins, P-gp, BCRP and MRP-1 have been linked to resistance mechanism in MM and other cancers. Bortezomib is a novel agent in the arsenal of chemotherapeutics in MM and its interaction with the MDR proteins has not been well characterised. To study the effects of bortezomib on MDR transport effectively, we used several lung cancer cell lines that had been developed by our institute. These cell lines overexpress P-gp, MRP-1 and BCRP. The cell lines and the MDR proteins they express are outlined in Table 3.1.1.

Cell Line		MDR proteins overexpressed	References
DLKP	parental	MRP-1	[272]
DLKP-A	subline	P-gp	[273]
DLKP-SQ/Mitox	subline	BCRP	Created by Helena Joyce, NICB [unpublished]
A549	parental	MRP-1, BCRP	[272], [274]
A549-taxol	subline	P-gp	[275]
RPMI-8226	parental	BCRP	[274]
RPMI-Dox40	subline	P-gp	[276]
NCI-Adr/res	parental	P-gp	[277]

Table 3.1.1 The MDR protein expression in cell lines used.

3.1.2. P-glycoprotein expression in various cell lines

P-gp expression was analysed in the panel of cell lines by Western blot (Figure 3.1.2). P-gp was detected in the doxorubicin-selected cell lines, DLKP-A and RPMI-Dox40. P-gp was also expressed in A549-Taxol [275] and in NCI-Adr/res cell line (consistent with previously published information, [277]). A549 and RPMI-8226 parent cell lines did not express measurable levels of P-gp by Western blot. The parental cell line DLKP had low levels of P-gp expression. The highest levels of P-gp protein in the drug-resistant variants were seen in DLKP-A and NCI-Adr/res followed by RPMI-Dox40 and the least amount of P-gp expressed by A549-taxol.

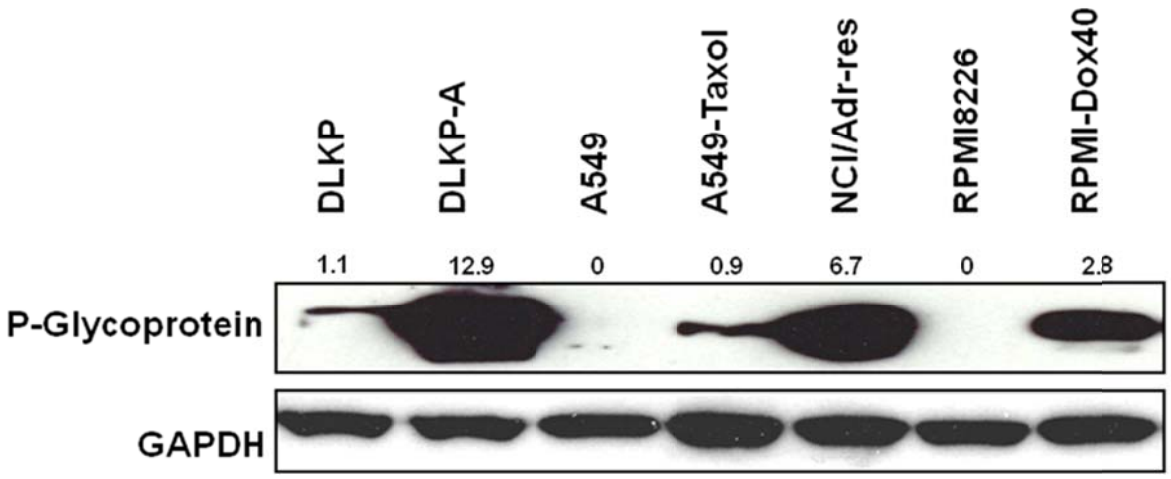

Figure 3.1.2 P-gp expression in various cell lines.

The western blot demonstrated the baseline P-gp expression level of different cell lines with their parental cell lines as comparator. Densitometry readings of each band were obtained by normalising the P-gp band to GAPDH band. The values obtained are indicated above the respective bands, with A549-taxol, RPMI-Dox40, NCI/Adr-res and DLKP-A having least P-gp to most P-gp expression. GAPDH levels were used as a loading control.

3.1.3. The effect of Bortezomib on p-glycoprotein-associated resistance

We investigated the effect of bortezomib on P-gp-associated resistance. Using the lung cancer cell line, DLKP-A which overexpresses P-gp [273], we were able to demonstrate that bortezomib was a substrate of P-gp by showing synergistic cytotoxicity in the presence of a P-gp inhibitor; elacridar (Fig. 3.1.3.1). DLKP-A cells were incubated with 60nM of bortezomib alone or with elacridar, 0.25μM, for 24hours. This data suggests that bortezomib is a P-gp substrate.

We wanted to demonstrate if this effect was sustained with a longer incubation period and if we were able to use lower drug doses. DLKP-A cells were incubated with 6nM and 12nM of bortezomib alone or with elacridar, 0.125μM, for 5 days. The single agent activity of bortezomib or elacridar alone was minimal and there was marked synergistic cytotoxicity seen (Fig. 3.1.3.2), indicating that bortezomib is likely a P-gp substrate.

The dose of bortezomib used was 10 times lower in the longer incubation period and the synergistic cytotoxicity was just as marked, therefore, the decision was made to carry out further experiments using the longer incubation period.

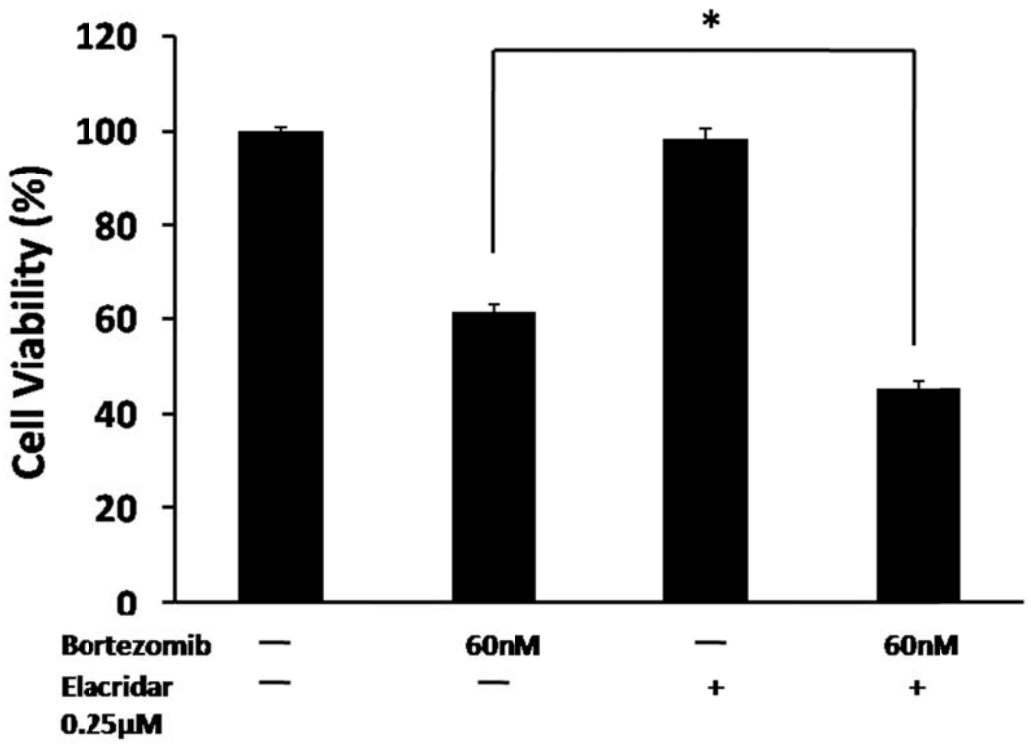

Figure 3.1.3.1 Bortezomib acts as a P-gp substrate.

The lung cancer cell line DLKP-A, which overexpresses P-gp, demonstrated that bortezomib was likely a substrate of P-gp by showing synergistic cytotoxicity in the presence of a P-gp inhibitor; elacridar. DLKP-A cells were incubated with 60nM of bortezomib alone or with elacridar, 0.25µM, for 24hours. Cell survival by alkaline phosphatase assay was expressed as percentage (mean ± SD) compared to vehicle treated control (60nM bortezomib). Experiment was repeated in triplicate. * is statistically significantly compared to control (P = 0.0012)

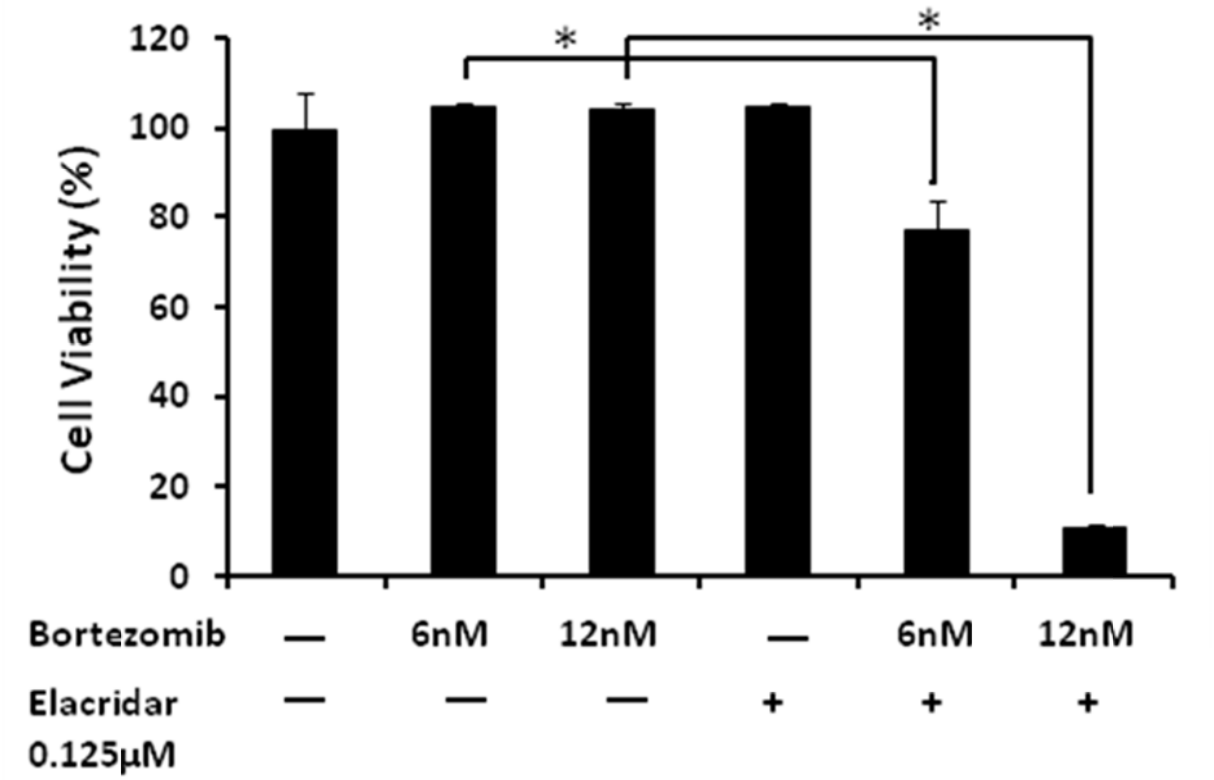

Figure 3.1.3.2 Bortezomib acts as a P-gp substrate.

The lung cancer cell line, DLKP-A which overexpresses P-gp, demonstrated that bortezomib was likely a substrate of P-gp by showing synergistic cytotoxicity in the presence of a p-gp inhibitor; elacridar. DLKP-A cells were incubated with 6nM and 12nM of bortezomib alone or with elacridar, 0.125μM, for 5 days. Cell survival by alkaline phosphatase assay was expressed as percentage (mean ± SD) compared to vehicle treated control (6nM, 12nM bortezomib). Experiment was repeated in triplicate. * is statistically significantly compared to control ($P < 0.05$)

As bortezomib is a P-gp substrate, we wanted to demonstrate if it has any inhibitory actions on P-gp activity. Using the same cell line that overexpresses P-gp, DLKP-A, we were able to demonstrate that bortezomib is not an effective P-gp inhibitor as synergistic cytotoxicity in the presence of a known P-gp substrate, doxorubicin, was only demonstrated at the highest dose of bortezomib, 12nM (Fig. 3.1.3.3). DLKP-A cells were incubated with 6nM and 12nM of bortezomib alone or with doxorubicin 1μg/ml for 5 days.

There have been reports that bortezomib and doxorubicin demonstrate synergistic cytotoxicity even in cell lines that are not known to express P-gp [44, 278]. Fig. 3.1.3.4 showed that in MM1.S cell line which does not express P-gp, bortezomib and doxorubicin were mildly synergistic. This suggests that bortezomib and doxorubicin synergy may be due to other factors rather than through P-gp inhibition.

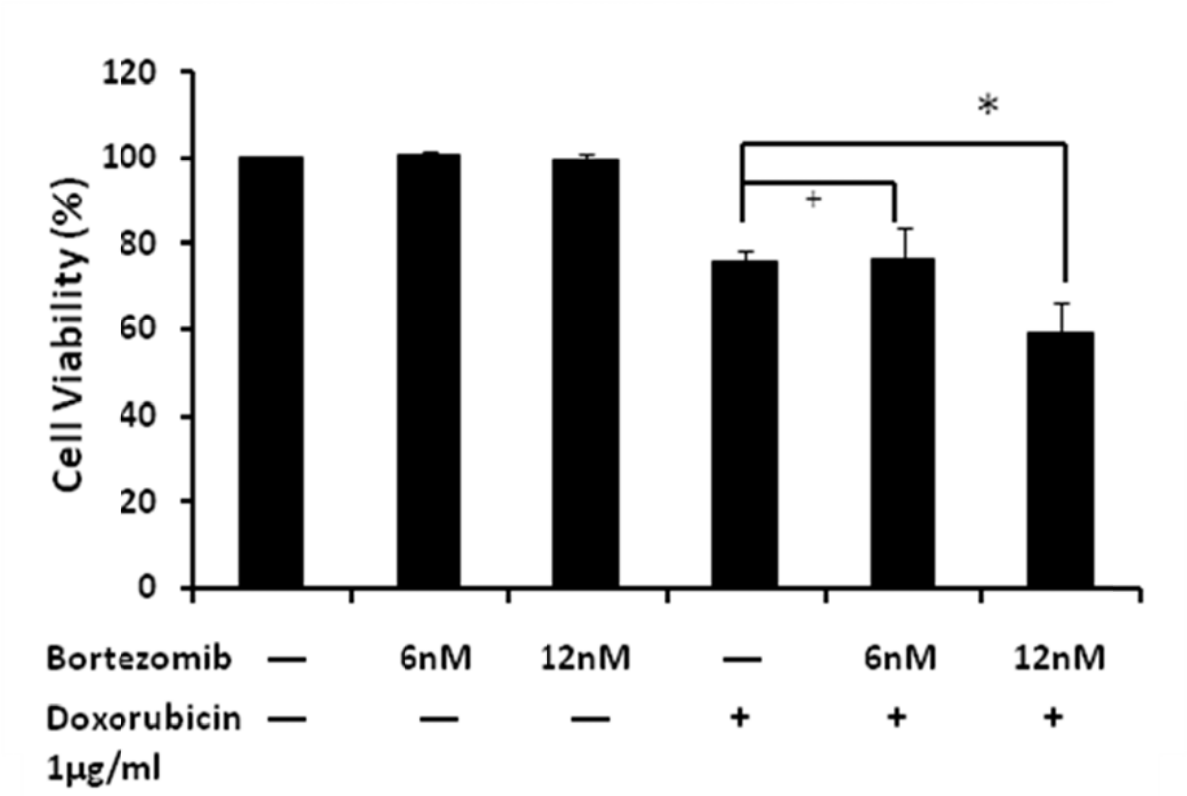

Figure 3.1.3.3 Bortezomib is a weak P-gp inhibitor.

The lung cancer cell line DLKP-A, which overexpresses P-gp, demonstrated that bortezomib is not an effective P-gp inhibitor as enhanced cytotoxicity in the presence of a known P-gp substrate, doxorubicin was only demonstrated at the highest dose of bortezomib, 12nM. DLKP-A cells were incubated with 6nM and 12nM of bortezomib alone or with doxorubicin 1µg/ml for 5 days. Cell survival assessed by alkaline phosphatase assay was expressed as percentage (mean ± SD) compared to vehicle treated control (6nM, 12nM bortezomib). Experiment was repeated in triplicate. + is not statistically significant, whereas * is statistically significantly compared to control ($P < 0.05$).

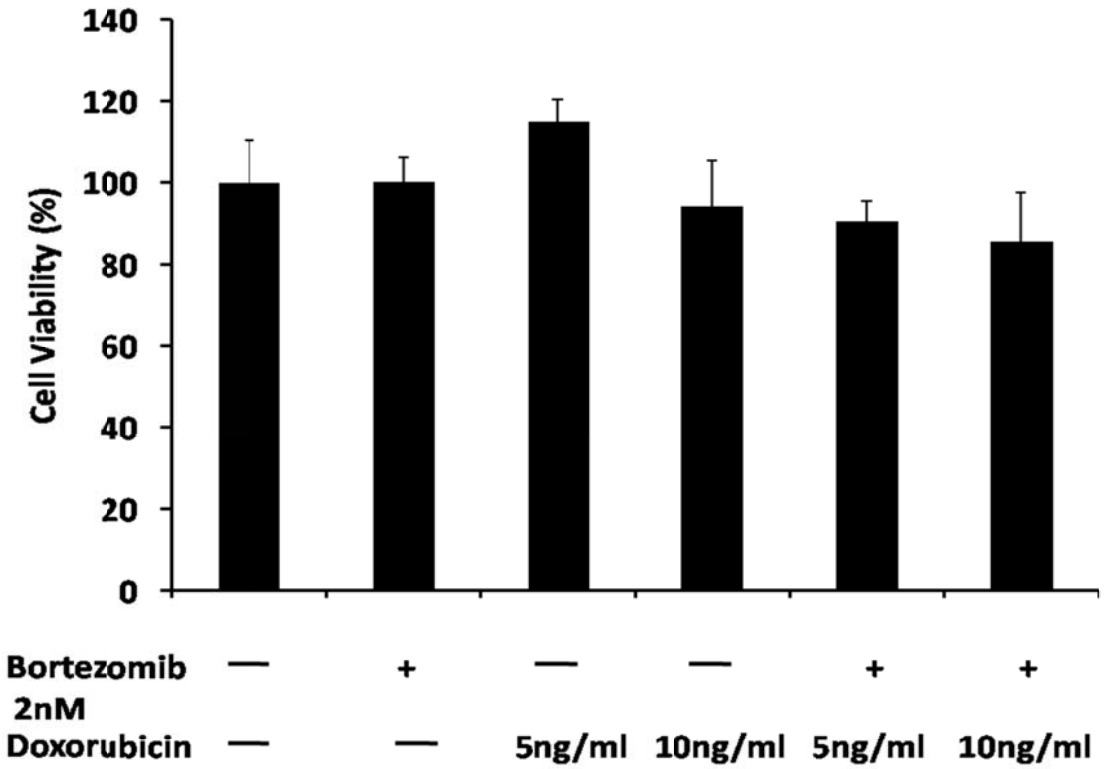

Figure 3.1.3.4 Bortezomib and doxorubicin is mildly synergistic even in a P-gp negative cell line.

MM1.S, a P-gp negative cell line, demonstrated that bortezomib and doxorubicin had mild synergistic cytotoxicity. MM1.S cells were incubated with 5ng/ml and 10ng/ml of doxorubicin in the presence and absence of bortezomib 2nM for 3 days. Cell survival assessed by MTT assay was expressed as percentage (mean ± SD) compared to vehicle treated control. Experiment was repeated in triplicate.

To investigate if the activity of bortezomib was affected by P-gp expression, we tested its single agent cytotoxicity in two cell lines that overexpress P-gp. DLKP-A, which expresses a high level of P-gp, and A549-taxol, which expresses a low level of P-gp. The activity of bortezomib was reduced in DLKP-A cell line compared to DLKP (Fig. 3.1.3.5A) whereas there was no reduction in activity in A549-taxol cell line compared to its parental cell line (Fig 3.1.3.5B). The cells were incubated with a range of bortezomib concentration for 5 days. This data suggest that P-gp expression causes resistance to bortezomib treatment but a minimal level of overexpression may be necessary to see a bortezomib resistance effect.

To determine that elacridar, as a single agent, had minimal single agent activity, we incubated DLKP-A cells with elacridar 0.25μM and 0.4μM for 5 days (Fig.3.1.3.6). After 5 days incubation, the cell viability, as measured by alkaline phosphatase assay, revealed minimal single agent activity of elacridar.

To ensure that the dose of elacridar used in this and subsequent experiments was adequate to inhibit the P-gp function. Fig. 3.1.3.7 demonstrates that 0.125μM of elacridar was adequate to inhibit P-gp activity as all doxorubicin doses showed synergistic activity with elacridar. The DLKP-A cell line was incubated with a range of doxorubicin doses alone or with elacridar 0.125μM for 5 days.

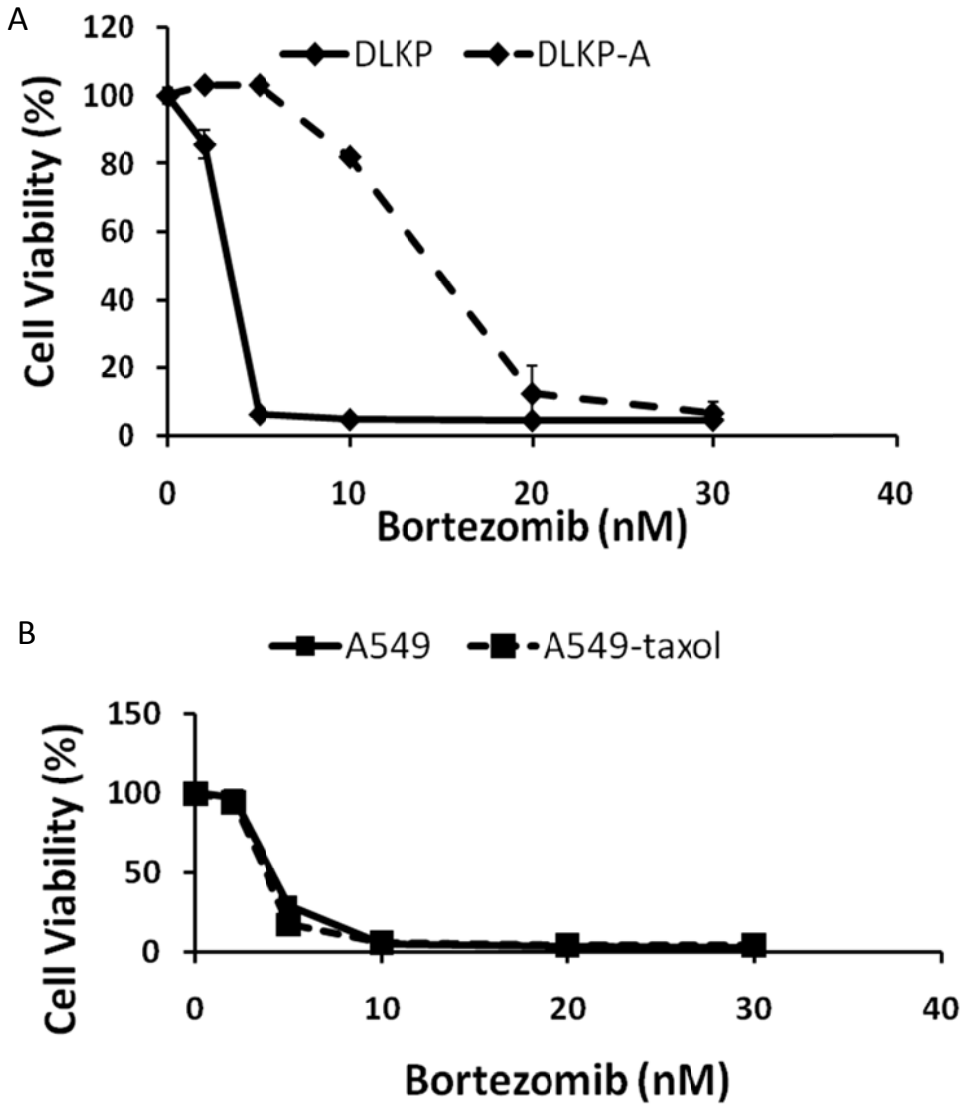

Figure 3.1.3.5 Bortezomib activity is reduced in the presence of high expression of P-gp.

Bortezomib activity was reduced in the DLKP-A cell line compared to DLKP (A) whereas there was no reduction in activity in A549-taxol cell line compared to its parental cell line (B). DLKP-A and A549-taxol are cell lines that overexpress P-gp compared to their parental counterpart. The cells were incubated with a range of bortezomib concentration for 5 days. Cell survival assessed by alkaline phosphatase assay was expressed as percentage (mean ± SD) compared to vehicle treated control. Experiment was repeated in triplicate.

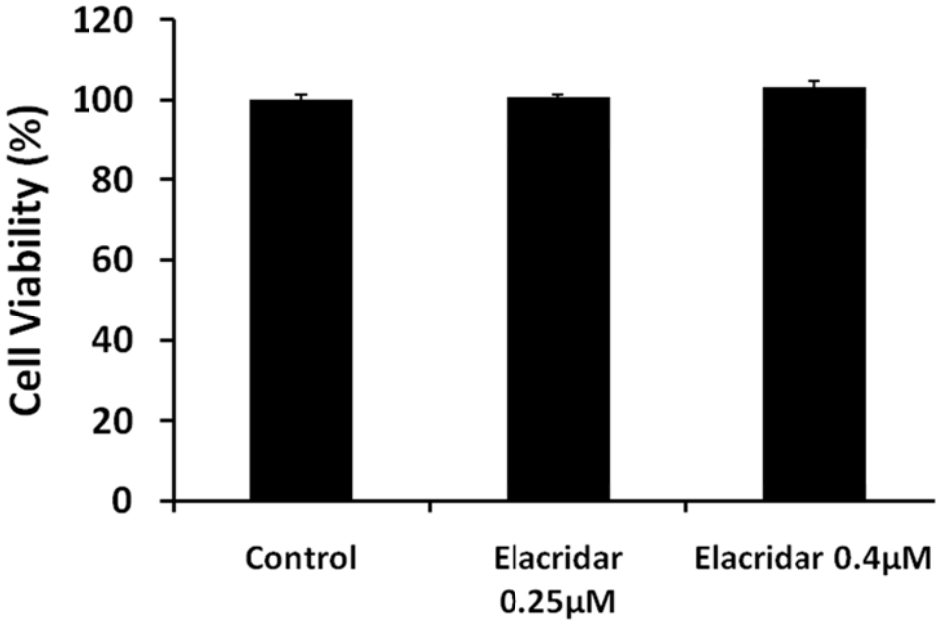

Figure 3.1.3.6 Elacridar as a single agent has minimal activity in DLKP-A.

This is to ensure that the doses of elacridar used were not going to have significant cytotoxicity on DLKP-A. The DLKP-A cell line was incubated with 0.25µM and 0.4µM of elacridar for 5 days Cell survival was expressed as percentage (mean ± SD) compared to vehicle treated control.

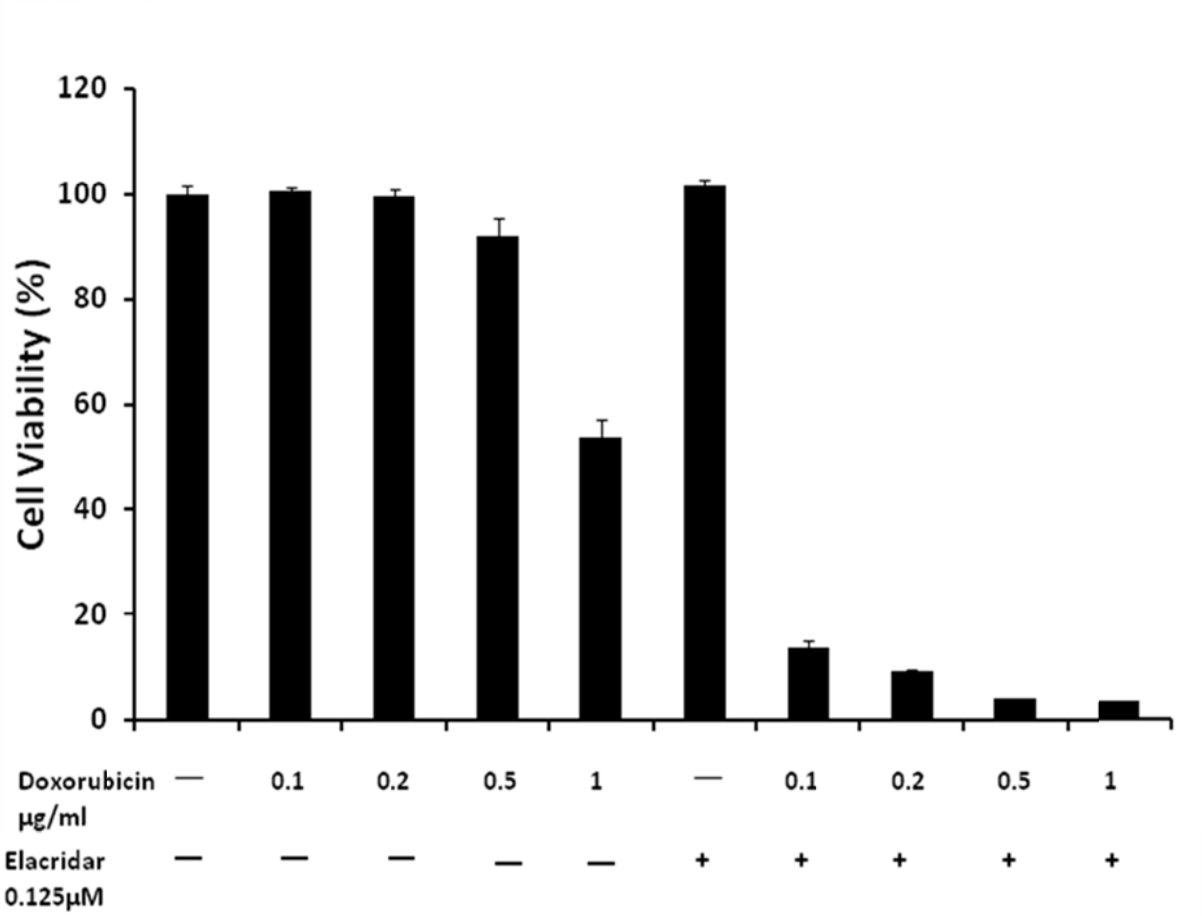

Figure 3.1.3.7 Elacridar 0.125µM is adequate to inhibit P-gp activity.

This demonstrates that the dose of elacridar used is adequate to inhibit P-gp activity as all doxorubicin doses show synergistic activity with elacridar. The DLKP-A cell line was incubated with a range of doxorubicin doses alone or with elacridar, 0.125µM, for 5 days Cell survival was expressed as percentage (mean ± SD) compared to vehicle treated control.

3.1.4. The effect of Bortezomib on MRP-1 associated resistance

Sulindac was previously found to be an MRP-1 inhibitor by our group [272]. Sulindac sulphide is a more potent MRP-1 metabolite of sulindac. To explore any possible interactions between bortezomib and the other MDR proteins, we first investigated if bortezomib combined with sulindac had any synergistic cytotoxicity. We used the lung cancer cell line, DLKP which overexpresses MRP-1, and were able to demonstrate that bortezomib is not a MRP-1 substrate as synergistic cytotoxicity in the presence of sulindac sulphide was not demonstrated (Fig. 3.1.4). DLKP cells were incubated with 2nM of bortezomib alone or with sulindac 1μM or 8 μM for 5 days.

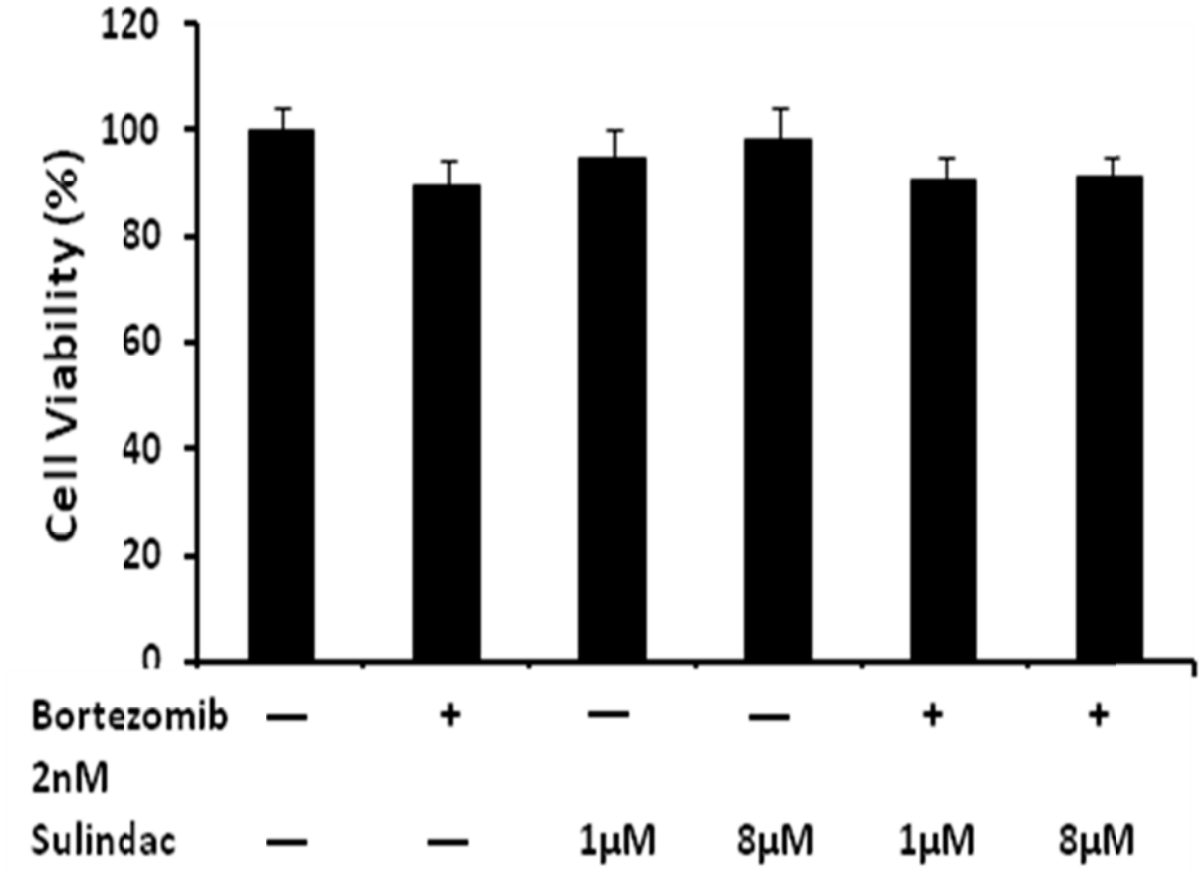

Figure 3.1.4 Bortezomib is not a MRP-1 substrate.

The lung cancer cell line, DLKP which overexpresses MRP-1, demonstrated that bortezomib is not a MRP-1 substrate as synergistic cytotoxicity in the presence of a known MRP-1 inhibitor; sulindac sulphide, was not demonstrated. DLKP cells were incubated with 2nM of bortezomib alone or with sulindac 1μM or 8 μM for 5 days. Cell survival was expressed as percentage (mean ± SD) compared to vehicle treated control (2nM bortezomib). Experiment was repeated in triplicate.

3.1.5. The effect of Bortezomib on BCRP-associated resistance

We next investigated the MDR protein, BCRP. Figure 3.1.5.1 demonstrates that bortezomib is not a BCRP substrate. DLKP-SQ/Mitox cells, which overexpresses BCRP [279], were incubated with 2nM and 4nM of bortezomib alone or in combination with elacridar, a known BCRP inhibitor, for 5 days. There was no demonstrable synergy seen.

This conclusion is further supported by the lack of resistance seen in DLKP-SQ/Mitox cells compared to DLKP with treated with single agent bortezomib for 5 days (Fig. 3.1.5.2).

We also showed that bortezomib is not a BCRP inhibitor by using the same cell line DLKP-SQ/Mitox. Bortezomib 2nM and 4nM was combined with 10nM SN38 for 5 days. SN38 is a known BCRP substrate. Fig. 3.1.5.3 demonstrates that this combination yielded no synergistic cytotoxicity.

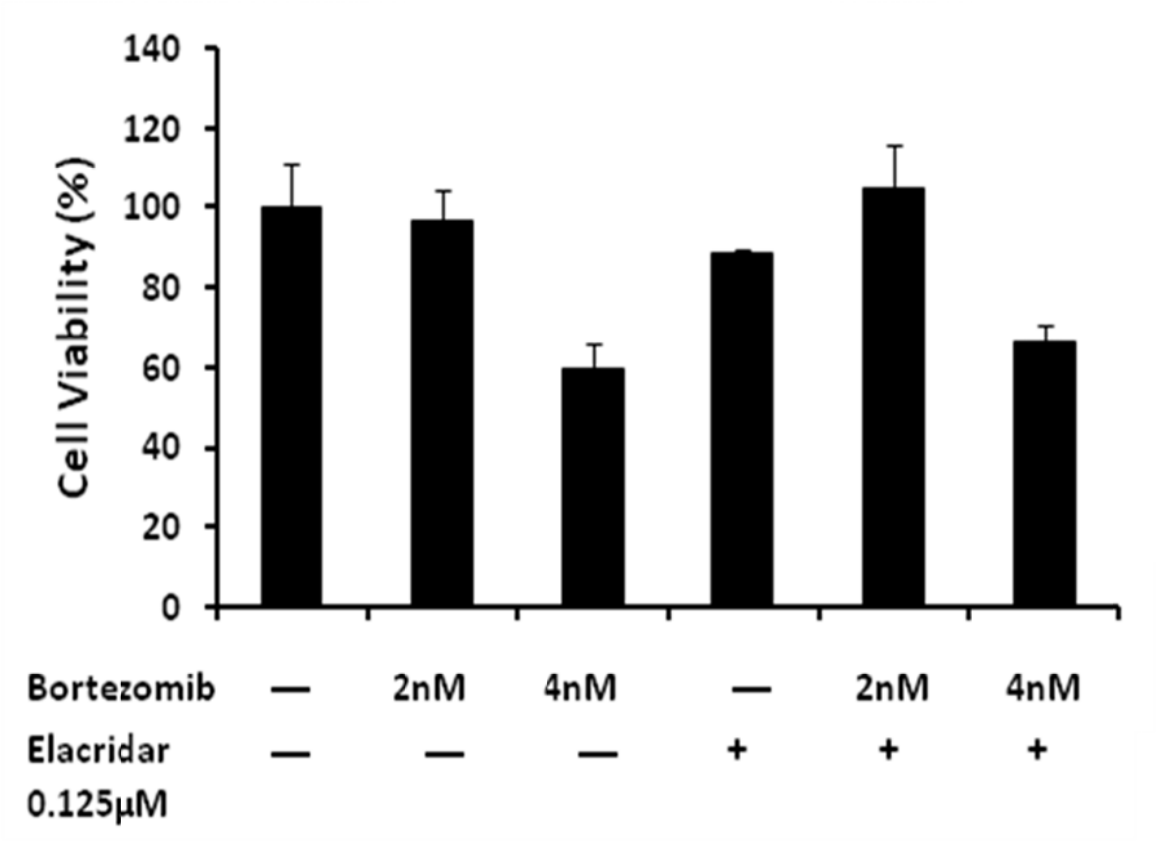

Figure 3.1.5.1 Bortezomib is not a BCRP substrate.

The lung cancer cell line, DLKP-SQ/Mitox which overexpresses BCRP, demonstrated that bortezomib is not a BCRP substrate as synergistic cytotoxicity in the presence of a known BCRP inhibitor; elacridar was not demonstrated. DLKPSQ/Mitox cells were incubated with 2nM and 4nM of bortezomib alone or with elacridar 0.125μM for 5 days. Experiment was performed in triplicate wells. Cell survival was expressed as percentage (mean ± SD) compared to vehicle treated control (2nM, 4nM bortezomib). Experiment was repeated in triplicate.

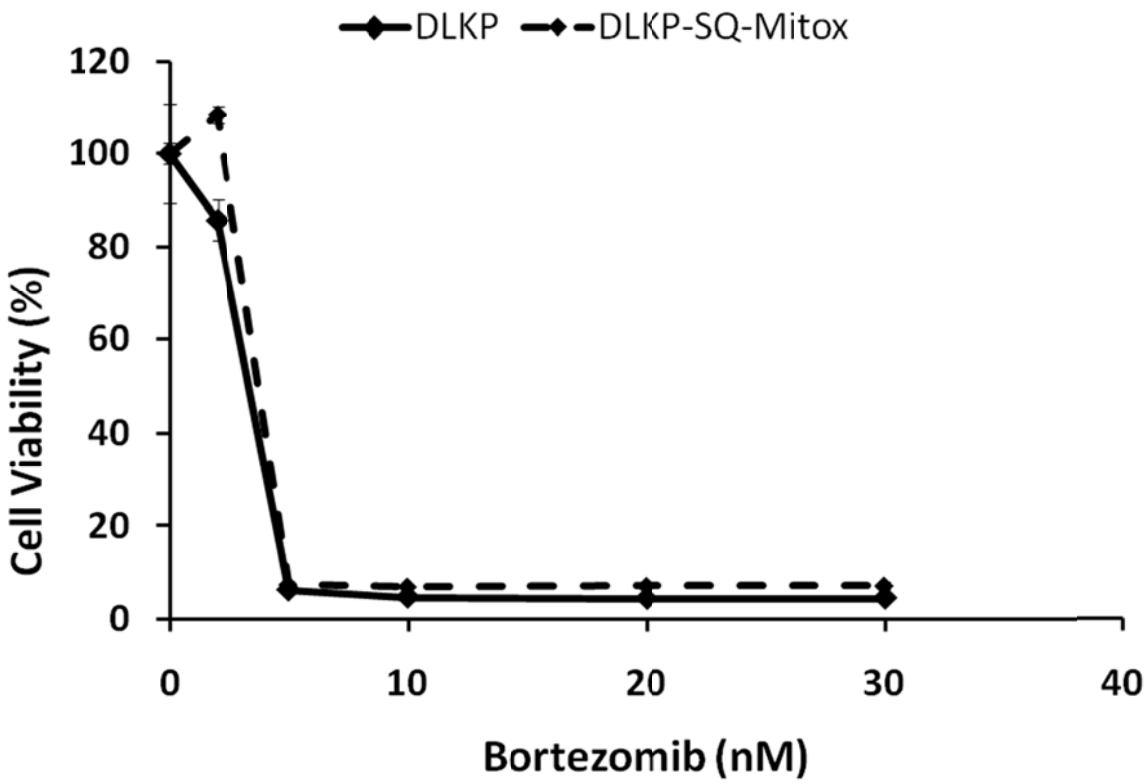

Figure 3.1.5.2 DLKP-SQ/Mitox cells do not demonstrate increased resistance with bortezomib treatment compared to DLKP.

BCRP overexpressing cell line DLKP-SQ/Mitox is not more resistant to single agent bortezomib compared to non-BCRP expressing DLKP. This demonstrates that BCRP does not confer resistance to bortezomib. The cell lines were incubated in the presence of bortezomib for 5 days. Cell survival was expressed as percentage (mean ± SD) compared to vehicle treated control. Experiment was repeated in triplicate.

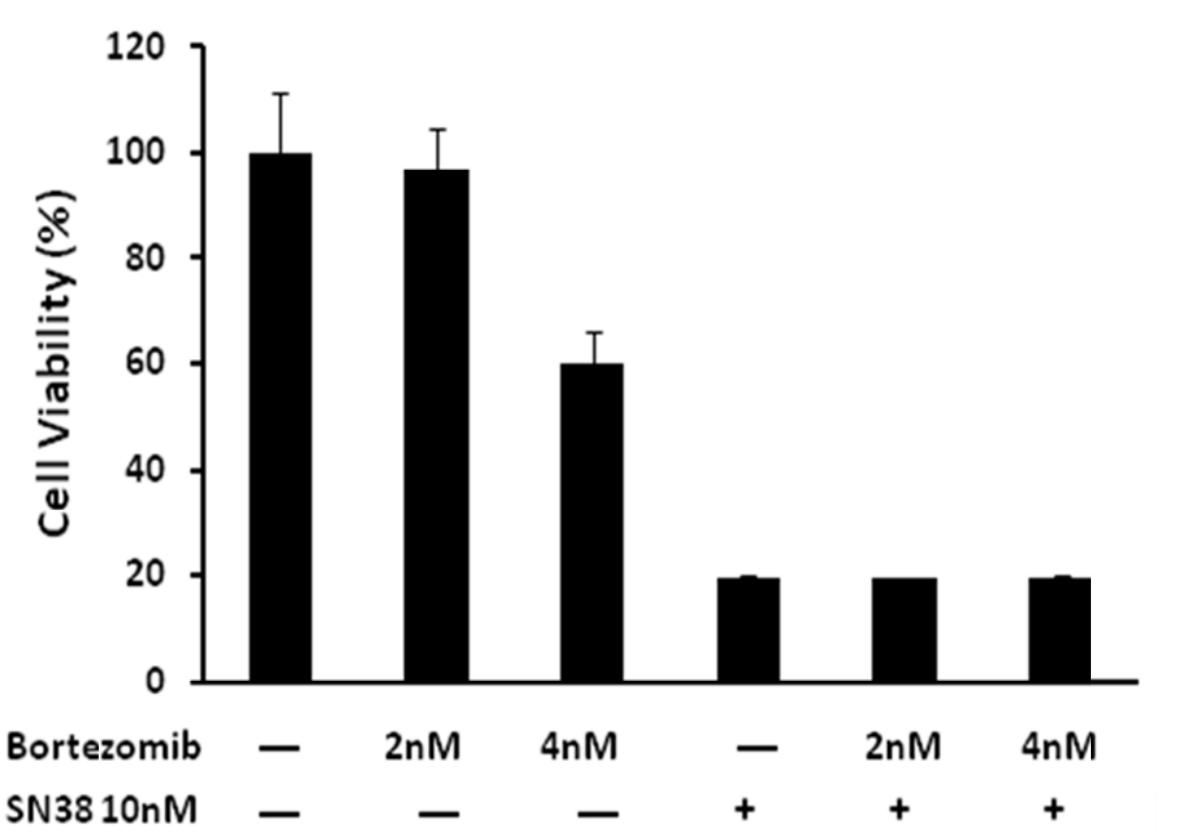

Figure 3.1.5.3 Bortezomib is not a BCRP inhibitor.

The lung cancer cell line, DLKP-SQ/Mitox which overexpresses BCRP, demonstrated that bortezomib is not a BCRP inhibitor as synergistic cytotoxicity in the presence of a known BCRP substrate; SN38 was not demonstrated. DLKPSQ/Mitox cells were incubated with 2nM and 4nM of bortezomib alone or with SN38 10nM for 5 days. Cell survival was expressed as percentage (mean ± SD) compared to vehicle treated control (2nM, 4nM bortezomib). Experiment was repeated in triplicate.

3.1.6. P-glycoprotein expression is associated with bortezomib's efficacy as a P-glycoprotein substrate

As seen in the Western blot analysis (Fig. 3.1.2), P-gp expression varies between the different cell lines. We have shown that the expression level of P-gp in each cell line corresponded to the degree of synergy seen when bortezomib was combined with elacridar, with cell lines that exhibited the highest levels of P-gp showing the most synergy when bortezomib was combined with elacridar (Fig. 3.1.6.1). Thus, DLKP-A and NCI-Adr/res had the most synergy when bortezomib was combined with elacridar, followed by RPMI-Dox40 and the least amount of synergy was seen with A549-taxol cells (Fig. 3.1.6.1). This synergy was confirmed by the calculated combination index (CIN) using Calcusyn software in Table 3.1.6.1. Synergy was indicated by a CIN value that <1. The lower the CIN value below 1, the higher the degree of synergism. The cell lines expression level of P-gp corresponds to the degree of synergy seen when bortezomib was combined with elacridar.

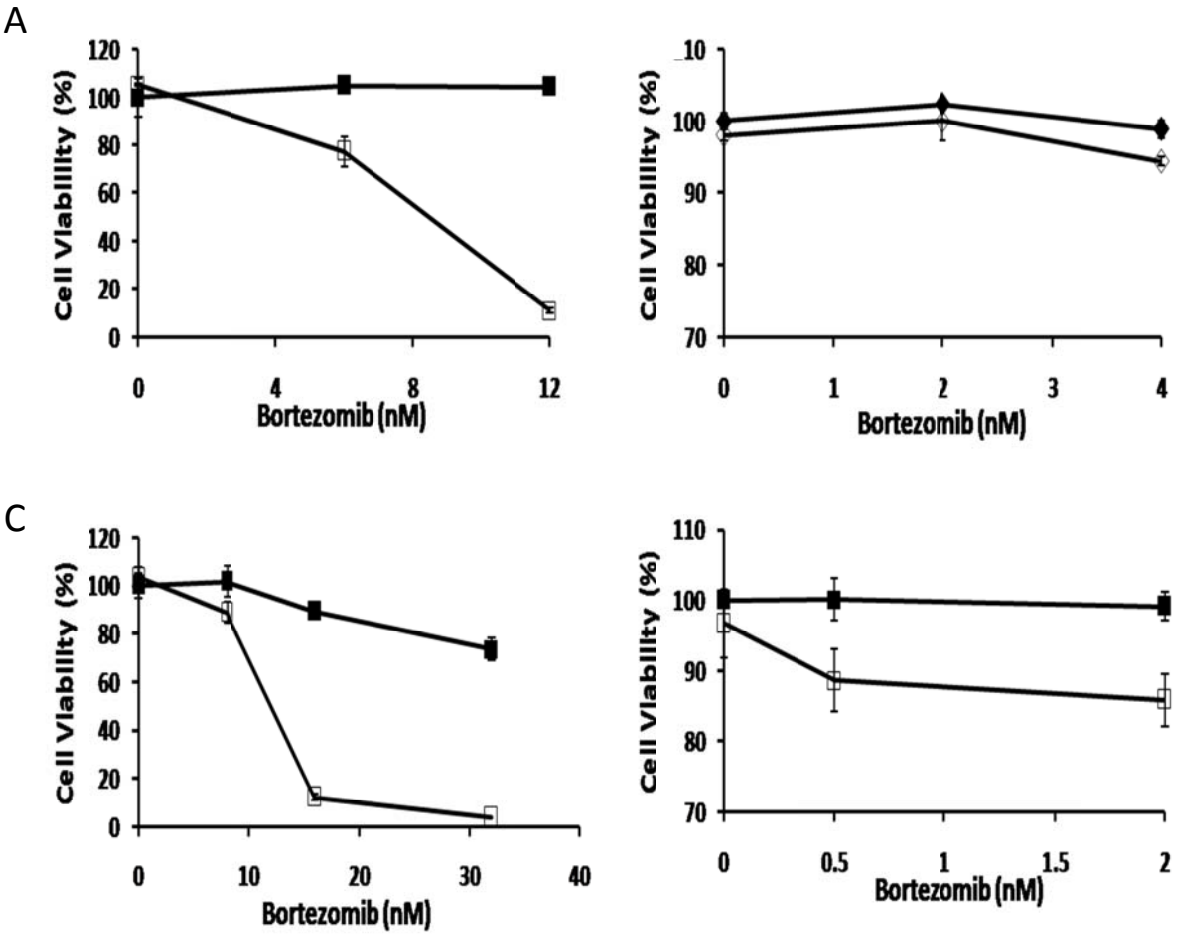

Figure 3.1.6.1 P-gp expression is associated with bortezomib's efficacy as a P-gp substrate

The cell lines expression level of P-gp corresponded to the degree of synergy seen when bortezomib was combined with elacridar. The cell lines that exhibit the highest levels of P-gp showed the most synergy when bortezomib is combined with elacridar for 5 days. DLKP-A (A) treated with Bortezomib (■ without elacridar, □ with elacridar 0.125μM). A549-taxol (B) treated with bortezomib (◆ without elacridar, ◇ with elacridar 0.4μM).NCI/Adr-res (C) and RPMI-Dox40 (D) treated with bortezomib (■ without elacridar, □ with elacridar 0.125μM). Cell survival was expressed as percentage (mean ± SD) compared to vehicle treated control. Experiment was repeated in triplicate.

Cell Lines	Bortezomib (nM)	Elacridar (ìM)	Fraction affected	CIN	P-gp expression
DLKP-A	12	0.125	0.888415	0.016	++++
A549-Taxol	4	0.4	0.0562078	1.369	+
NCI-Adr/res	16	0.125	0.878684	0.356	+++
RPMI-Dox40	2	0.125	0.140981	0.398	++

Table 3.1.6.1 Combination index for the various cell lines when bortezomib is combined with elacridar demonstrating that the degree of synergy correspond to the P-gp expression levels.

A representative combination dose for each cell line outlined in Figure 3.1.6.1 was calculated using Calcusyn software. CIN values were interpreted as follows: antagonistic effect when CIN > 1.1, additive effect when CIN = 0.9–1.1, slight synergism when CIN = 0.7–0.9, synergism when CIN = 0.3–0.7, strong synergism when CIN = 0.1–0.3, and very strong synergism when CIN < 0.1. The cell lines expression level of P-gp corresponds to the degree of synergy seen when bortezomib was combined with elacridar.

In the literature, P-gp mediated resistance can be induced after exposure to anthracyclines. We wanted to examine if this synergy between bortezomib and elacridar was preserved in the same cell line that had different P-gp levels. RPMI-Dox40 was selected to be P-gp positive by exposure to doxorubicin. To ensure continued P-gp positivity, this cell line had to be cultured in the presence of low dose doxorubicin (400nM). In our cell line bank, we had a version of RPMI-Dox40 that was not cultured in doxorubicin and thus, the P-gp levels were lower. Using these two RPMI-Dox40s; RPMI-Dox40 with low P-gp (RPMI-Dox40 LP) and RPMI-Dox40 with high P-gp (RPMI-Dox40 HP), we wanted to address the question whether the level of P-gp affects synergy in the same cell line. As shown in Fig. 3.1.6.2., the RPMI-Dox40 (HP) had an increase in resistance to both bortezomib and doxorubicin compared to the RPMI-Dox40 (LP). By using a phycoerythrin (PE) conjugated P-gp antibody, we demonstrated that RPMI-Dox40 (HP) has a higher expression of PE compared to RPMI-Dox40 (LP) as seen in Fig. 3.1.6.3 (A). This decrease in sensitivity to both drugs was associated with a higher P-gp expression in the RPMI-Dox40 (HP). The combination of elacridar and bortezomib demonstrated a stronger synergy in the RPMI-Dox40 (HP) compared to RPMI-Dox40 (LP) (Fig. 3.1.6.3. B and C). The calculated CIN values were shown in Table 3.1.6.3. and showed similar results. Experiment was repeated in triplicate.

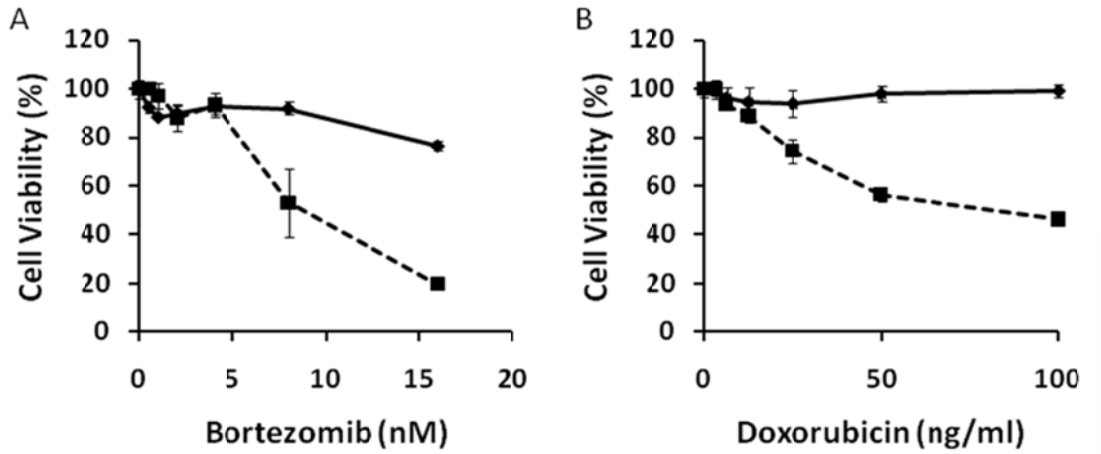

Figure 3.1.6.2 RPMI-Dox40 (HP) demonstrating an increase in resistance to both bortezomib and doxorubicin

Bortezomib (A) and doxorubicin (B) activity was reduced in RPMI-Dox40 (HP) (solid line) compared to RPMI-Dox40 (LP) (dotted line). The cells were incubated with a range of drug concentrations for 5 days. Cell survival was expressed as percentage (mean ± SD) compared to vehicle treated control. Experiment was repeated in triplicate.

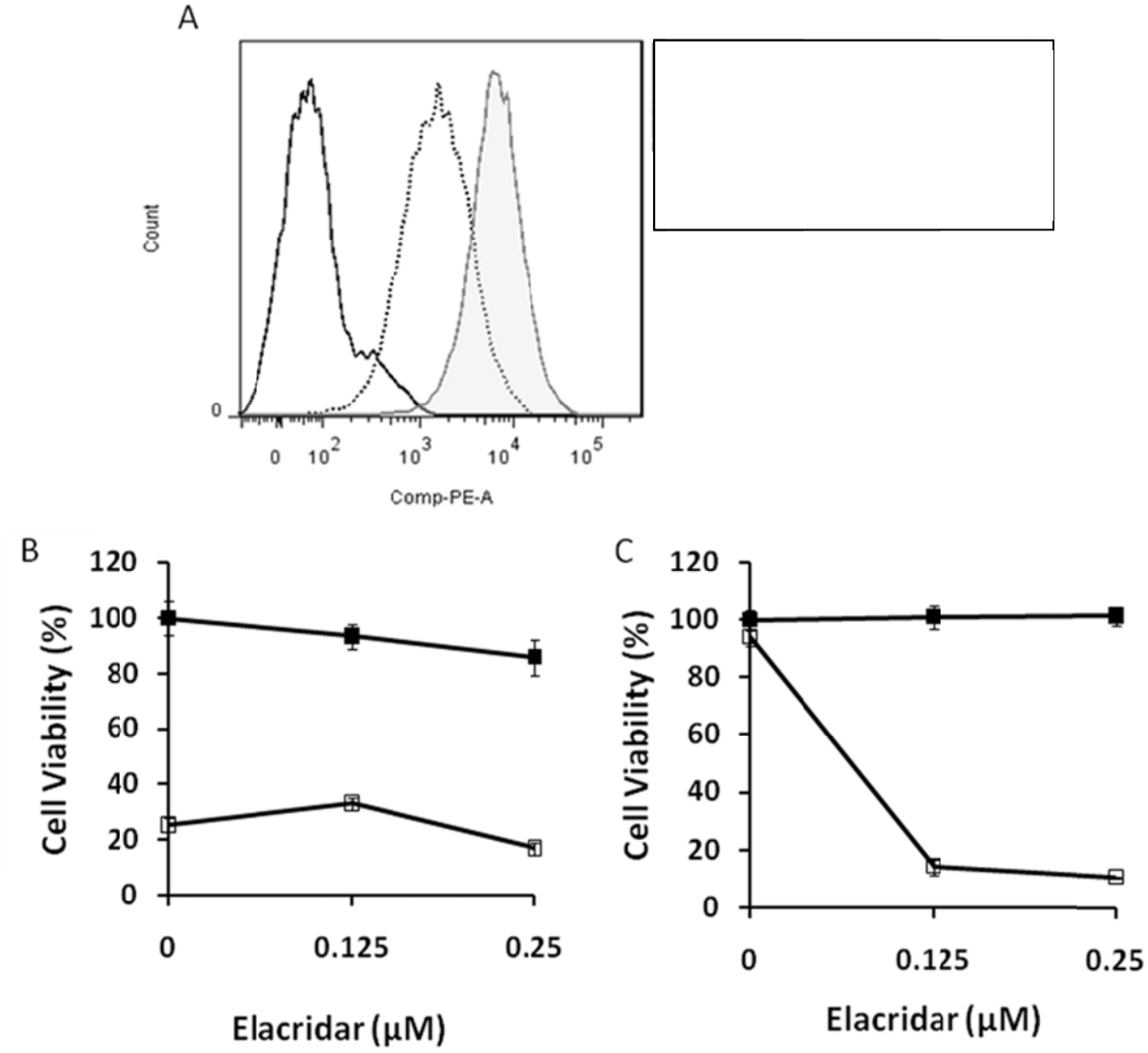

Figure 3.1.6.3 RPMI-Dox40 cell line with a higher expression of P-gp demonstrates a higher degree of synergy.

(A) As demonstrated via flow cytometry analysis, RPMI-Dox40 (HP) had a higher expression of P-gp compared to RPMI-Dox40 (LP). The combination of elacridar and bortezomib demonstrated a lower degree of synergy in RPMI-Dox40 (LP) (B) compared to RPMI-Dox40 (HP) (C). RPMI-Dox40 (LP and HP) treated with elacridar (■ without bortezomib, □ with bortezomib 8nM). Cell survival was expressed as percentage (mean ± SD) compared to vehicle treated control. Experiment was repeated in triplicate.

	Bortezomib (nM)	Elacridar (ìM)	Fraction affected	CIN
RPMI-Dox40 LP	8	0.125	0.67002	1.139
	8	0.25	0.83151	0.965
RPMI-Dox40 HP	8	0.125	0.85873	0.097
	8	0.25	0.89529	0.082

Table 3.1.6.3 Combination index for both RPMI-Dox40 versions when bortezomib is combined with elacridar demonstrating that the degree of synergy correspond to the P-gp expression levels.

The combination dose for each cell line outlined in Figure 3.1.6.3 was calculated using Calcusyn software. CIN values were interpreted as follows: antagonistic effect when CIN > 1.1, additive effect when CIN = 0.9–1.1, slight synergism when CIN = 0.7–0.9, synergism when CIN = 0.3–0.7, strong synergism when CIN = 0.1–0.3, and very strong synergism when CIN < 0.1. RPMI-Dox40 HP which has a higher level of P-gp showed a greater degree of synergism when bortezomib was combined with elacridar.

3.1.7. Bortezomib and elacridar combination overcomes the stromal-derived protection of Multiple Myeloma cells

The role of the local microenvironment in MM growth, proliferation and survival is well established [60, 61]). For instance, it has been demonstrated that the response of MM to doxorubicin is attenuated by the presence of bone marrow stromal cells (BMSCs) [27, 62-64]. This is of clinical importance as P-gp expression also contributes to resistance to doxorubicin. On the other hand, bortezomib is known to be able to overcome the protective effects of the BMSCs. To ensure that the combination of bortezomib and elacridar might be useful clinically, we need to establish if the combination is able to have the same activity in the presence of BMSCs.

Using the compartment-specific bioluminescence imaging (CS-BLI) approach, we were able to evaluate the MM cells when cocultured with another accessory cell. The MM cell line RPMI-Dox40-MCherry/luc was cultured in the presence of HS-5 stromal cells for 5 days, which triggered cell proliferation (Fig 3.1.7.1). Using the same technique, MM cells were treated with bortezomib and elacridar combination and cell viability measured at 5 days. Cell viability was normalized to each respective drug-free control and synergistic cytotoxicity was evident at all combination doses indicated (Fig. 3.1.7.2). The presence of the stroma cells mildly attenuated the activity of the combination of bortezomib and elacridar but the synergistic cytotoxicity was still statistically significant.

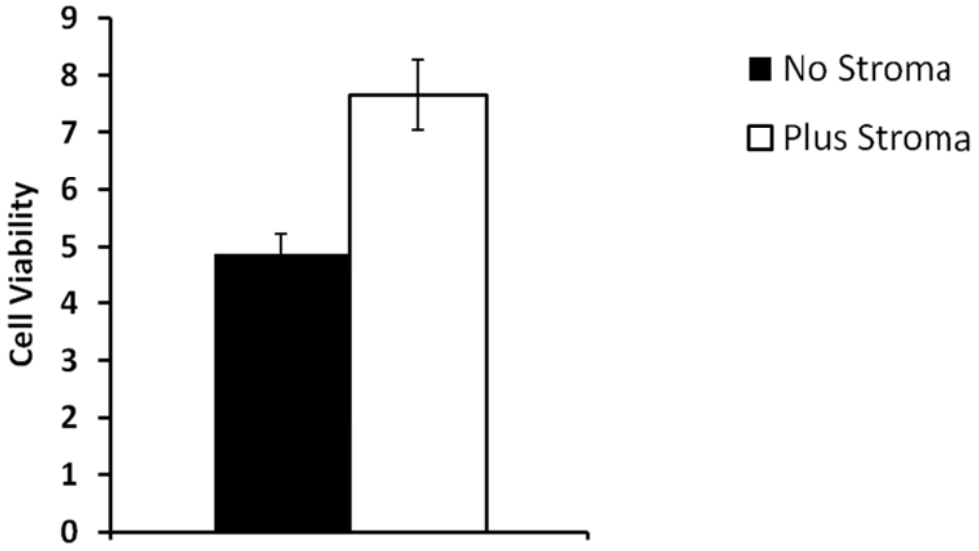

Figure 3.1.7.1. Cell proliferation in RPMI-Dox40 when co-cultured with BMSCs

Using the compartment-specific bioluminescence imaging (CS-BLI) approach, when RPMI Dox40 cells were cocultured with BMSCs for 5 days, there was an increase in MM cells in the presence of BMSCs compared to absence. Experiment was repeated in triplicate.

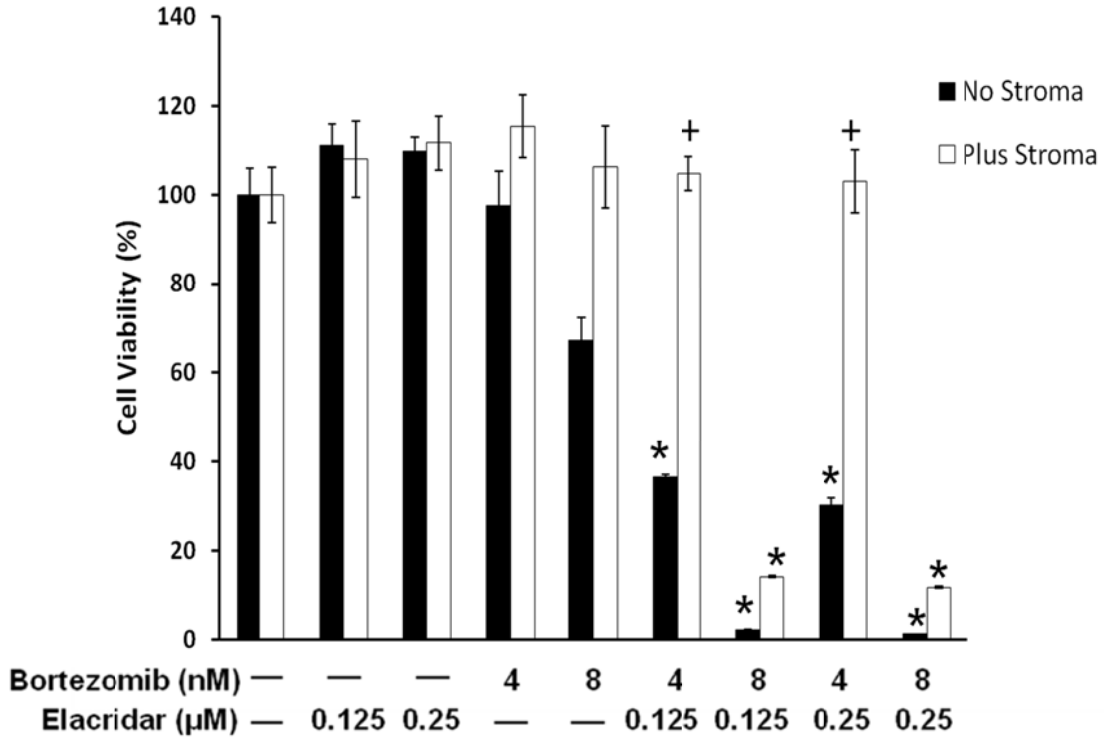

Figure 3.1.7.2. Synergy between bortezomib and elacridar persists in the protective effect of the BM microenvironment

Using the compartment-specific bioluminescence imaging (CS-BLI) approach, we evaluated the combination of bortezomib and elacridar on multiple myeloma RPMI-Dox40-MCherry/luc cells cultured in the presence vs. absence of HS-5 stromal cells and treated with bortezomib 4 and 8nM and elacridar 0.125, 0.25μM for 5 days. RPMI-Dox40-MCherry/luc survival was expressed as percentage (mean ± SD) compared to vehicle treated control. Experiment was repeated in triplicate. Synergistic cytotoxicity of the combination of bortezomib and elacridar persisted despite coculture with BMSCs. (+: $p < 0.05$, *: $p < 0.001$)

3.1.8. Bortezomib affects P-glycoprotein expression and function

We next investigated the direct effect of bortezomib on P-gp expression. RPMI-Dox40 cells and DLKP-A cells were treated with 4nM and 16nM of bortezomib respectively for 0-72 h. P-gp expression was analyzed by Western blot and demonstrated a reduction in P-gp levels with bortezomib treatment by 24 h for both cell lines (Fig. 3.1.8.1).

To determine if the P-gp function was similarly inhibited, we performed a rhodamine-123 (Rh-123) efflux assay and analysed using flow cytometry. Verapamil was the P-gp inhibitor used in this study. Fig. 3.1.8.2 demonstrated that in this experiment, verapamil was able to inhibit P-gp function causing an accumulation of Rh-123 in the MM cells.

RPMI-Dox40 cells were then treated with bortezomib 6, 10 and 15nM for 72 h. The cells were then washed and Rh-123 efflux assay performed. The results were expressed as the mean of the median Rh-123 fluorescence intensity as shown in Fig. 3.1.8.3. RPMI-Dox40 cells treated with bortezomib demonstrated a reduction in Rh-123 efflux indicating a reduction in P-gp function at all doses tested with maximal inhibition of Rh-123 efflux at 120 mins. We have shown that bortezomib treatment reduces the expression of P-gp and its function was also reduced as well.

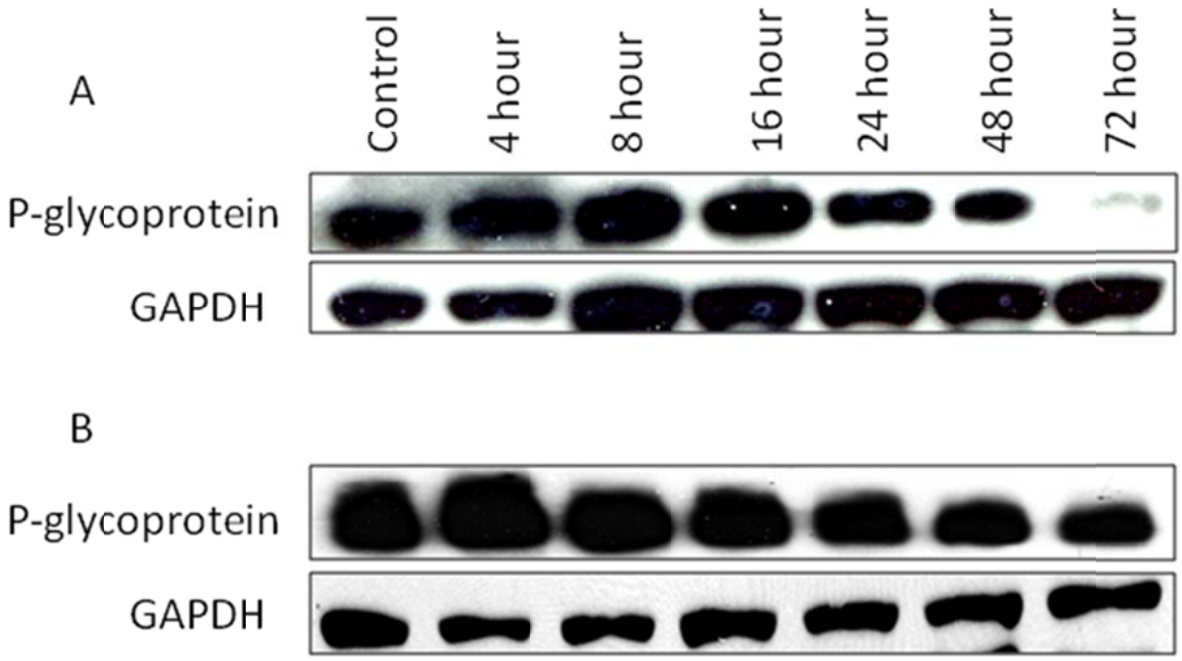

Figure 3.1.8.1 Bortezomib affects P-gp expression

When P-gp expressing cell lines RPMI-Dox40 (A) and DLKP-A (B) were treated with bortezomib 4nM and 16nM respectively, immunoblot analysis demonstrated a reduction in the level of P-gp expression by 24h treatment. GAPDH levels were used as a loading control.

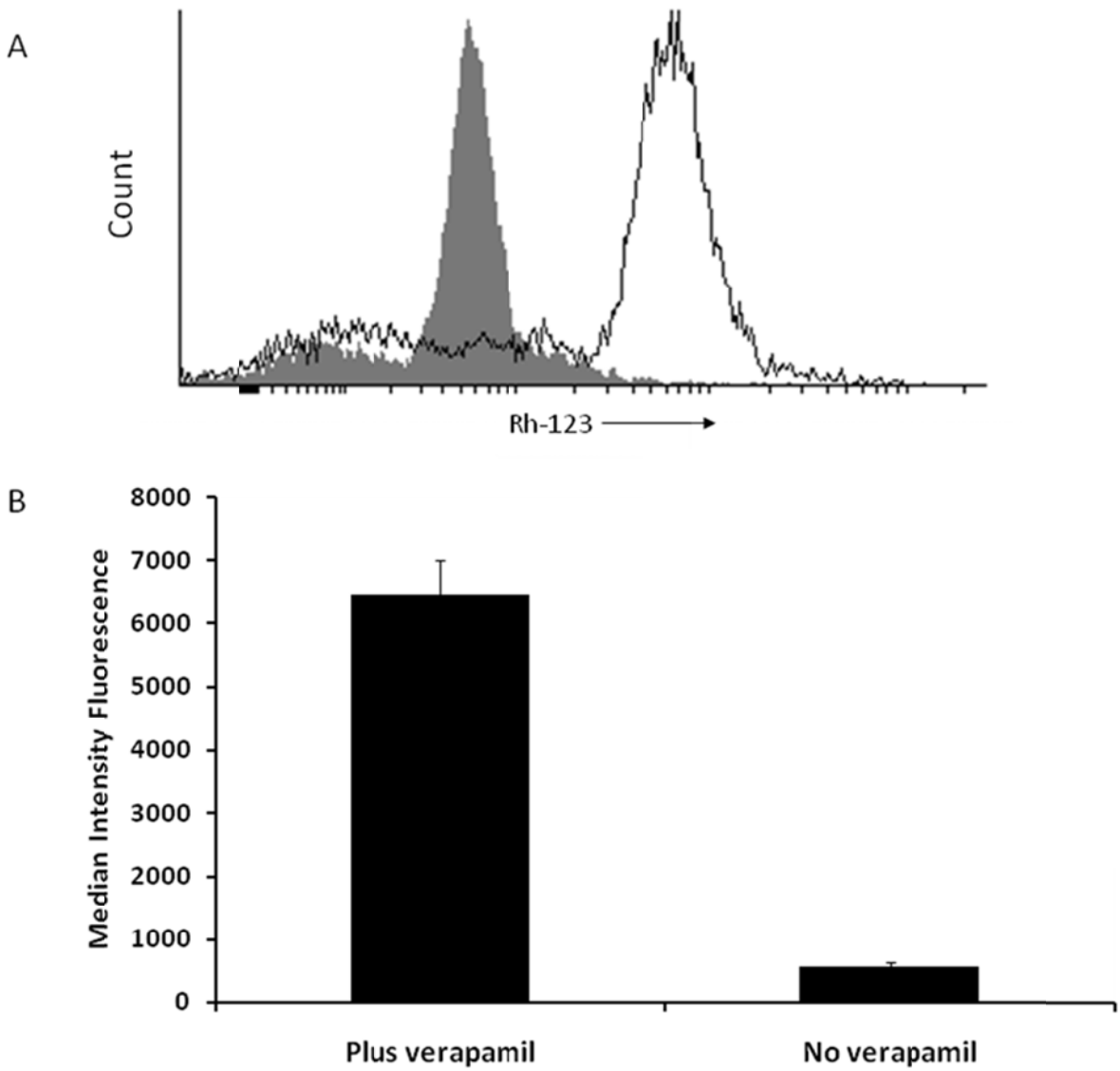

Figure 3.1.8.2 Verapamil inhibits P-gp and causes accumulation of Rh123

Rhodamine 123 efflux assay demonstrated that verapamil inhibits P-gp and this causes the accumulation of Rh123. (A) Histogram of RPMI-Dox40 with (*black line, unshaded*) and without (*gray line, shaded*) verapamil demonstrated a higher expression of Rh-123 in the cells treated with verapamil. (B) RPMI-Dox40 cells treated with verapamil demonstrated an accumulation of Rh123 reflected in the higher median intensity fluorescence of GFP. Experiment was repeated in triplicate.

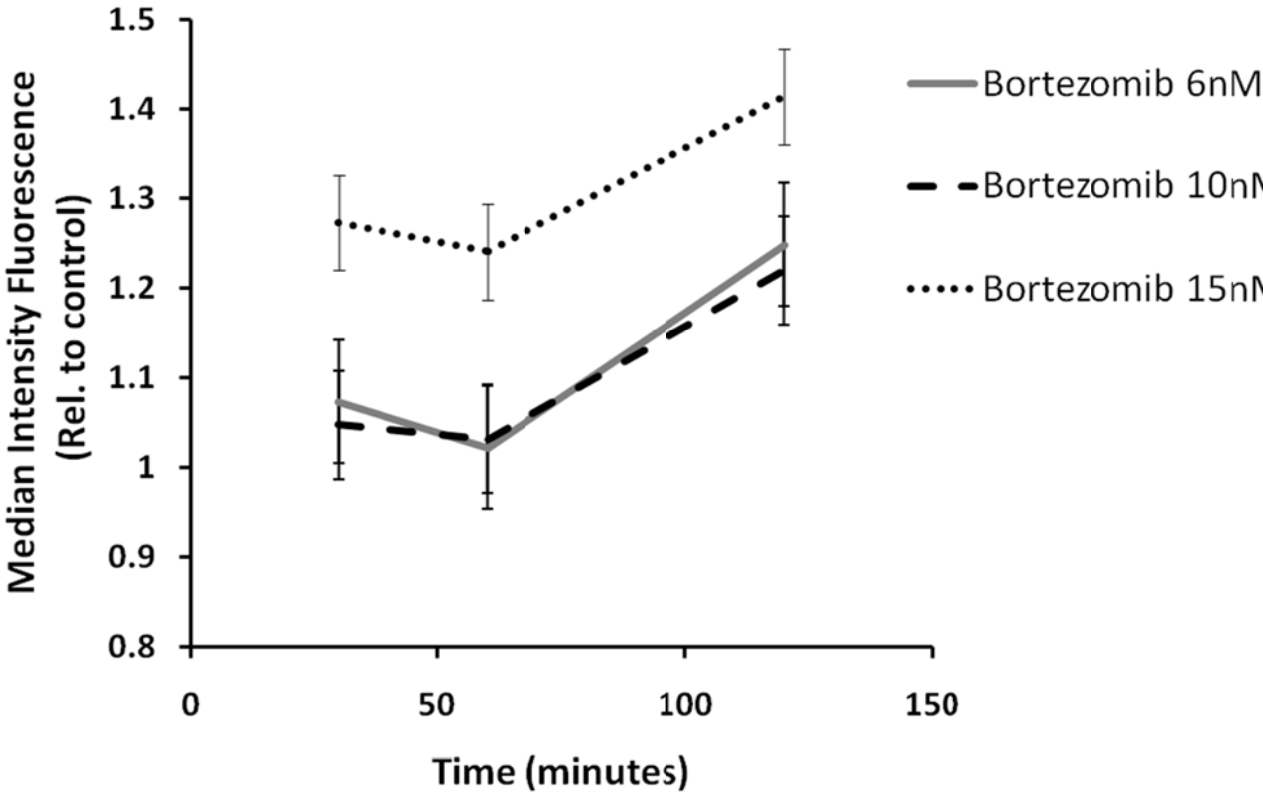

Figure 3.1.8.3 Bortezomib is able to reduce the function of P-gp

Bortezomib treatment at the doses indicated inhibited rhodamine-123 efflux in RPMI-Dox40 cells with maximum inhibition seen at 120 mins for all doses tested. The experiment was performed in triplicate and results were expressed relative to control at each time point. (mean of the median intensity of rhodamine-123 fluorescence ± SEM).

3.1.9. P-glycoprotein expression and function is affected by the local microenvironment

As the BM microenvironment confers protection to MM cells [280] we hypothesized that P-gp expression might be upregulated when MM cells are cocultured with BMSCs, because doxorubicin is known to be attenuated in the presence of BMSCs. We also wanted to examine if the reduction of P-gp expression and function when treated with bortezomib was affected by the BM microenvironment.

To answer these two questions, we performed the next set of experiments. RPMI-Dox40 cells were co-cultured with BMSCs and treated with bortezomib 4nM for up to 48 h before collection of cell lysates. Contrary to our hypothesis, we saw a reduction in P-gp expression in the coculture setting when compared to MM cells alone in the control lysates (Fig 3.1.9.1). After treatment with bortezomib 4nM, the immunoblot demonstrated a reduction in P-gp levels in the MM cells that were cocultured, compared to MM cells alone, at each time point (Fig. 3.1.9.1). This data suggest that the attenuation of doxorubicin when cocultured with BMSCs is unrelated to P-gp expression in the MM cells, as the cocultured MM control cells did not show an increase in P-gp expression. Fig 3.1.9.1 further showed that with bortezomib treatment, the P-gp expression was reduced in the MM cells alone and further reduced when MM cells were cocultured with stroma.

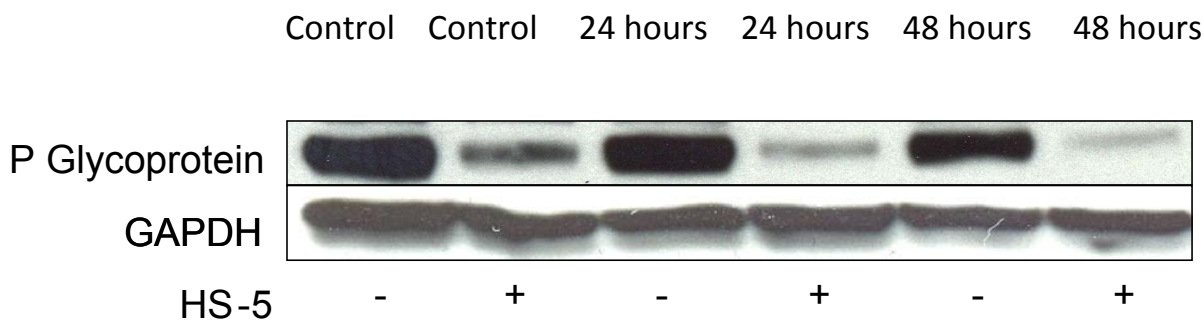

Figure 3.1.9.1 P-gp expression is downregulated when MM cells are co-cultured with BMSCs

RPMI-Dox40 cells were cocultured with BMSCs HS-5 and treated with bortezomib 4nM for up to 48 h. Immunoblot analysis demonstrated a reduction of P-gp expression in the MM cells that were co-cultured with BMSCs (see control cells). Upon treatment with bortezomib, as seen before, P-gp expression was reduced in the MM cells alone and further reduced in the MM cells cocultured with stroma. GAPDH levels were used as a loading control.

The finding that P-gp expression was reduced in MM cells when cocultured with stroma was unexpected. To determine if the P-gp mediated efflux, i.e. function was similarly reduced in MM cells when cocultured, a Rh-123 assay was performed. We used RPMI-Dox40 cells and cocultured them with BMSCs HS-5. The RPMI-Dox40 cell population was distinguished from the stroma cells by prelabelling with CellVue claret dye. Fig. 3.1.9.2 demonstrates clearly the two cell populations using flow cytometry. Fig. 3.1.9.3 demonstrated that in this experiment, verapamil was able to inhibit P-gp function causing an accumulation of Rh-123 in the MM cells.

RPMI-Dox40 cells were then cocultured with BMSCs HS-5 for 72 h. The cells were then washed and Rh-123 efflux assay performed. The results were expressed as the mean of the median Rh-123 fluorescence intensity as shown in Fig. 3.1.9.4. RPMI-Dox40 cells cocultured with stroma demonstrated a reduction in Rh-123 efflux indicating a reduction in P-gp function at all doses tested with maximal inhibition of Rh-123 efflux at 2 h.

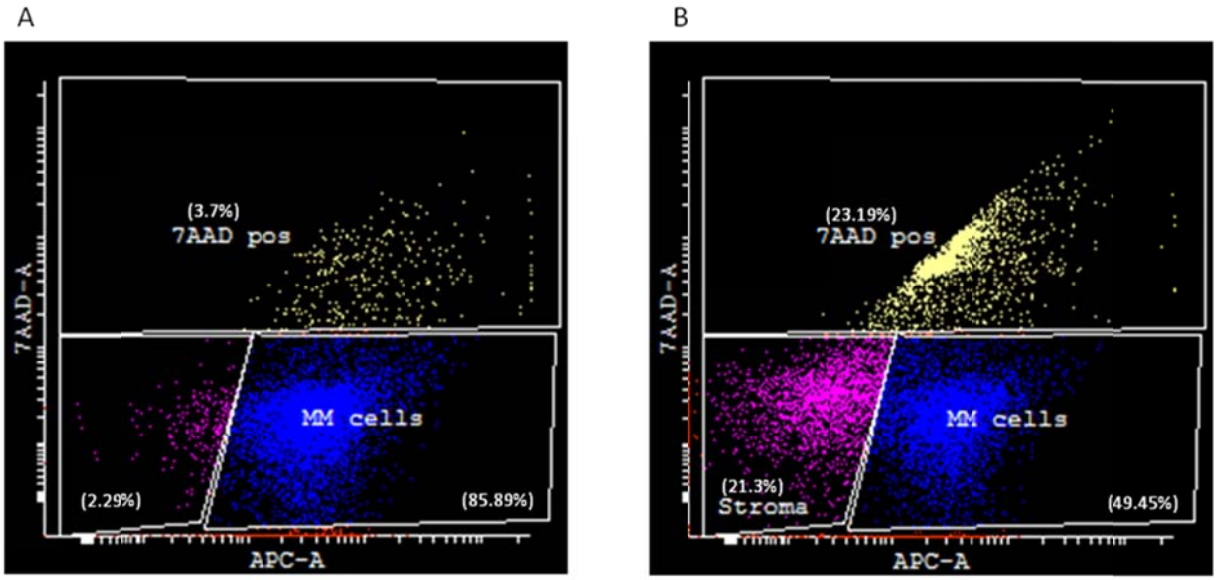

Figure 3.1.9.2 Flow cytometry distinguishing MM cells from stroma when cocultured

By staining the RPMI-Dox40 cells with CellVue claret dye, the MM cell population was able to be separated from the stroma cell population. (A) RPMI-Dox40 cells alone and (B) RPMI-Dox40 cells cocultured with stroma. Experiment was repeated in triplicate.

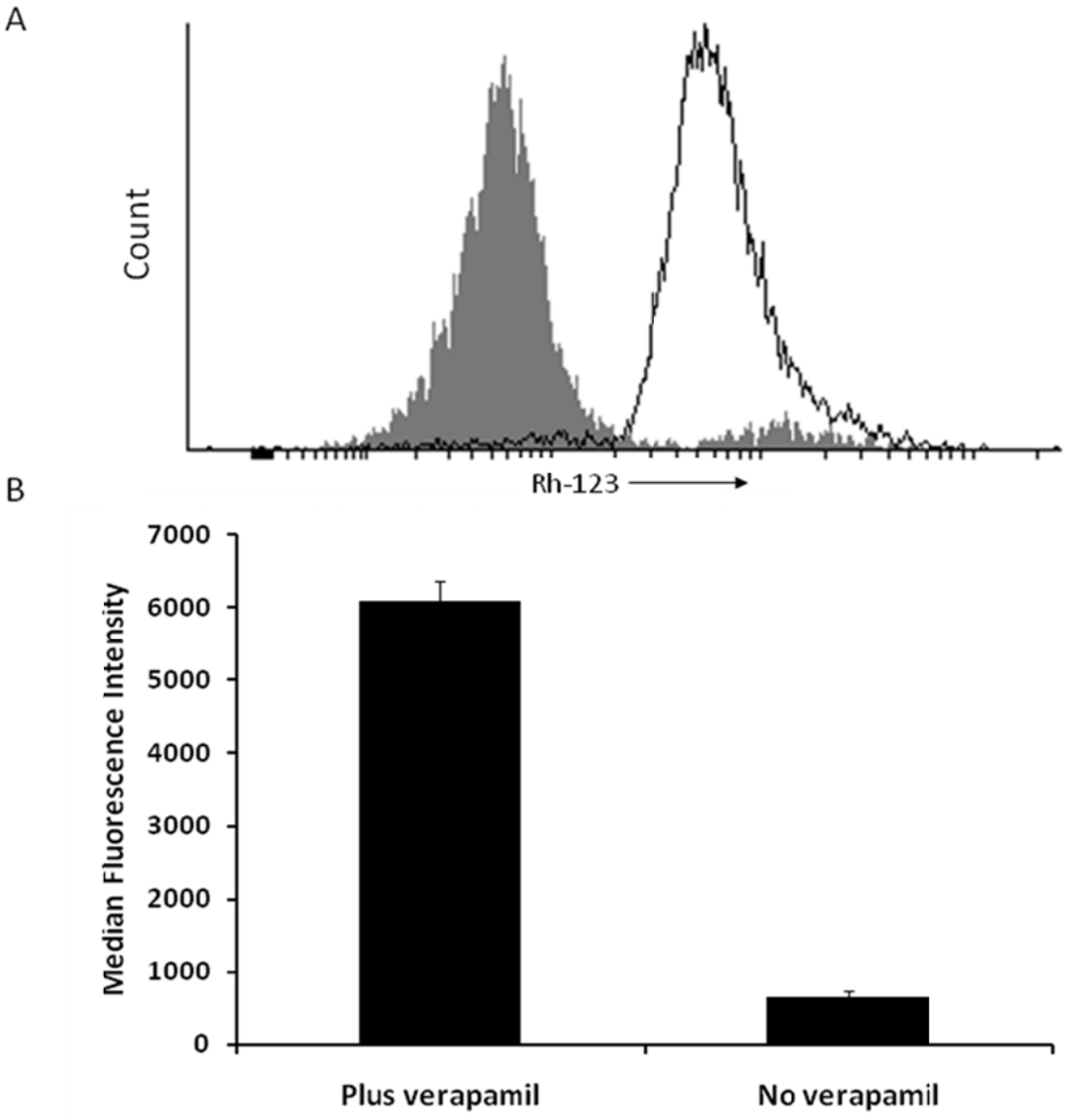

Figure 3.1.9.3 Verapamil inhibits P-gp and causes accumulation of Rh123

RPMI-Dox40 cells prelabelled with CellVue claret were cocultured with stroma for up to 72 h and Rh-123 assay was performed. The MM cell population was distinguished from the stroma cells and analysed. Verapamil was shown to inhibit P-gp and this causes the accumulation of Rh123. (A) Histogram of RPMI-Dox40 with (*black line, unshaded*) and without (*gray line, shaded*) verapamil. (B) RPMI-Dox40 cells treated with verapamil demonstrated an accumulation of Rh123 reflected in the higher median intensity fluorescence of GFP

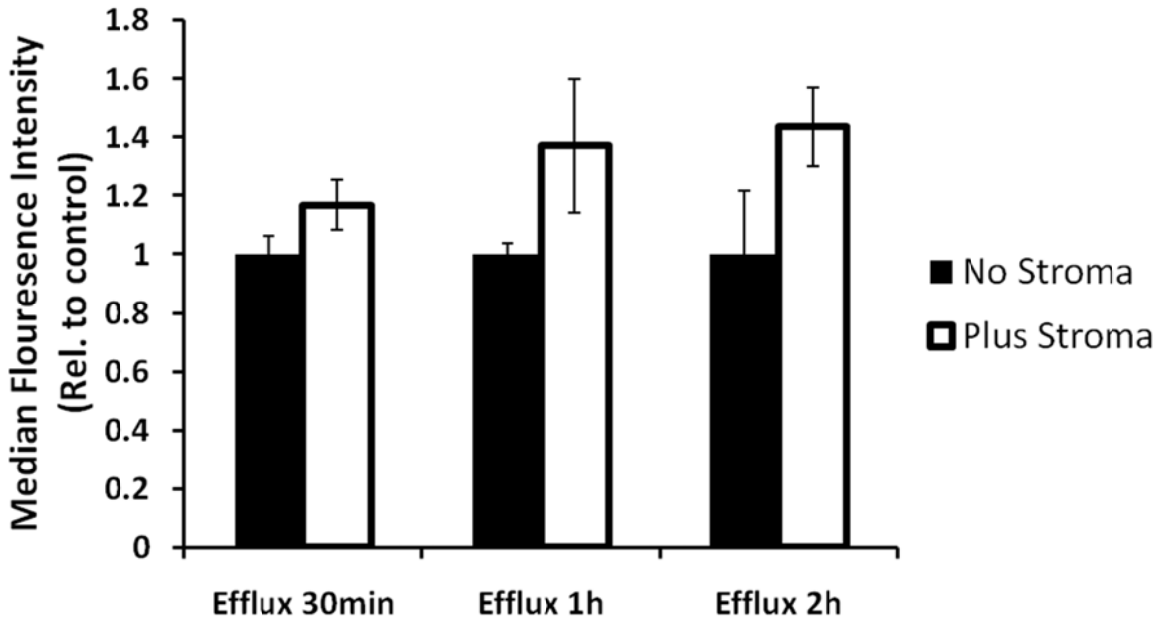

Figure 3.1.9.4 MM cells cocultured with stroma shows reduced function of P-gp

RPMI-Dox40 cells prelabelled with CellVue claret were cocultured with BMSCs HS-5. Analysing only the MM cell population, inhibition of Rh-123 efflux was demonstrated in RPMI-Dox40 cells that were cocultured with BMSCs when compared to RPMI-Dox40 cells alone. The experiment was performed in triplicate and results were expressed relative to absence of BMSCs control at each time point (mean of the median intensity of rhodamine-123 fluorescence ± SEM).

To further probe the relationship between P-gp and the BM microenvironment, we looked at the BMSCs fraction after coculturing with P-gp-positive RPMI-Dox40 cells. BMSCs do not express P-gp (Fig. 3.1.9.5). A study by Levchenko *et al.* [281] showed that intercellular transfer of functional P-gp from P-gp-positive to P-gp-negative cells *in vitro* and *in vivo* was possible. The authors demonstrated that intercellular transfer of functional P-gp occurs between different tumour cell types and results in increased drug resistance both *in vitro* and *in vivo*. They also showed that P-gp transfer also occurs to putative components of tumour stroma, such as fibroblasts, raising the possibility that multidrug resistance could be conferred by resistant tumour cells to critical stromal elements within the tumour mass. Fig 3.1.9.6 demonstrated that the previously P-gp-negative BMSCs, became P-gp-positive after coculturing with RPMI-Dox40 for 72 h. This suggests the transference of P-gp from the cancer cells to the normal tumour stroma as demonstrated by Levchenko [281]. However, this transferred P-gp does not appear to be functional as there was no extrusion of Rh-123 in the absence of verapamil (Fig. 3.1.9.7). The transference of P-gp from MM cells to BMSCs may account for the reduction in the P-gp expression in the MM cells after coculture.

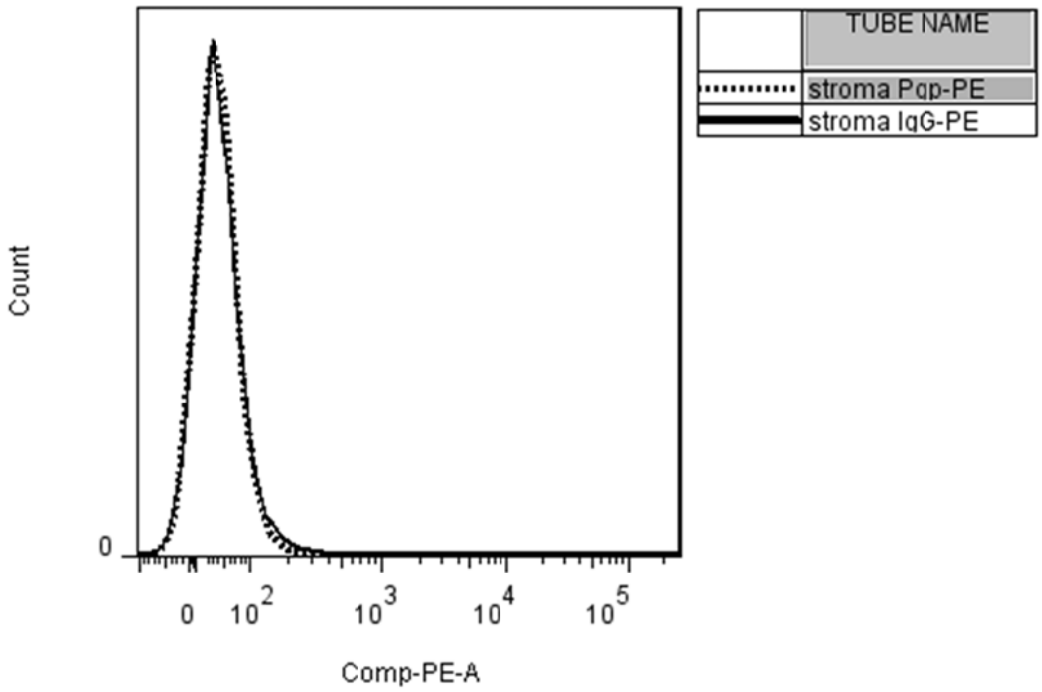

Figure 3.1.9.5 BMSCs cells do not express P-gp

BMSCs were analysed using flow cytometry and does not show expression of P-gp. BMSCs labelled with an isotype control (*solid black line*) and P-gp antibody conjugated with phycoerythrin (*shaded gray*).

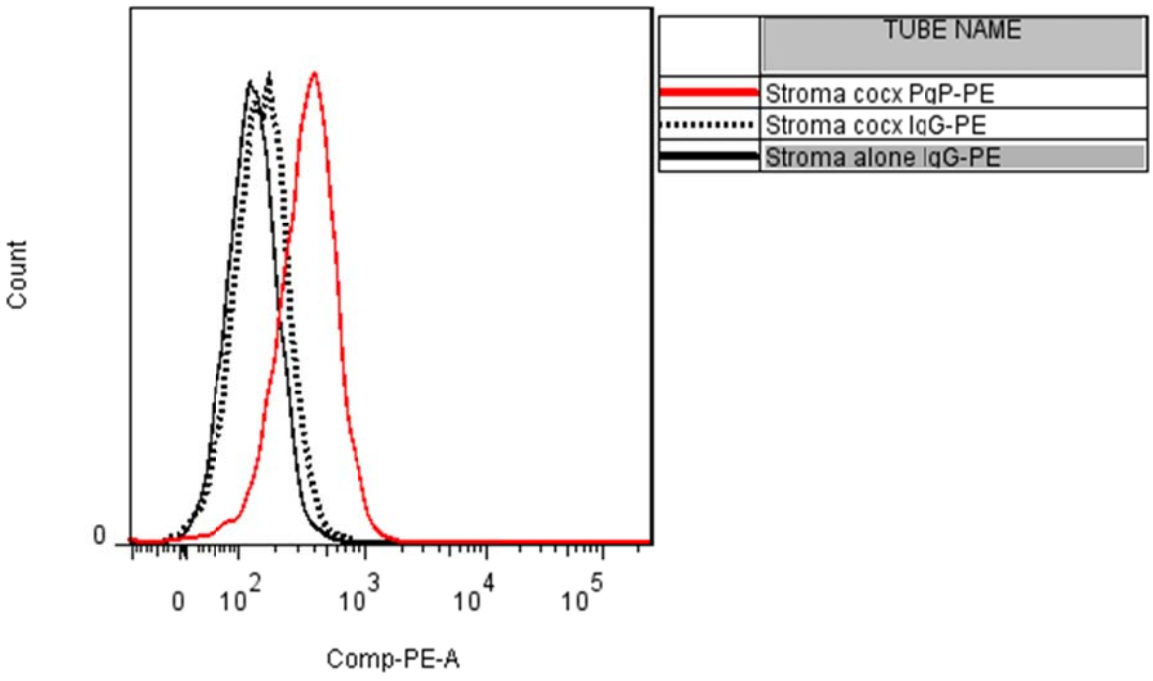

Figure 3.1.9.6 The stroma fraction shows increased expression of P-gp after coculture with P-gp-positive MM cells.

RPMI-Dox40 cells prelabelled with CellVue claret were cocultured with BMSCs HS-5 for 72 h. Analysing only the stroma cell population, there was an increase in the P-gp expression in the previously P-gp-negative stroma cells. Shown in black (*solid: BMSCs alone; dotted: BMSCs fraction after* coculture) is the IgG-phycoerythrin antibody. The solid red line demonstrated the stroma fraction after coculture with a P-gp-phycoerythrin antibody.

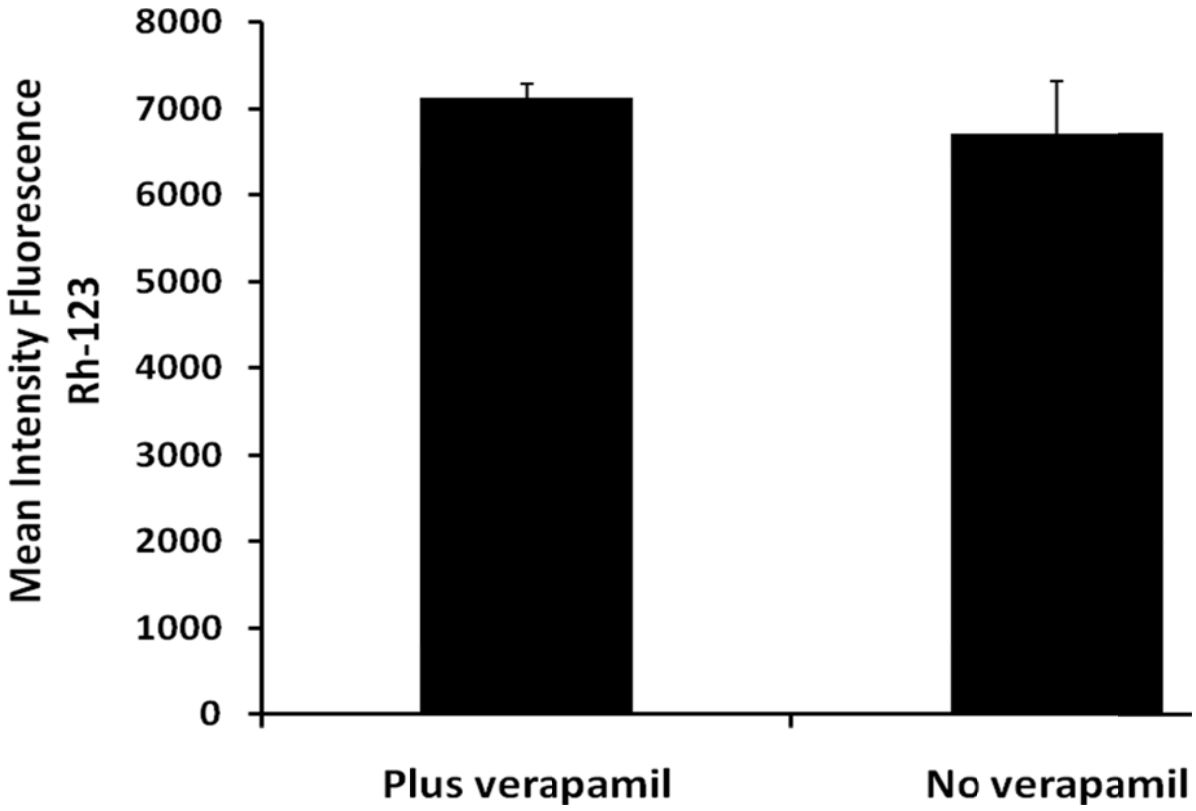

Figure 3.1.9.7 Characterization of P-gp transfer in the stroma fraction after coculturing with MM cells.

RPMI-Dox40 cells prelabelled with CellVue claret were cocultured with stroma for up to 72 h and Rh-123 assay was performed. The MM cell population was distinguished from the stroma cells and only the stroma fraction was analysed. The transferred P-gp was not functional as evidenced by the lack of rhodamine 123 extrusion in the absence of verapamil. The experiment was performed in triplicate (average of the mean intensity of rhodamine-123 fluorescence ± SD).

3.2. Investigation of p53 signalling perturbations in Multiple Myeloma resistance

3.2.1. Introduction

TP53 (the human gene that encodes p53) inactivating mutations affect 11 million cancer patients and another 11 million people have tumours in which the p53 pathway is partially abrogated through the inactivation of other signalling or effector components [282]. Therefore, the p53 pathway is a prime target to investigate resistance mechanisms and for new cancer drug development strategies,

Bortezomib, a proteasome inhibitor, is known to stabilize and prevent the degradation of many tumour-suppressing and pro-apoptotic proteins, including p53. It has also been shown that DNA-damaging, p53-activating agents, such as doxorubicin and melphalan, can demonstrate synergistic toxicity with bortezomib [44]. In the meantime, nutlin-3, a Mdm2 inhibitor, can stabilise p53, increase its protein levels and activate the p53 apoptotic pathway. The added advantage of nutlin-3 is that it stabilises p53 levels without genotoxicity which would be of benefit to normal tissues.

We hypothesized that nongenotoxic stabilisation of p53, caused by nutlin-3, through suppression of Mdm2-mediated p53 ubiquination, might synergise with accumulation of p53 caused by bortezomib through proteasome inhibition, leading to increased antitumour activity.

3.2.2. Nutlin-3 activity in Multiple Myeloma and carcinoma cell lines

A panel of MM and carcinoma cell lines were treated with nutlin-3. MM cell lines were sensitive to nutlin-3, with decreased cell viability upon treatment; representative results for MM1.S, MM1.R and OPM-2 are shown in Fig. 3.2.2A. Epithelial tumour cell lines such as thyroid carcinoma were also sensitive to nutlin-3, although typically to lesser extent than to MM cells (Fig. 3.2.2B).

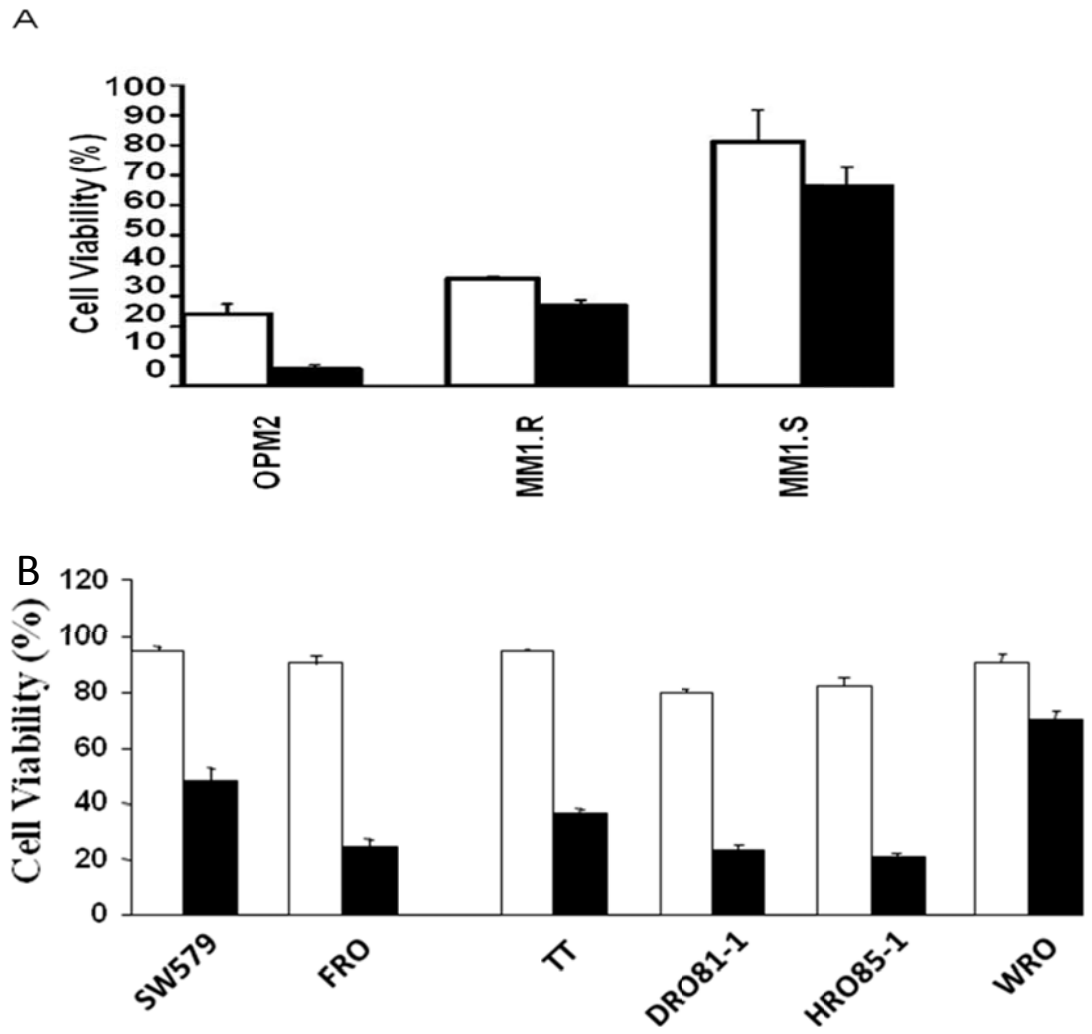

Fig 3.2.2 Nutlin-3 activity in MM and carcinoma cell lines

(A) MM cell lines are sensitive to nutlin-3. Viability of the MM1.S, MM1.R and OPM2 cell lines after exposure to nutlin-3 (*white columns,* 5μM; *black columns*, 10μM) for 48 h was assessed by MTT. Cell survival was expressed as a percentage (mean ± SD) compared with vehicle treated controls. The treatment was repeated thrice with similar results. (B) shows the response of a panel of 6 carcinoma cell lines (SW579, papillary thyroid; FRO, anaplastic thyroid; TT, DRO81-1 and HRO85-1, medullary thyroid; WRO, follicular thyroid) to treatment with nutlin-3 (*white columns* 10μM; *black columns,* 30μM) for 48 h as assessed by MTT. Cell survival was expressed as a percentage (mean ± SD) compared with vehicle treated controls. The treatment was repeated thrice with similar results.

3.2.3. Nutlin-3 upregulates expression of p53-dependent targets

As an Mdm2 inhibitor, nutlin-3 is able to upregulate expression of several p53-dependent targets including Bax, PUMA, Noxa, p21, and Mdm2 itself (Table 3.2.3). Table 3.2.3 demonstrated the mRNA levels of p53-responsive transcripts after FRO cells were treated with bortezomib for 0, 24 and 48h.

The cellular response to genotoxic stress that damages DNA includes cell cycle arrest, activation of DNA repair and, in the event of irreparable damage, induction of apoptosis. When cells encounter genotoxic stress, certain sensors for DNA lesions eventually stabilize and activate p53. p53 causes apoptotic cell death by induction of caspase-3 cleavage (Fig. 3.2.3A). However, the pro-apoptotic effect of nutlin-3 was partially attenuated by the pan-caspase inhibitor, ZVAD-FMK (Fig. 3.2.3B), suggesting that caspase activity is not the sole mechanism of nutlin-3-induced cell death.

2-ΔΔCT	24h	48h
BAK	4.2	2.2
BAX	5.5	2.7
PUMA (BBC3)	7.8	2.6
BTG1	4.8	4.0
CDKN1A (p21/CIP1/WAF1)	11.0	5.5
CDKN1B (p27/KIP1)	10.8	3.3
CDKN1C (p57/KIP2)	2.4	1.6
CDKN2B (p15/INK4B)	2.6	11.5
GADD45B	4.3	1.9
GADD45G	19.7	12.2
HSP90AA1	5.5	3.7
HSP90B1 (GRP94)	7.0	5.7
HSPCB (HSP90AB1)	4.0	2.9
MDM2	7.5	2.6
PMAIP1 (NOXA)	8.8	2.9
VEGF	1.8	4.7
CD44, iso 1-4	0.6	0.6

Table 3.2.3 Nutlin-3 upregulated expression of several p53-dependent targets

FRO cells were treated with nutlin-3 (30 μM) for 0, 24 and 48h. mRNAs levels for a panel of p53-responsive transcripts were then analyzed by qRT-PCR and expressed fold change relative to control cells (i.e., controls are assigned a value of 1 by definition). Experiment was performed with three technical replicates.

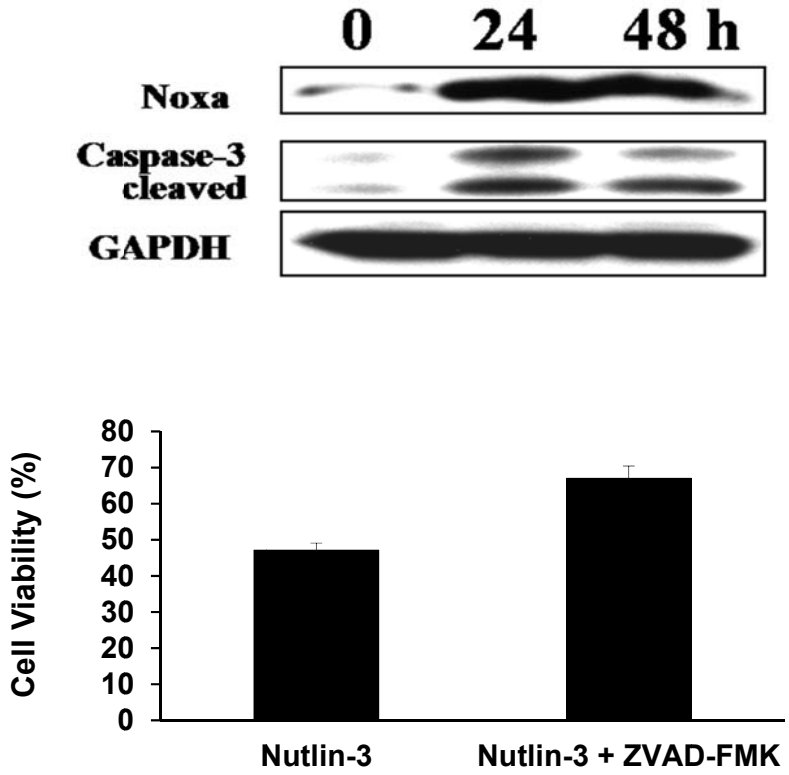

Fig. 3.2.3 Nutlin induces caspase-3 cleavage

Total cell lysates were assayed by immunoblotting for the presence of Noxa and cleaved caspase-3 (A). FRO cells were treated with nutlin-3 (30 μM) for 0, 24 and 48 h. GAPDH was a loading control. (B) FRO cells were treated with nutlin-3 (20 μM) for 48 h in the presence or absence of the pancaspase inhibitor ZVAD-FMK (20 μM). Cell survival was quantified by MTT and expressed as a percentage (mean±SD) compared with vehicle-treated controls. * $p<0.001$

3.2.4. Differential effect of Nutlin-3 on activity of sublethal doses of bortezomib against Multiple Myeloma vs. epithelial tumour cells.

We have previously reported that bortezomib increases p53 protein levels, at least in part due to inhibition of its proteasomal degradation, as well as upregulates p53 mRNA expression and induces p53 phosphorylation (Ser15) [278, 283]. We hypothesized that combined treatment with the Mdm2 ubiquitin ligase inhibitor nutlin-3 would enhance the p53-stabilizing activity and hence the pro-apoptotic effect of bortezomib. MM cell lines are highly sensitive to *in vitro* single-agent bortezomib, including MM.1S, MM.1R, KMS-11, and NCI-H929 (Fig. 3.2.4.1); and combinations of sublethal concentrations of nutlin-3 and bortezomib demonstrated a lack of synergistic cytotoxicity. This is reflected in Table 3.2.4.1 which showed the calculated combination index of the combinations above; the CIN was >1 for all cell lines except for KMS11 showing a lack of synergy. Although according to Chou and Talalay [271], a CIN value of >1.1 is indicative of antagonism, it was obvious that in this combination tested there was no antagonism seen, more an additive effect. Thus, in this study, we have regarded a CIN >0.9, < 1.5 as additive. For the KMS11 cell line, the two highest doses of nutlin-3 demonstrated synergy when combined with bortezomib (in *italics).*

In contrast, in epithelial cancer cell lines with little single agent activity to bortezomib or nutlin-3 alone, there was synergistic cytotoxicity when bortezomib was combined with nutlin-3. Fig. 3.2.4.2 demonstrated the impressive synergy against epithelial tumour cell lines including thyroid, breast and prostate carcinomas with the corresponding CIN values in Table 3.2.4.2.

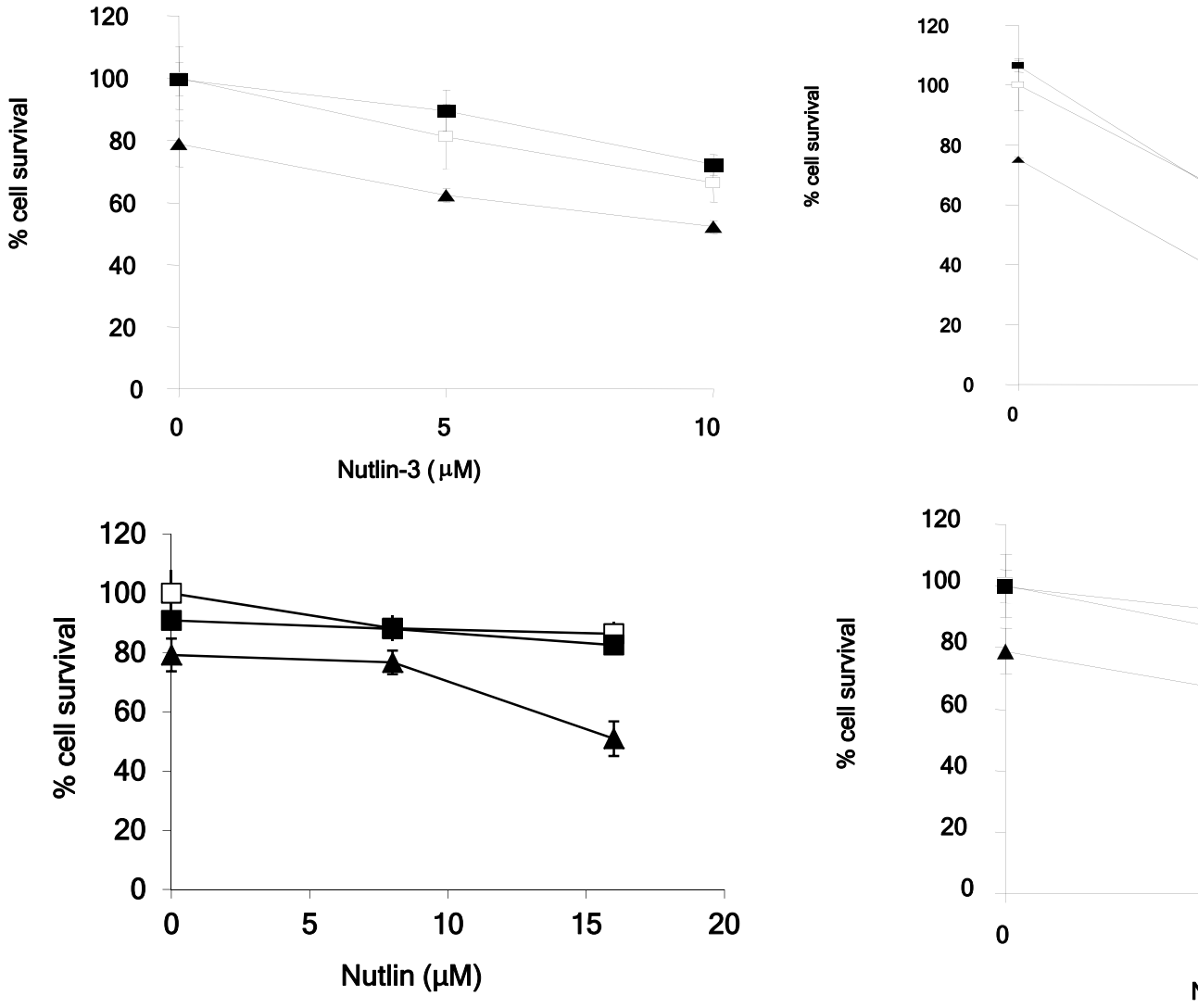

Fig. 3.2.4.1 Effect of combined Mdm2 and proteasome inhibition on Multiple Myeloma cells.

Treatment of the MM cell lines MM1.S, MM1.R, KMS-11 and NCI-H929 with combinations of sublethal concentrations of nutlin-3 and bortezomib exhibited lack of synergistic cytotoxicity. Data from representative cell lines are shown: (A) MM1.S cells were treated for 48h with nutlin-3 (0-10 μM) in the absence (□) or presence of bortezomib (■ : 2 nM, ▲ : 4 nM).) (B) MM1.R cells were treated for 48h with nutlin-3 (0-10 μM) in the absence (□) or presence of bortezomib (■: 2 nM, ▲ 4 nM). (C) KMS-11 cells were treated for 48h with nutlin-3 (0-16 μM) in the absence (□) or presence of bortezomib (■ : 2 nM, ▲ : 4 nM). (D) NCI-H929 cells were treated for 48h with nutlin-3

□ ■ ▲

(0-10 μM) in the absence ( ) or presence of bortezomib (: 2 nM, : 4 nM). Cell survival was quantified by MTT and expressed as a percentage (mean±SD) relative to vehicle-treated controls.

Cell lines	Nutlin (ìM)	Bortezomib (nM)	Fraction affected	CIN
MM1.S	5	2	0.10489	2.402
	5	4	0.37611	1.307
	10	2	0.279224	1.741
	10	5	0.478134	1.618
MM1.R	5	2	0.542056	1.264
	5	4	0.786957	1.036
	10	2	0.725317	1.072
	10	4	0.850924	1.055
KMS11	8	1	0.120185	1.726
	8	2	0.23333	0.934
	16	1	0.174699	*0.885*
	16	2	0.490668	*0.392*
NCI-H929	5	2	0.10489	2.376
	5	4	0.37611	1.348
	10	2	0.279224	1.75
	10	4	0.478134	1.471

Table 3.2.4.1 Combination index for Nutlin-3 plus Bortezomib in MM cells

Using Calcusyn software, the combination index (CIN) for the combination of Nutlin-3 and bortezomib was calculated. For the MM cells, the CIN was >1 for all cell lines except for KMS11 showing a lack of synergy. For the KMS11 cell line, the two highest doses of nutlin-3 demonstrated synergy when combined with bortezomib (in *italics).* (Synergy – CIN <0.9, additive effect - CIN >0.9, <1.5).

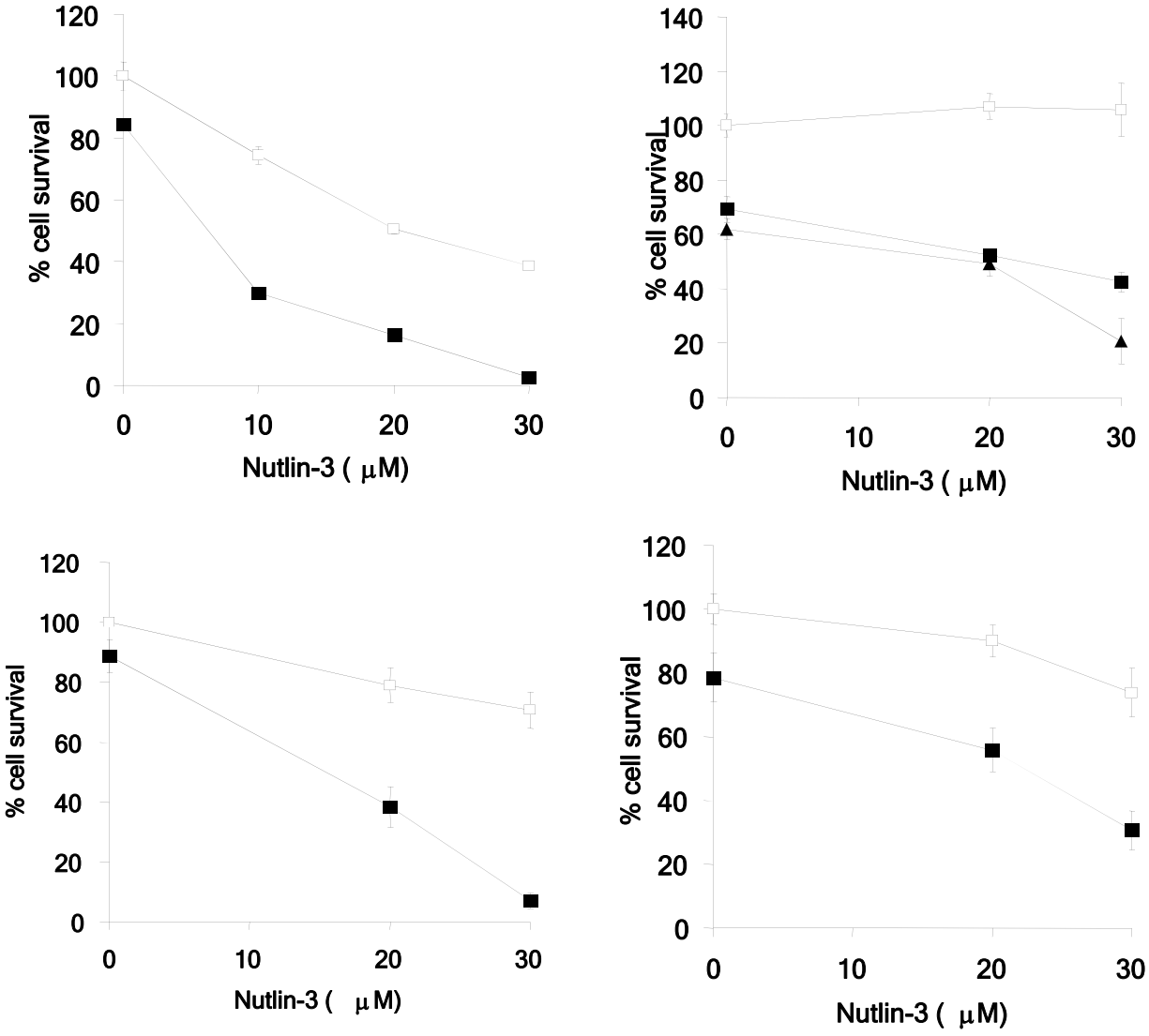

Fig. 3.2.4.2 Effect of combined Mdm2 and proteasome inhibition on epithelial cancer cells.

Nutlin-3 also potentiates the activity of sublethal concentrations of bortezomib against several types of epithelial tumours, including thyroid, breast and prostate carcinomas. (A). Anaplastic thyroid carcinoma FRO cells were treated for 48h with nutlin-3 (0-30 μM) in the absence (□) or presence (■) of bortezomib (4 nM). (B) Follicular thyroid carcinoma WRO cells were treated for 48h with nutlin-3 (0-30 μM) in the absence (□) or presence of bortezomib (■: 20 nM, ▲: 40 nM). (C) Prostate carcinoma DU145 cells were treated for 48h with nutlin-3 (0-30 μM) in the absence (□) or presence (■) of

bortezomib (5 nM). (D) Breast carcinoma MDA-MB-231met-LN cells were treated for 48h with nutlin-3 (0-30 µM) in the absence ( ) or presence ( ) of bortezomib (5 nM). Cell survival was quantified by MTT and expressed as a percentage (mean±SD) relative to vehicle-treated controls.

Cell lines	Nutlin (ìM)	Bortezomib (nM)	Fraction affected	CIN
FRO	10	4	0.7004	0.549
	20	4	0.8387	0.489
	30	4	0.97456	0.179
WRO	20	20	0.47584	0.216
	20	40	0.50929	0.324
	30	20	0.57572	0.091
	30	40	0.79245	0.02
DU145	20	5	0.44151	*1.1*
	30	5	0.69336	0.92
MDA-MB-231met-LN	20	5	0.30712	0.024
	30	5	0.83598	0.001

Table 3.2.4.2 Combination index for Nutlin-3 plus Bortezomib in epithelial cancer cells

Using Calcusyn software, the combination index (CIN) for the combination of Nutlin-3 and bortezomib was calculated. For the epithelial cancer cells, the CIN was <1 for all cell lines except for one dose in the DU145 cell line (in *italics*) demonstrating synergy. For the DU145 cell line, the combination of 20ìM Nutlin-3 and Bortezomib 5nM yielded an additive effect. (Synergy - CIN<0.9, additive effect - CIN >0.9, <1.5).

3.2.5. Nutlin-3 enhances the activation of the p53 apoptotic pathway by sublethal concentrations of bortezomib in epithelial carcinoma cell lines, but not in bortezomib-sensitive Multiple Myeloma cells.

We next investigated the mechanism for the differential sensitivity of MM vs. epithelial cell lines to the combination of bortezomib with nutlin-3. Western blot analysis of MM1.S cells treated with this combination for 8h or 24h demonstrated no evidence of synergistic activation of p53 pathway and apoptosis mediators (Fig. 3.2.5), consistent with the lack of enhanced killing effect. In contrast, FRO cells treated with sublethal concentrations of nutlin-3 and bortezomib for 8h or 24h revealed synergistic activation of p53 pathway and apoptosis, associated with upregulation in p53, Hdm2, Noxa, and PUMA expression, as well as enhanced cleavage of PARP and caspase-3 (Fig. 3.2.5), consistent with the synergistic activity of this drug combination.

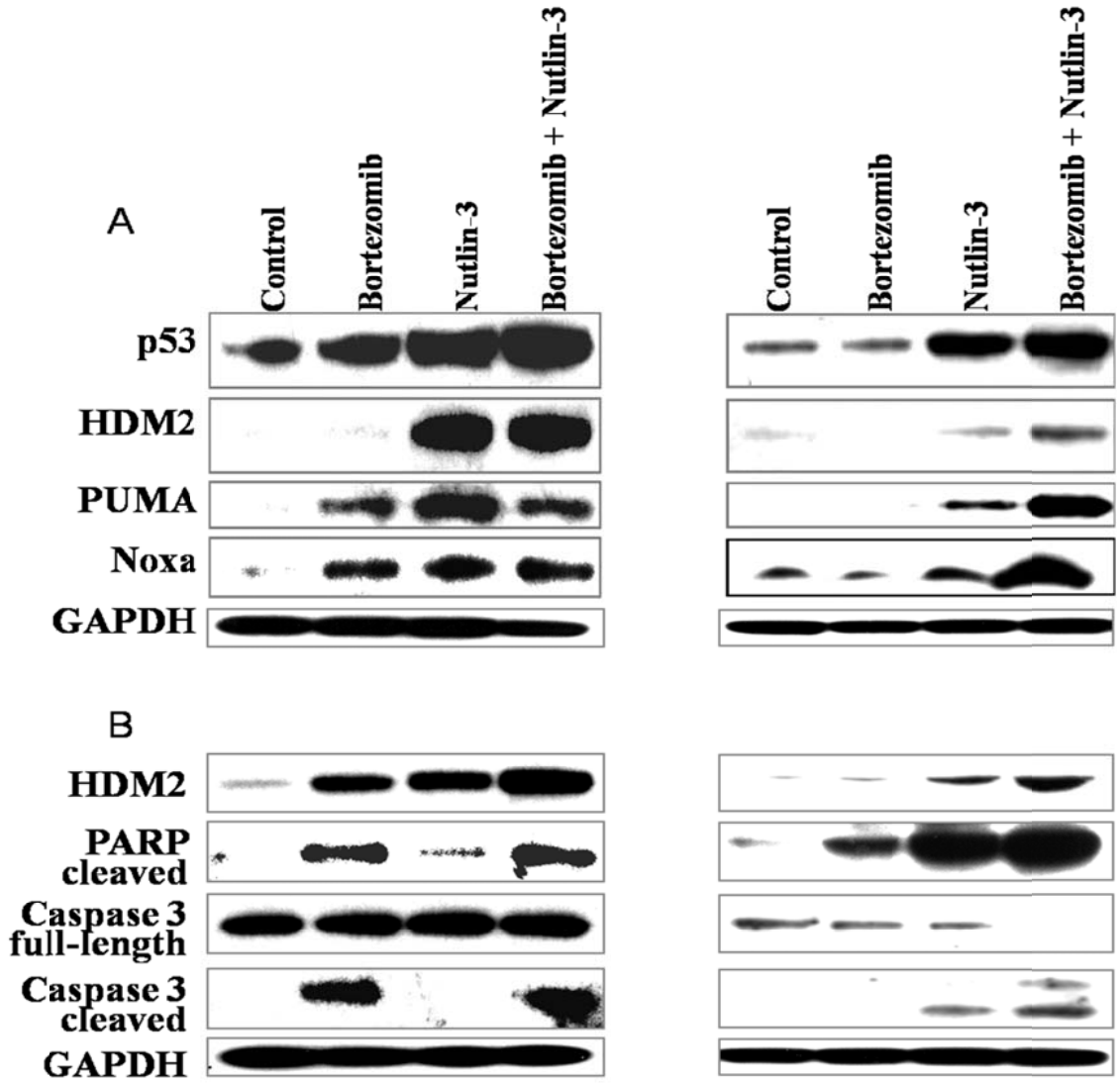

Fig. 3.2.5 Immunoblotting analysis of MM1.S (left panel) and FRO (right panel) cells treated with sublethal concentrations of nutlin-3 and bortezomib for 8h (A) or 24h (B).

Total cell lysates were assayed for p53, Hdm2, Noxa, PUMA, and cleaved PARP and caspase-3. There was no synergistic activation of p53 pathway and apoptosis in MM1S cells (nutlin-3: 2μM, bortezomib: 2 nM). In contrast, the combination of nutlin-3 (10μM)

with bortezomib (4nM) resulted in synergistic activation of p53 pathway and apoptosis in FRO cells.

3.2.6. The impact of bone marrow stroma cells coculture on p53 activity and sensitivity to nutlin-3 in Multiple Myeloma cells.

BMSCs confer a protective effect on MM cells against several conventional pro-apoptotic agents, such as dexamethasone or cytotoxic chemotherapy [27]. We therefore next investigated the effect of co-culture with BMSCs to the activation of the p53 pathway in MM cells and to sensitivity to nutlin-3. Human MM1.S-GFP/luc cells were co-cultured with HS-5 BMSCs for 24 hours and separated using a FACS cell sorter. Quantitative RT-PCR of MM1S cells co-cultured with BMSCs demonstrated decreased expression of p53 and gene transcripts known to be induced by p53 including Hdm2 [284], Bax [285], Noxa [286], PUMA [287], BTG1, DAPK1 [288], GADD45B, ID2, Jun, Plk1, and Plk2 [289] (Fig. 3.2.6.1). These results suggest that co-culture with BMSCs triggers downregulation of the p53 pathway in MM cells, which can contribute to resistance to apoptosis.

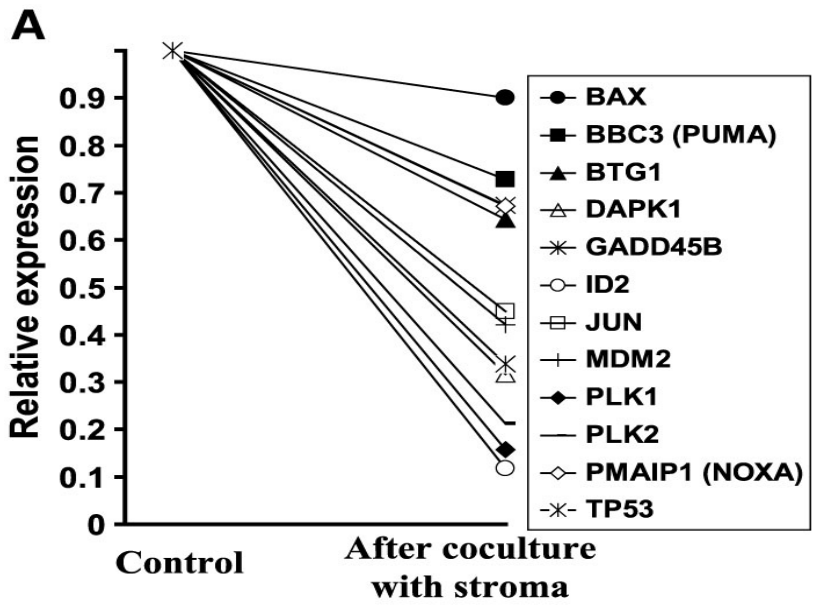

Fig 3.2.6.1 Coculture with BMSCs suppress levels of p53 responsive transcripts

MM.1S-GFP/luc cells were cultured for 24 h in the presence or absence of BMSCs line HS-5, and then sorted by FACS. Levels of mRNAs for a panel of p53-responsive transcripts were quantified by qRT-PCR and expressed relative to the respective levels in control cells. Co-culture with BMSCs suppressed levels of these p53-responsive transcripts. Experiment was performed with three technical replicates.

We next assessed the impact of co-culture with BMSCs on MM cell sensitivity to nutlin-3. Using the compartment-specific bioluminescence imaging (CS-BLI) approach, we found that MM1.SGFP/luc cells were less sensitive to the pro-apoptotic effect of nutlin-3 in the presence of HS-5 BMSCs (Fig. 3.2.6.2). This may have implications in the single agent treatment of nutlin-3 in MM.

We next wanted to assess if the downstream effectors of p53 would be upregulated upon nutlin-3 treatment in the presence of stroma, since its activity was attenuated. Importantly, however, treatment with nutlin-3 was able to induce the expression of Hdm2 (Fig. 3.2.6.3A) and PUMA (Fig. 3.2.6.3B) even in the presence of BMSCs. This implies that the drug is still having an effect although somewhat blunted.

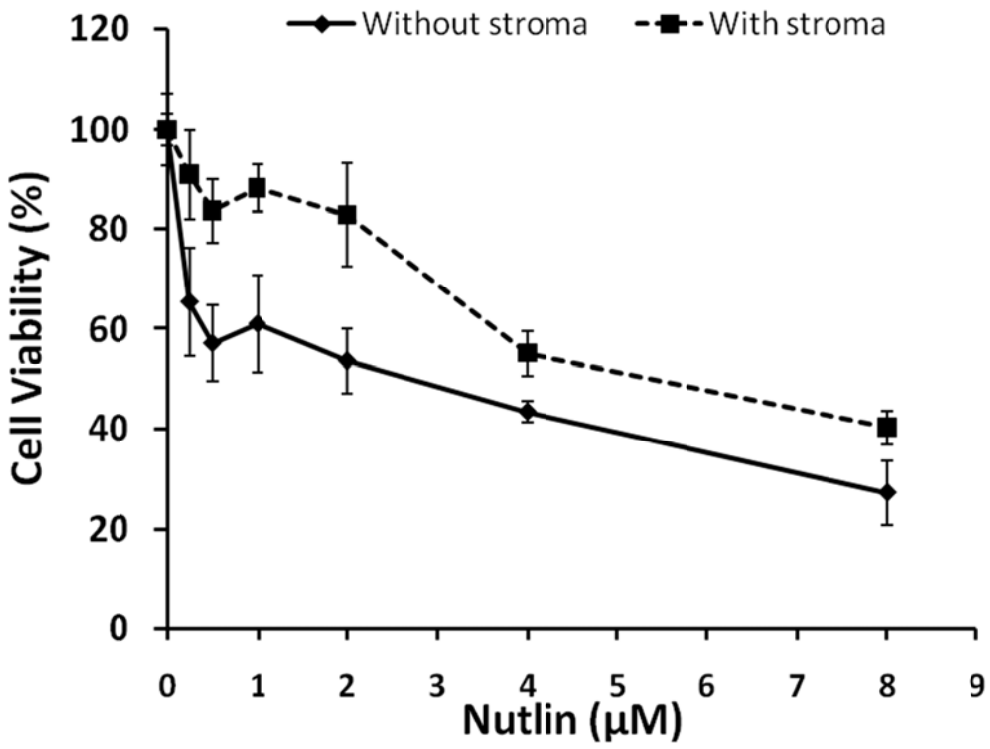

Fig. 3.2.6.2 Nutlin-3 cocultured with BMSCs in MM cells.

MM1.S-GFP/luc cells were treated with nutlin-3 for 48 h, in the presence or absence of BMSCs. MM cell viability was assessed using the compartment-specific bioluminescence imaging (CS-BLI) approach and expressed as a percentage (mean ± SD) relative to vehicle-treated controls. Coculture with BMSCs partially attenuated the pro-apoptotic effect of nutlin-3 on MM1S. Experiment was performed in triplicate.

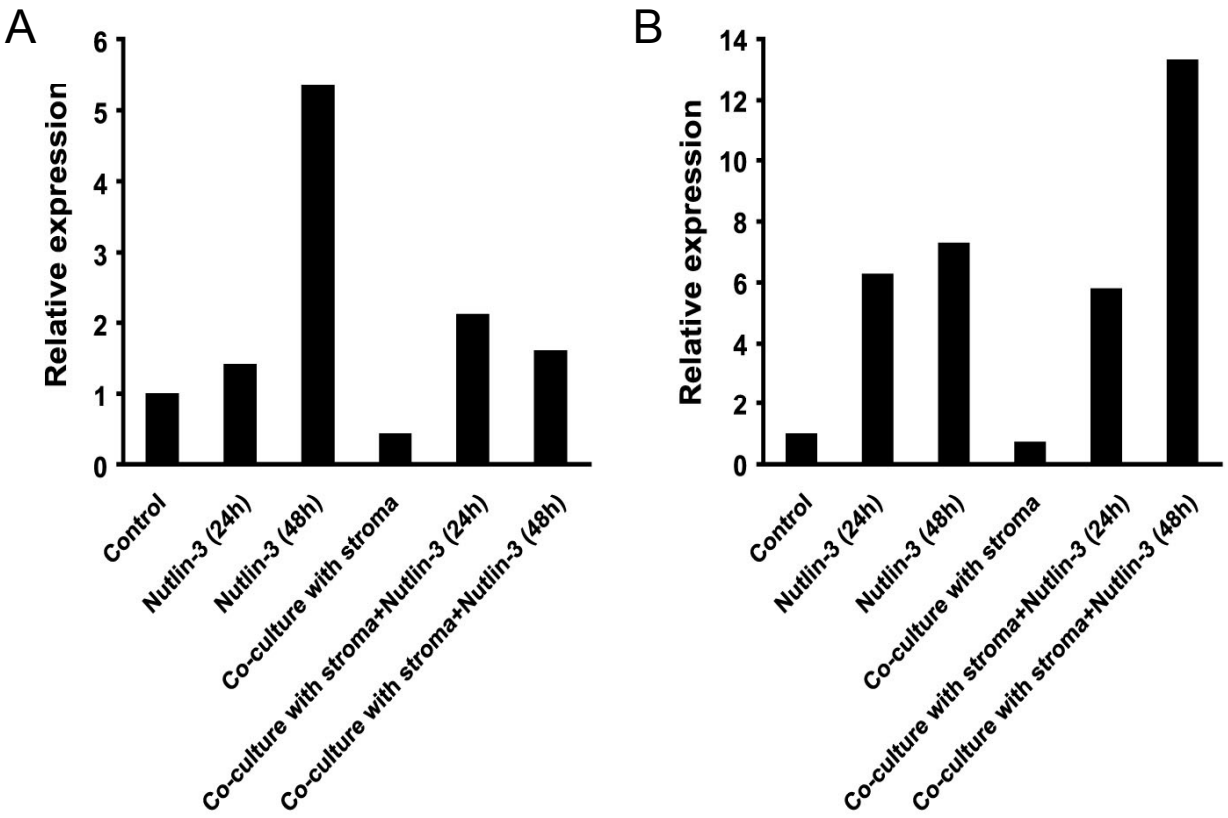

Fig. 3.2.6.3 Nutlin-3 is able to induce expression of Hdm2 and PUMA even in the presence of BMSCs in MM cells.

The effect of nutlin-3, in the presence or absence of BMSC, on the expression of Hdm2 (A) and PUMA (B) in MM cells. MM.1S-GFP/luc cells were treated with nutlin-3 (8 μM) for 0, 24 or 48 hours in the presence or absence of the BMSC line HS-5, and then sorted by FACS. Levels of Hdm2 and PUMA mRNA were quantified by qRT-PCR and expressed as a ratio relative to respective levels in control cells. Experiment was performed with three technical replicates.

3.2.7. Impact of bone marrow stroma cells on p53 activity and sensitivity to nutlin-3 in epithelial carcinoma cells

As noted above, the combination of nutlin-3 with bortezomib mediates additive cytotoxicity against MM cells, but triggers synergistic cytotoxicity against epithelial carcinoma cell lines. We investigated whether this latter effect persists in the presence of BMSC. This is important to evaluate as other cancer types also metastasise to the BM. Using the compartment-specific bioluminescence imaging (CS-BLI) approach, we evaluated the impact of BSMCs on the effect of the combination of nutlin-3 with bortezomib on MDA-MB-231 met-luc-neo cells stably transfected with a luciferase vector. Coculture with BSMCs did not protect against the synergistic pro-apoptotic effect of the combination of nutlin-3 with bortezomib in this epithelial carcinoma model (Fig. 3.2.7). These data suggest that the enhanced activity of nutlin-3 combined with bortezomib against epithelial models of cancer is unlikely to be inhibited by microenvironmental interactions.

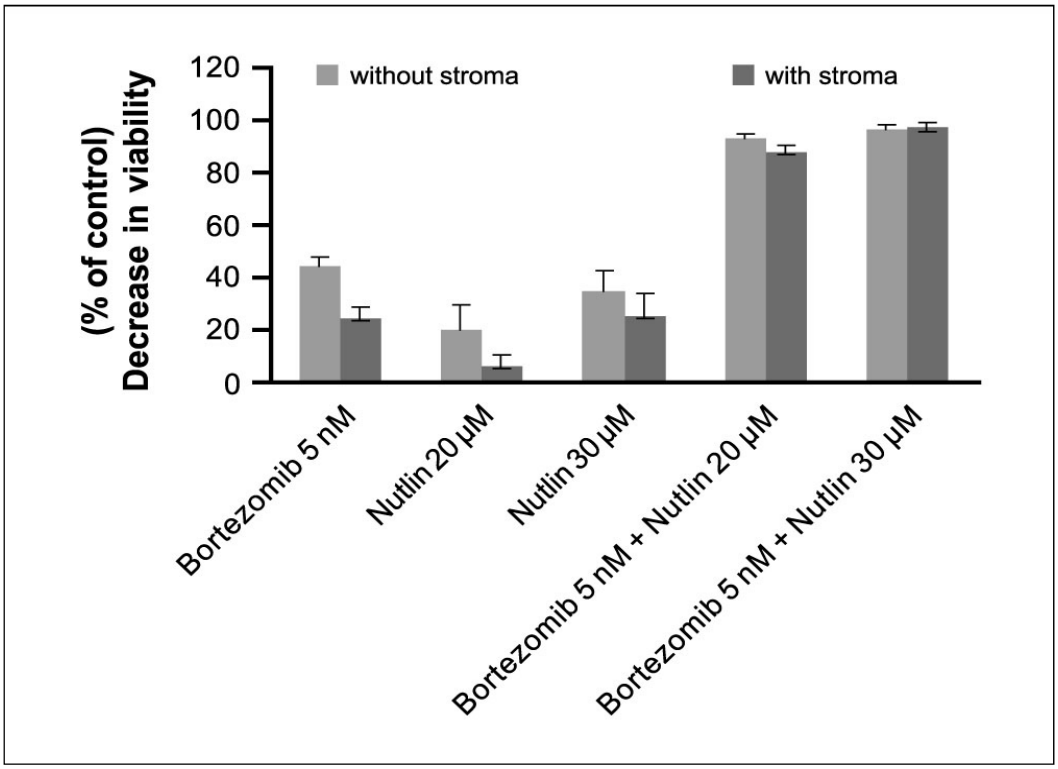

Fig. 3.2.7 Impact of coculture with BMSCs on effect of combined Hdm2 and proteasome inhibition.

MDA-MB-231met-LN cells stably expressing luciferase were treated with nutlin-3 (0, 20 or 30 µM) and bortezomib (5 nM) for 48 hrs, in the presence or absence of HS-5 stromal cells. MDA-MB-231met-LN viability was assessed using the compartment-specific bioluminescence imaging (CS-BLI) approach. Synergistic cytotoxicity of the combination of nutlin-3 and bortezomib persisted despite coculture with BMSCs. Experiment was performed in triplicate.

3.2.8. Transcriptional signature of nutlin-3 suppressed genes correlates with clinical outcome in bortezomib treated Multiple Myeloma patients.

To probe the clinical relevance of molecular sequelae triggered by nutlin-3, we next evaluated whether the transcriptional signature of tumour cell response to nutlin-3 treatment was enriched in genes which may correlate with clinical outcome. To test this hypothesis, a previously reported signature of genes suppressed in tumour cells by nutlin-3 treatment [180] was used to classify bortezomib-treated MM patients enrolled in phase II SUMMIT and phase III APEX trials into cohorts with high vs. low expression of nutlin-3-suppressed genes. Bortezomib-treated patients who had, at baseline, high expression of nutlin-3-suppressed genes had significantly shorter progression-free survival (panel A, p=0.001, log-rank test) and OS (panel B, p=0.002, log-rank test) compared to those with low expression levels (Fig 3.2.8). The clinical significance of this finding is discussed further in Section 4.2.7.

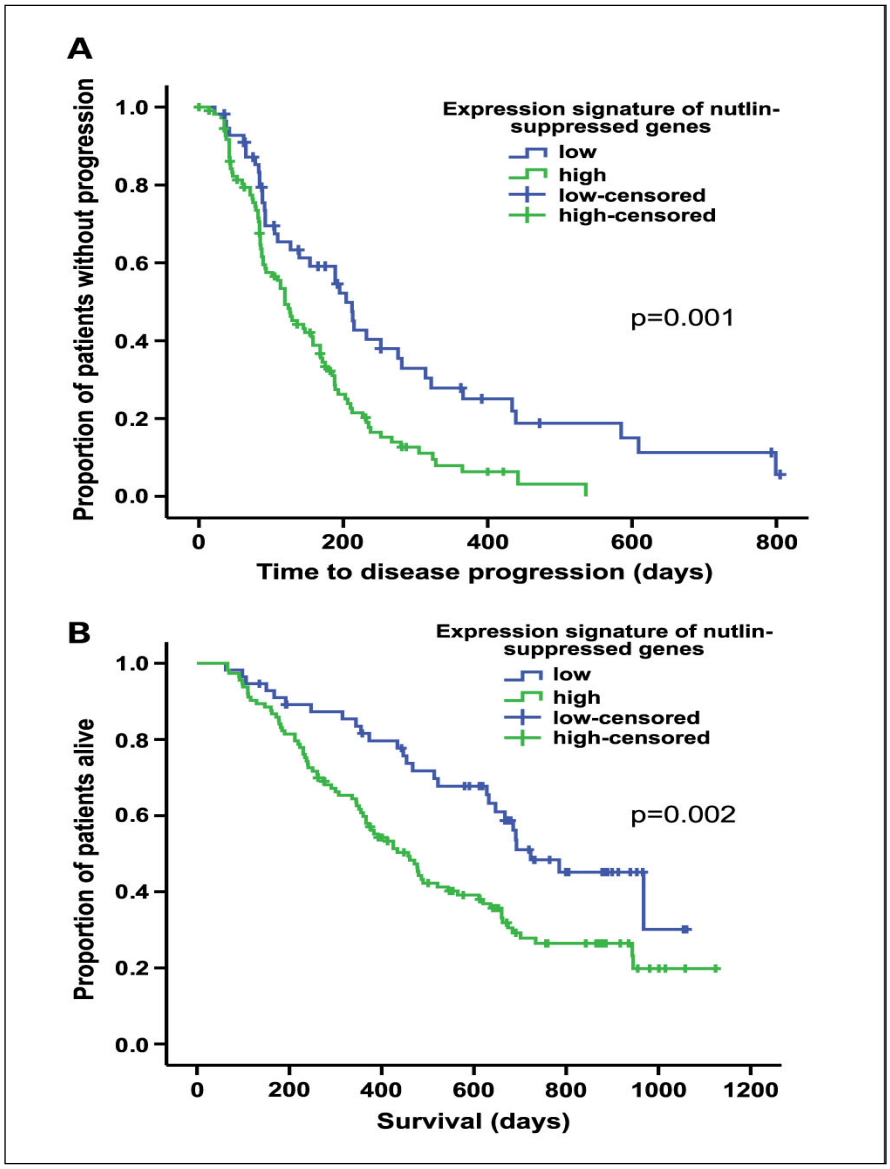

Fig. 3.2.8 A transcriptional signature of nutlin-responsive genes correlates with clinical outcome in bortezomib-treated MM patients.

Gene expression data were analyzed from tumour cells of bortezomib-treated MM patients (relapsed and/or refractory) enrolled in the phase II SUMMIT and phase III APEX trials. A previously reported signature of genes suppressed in tumour cells by nutlin-3 treatment was used to classify bortezomib-treated patients having high vs. low expression of nutlin-3-suppressed genes. Bortezomib-treated patients who had baseline high expression of nutlin-3-suppressed genes had significantly shorter progression-free (panel A, p=0.001, log-rank test) and OS (panel B, p=0.002, log-rank test) compared to those with low expression levels.

3.2.9. Nutlin-3 and bortezomib activity is independent of p53 .

There have been studies showing that nutlin-3 have activity in p53-deleted or p53-mutated cells, Nutlins are able to activate alternative transcription factors, in particular E2F1 [181, 182]. E2F1 can induce proliferation or apoptosis depending on the cell context and depending on the simultaneous activation of the Akt-prosurvival pathway [183]. Another study has demonstrated that nutlin-3 is able to induce apoptosis in p53-null cells through activation of p73 [184]. p73 is a homolog of p53 and is able to transactivate proapoptotic genes and induce cell death. It is also regulated by Mdm2. These two targets make nutlin a viable therapeutic option even when p53 is deleted or mutated.

To demonstrate if the synergy between bortezomib and nutlin-3 persists if p53 is not involved, we utilised two p53 mutated cell lines; OPM2 and ANBL6. Fig. 3.2.9.1 showed that in both these cell lines, there was synergistic cytotoxicity in the combination except for in the lower dose of bortezomib 2nM used in cell line OPM2. Calculated combination index using Calcusyn software showed in Table 3.2.9. Of note, these two cell lines are MM cell lines.

We then wanted to study if the combination of bortezomib and nutlin-3 would persist in a bortezomib-resistant cell line. Using the subline of ANBL6 which developed bortezomib resistance *in vitro* with repeated exposure to bortezomib 5nM; ANBL6-VR5 (courtesy of Dr Robert Orlowski, MD Anderson Cancer Center); we showed that the combination of bortezomib and nutlin-3 was effective in producing synergy as well (Fig. 3.2.9.2A). Table 3.2.9 demonstrated the combination index of the nutlin/bortezomib calculated using Calcusyn. Fig 3.2.9.2B demonstrated the attenuation of bortezomib in the resistant cell line ANBL6-VR5 compared to its parental control.

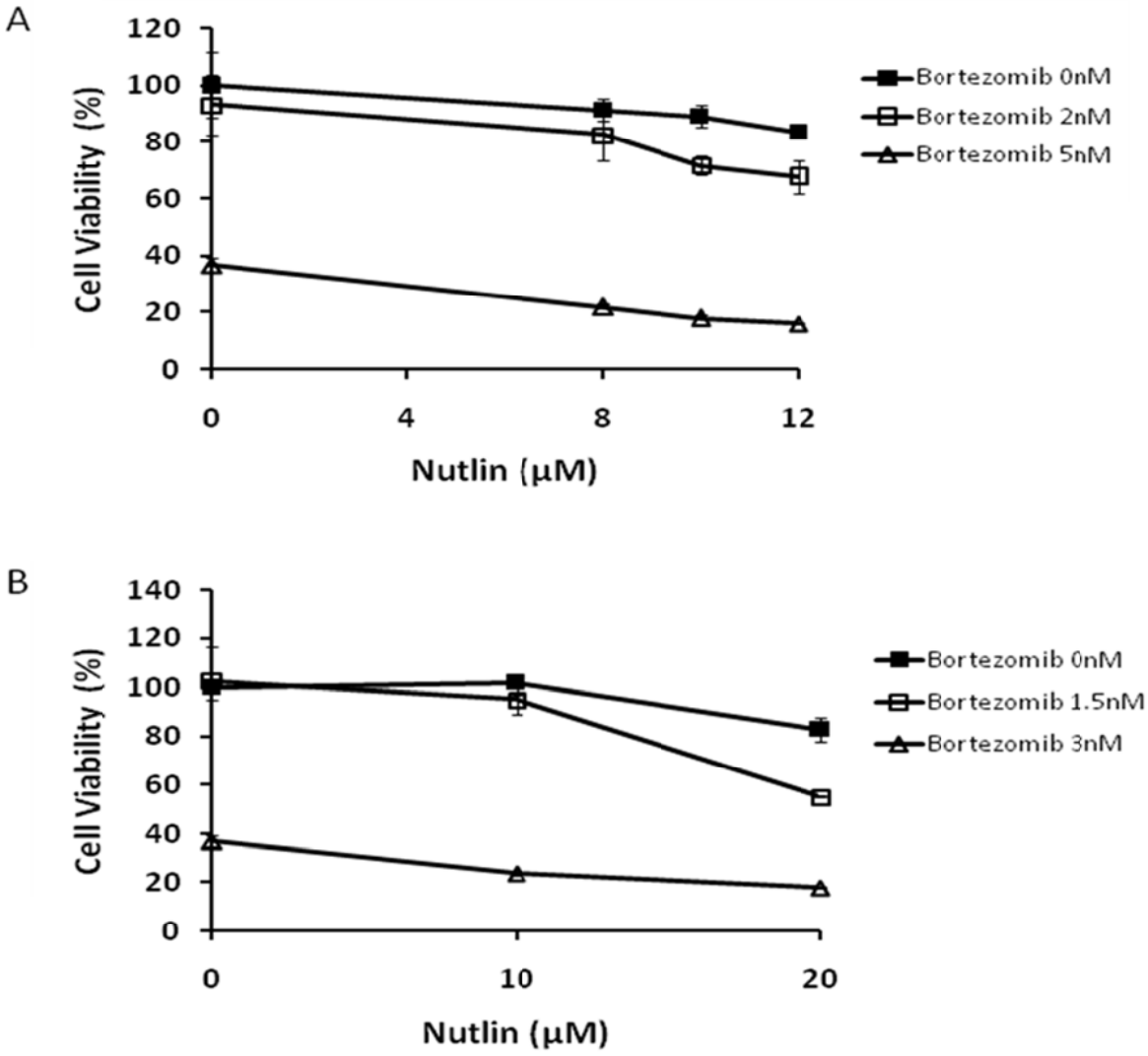

Fig. 3.2.9.1 Nutlin-3 and bortezomib combination demonstrates synergy independent of p53.

Nutlin-3 also potentiates the activity of bortezomib against MM cell lines that are p53 mutated. (A) OPM2 cells were treated for 48h with nutlin-3 (0-12 μM) in the absence (■) or presence of bortezomib (□ : 2nM ;△ : 4nM). (B) ANBL6 cells were treated for 48h with nutlin-3 (0-20 μM) in the absence (■) or presence of bortezomib (□ : 1.5 nM, :△ 3 nM). Cell survival was quantified by MTT and expressed as a percentage (mean±SD) relative to vehicle-treated controls. Experiment was performed in triplicate.

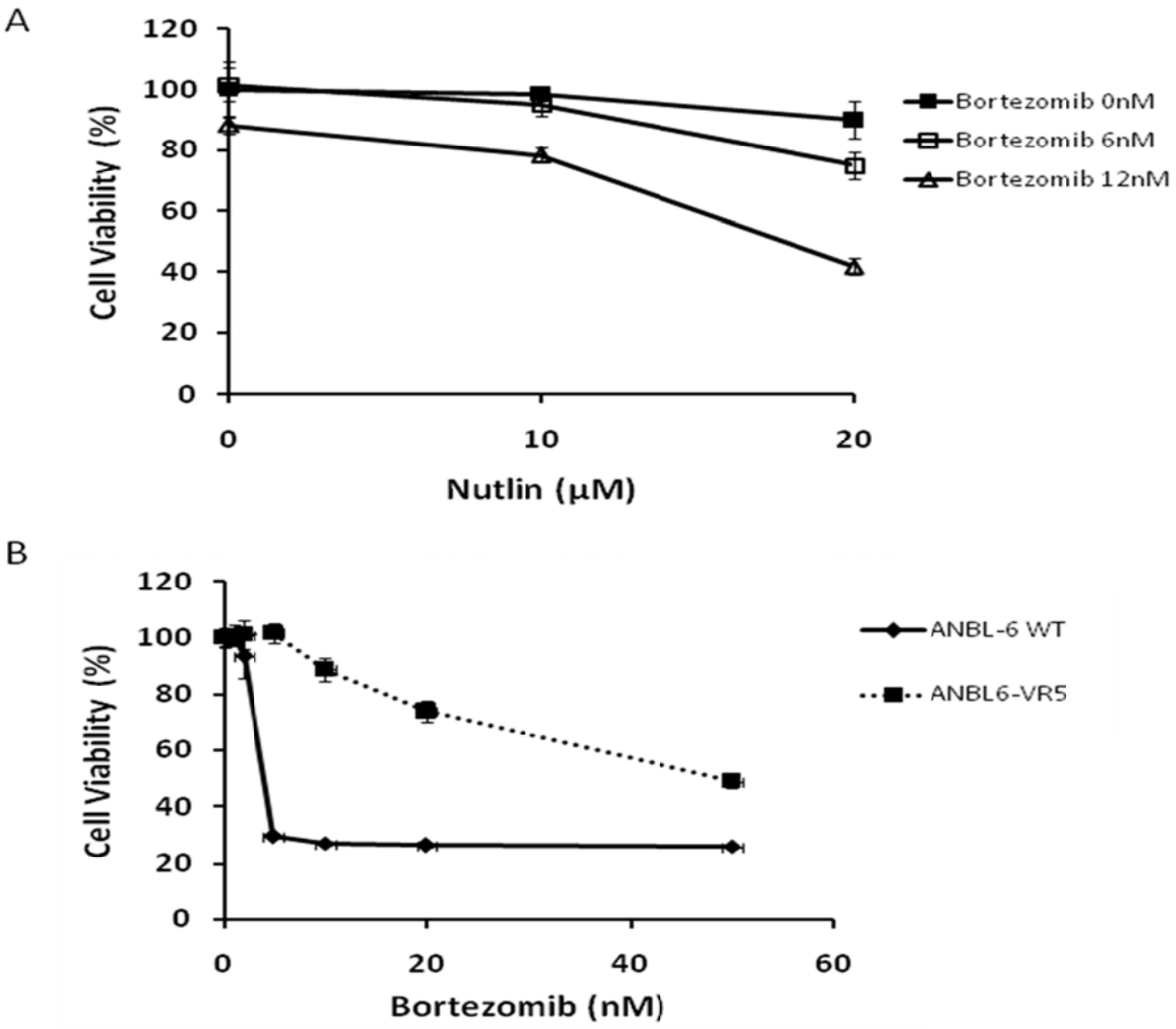

Fig. 3.2.9.2 ANBL6-VR5 demonstrates synergy in bortezomib and nutlin-3 combination.

Nutlin-3 also potentiates the activity of bortezomib against a bortezomib resistant MM cell line; ANBL6-VR5. (A) ANBL6-VR5 cells were treated for 48h with nutlin-3 (0-20 μM) in the absence (■) or presence of bortezomib (□: 6 nM,△ : 12 nM). (B) ANBL6-VR5 demonstrate cross resistance to bortezomib compared to ANBL6-WT (parental cell line). Cell survival was quantified by MTT and expressed as a percentage (mean±SD) relative to vehicle-treated controls. Experiment was performed in triplicate.

Cell lines	Nutlin (ìM)	Bortezomib (nM)	Fraction affected	CIN
OPM2	8	2	0.17389	1.362
	8	5	0.78176	0.94
	10	2	0.282	1.168
	10	5	0.82063	0.897
	12	2	0.323	1.177
	12	5	0.83962	0.884
ANBL6	10	1.5	0.04951	0.971
	10	3	0.76244	0.904
	20	1.5	0.44693	0.651
	20	3	0.82083	0.896
ANBL6-VR5	10	6	0.04933	1.035
	10	12	0.2169	0.787
	20	6	0.24912	0.807
	20	12	0.58065	0.61

Table 3.2.9 Combination index for Nutlin-3 plus Bortezomib in p53 mutated cell lines

Using Calcusyn software, the combination index (CIN) for the combination of Nutlin-3 and bortezomib was calculated. For the p53 mutated cell lines, the CIN was <1 for all cell lines except for the combination of nutlin with bortezomib 2nM in OPM2 cell line, demonstrating synergy. (Synergy - CIN<0.9, additive effect - CIN >0.9).

3.3. Activation of AMP-kinase pathway as an alternative to overcome drug resistance in Multiple Myeloma

3.3.1. Introduction

Several groups have reported that activation of AMPK suppresses mTOR signalling by growth factors and amino acids [198-200]. Activation of AMPK by metformin, AICAR or thiazolidinediones or expression of constitutively active mutants has been shown to cause apoptosis or cell cycle arrest of various cancer cells.

PI3K-Akt-mTOR signalling is important in MM. In fact, perifosine, an Akt inhibitor, is already in clinical trials after having good preclinical activity in MM [211]. AMPK activation as an anticancer strategy has only begun to be studied but current preclinical data is encouraging. We are interested in this pathway as a novel and perhaps alternative pathway to overcome drug resistance in MM.

3.3.2. Activity of Metformin on cancer cell lines

A panel of MM and solid tumour cell lines were treated with metformin (0.1-5mM) for a period of 96 h, and viability was assessed by MTT colorimetric survival assay (Fig. 3.3.2.1). MM cell lines were sensitive to metformin, with comparable or decreased sensitivity seen in solid tumour cell lines.

BM microenvironmental factors confer a protective effect on MM cells against several conventional anti-MM agents, such as dexamethasone or cytotoxic chemotherapy [44]. Therefore, we next investigated the effect of coculture with BMSCs and differentiated osteoclasts on the sensitivity of metformin. Three MM cell lines, NCI-H929-GFP/luc, JJN3-GFP/luc and MM.1S-GFP/luc cells were treated with metformin, in the presence or absence of HS-5 stromal cells or differentiated osteoclasts (Fig. 3.3.2.2), and the viability assessed by compartment-specific bioluminescence imaging (CS-BLI). Metformin was as or more active in the presence of stromal cells or osteoclasts across the range of concentrations tested.

Fig. 3.3.2.3 demonstrated the signalling pathways that were activated by metformin treatment. RPMI8226 cells treated with metformin 10mM demonstrated activation of phospho-AMPK (Thr 172) and AMPK with subsequent downregulation of phospho-

p70S6k (Thr 389), p70S6k, phospho-S6 ribosomal (Ser 235/236) and S6 ribosomal protein as early as 8hr after treatment (Fig. 3.3.2.3). Cell cycle proteins (Cyclin D1, Cdk4, Cyclin B1 and Cdc2) were also downregulated by metformin treatment (Fig. 3.3.2.3). By 8 hrs of treatment, metformin was able to decrease the levels of Cyclin D1.

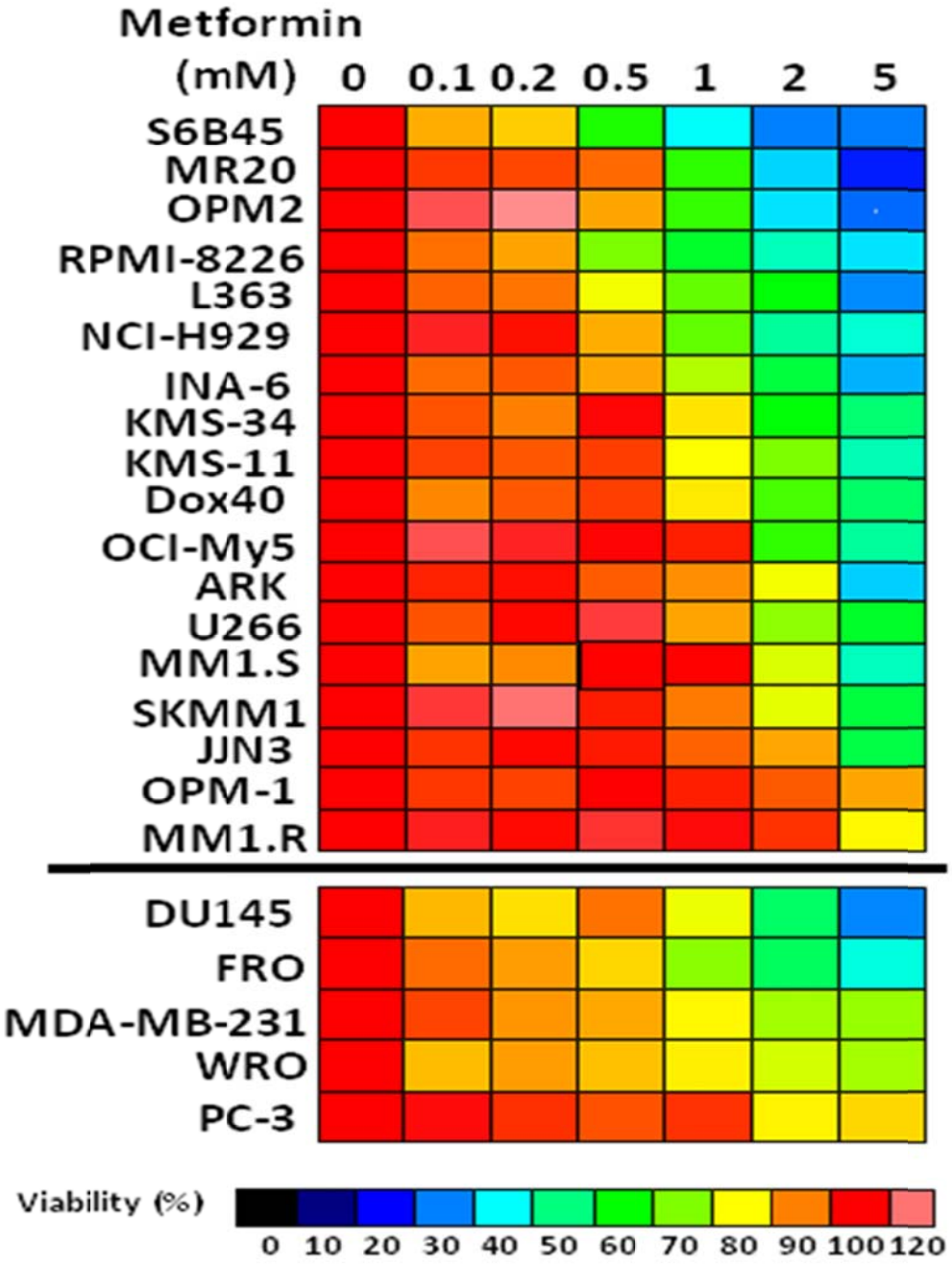

Figure 3.3.2.1 Antimyeloma activity of Metformin.

A panel of MM (upper panel) and solid tumour cell lines (lower panel) were treated with Metformin (0.1-5mM) for a period of 96 h, and viability was assessed by MTT assay. Cell viability was calculated as percentage of vehicle treated control and expressed as a heat map. Experiment was performed in triplicate.

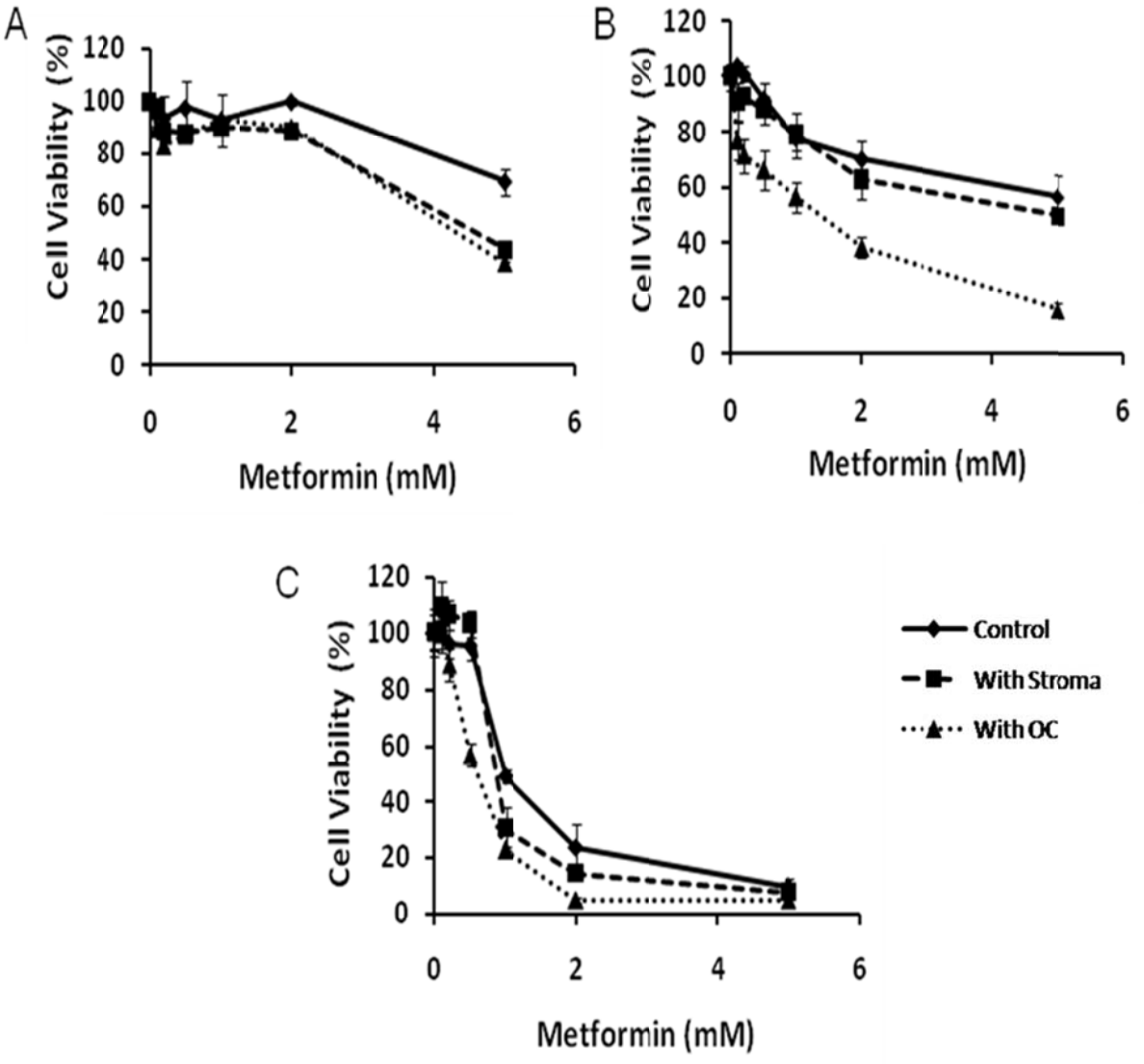

Fig. 3.3.2.2 Metformin is able to overcome BM microenvironmental protective effect.

Using the compartment-specific bioluminescence imaging (CS-BLI) approach, we evaluated the effect of Metformin on (A) NCI-H929-GFP/luc cells, (B) JJN3-GFP/luc cells and (C) MM.1S-GFP/luc cells cultured in the presence vs. absence of HS-5 stromal cells or mature osteoclasts for 96 h. Metformin is as or more active in the presence of stromal cells or osteoclasts across the range of concentrations tested. Experiment was performed in triplicate.

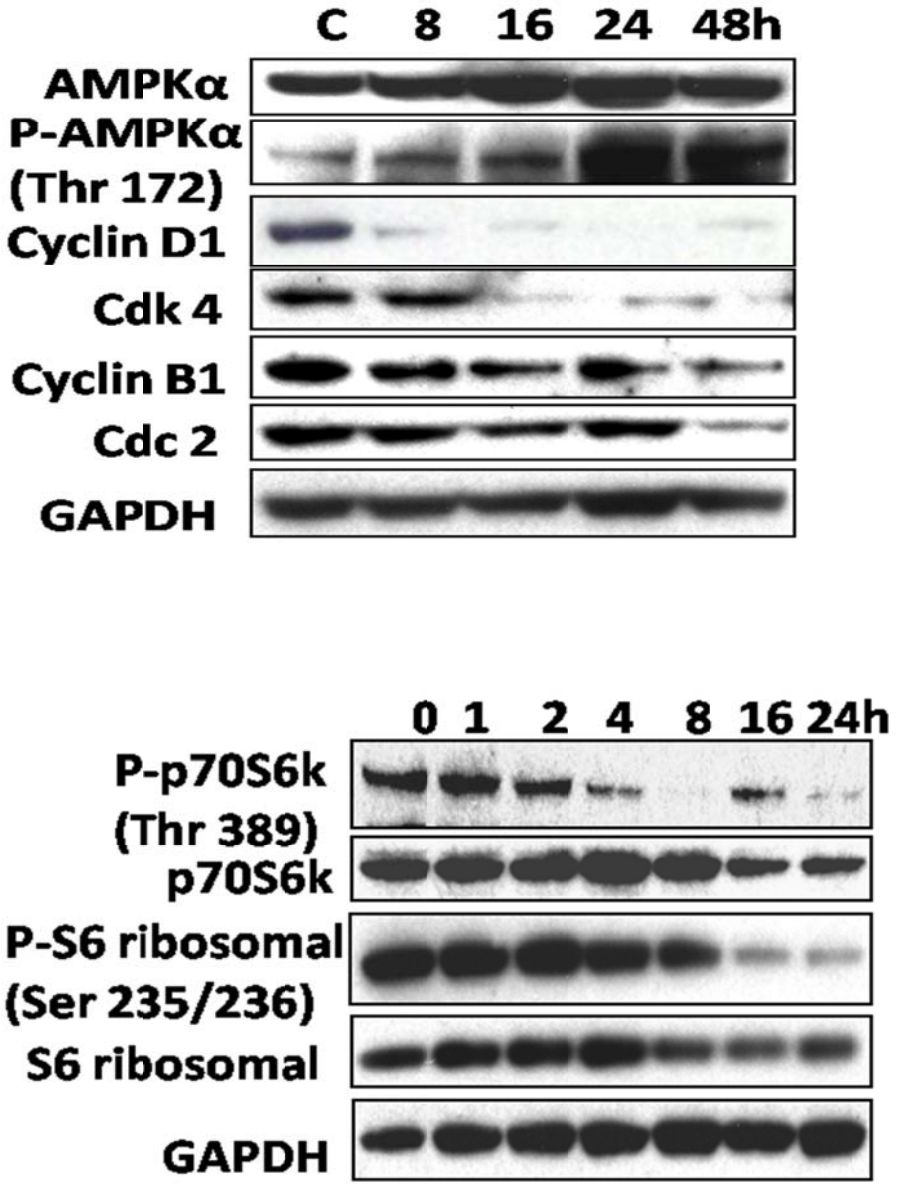

Figure 3.3.2.3 Metformin signalling pathway.

Metformin signalling pathways are demonstrated in Western blots. RPMI8226 cells treated with metformin 10mM demonstrated activation of AMPK and downregulation of p70S6k and s6 ribosomal proteins (lower panel). Cell cycle proteins (cyclin D1, cdk4, cyclin B1 and cdc2) were also downregulated by metformin treatment (upper panel). GAPDH levels were used as loading control.

3.3.3. Activity of AICAR on cancer cell lines

We next evaluated another AMPK activator, AICAR. A panel of MM and solid tumour cell lines were treated with AICAR (20-1000μM) for a period of 96 hrs, and viability was assessed by MTT colorimetric survival assay (Fig. 3.3.3.1). MM cell lines were sensitive to AICAR with decreased cell viability upon treatment. Solid tumour cell lines were also sensitive to AICAR, although typically to a lesser extent than MM cells.

As metformin was able to overcome the BM microenvironmental effects, we wanted to investigate if AICAR was also able to overcome stromal and osteoclast-derived protection of MM cells. NCI-H929-GFP/luc, JJN3-GFP/luc and MM.1S-GFP/luc cells were treated with AICAR, in the presence or absence of HS-5 stromal cells or differentiated osteoclasts (Fig. 3.3.3.2), and the viability assessed by compartment-specific bioluminescence imaging (CS-BLI). AICAR was more active in the presence of stromal cells or osteoclasts across the range of concentrations tested.

The signalling pathway of AICAR was examined next. RPMI8226 cells treated with 150μM AICAR was able to activated AMPK with an increase in phospho-AMPK (Thr 172) as shown on Western blot (Fig. 3.3.3.3). There was also a corresponding decrease of phospho-GSK3α/β (Ser 21/9), GSK3α/β, phospho-p70S6k (Thr 389), phospho-S6 ribosomal (Ser 235/236) and S6 ribosomal protein (Fig. 3.3.3.3). Cell cycle proteins such as Cyclin D1, Cdk4, and Cdc2 were also downregulated by AICAR treatment. In fact, by 16 hrs, Cyclin D1 levels were no longer detectable. However, Cyclin B1 showed a late increase with AICAR treatment.

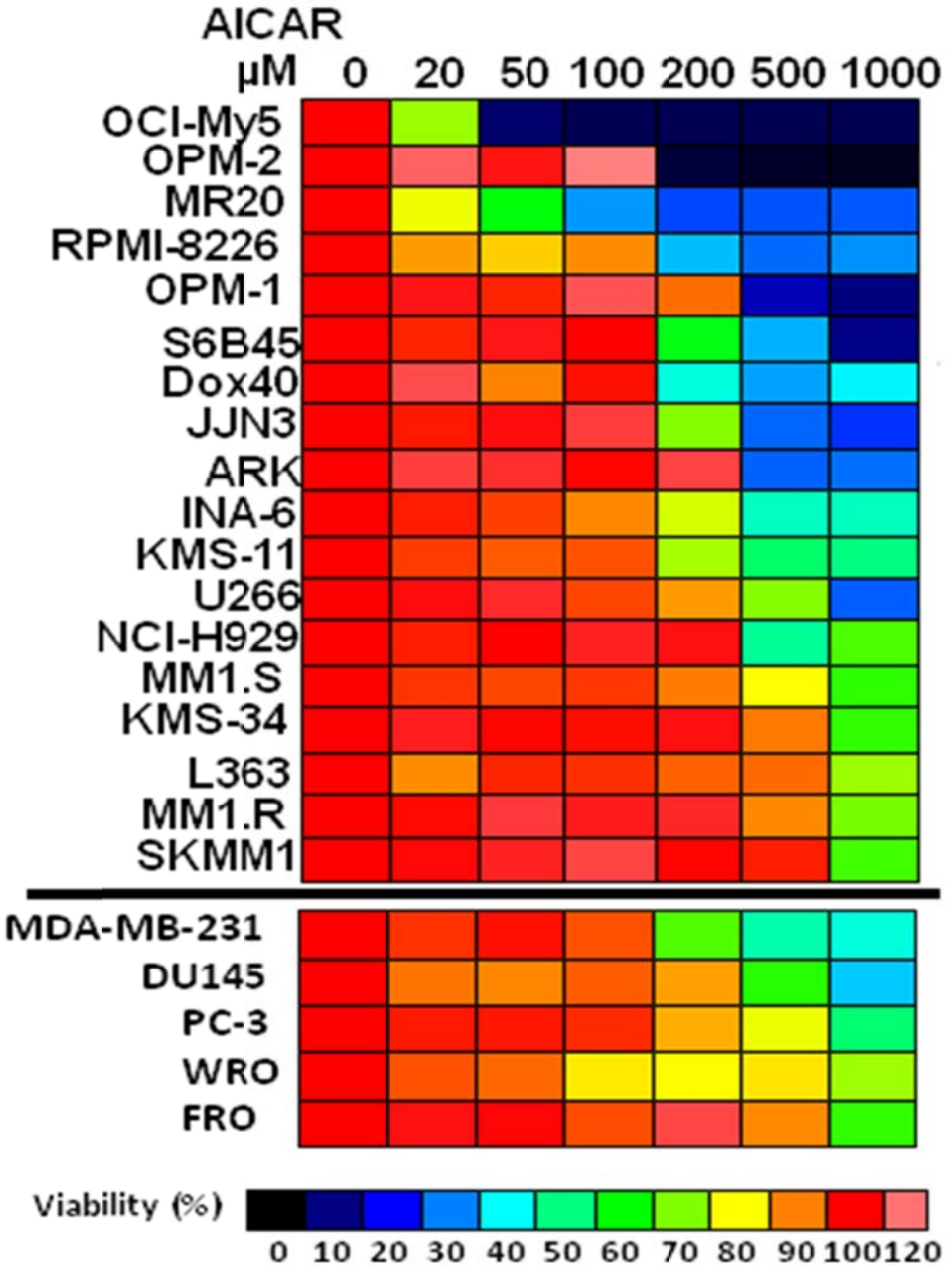

Figure 3.3.3.1 Antimyeloma activity of AICAR.

A panel of MM (upper panel) and solid tumour cell lines (lower panel) were treated with AICAR (20-1000μM) for a period of 96 h, and viability was assessed by MTT assay. Cell viability was calculated as percentage of vehicle treated control and expressed as a heat map. Experiment was performed in triplicate.

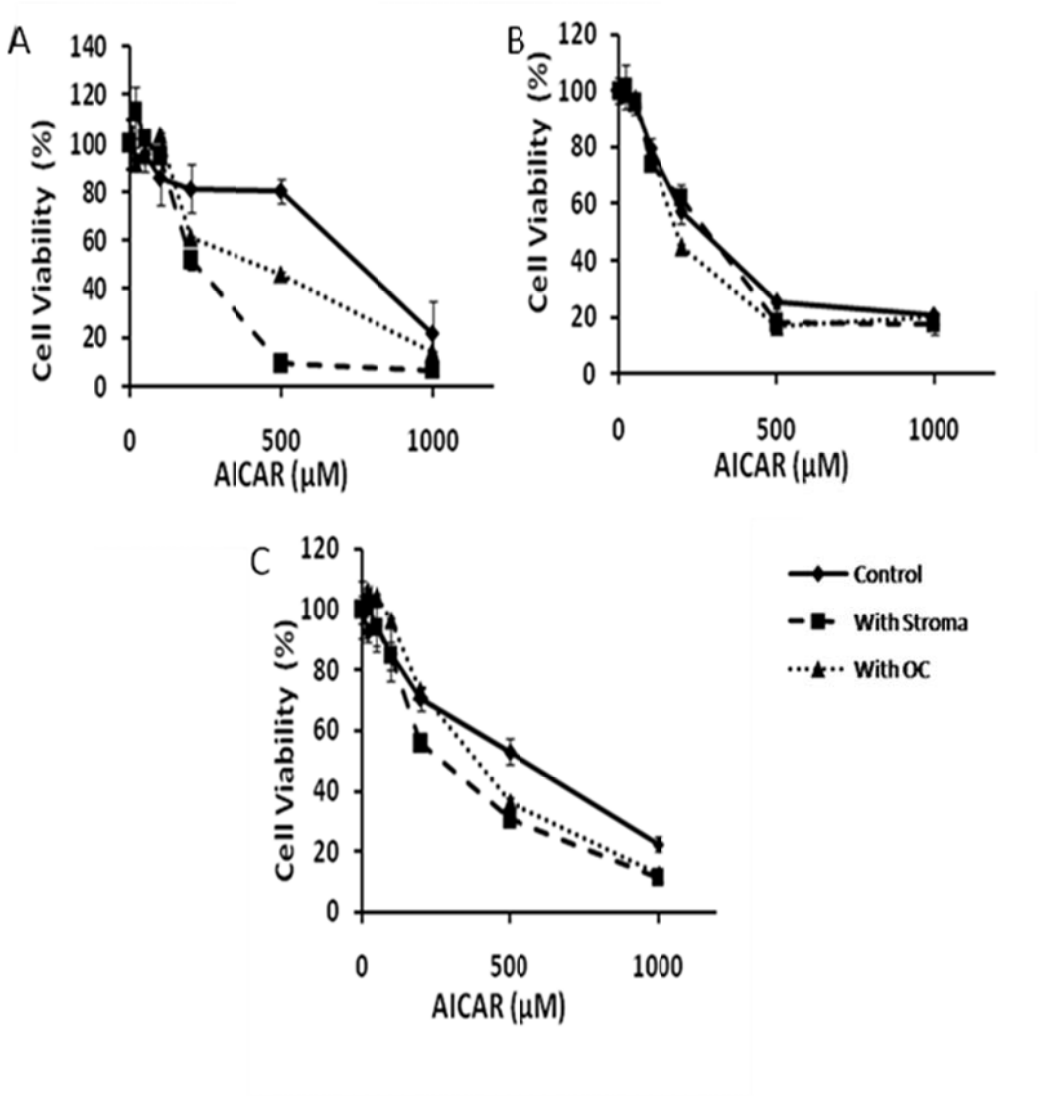

Figure 3.3.3.2 AICAR overcomes the protective effects of microenvironmental factors.

Using the compartment-specific bioluminescence imaging (CS-BLI) approach, we evaluated the effect of AICAR on (A) NCI-H929-GFP/luc cells, (B) JJN3-GFP/luc cells and (C) MM.1S-GFP/luc cells cultured in the presence vs. absence of HS-5 stromal cells or mature osteoclasts for 96 h. AICAR was more active in the presence of stromal cells or osteoclasts across the range of concentrations tested. Experiment was performed in triplicate wells. Cell survival was expressed as percentage (mean ± SD) compared to vehicle treated control.

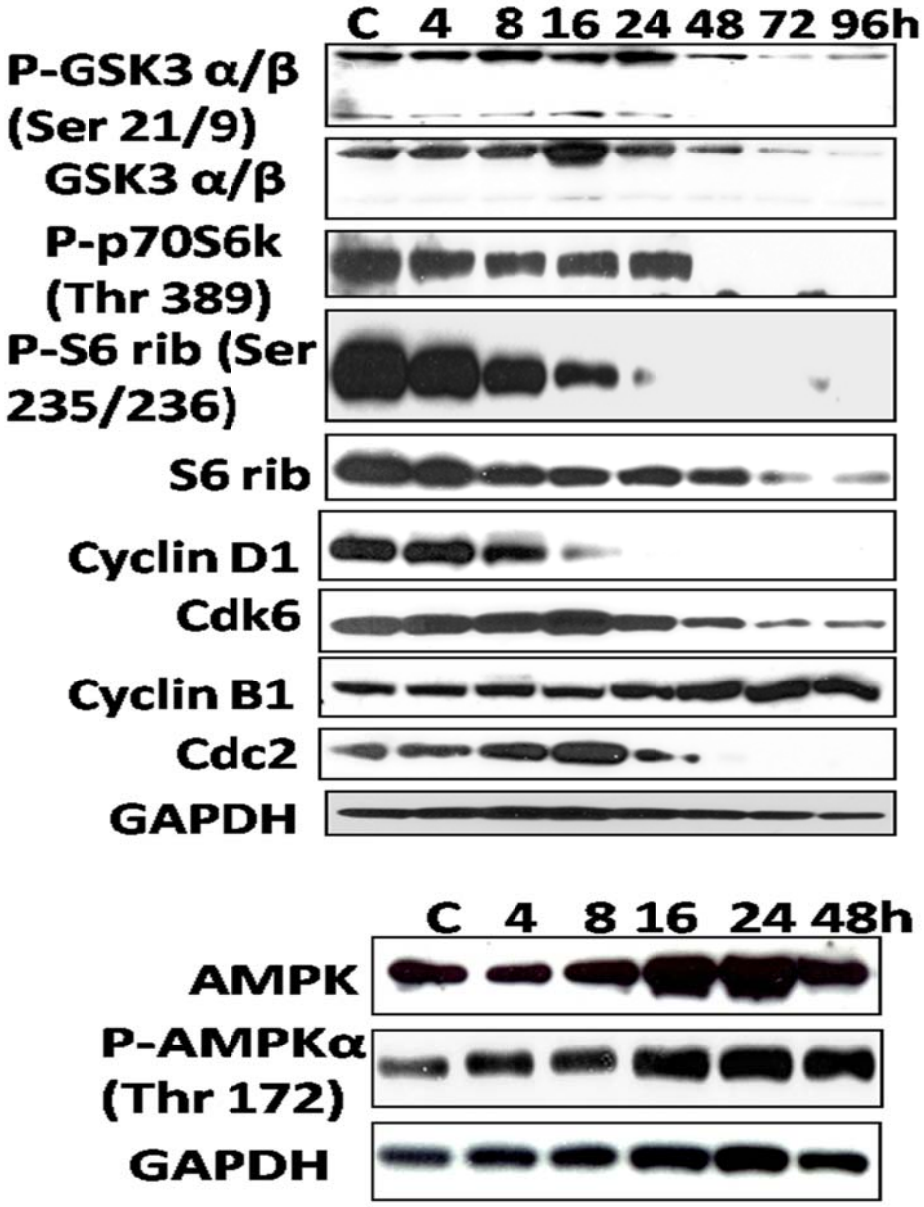

Figure 3.3.3.3 AICAR signalling pathway

AICAR signalling pathways are demonstrated by Western blots. RPMI8226 cells treated with AICAR 150μM showed activation of AMPK and downregulation of p70S6k, s6 ribosomal and GSK3 as well as their phosphorylated counterparts. Cell cycle proteins (cyclin D1, Cdk6, cyclin B1 and cdc2) were also downregulated by AICAR treatment. GAPDH levels were used as loading control.

3.3.4. Activity of AICAR and Metformin on patient samples

Bone marrow aspirates from MM patients were processed using Miltenyi anti-CD138 microbeads for purification of MM cells. These patient tumour cells were treated with increasing doses of AICAR for 96h and viability assessed. AICAR induced cytotoxicity in 3 / 4 MM patient samples, with IC50 values <500 μM (Fig. 3.3.4A). Metformin activity on patient samples was also tested. Only 1 / 3 MM patient showed a response to metformin. This data suggest that AICAR may be the more potent and broadly active anti-MM agent of the two.

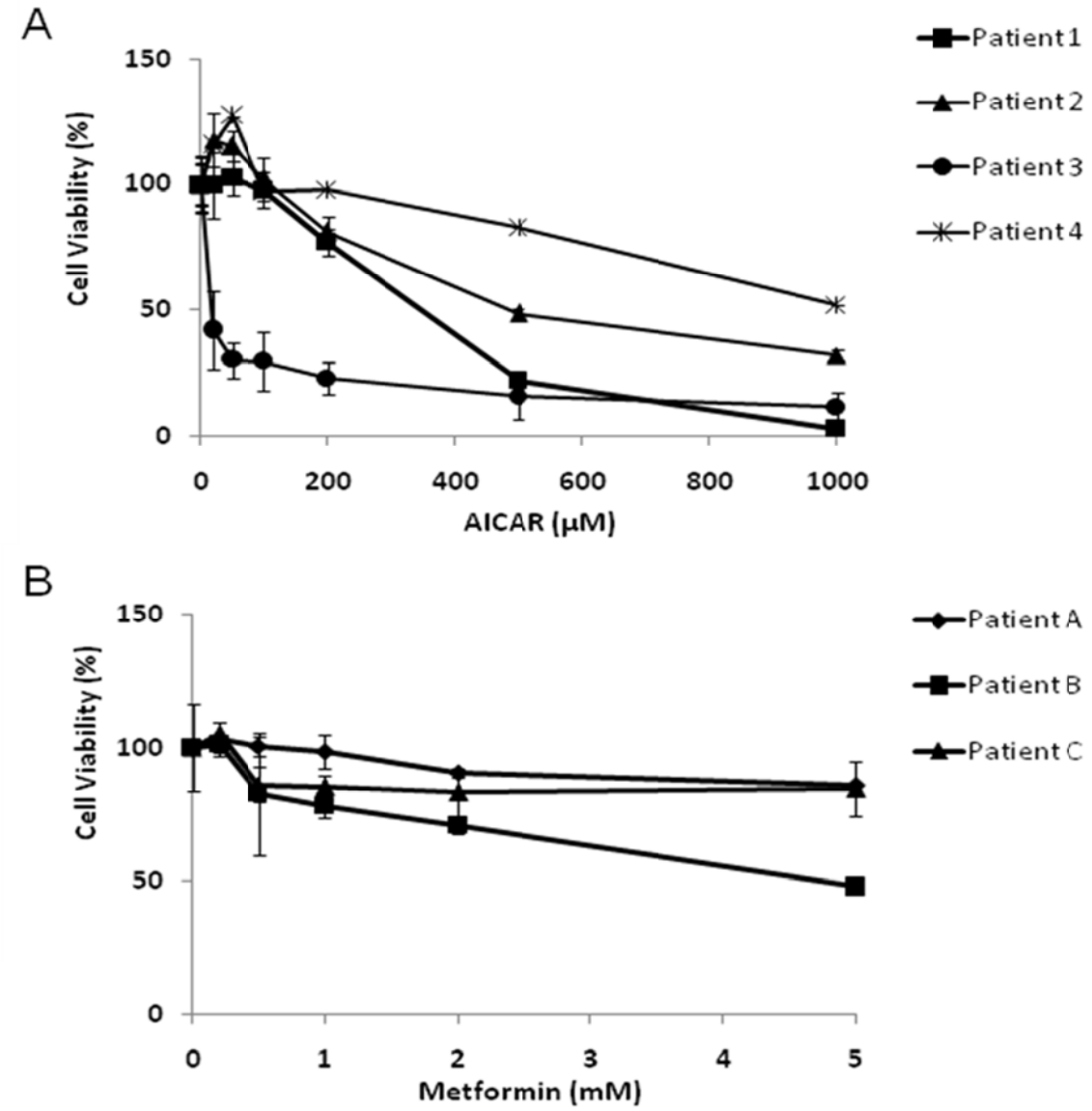

Figure 3.3.4 Activity of AICAR and Metformin on patient samples

Bone marrow aspirates from MM patients were processed using Miltenyi anti-CD138 microbeads for purification of MM cells. Viability of MM cells treated with or without increasing doses of AICAR (A) and metformin (B) for 96h was assessed by CellTitreGlo assay and measured by a luminometer. Experiment was performed in quadruplet wells. Cell survival was expressed as percentage (mean ± SD) compared to vehicle treated control.

3.3.5. Activity of AICAR and Metformin on non-neoplastic cells

We next evaluated the impact of AICAR on non-neoplastic tissues. Non-malignant cells were also treated with AICAR, and their viability was assessed by MTT assay. The BMSC line HS-5 and the immortalized hepatocyte cell line THLE-3 were shown to be insensitive to AICAR with calculated EC_{50} values >1000μM (Fig. 3.3.5.1). In addition, PBMCs from healthy donors were PHA-stimulated to induce their cycling and proliferation, which resulted in a 2.7-5.7 fold increase in the number of viable cells following 96 h of culture. Moreover, the percentage of viable PBMCs was >50% AICAR treatment, suggesting a favourable therapeutic index (Fig. 3.3.5.2).

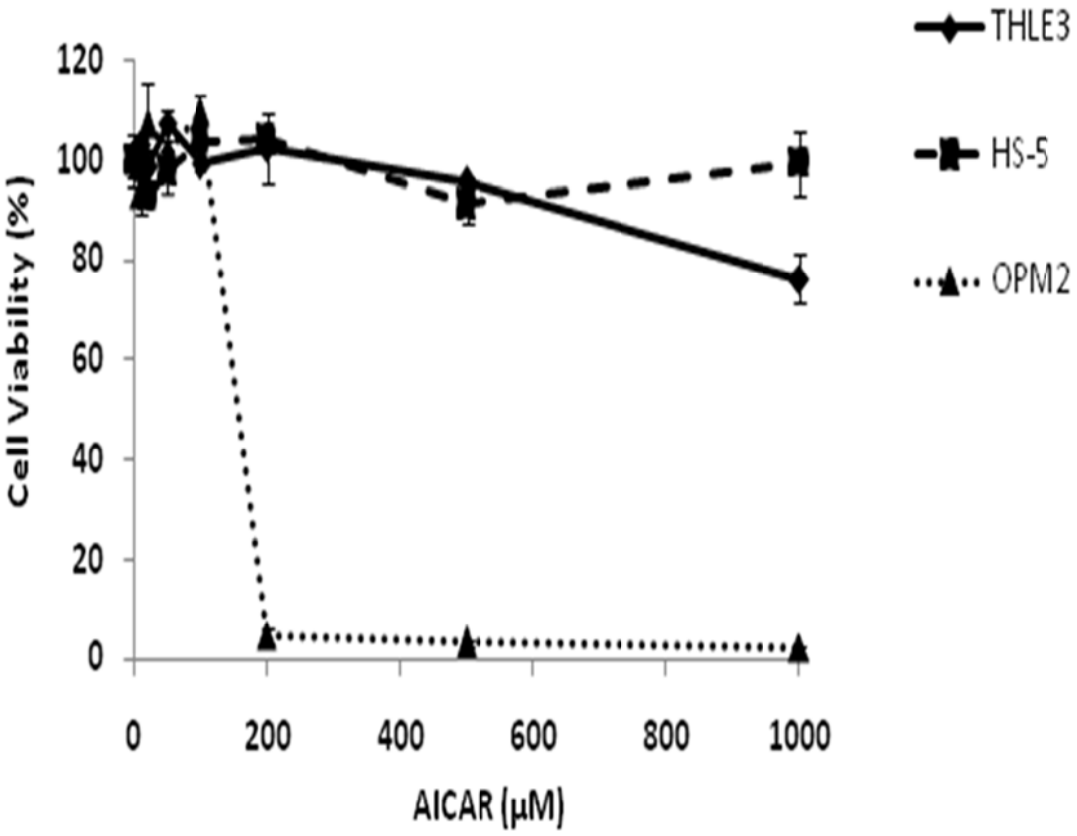

Figure 3.3.5.1 Activity of AICAR on non-neoplastic cells

Nonmalignant cells were also treated with AICAR, and their viability was assessed by MTT assay. The BMSC line HS-5 and the immortalized hepatocyte cell line THLE-3 were exposed to AICAR (20-1000μM) for 96h and compared with the MM cell line OPM2. Experiment was performed in triplicate.

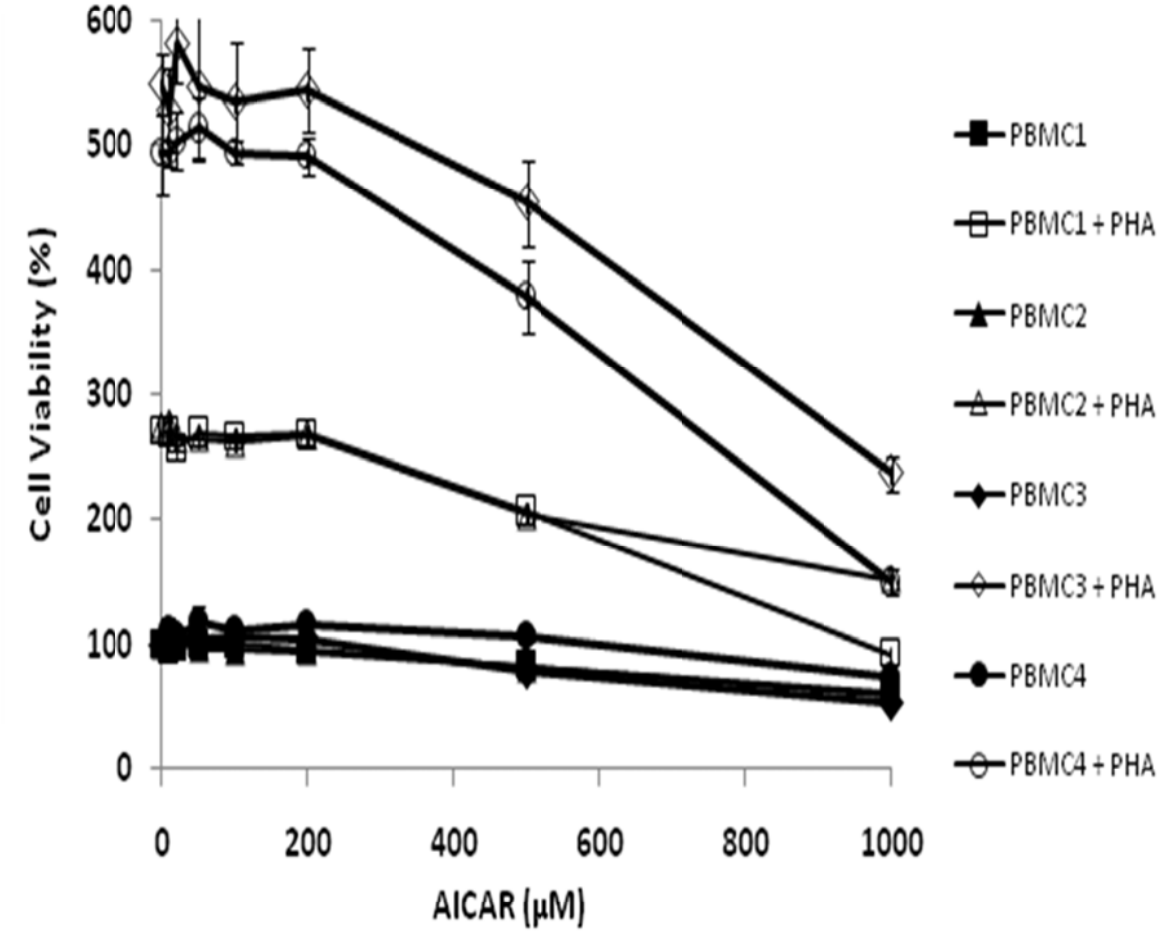

Figure 3.3.5.2 Activity of AICAR on non-neoplastic cells

Both unstimulated and PHA (5 µg/mL)–stimulated PBMCs were exposed to AICAR (20-1000µM) for 96h, and their viability was assessed by MTT. Due to cell stimulation, there was an increase in viable PBMCs following 96h in the absence of the drug; cells remained >50% viable at drug concentrations up to 1000µM. Values were normalized to the non-stimulated drug-free control. Experiment was performed in triplicate wells.

3.3.6 The AMPK inhibitor Compound C does not attenuate the direct anticancer activity of metformin

Both metformin (indirect AMPK activator) and AICAR (direct AMPK activator) have demonstrated anticancer activity in our *in vitro* models. We wanted to examine the impact of AMPK inhibition on the anticancer activity of metformin. Compound C is known to function as an ATP-competitive inhibitor of AMPK. We found that the AMPK inhibitor compound C did not attenuate the anticancer activity of metformin against RPMI8226, MM1.S and FRO cells (Fig. 3.3.6.1). These results suggest that, while direct AMPK activation (by AICAR) can have anticancer activity, metformin itself can also promote AMPK-independent anticancer effects.

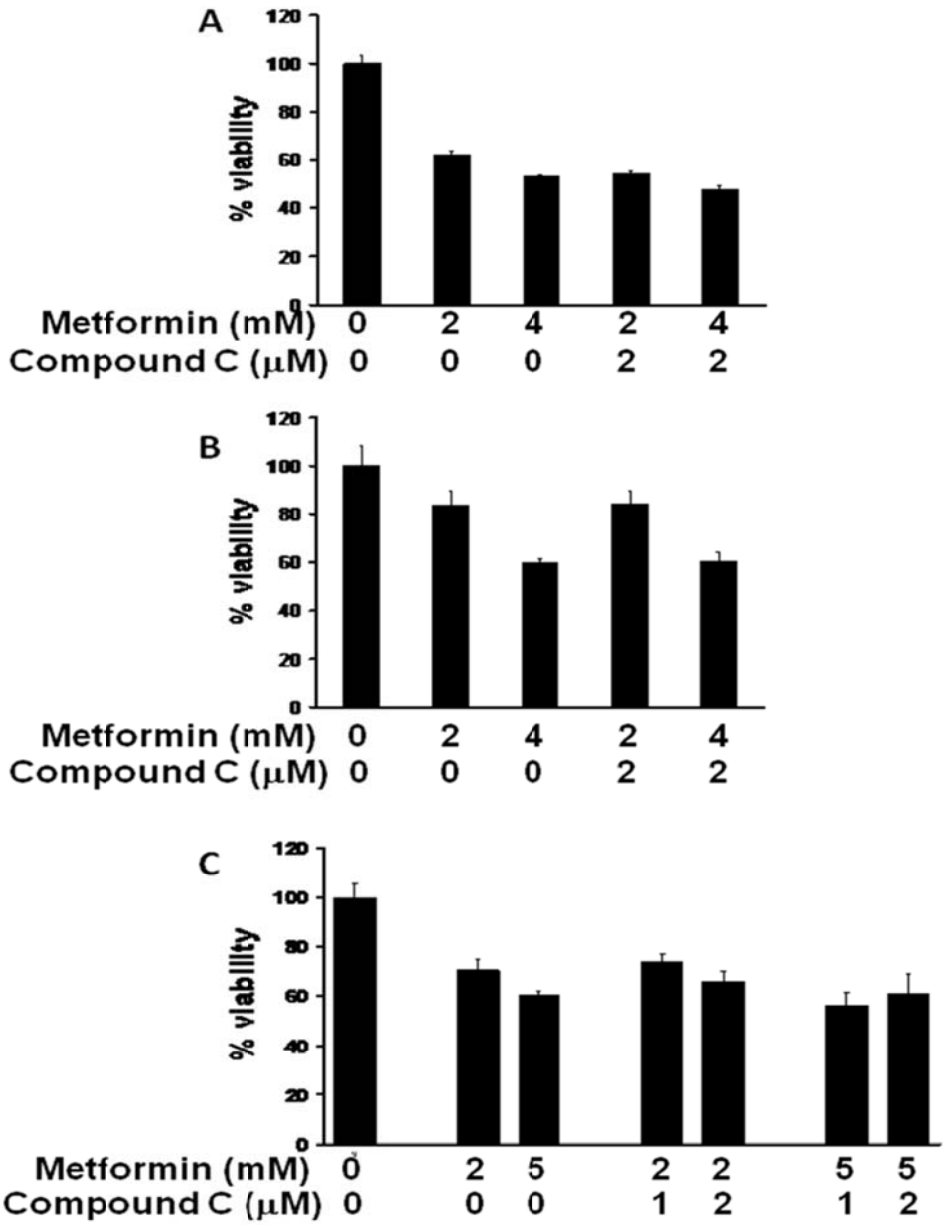

Figure 3.3.6 The AMPK inhibitor Compound C does not attenuate the direct anticancer activity of metformin.

RPMI8226 (A), MM1.S (B) and FRO (C) cells were treated with metformin at the indicated concentrations for 96 hrs in the presence or absence of the AMPK inhibitor compound C.. Experiment was performed in triplicate wells. Cell survival was expressed as percentage (mean ± SD) compared to vehicle treated control.

3.3.7. Analysis of effect of AICAR and Metformin on induction of apoptosis and mitochondrial membrane depolarization in Multiple Myeloma cells

Western blot analysis of RPMI8226 cells treated with 150 μM AICAR revealed molecular signalling events consistent with initiation of cell death. By 24 hrs of AICAR treatment, apoptosis was associated with cleavage of caspase 3 and PARP (Fig. 3.3.7.1).

We next carried out Annexin V/PI staining on MM cells exposed to AICAR and metformin. RPMI8226 cells were exposed to 150 μM of AICAR and 2mM of metformin for 0-96 hrs. Cells were collected, washed, stained for Annexin V and propodium iodide (PI), and analyzed using flow cytometry. Annexin V detects apoptotic events whilst PI detects necrotic events. Exposure to AICAR resulted in time-dependent increases in only Annexin V positive events, with increased Annexin V+, PI+ events at later time points, indicating apoptotic cell death of RPMI8226 cells (Fig. 3.3.7.2). However, treatment with metformin 2mM showed mild increase in non-viable cells but not through apoptosis (Fig. 3.3.7.3). These data suggest that AICAR is more effective in killing MM cells as they have the added advantage of being able to cause cell death through the apoptosis mechanism, whereas metformin seem to act in a cytostatic manner as there is decrease in viability (Section 3.3.2) but little apoptosis or even necrosis seen in Annexin V/PI staining. The amount of necrotic cell death with Annexin V/PI staining was 26% (Fig. 3.3.7.3) vs. 54% calculated cell death seen with MTT (Fig. 3.3.7.4).

The JC-1 assay was utilised to study the mitochondrial membrane potential. JC-1 dye exhibits potential-dependent accumulation in the mitochondria, indicated by a fluorescence emission shift from green (~529nm) to red (~590nm). The green fluorescence measures JC-1 monomers and the red fluorescence measures JC-1 aggregates. Consequently, mitochondrial depolarization is indicated by a decrease in the red/green fluorescence intensity ratio caused by accumulation of the monomers. RPMI8226 cells were exposed to 150 μM of AICAR (Fig. 3.3.7.5) and 2mM of metformin (Fig. 3.3.7.6), stained with JC-1 dye and analyzed using flow cytometry. AICAR, but not metformin, caused mitochondrial membrane depolarization by 24 hrs.

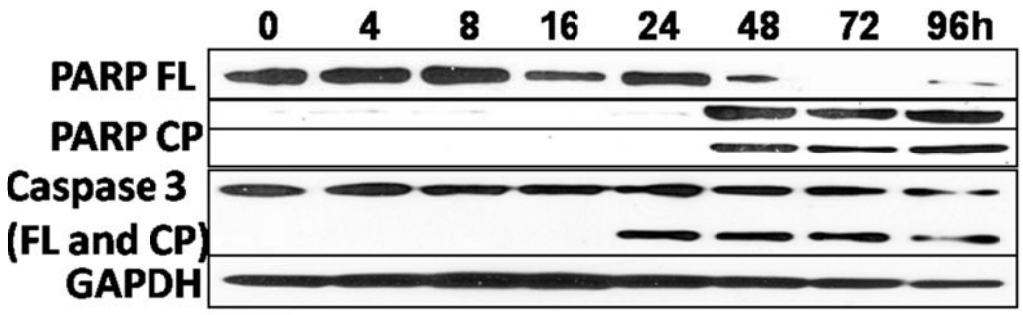

Figure 3.3.7.1 Treatment with AICAR induces caspase-3 and PARP cleavage

RPMI8226 cells were treated with 150 μM AICAR for up to 96h. Activation of apoptotic pathway was demonstrated by cleavage of caspase-3 and PARP by 24h. GAPDH levels were used a loading control.

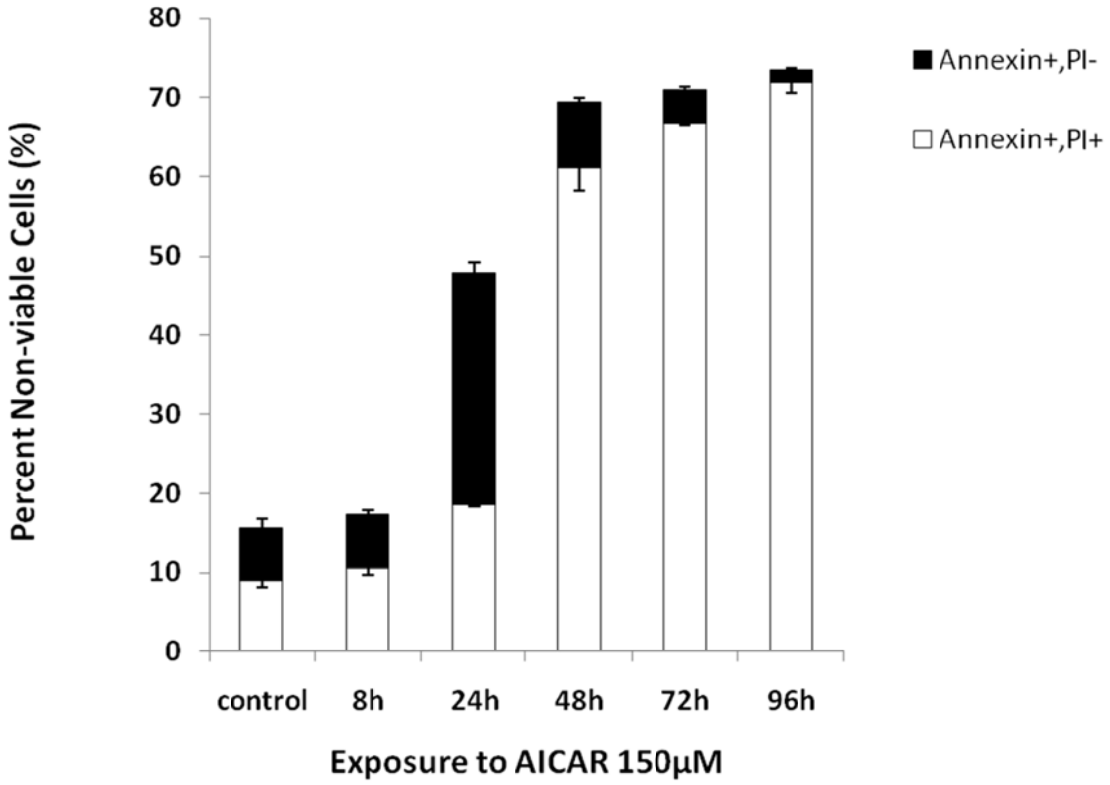

Figure 3.3.7.2 AICAR induces apoptosis in MM cells

RPMI8226 cells were exposed to 150 µM of AICAR for 0-96 h. Cells were collected, washed, stained for Annexin V and PI, and analyzed using flow cytometry. Exposure to AICAR resulted in time dependent increases Annexin V positive events, with increased AnnexinV+PI+ events at later time points indicating apoptotic cell death of RPMI8226 cells. Experiments were performed in triplicate and presented as average ± SD.

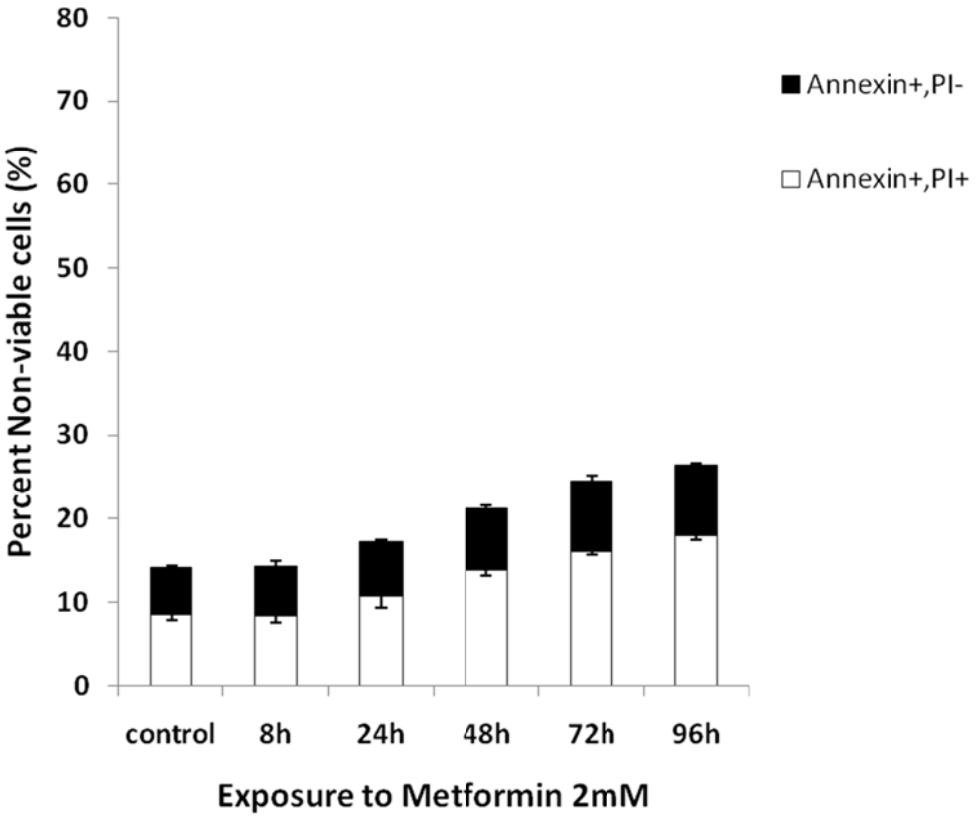

Figure 3.3.7.3 Metformin does not induce apoptosis in MM cells

RPMI8226 cells were exposed to 2mM of Metformin for 0-96 h. Cells were collected, washed, stained for Annexin V and PI, and analyzed using flow cytometry. Exposure to metformin showed an increase in non-viable cells but not through apoptosis. There was also considerably less necrotic cells observed compared to the results of the viability assay. Experiments were performed in triplicate and presented as average ± SD.

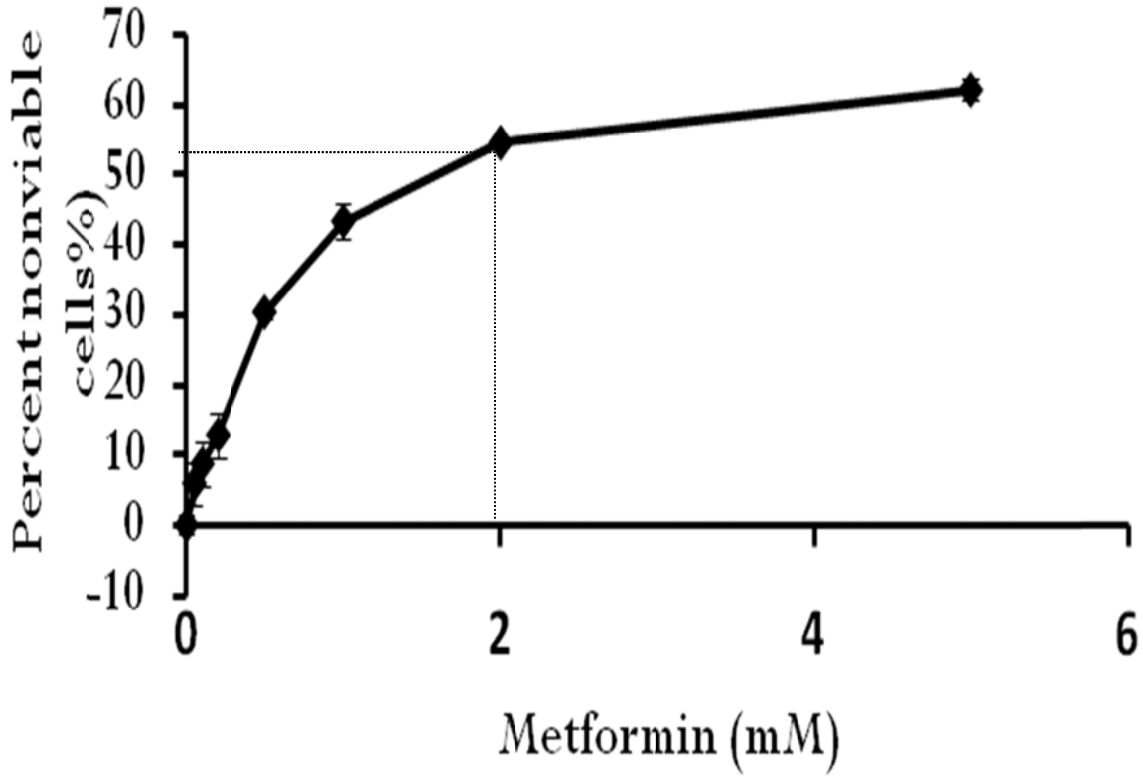

Figure 3.3.7.4 Metformin has a cytostatic rather than cytotoxic role in cancer cell death

RPMI-8226 MM cell line was treated with Metformin (0.1-5mM) for a period of 96 h, and viability was assessed by MTT assay. At 2mM metformin, the cell viability by MTT was 54%. Experiment was performed in triplicate wells. Cell survival was expressed as percentage (mean ± SD) compared to vehicle treated control.

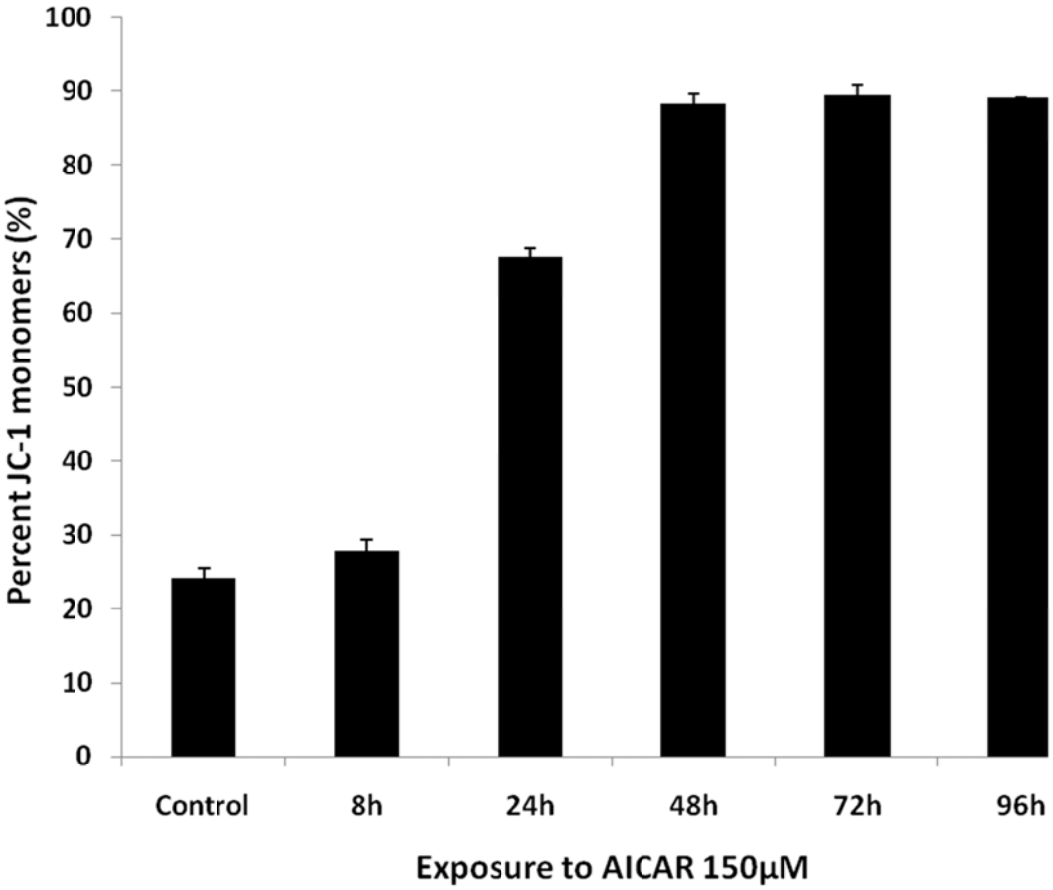

Fig 3.3.7.5 AICAR induced mitochondrial membrane depolarization in MM cells

RPMI8226 cells were exposed to 150 µM of AICAR, stained with JC-1 dye and analyzed using flow cytometry. The green fluorescence measures JC-1 monomers and red fluorescence measures JC-1 aggregates. AICAR was able to induce mitochondrial membrane depolarization, by accumulation of monomers and a reduction in the red/green fluorescence intensity ratio, as early as by 24h of treatment. Experiments were performed in triplicate and presented as average ± SD.

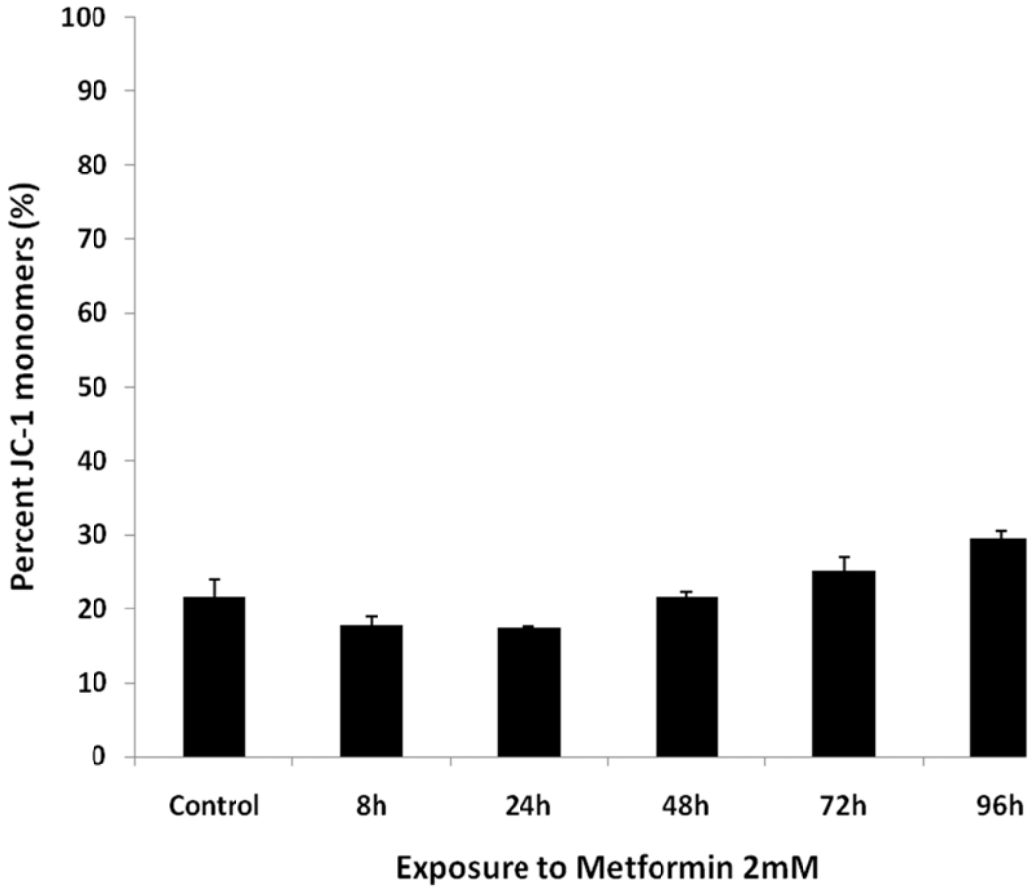

Fig 3.3.7.6 Metformin is unable to cause mitochondrial membrane depolarization in MM cells

RPMI8226 cells were exposed to 2mM of metformin, stained with JC-1 dye and analyzed using flow cytometry. The green fluorescence measures JC-1 monomers and orange fluorescence measures JC-1 aggregates. Metformin exposure to RPMI8226 did not have an effect on mitochondrial membrane depolarization as there was minimal accumulation of monomers, and thus no decrease in the red/green fluorescence intensity ratio. Experiments were performed in triplicate and presented as average ± SD.

3.3.8. AICAR-induced apoptosis is attenuated by overexpression of Bcl-2 and enhanced by activation of the Akt pathway

Akt and Bcl-2 overexpression are known hallmarks of cancer activation. The Akt pathway is of interest in this study as both metformin and AICAR are AMPK activators, which affect events upstream of Akt. We wanted to examine what effects both these agents had on cells overexpressing Akt. Meanwhile, Bcl-2 stabilizes mitochondrial membrane potential and inhibits mitochondrial-mediated apoptosis. Having demonstrated that AICAR can potently induce mitochondrial membrane depolarization and apoptosis, we next examined the impact of the modulation of apoptotic pathways by Bcl-2 on AICAR-induced apoptosis.

Stable overexpression of Bcl-2 attenuated the anticancer effect of AICAR (Fig. 3.3.8.1A). Constitutive activation of the Akt pathway (via overexpression of myristoylated Akt) led to enhanced sensitivity to AICAR (Fig. 3.3.8.1A). Bcl-2 and Akt overexpression did not substantially modulate the effect of metformin (Fig. 3.3.8.1B).

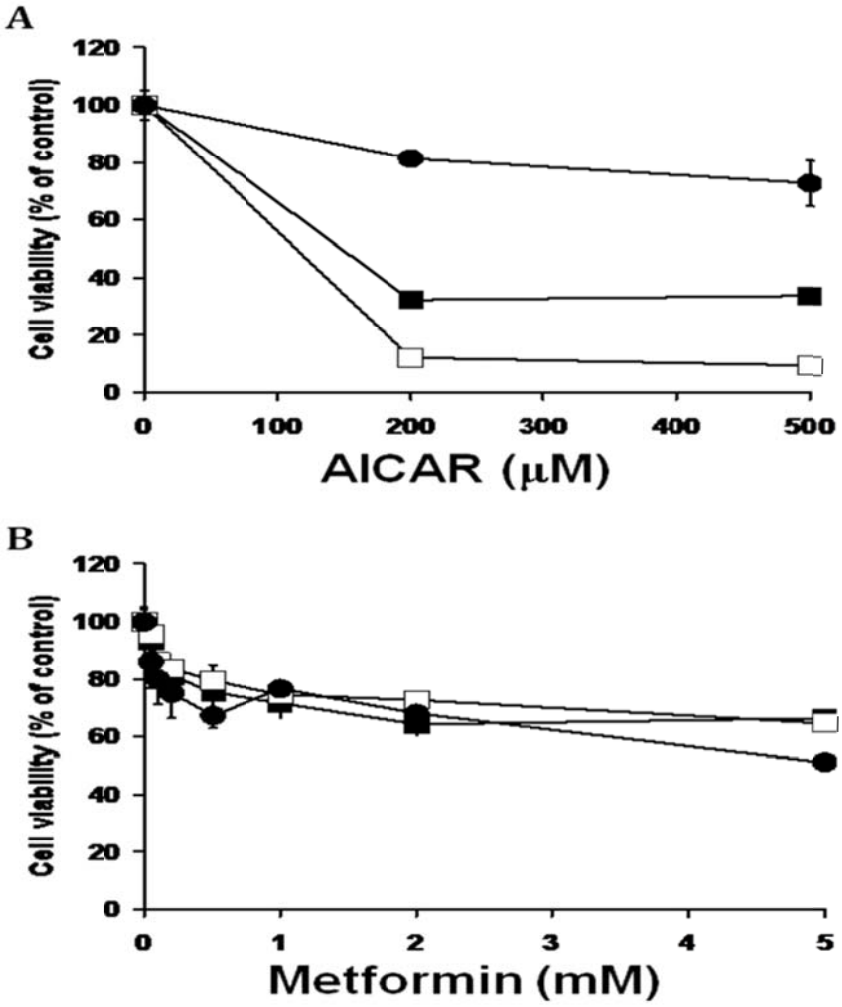

Figure 3.3.8.1 AICAR-induced apoptosis is attenuated by overexpression of Bcl2 and enhanced by activation of the Akt pathway

FRO cells stably transfected with Bcl-2 (●), myristoylated (constitutively active) Akt (□) or empty vector (■) were treated with AICAR (0-500 μM) or metformin (0-5 mM) for 96 hrs. Experiments were performed in triplicate and cell viability measured by MTT was presented as average ± SD. Overexpression of Bcl-2 attenuated the anticancer effect of AICAR (A), while constitutive activation of the Akt pathway (via overexpression of myristoylated Akt) led to enhanced sensitivity to AICAR (A). Bcl2 and Akt overexpression did not substantially modulate the effect of metformin on FRO cells (B).

3.3.9. *In vivo* activity of AICAR

In vivo testing of AICAR in a subcutaneous xenograft model was performed in NOD.CB17 SCID mice. These mice are homozygous for the severe combined immune deficiency spontaneous mutation *Prkd*^{scid} and are characterised by an absence of functional T cells and B cells, lymphopaenia, hypogammaglobulinaemia but with a normal haematopoietic microenvironment. OPM2-GFP/luc cells (10^6 cells per mouse) were injected subcutaneously into the mice in between the shoulder blades. Following 7 days of tumour engraftment, mice were randomly assigned to receive 600 mg/kg AICAR or vehicle (PBS) i.p. Tumour load (by calliper measurement), survival, and weights were assessed.

There were 7 mice in the control group and 8 mice in the treatment group. AICAR treatment significantly decreased tumour burden compared to controls (Fig. 3.3.9.1; P=0.005; unpaired one-tailed T-test). In addition, the survival of the treated mice was statistically significant compared to controls (Fig. 3.3.9.2; P=0.003; log-rank test) on Kaplan-Meier method. Furthermore, there was no significant change in the weights of treated mice (Fig. 3.3.9.3) indicating that the mice tolerated the treatment well. There were also no potential toxicities observed during the course of treatment with AICAR.

AICAR treated mice responded to the treatment in a rapid fashion. Due to the rapid disappearance of the tumours, there was development of ulcers in the central portion of the tumour. As a result of the ulcer formation, the Animal Care and Use Committee of the Dana-Farber Cancer Institute instructed us to sacrifice the mice, despite the shrinking tumour load. As a result, we had to censor the groups to get an accurate Kaplan-Meier calculation.

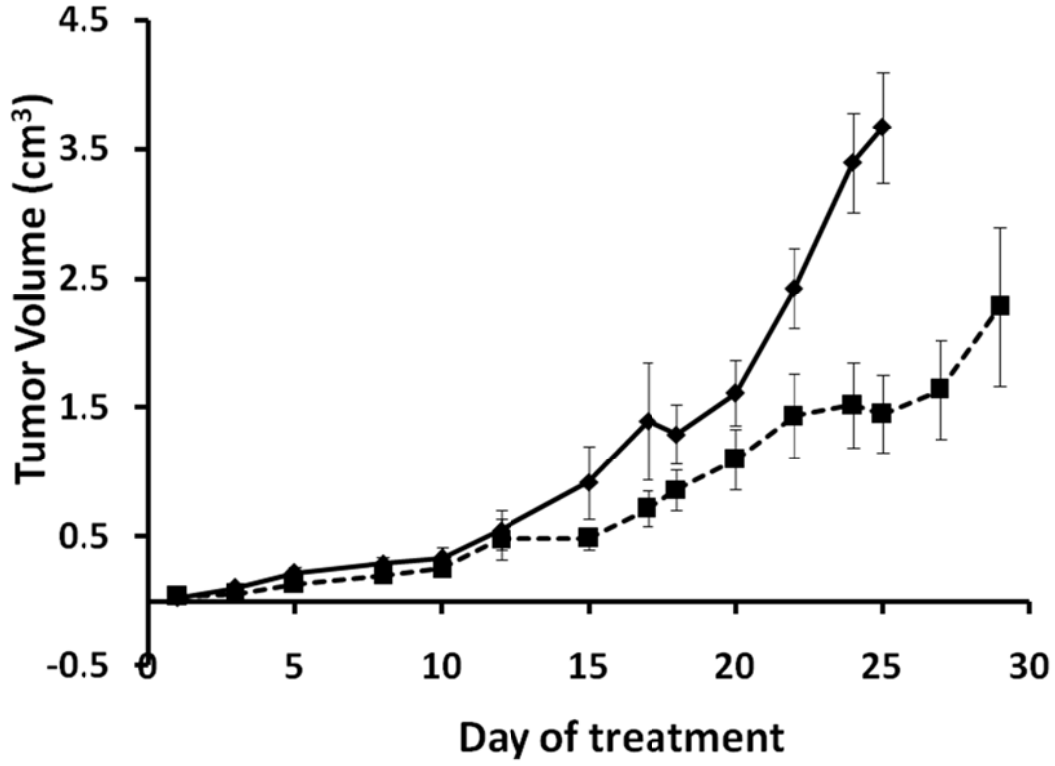

Figure 3.3.9.1 AICAR is able to reduce tumour burden in treated mice.

1 million OPM2-GFP/luc cells were injected subcutaneously into CB17 SCID mice. Following 7 days of tumour engraftment, mice were randomly assigned as per section 2.12.1 to receive 600 mg/kg AICAR (*broken line)* or vehicle (PBS- *solid line*) intraperitoneally. Tumour load (by calliper measurement) was assessed twice a week. Mouse tumour burden was significantly reduced in the subcutaneous model (P=0.005; Avg tumour size ± SEM; unpaired one-tailed T-test) compared to controls. (n= 7 in controls, n= 8 in treatment group)

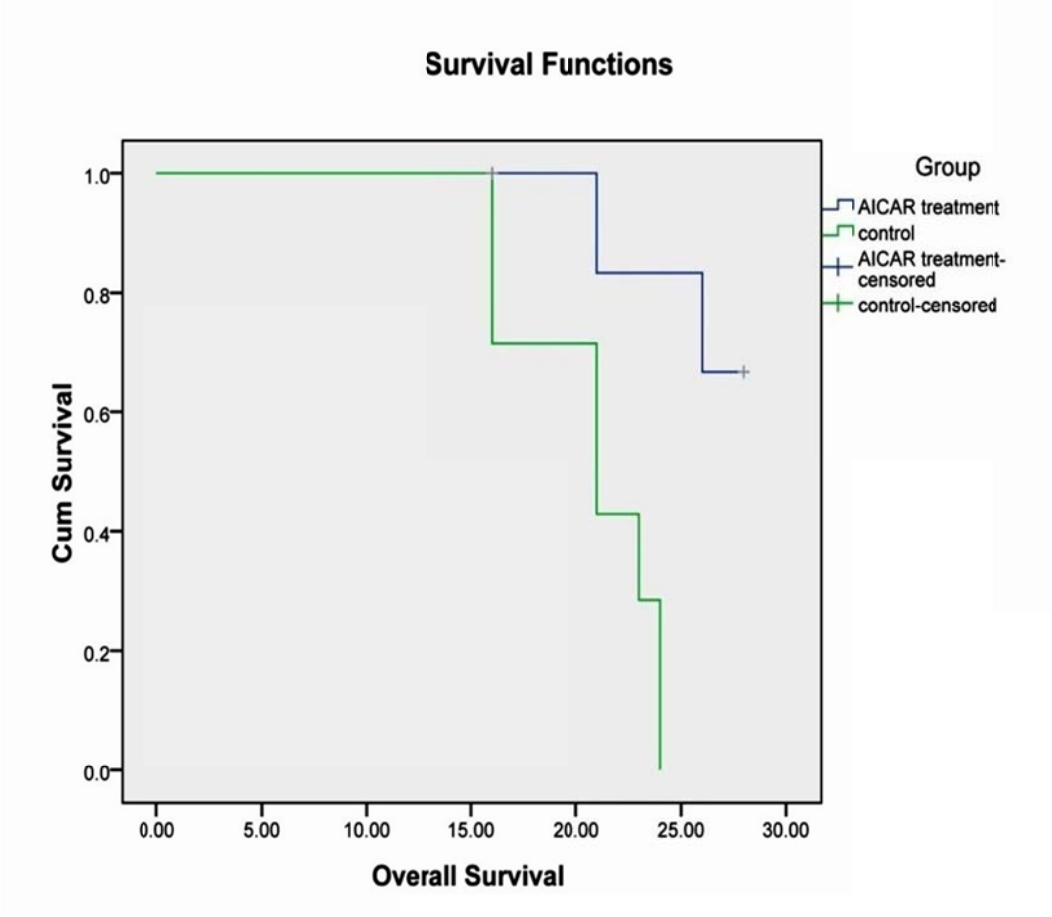

Figure 3.3.9.2 AICAR treated mice survive longer than controls

The survival of the subcutaneous model was statistically significant (C; P=0.003; log-rank test). Survival was defined as time between initiation of treatment and sacrifice or death and calculated using the Kaplan-Meier method. (There was censorship in both groups as some mice had to be sacrificed early upon instructions by the Animal Care and Use Committee of the Dana-Farber Cancer Institute) (n= 7 in controls, n= 8 in treatment group)

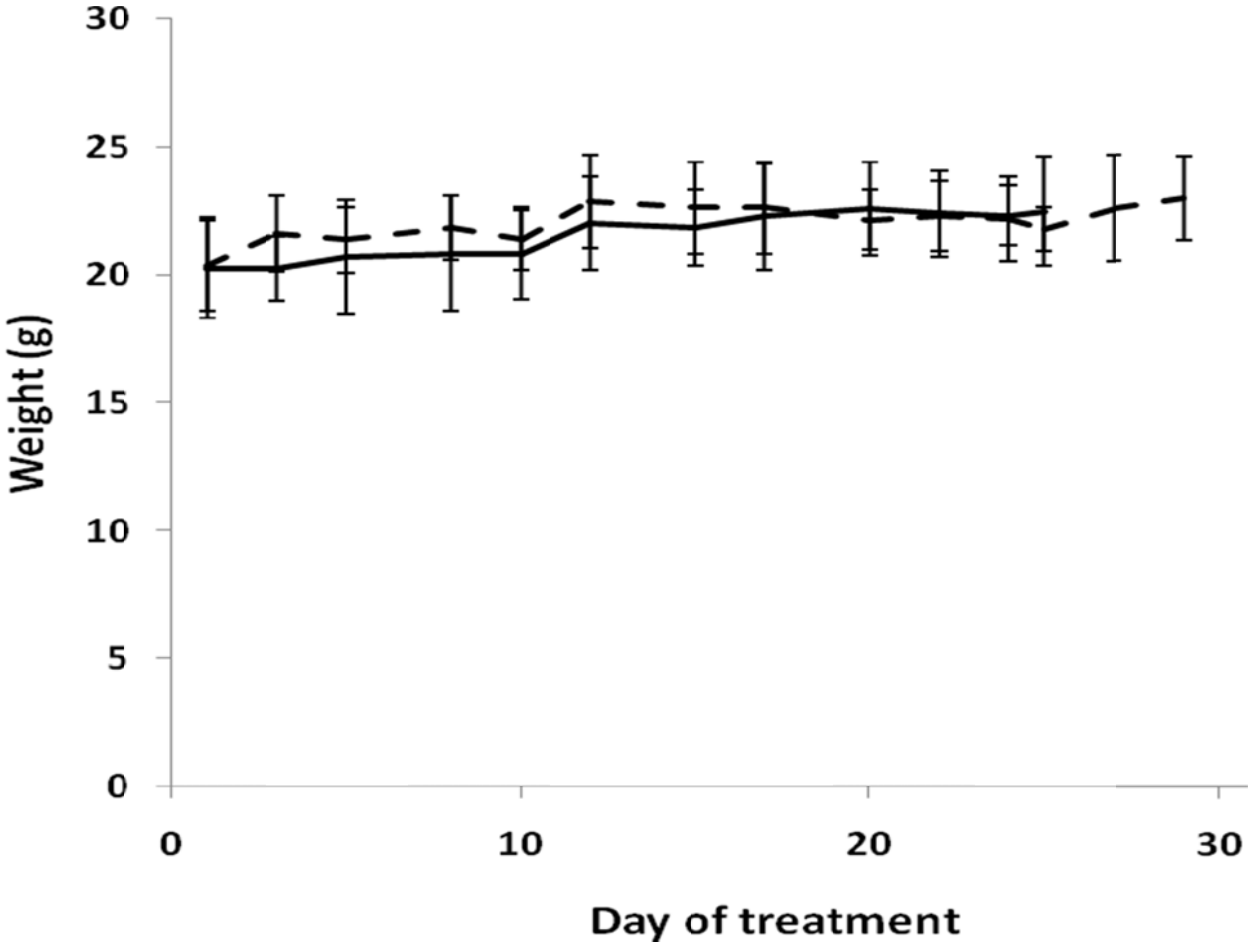

Figure 3.3.9.3 AICAR treated mice show no change in weight compared to controls

Mice in the treatment group (AICAR 600mg/kg – *broken line*) showed no difference in weights compared to mice in the control group (*solid line).* This indicated that the mice tolerated the treatment well. (n= 7 in controls, n= 8 in treatment group)

3.3.10. Synergy of AICAR and Metformin with glycolysis inhibitors

According to the Warburg hypothesis, tumour cell survival and proliferation critically depend on aerobic glycolysis rather than mitochondrial glucose oxidative metabolism [290]. Because metformin inhibits the mitochondrial respiratory chain and AICAR decreases mitochondrial membrane potential, we hypothesized that combined treatment of metformin or AICAR with a glycolysis inhibitor would significantly reduce the capacity of the cancer cell to generate energy, as it would target concurrently both key ATP-producing pathways. We treated MM1.S and FRO cells with 3-bromopyruvate (3BP), an inhibitor of hexokinase II, and 2-deoxyglucose (2DG), a stable glucose analogue that is actively taken up by the hexose transporters and inhibits phosphoglucose isomerase in a competitive, and hexokinase in a noncompetitive, manner [291], in combination with AICAR or metformin.

The doses used for the combinations were in the range of IC_{70} to IC_{90} for single agent activity. 3BrPA dose of 7.5μM and 15μM for MM1.S and 15μM and 30μM for FRO cells were picked based on the dose response curve in Fig 3.3.10.1. As 2-DG had minimal single agent activity at doses <1000μM, the dose of 125μM and 250μM were picked to represent the lowest dose that will still yield synergy with AMPK activators.

MM1.S and FRO cells were treated for 96h with a combination of AICAR or metformin plus 3BP or 2DG. This combination exhibited synergistic cytotoxicity in almost all doses, more with AICAR than metformin (Fig. 3.3.10.2 and 3.3.10.3). The Calcusyn software calculated the combination index (CIN) using the Chou and Talalay method [270, 271]. In Table 3.3.10.1 and 3.3.10.2, the CIN for both MM1.S and FRO cells treated with AICAR or metformin plus glycolysis inhibitors, 3BP or 2DG are shown. With the use of this method, a combination index < 0.9 indicates synergy, a combination index >0.9 indicates additive effect. All CIN values for MM1.S cells were <0.9 except for the combination of metformin 1.5 mM and 3BP 15 μM and metformin 3mM and 3BP 15 μM which showed a calculated CIN of > 0.9. The combinations that were < 0.9 were synergistic, whereas the two combinations in *italics* indicated that the combination of metformin with 3BP was additive. The same synergistic results were seen with the FRO cells except for two combinations which were highlighted in *italic*. The combination of AICAR 600 μM with 3BP 30 μM was slightly antagonistic and the combination of metformin 2mM with 2DG 250 μM was additive.

The combination of AMPK activators and glycolysis inhibitors demonstrated synergistic cytotoxicity by enhancing apoptotic activity. Fig. 3.3.10.4 showed that the combination of AICAR with glycolysis inhibitors led to enhanced cleavage of caspase 3 and PARP.

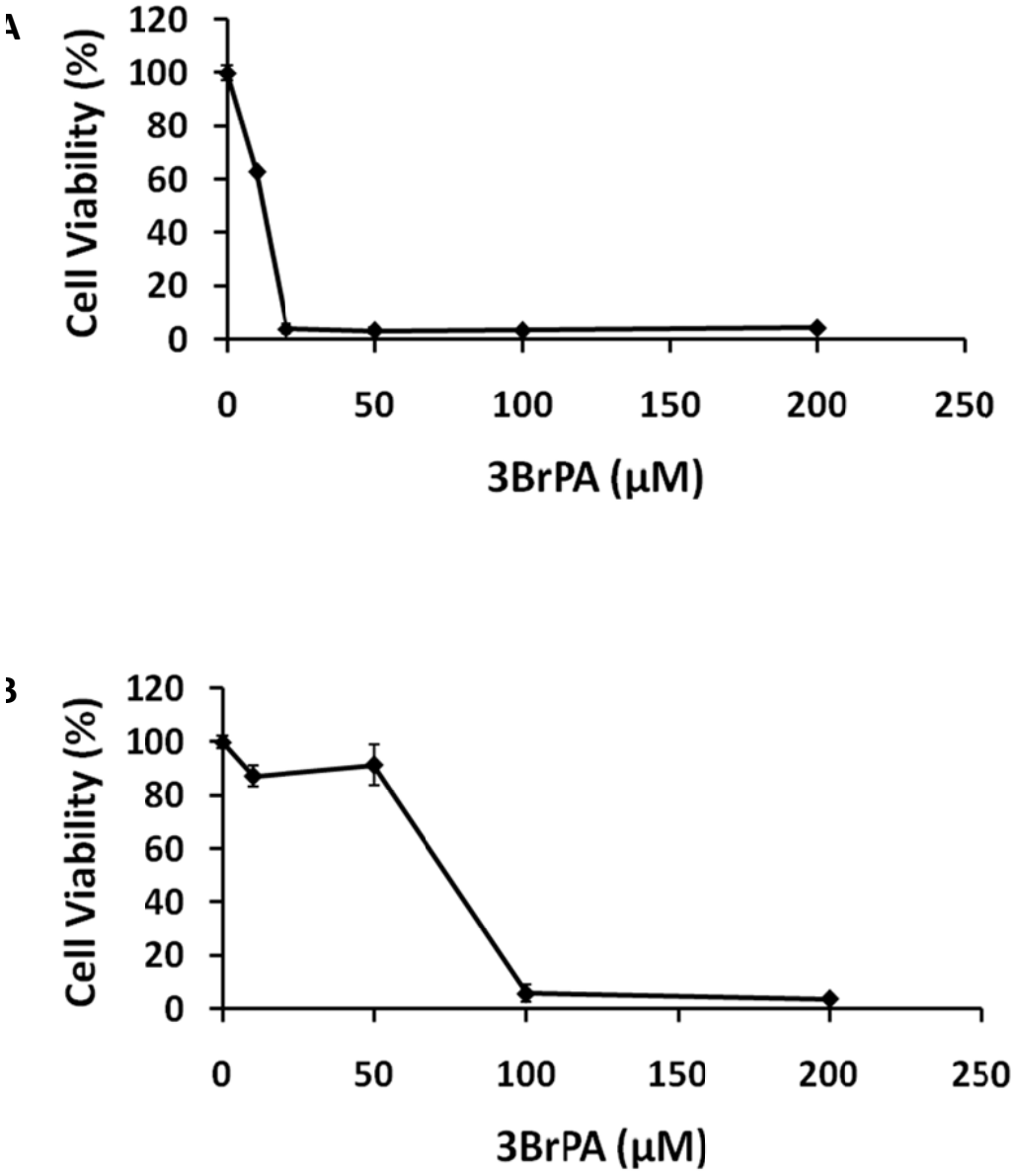

Figure 3.3.10.1 3BrPA dose response curve in MM1.S (A) and FRO (B).

A dose response curve was established for 3BrPA on MM1.S and FRO cells. Cells were treated for 96h. Cell viability was assessed by MTT assay and values expressed as percentage (mean ± SD) compared to vehicle treated control. Experiments were performed in triplicate.

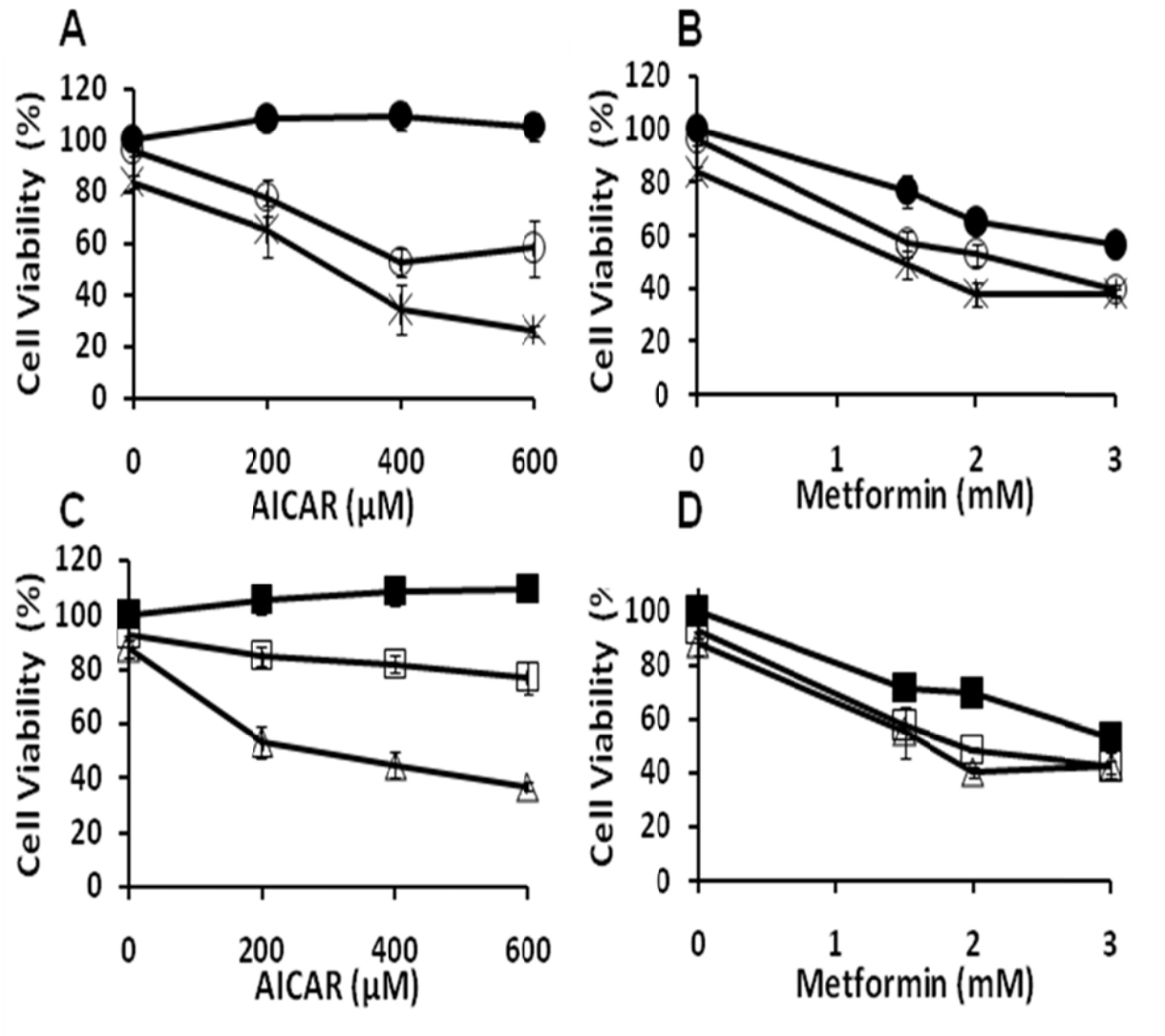

Figure 3.3.10.2 AICAR and Metformin synergises with glycolysis inhibitors in MM cells.

(A,B) MM1.S cells were treated for 96h with increasing doses of AICAR or metformin in the absence (●) or presence of 3-Bromopyruvate 7.5µM (○) or 15µM (✱), demonstrating synergy. The same experiment was performed in the absence (■) or presence of 2 deoxy-glucose 125µM (□) or 250µM (Δ) (C,D). Experiments were performed in triplicate and presented as average ± SD.

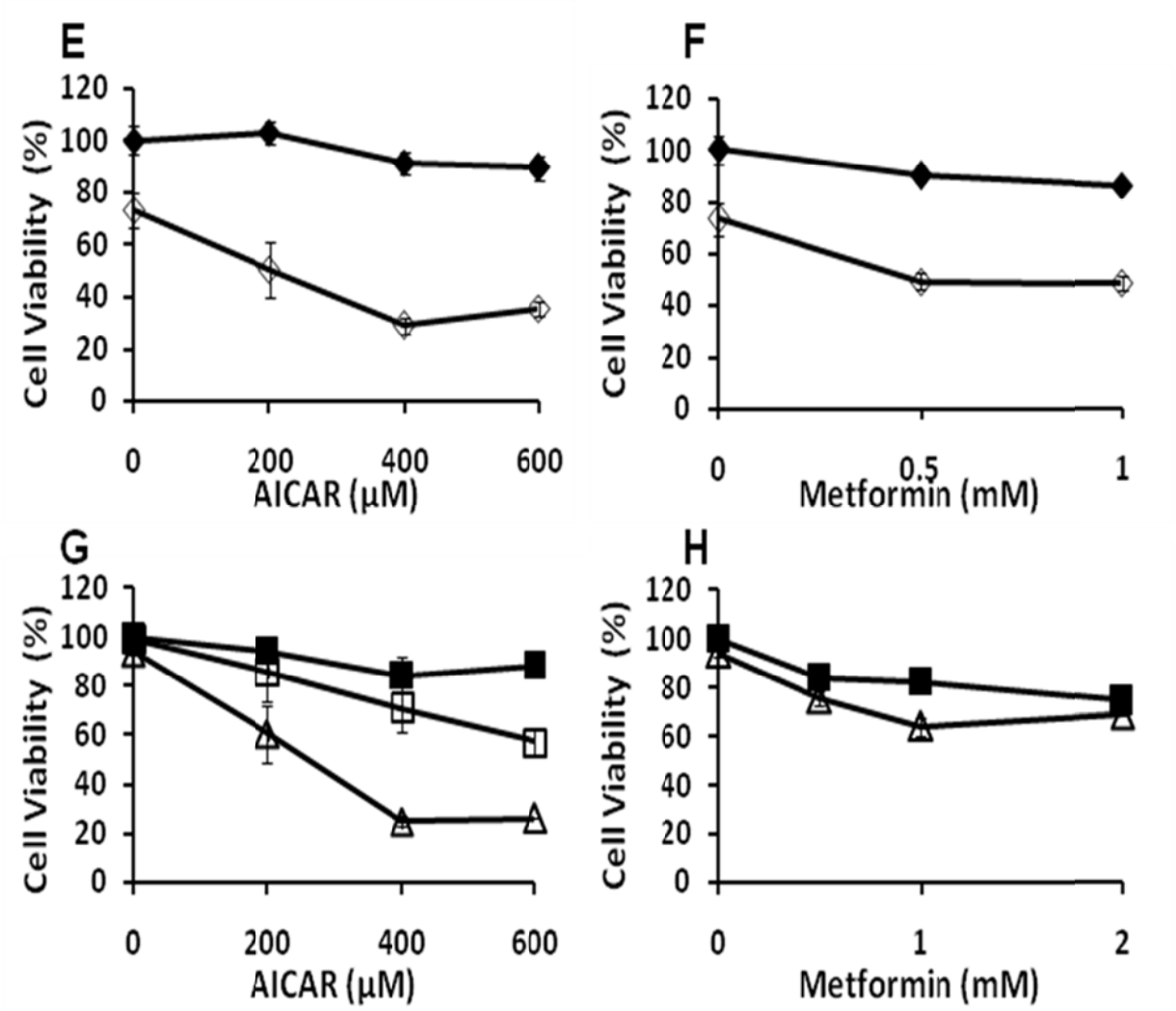

Figure 3.3.10.3 AICAR and Metformin synergises with glycolysis inhibitors in FRO cells.

Using FRO cells (E,F), AICAR or Metformin without (◆) and with 30µM 3-Bromopyruvate (◇) showed synergistic activity. The same results were seen in the absence (■) or presence of 2 deoxy-glucose 125µM (□) or 250µM (Δ) in FRO cells (G,H). Experiments were performed in triplicate and presented as average ± SD.

AICAR (μM)	3-Bromopyruvate (μM)	Fraction affected	CIN
200	7.5	0.221805	0.426
200	15	0.350624	0.638
400	7.5	0.474641	0.256
400	15	0.660006	0.361
600	7.5	0.419226	0.285
600	15	0.739868	0.305

Metformin (mM)	3-Bromopyruvate (μM)	Fraction affected	CIN
1.5	7.5	0.431177	0.805
1.5	15	0.506741	*0.901*
2	5	0.471601	0.797
2	15	0.621679	0.784
3	7.5	0.603879	0.831
3	15	0.620715	*0.986*

AICAR (μM)	2 deoxy-glucose (μM)	Fraction affected	CIN
200	125	0.153206	0.344
200	250	0.471292	0.099
400	125	0.182012	0.267
400	250	0.552601	0.066
600	125	0.228841	0.188
600	250	0.630215	0.045

Metformin (mM)	2 deoxy-glucose (μM)	Fraction affected	CIN
1.5	125	0.423288	0.612
1.5	250	0.446638	0.619
2	125	0.515034	0.576
2	250	0.598452	0.456
3	125	0.576538	0.682
3	250	0.570363	0.728

Table 3.3.10.1 Combination index (CIN) for AICAR/Metformin + Glycolysis inhibitors (3-Bromopyruvate or 2-deoxyglucose) for MM1S cells.

Using Calcusyn software, the combination index (CIN) for the combination of AICAR/Metformin and glycolysis inhibitors was calculated. The CIN values were <0.9 (except the combination in *italics)*, indicating that the combination of AICAR or metformin with 2DG or 3BP were synergistic. The value in *italics* indicated that the combination was additive.

AICAR (μM)	3-Bromopyruvate (μM)	Fraction affected	CIN
200	30	0.494308	0.879
400	30	0.711659	0.86
600	30	0.645551	*1.204*

Metformin (mM)	3-Bromopyruvate (μM)	Fraction affected	CIN
0.5	30	0.508185	0.589
1	30	0.519125	0.584

AICAR (μM)	2 deoxy-glucose (μM)	Fraction affected	CIN
200	125	0.137895	0.744
200	250	0.394176	0.586
400	125	0.288792	0.518
400	250	0.749566	0.364
600	125	0.427672	0.404
600	250	0.737363	0.38

Metformin (mM)	2 deoxy-glucose (μM)	Fraction affected	CIN
0.5	250	0.2487	0.868
1	250	0.36224	0.675
2	250	0.3132	*1.015*

Table 3.3.10.2 Combination index (CIN) for AICAR/Metformin + Glycolysis inhibitors (3-Bromopyruvate or 2-deoxyglucose) for FRO cells.

Using Calcusyn software, the combination index (CIN) for the combination of AICAR/Metformin and glycolysis inhibitors was calculated. The CIN values were <0.9 (except the combination in *italics)*, indicating that the combination of AICAR or metformin with 2DG or 3BP were synergistic. The value in *italics* indicated that the combination was additive.

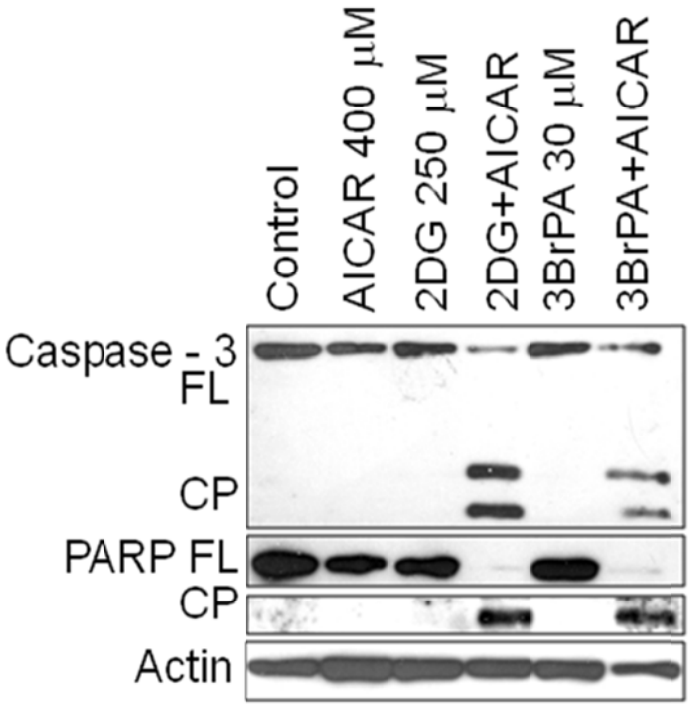

Figure 3.3.10.4 The combination of AICAR with glycolysis inhibitors lead to enhanced pro-apoptotic activity

Immunobloting revealed that the combination of AICAR (400 µM) and the glycolysis inhibitors 2-deoxyglucose (250 µM) or 3-bromopyruvate (30 µM), resulted in enhanced cleavage of caspase 3 and PARP. FRO cells were treated for 96h with AICAR 400 µM and 2DG 250 µM or 3BrPA 30 µM. GAPDH levels were used as loading control.

3.4. Proteomic analysis to examine bortezomib resistance

3.4.1. Introduction

To study further the resistance mechanisms in MM, specifically resistance to bortezomib treatment, we utilised proteomic technologies; the comparative proteomic approach which enabled us to study multiple signalling pathways simultaneously and mechanism of resistance to bortezomib.

As most MM cell lines are exquisitely sensitive to bortezomib treatment, there was difficulty in locating a resistant cell line to act as a negative control. At this time, a paired isogenic bortezomib resistant MM cell line has not been generated. The MM cell lines used in this study were MM1.S (sensitive) and OPM2 (intermediate resistant cell line). Thus, the decision to use paired sensitive and resistant thyroid carcinoma cell lines (KAT18 and WRO) was twofold. One of the reasons was to have a totally resistant cell line to act as a negative control; the other reason was to account for any artefacts that may have arisen as non-isogenic cell lines were used.

To determine expression differences between bortezomib sensitive and bortezomib resistant cell lines, proteomic analysis was carried out on sensitive (MM1.S and KAT18) and resistant (OPM2 and WRO) cell lines treated with bortezomib for 24 hrs (see Table 3.4.1 for dose of treatment). The dose used corresponded to the IC_{50} of each cell line. Investigations into differential protein expression between the responses of the cell lines to bortezomib treatment could potentially identify proteins that respond or do not respond to bortezomib and may be critical for understanding resistant mechanisms to this drug.

Cell lines	Bortezomib dose
MM1.S	4nM
OPM2	10nM
KAT18	20nM
WRO	100nM

Table 3.4.1 Samples used in proteomic experiment

3.4.2. Experimental outline for 2D-DIGE analysis of the samples

2D-DIGE protein separation was performed by separating proteins first by isoelectric point and then by molecular weight. Protein spots in a gel were visualised using fluorescent markers. 2-D DIGE enables the incorporation of the same internal standard on every 2-D gel. The internal standard is a pool of all the samples within the experiment, and therefore contains every protein from every sample. Duplicate technical repeats were also carried out as well as reverse labelling. Once proteins were separated and quantified, they were identified by MALDI-TOF MS (Chapter 2.9.8). Identification of proteins enabled lists to be generated detailing differentially regulated proteins between samples.

Gel	Cy2	Cy3	Cy5
1	pooled sample	MM1S control	MM1S treatment
2	pooled sample	MM1S treatment	MM1S control
3	pooled sample	OPM2 control	OPM2 treatment
4	pooled sample	OPM2 treatment	OPM2 control
5	pooled sample	KAT18 control	KAT18 treatment
6	pooled sample	KAT18 treatment	KAT18 control
7	pooled sample	WRO control	WRO treatment
8	pooled sample	WRO treatment	WRO control

Table 3.4.2 Labelling of samples for proteomic experiment

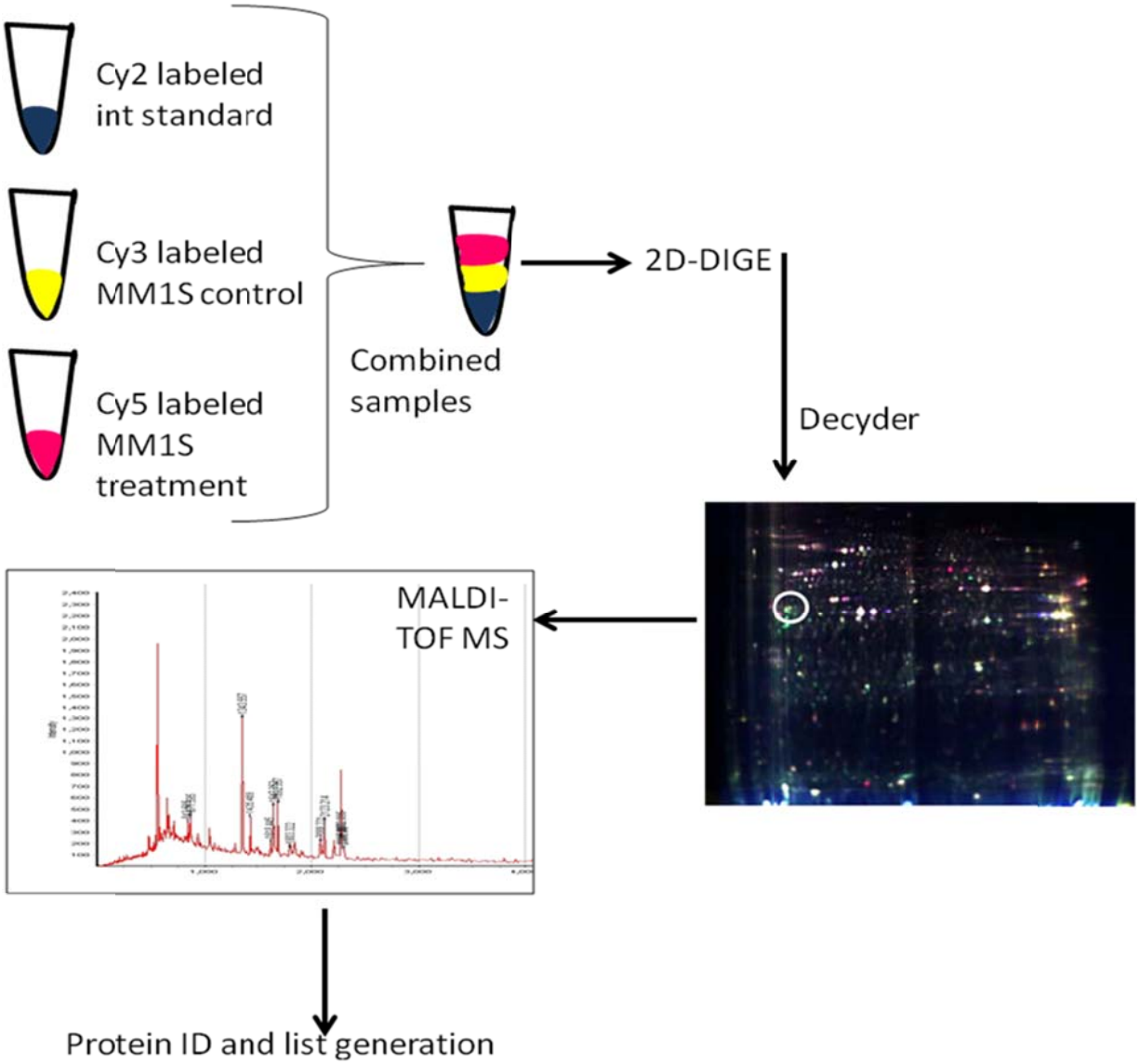

Figure 3.4.2 Labelling of samples and generation of protein list and ID

Normalised pool comprising all the samples from all samples (MM1.S, OPM2, KAT18 and WRO control and treated) is labelled with Cy2 dye. Each 2D-DIGE gel comprises pool (Cy2), condition 1 (Cy3/Cy5) and condition 2 (Cy3/Cy5) samples. The three scanned images from each 2D-DIGE are further analysed by DeCyder Image analysis software to generate the differentially regulated protein spots. The differentially regulated protein spots, as depicted in the 2D gel, are further processed by MALDI-TOF MS for peptide mass fingerprinting for protein identification.

3.4.2.1. Identification of differentially regulated proteins

Differential protein expression between sensitive and resistant cell lines to bortezomib was examined using 2D-DIGE. DeCyderTM 6.5 software was used to identify differentially regulated proteins in each comparison.

To evaluate the differentially expressed proteins after 24 hrs of exposure to bortezomib in the cell lines MM1S, OPM2, KAT18 and WRO, four comparative protein lists were generated. These four lists comprised of differentially expressed proteins between control and treated MM1.S (list 1), control and treated KAT18 (list 2), control and treated OPM2 (list 3) and control and treated WRO (list 4). The generated protein list and analysis was looking at the trend of change in the cell lines before (control) and after (24h) treatment with bortezomib.

3.4.2.2. Identification of unique proteins demonstrating the same trend in sensitive vs. resistance cell lines

In order to further determine the significance of these differentially changed proteins, the design analysis was planned to specifically identify proteins that were altered in the same trend in both of the sensitive lines (MM1S, KAT18) vs. the resistant lines (OPM2, WRO), e.g. protein x upregulated in sensitive lines and downregulated in resistant lines. Biological variation analyses of these spots showing greater than 1.2-fold change in expression with a t-test score of less than 0.05 were identified. A total number of 50 spots containing proteins of interest were identified as being significant (Table 3.4.2.1). Fig 3.4.2.1 showed the preparative gel where the 50 spots were located. 30 spots contained proteins that were downregulated in the sensitive cell lines, 16 spots contained proteins that were upregulated in the sensitive cell lines and 4 spots contained proteins that were unchanged in the sensitive cell lines but increased in the resistant cell line.

Out of these 50 spots, only 39 spots were able to be identified and picked from the preparative gel (Fig 3.4.2.2). The other 11 spots contained proteins that were of too low abundance to be identified from the preparative gel. These 39 spots were then trypsin digested and further analysed on the mass spectrometer (Chapter 2.9.8). The peptides generated from the mass spectrometer was then analysed by the MASCOT software (Chapter 2.9.8). Of these 39 spots, 14 spots contained proteins that were identified with confidence by the software and 1 spot contained a protein that was identified with borderline confidence (Table 3.4.2.2A and B). Further details on the Mascot software identification using KHSRP protein and Heterogenous nuclear ribonuclearprotein A2/B1 isoform B were provided in Appendix A.

	Sensitive - MM1.S		Resistant - OPM2	
Spot ID	**Fold change**		**Fold change**	
155	-1.59	Decreased	-1.04	Unchanged
222	-1.59	Decreased	-1.06	Unchanged
228	-1.45	Decreased	-1.01	Unchanged
272	1.08	Unchanged	1.38	Increased
280	-1.49	Decreased	-1	Unchanged
283	-1.87	Decreased	-1.08	Unchanged
297	1.74	Increased	1.08	Unchanged
323	-1.56	Decreased	1.13	Unchanged
329	-2.33	Decreased	-1.07	Unchanged
339	-1.93	Decreased	1.01	Unchanged
387	-1.95	Decreased	-1.05	Unchanged
443	-2.07	Decreased	1.06	Unchanged
447	3.45	Increased	-1.19	Unchanged
457	1.7	Increased	-1.08	Unchanged
505	-1.36	Decreased	1.25	Increased
603	-1.61	Decreased	1.06	Unchanged
605	-1.61	Decreased	1.08	Unchanged
609	-1.48	Decreased	-1.03	Unchanged
610	-1.45	Decreased	-1.03	Unchanged
614	1.53	Increased	-1.06	Unchanged
636	1.06	Unchanged	-1.11	Unchanged
669	-1.41	Decreased	1.08	Unchanged
670	-1.55	Decreased	1.08	Unchanged
675	-1.18	Unchanged	1.79	Increased
676	-1.82	Decreased	1.07	Unchanged
718	-1.51	Decreased	1.03	Unchanged
868	1.61	Increased	1.1	Unchanged
914	1	Unchanged	1.5	Increased
1088	2.29	Increased	-1.49	Decreased
1166	1.77	Increased	1.03	Unchanged
1265	1.73	Increased	1.06	Unchanged
1306	-1.08	Decreased	1.16	Unchanged
1330	5.36	Increased	1.04	Unchanged
1351	-1.31	Decreased	1.03	Unchanged
1387	-1.84	Decreased	1.12	Unchanged
1436	-1.45	Decreased	1	Unchanged
1465	-2.03	Decreased	1.16	Unchanged
1479	-1.62	Decreased	-1.19	Unchanged
1480	1.4	Increased	-1.06	Unchanged
1552	-1.98	Decreased	1.15	Unchanged
1649	-1.39	Decreased	-1.1	Unchanged
1669	1.24	Increased	1.02	Unchanged

Table 3.4.2.1 Proteins identified with a significant trend

	Sensitive - MM1.S		Resistant OPM2	
Protein ID	**Fold change**		**Fold change**	
1729	1.24	Increased	1.02	Unchanged
1732	1.87	Increased	1.09	Unchanged
1788	1.34	Increased	-1.06	Unchanged
1844	1.03	Decreased	1.42	Increased
1932	13.06	Increased	1.31	Increased
2275	-1.3	Decreased	1.12	Unchanged
2403	-1.77	Decreased	1.19	Unchanged
2525	6.25	Increased	1.53	Increased

Table 3.4.2.1 Spots containing proteins identified with a significant trend

The spots containing proteins identified when comparing the sensitive vs. resistant cell lines showing a significant trend. The fold change and the trend of change (whether upregulated or downregulated) of the protein after treatment with bortezomib when compared to its respective untreated control is shown.

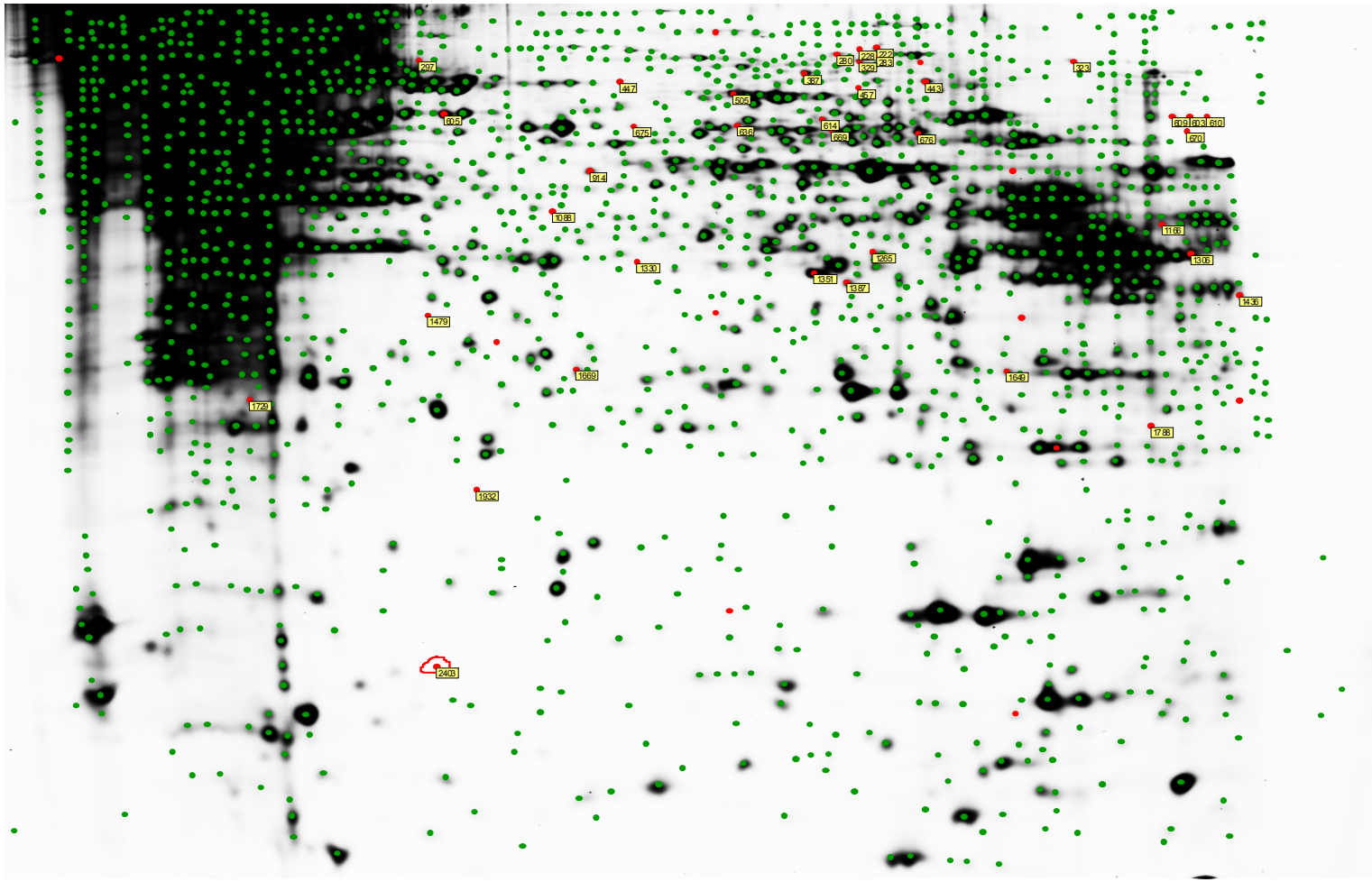

Fig. 3.4.2.1 – Spots identified on the preparative gel

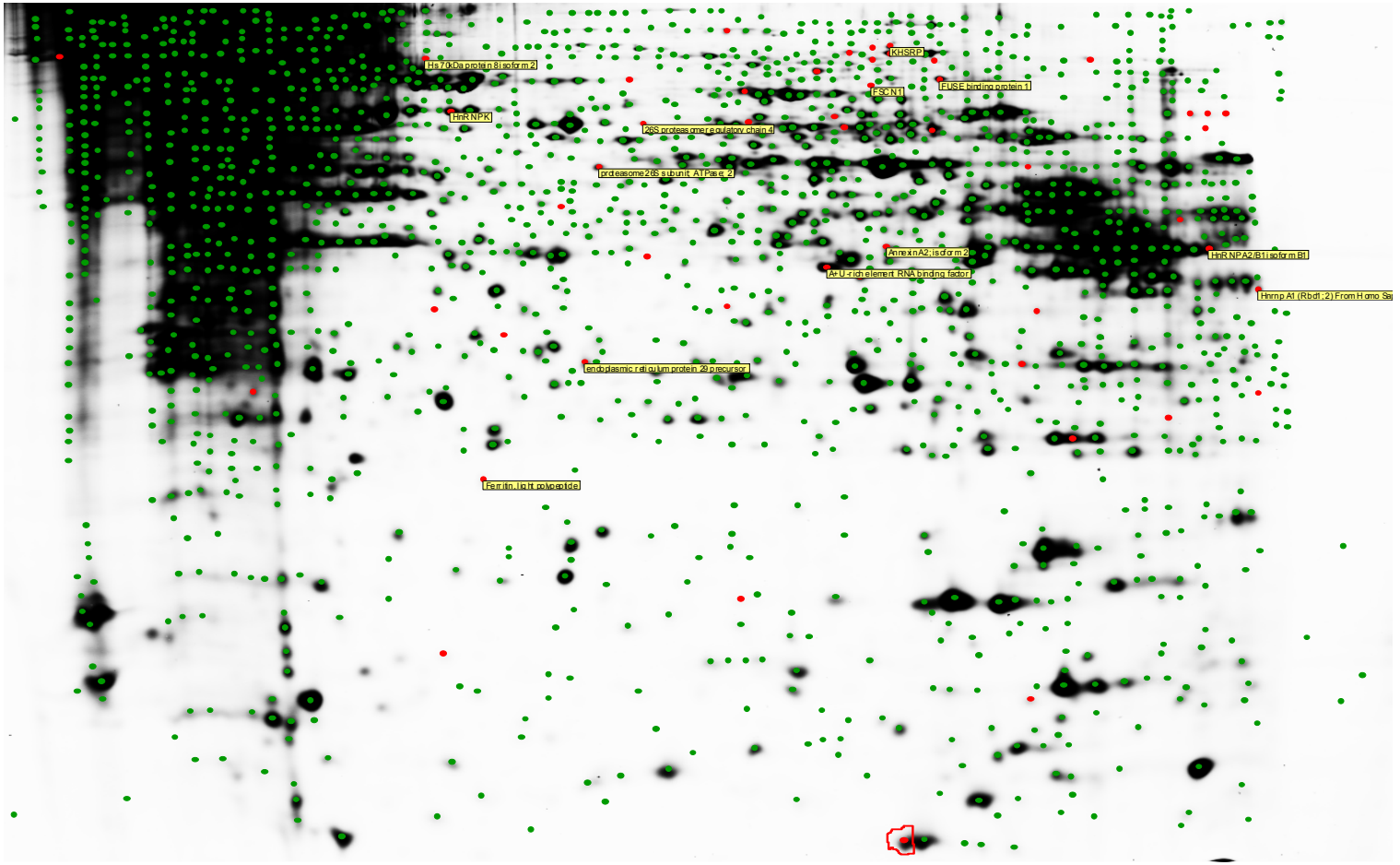

Fig. 3.4.2.2 – Spots containing proteins identified by Mascot software

Protein ID	Protein Name	Sensitive - MM1.S		Resistant - OPM2	
		Fold change		Fold change	
222	KHSRP protein	-1.59	Decreased	-1.06	Unchanged
297	Heat shock 70kDa protein 8 isoform 2	1.74	Increased	1.08	Unchanged
443	Far upstream element binding protein 1	-2.07	Decreased	1.06	Unchanged
457	FSCN1 protein	1.7	Increased	-1.08	Unchanged
605	Heterogeneous nuclear ribonucleoprotein K	-1.61	Decreased	1.08	Unchanged
675	26S protease (S4) regulatory subunit	-1.18	Unchanged	1.79	Increased
914	Proteasome 26S subunit, ATPase 2	1	Unchanged	1.5	Increased
1088	Proteasome 26S subunit, ATPase 2	2.29	Increased	-1.49	Decreased
1265	Annexin A2, isoform 2	1.73	Increased	1.06	Unchanged
1306	Heterogeneous nuclear ribonucleoprotein A2/B1 isoform B1	-1.08	Decreased	1.16	Unchanged
1351	A+U-rich element RNA binding factor	-1.31	Decreased	1.03	Unchanged
1436	Heterogenous nuclear ribonucleoprotein A1 (Rbd1,2)	-1.45	Decreased	1	Unchanged
1465	Caspase-3	-2.03	Decreased	1.16	Unchanged
1669	Endoplasmic reticulum protein 29	1.24	Increased	1.02	Unchanged
1932	Ferritin, light polypeptide	13.06	Increased	1.31	Increased

Table 3.4.2.2A – Proteins with a significant trend that are identified from the list generated (Table 3.4.2)

Protein ID	Protein Name	Ascension	Mass (Dalton)	Mascot Score	Peptides match	Sequence coverage
222	KHSRP protein	gi|54648253	73307	149	22	26%
297	Heat shock 70kDa protein 8 isoform 2	gi|24234686	53598	164	19	36%
443	Far upstream element binding protein 1	gi|37078490	67603	112	16	23%
457	FSCN1 protein	gi|14043107	55729	63*	13	25%
605	Heterogeneous nuclear ribonucleoprotein K	gi|55958544	47756	142	17	32%
675	26S protease (S4) regulatory subunit	gi|403456	49326	67	18	36%
914	Proteasome 26S subunit, ATPase 2	gi|51095169	49002	130	14	23%
1088	Proteasome 26S subunit, ATPase 2	gi|51095169	49002	207	24	49%
1265	Annexin A2, isoform 2	gi|16306978	38822	116	17	43%
1306	Heterogeneous nuclear ribonucleoprotein A2/B1 isoform B1	gi|14043072	37464	370	24	50%
1351	A+U-rich element RNA binding factor	gi|2547076	30337	114	14	29%
1436	Heterogenous nuclear ribonucleoprotein A1 (Rbd1,2)	gi|2194069	21116	114	11	50%
1465	Caspase-3		31587		3	21%
1669	Endoplasmic reticulum protein 29 precursor	gi|5803013	29032	134	10	26%
1932	Ferritin, light polypeptide	gi|18203882	20106	98	10	36%

Table 3.4.2.2B – Proteins with a significant trend that are identified from the list generated (Table 3.4.2)

The masses were calculated from the sequence of the protein in the database. The sequence coverage is the amount of the protein sequence covered by the matched peptides. For protein identification, all proteins were digested and identified at least twice from separate gels with MALDI-TOF MS. Mascot scores greater than 64 are significant ($p<0.05$). * is a protein that was identified with borderline confidence.

3.4.3. Proteins identified that are known to be affected by bortezomib treatment

3.4.3.1. Heat shock protein 70kD

One of the proteins identified was Heat shock protein 70 (Hsp70). This protein was induced by bortezomib treatment whereas in bortezomib resistant cells, there was no change in this protein after exposure to bortezomib (Fig. 3.4.3.1). We validated this result in the bortezomib sensitive cell line MM1.S by Western blot (Fig. 3.4.3.3) showing an increase in Hsp70 after treatment with bortezomib.

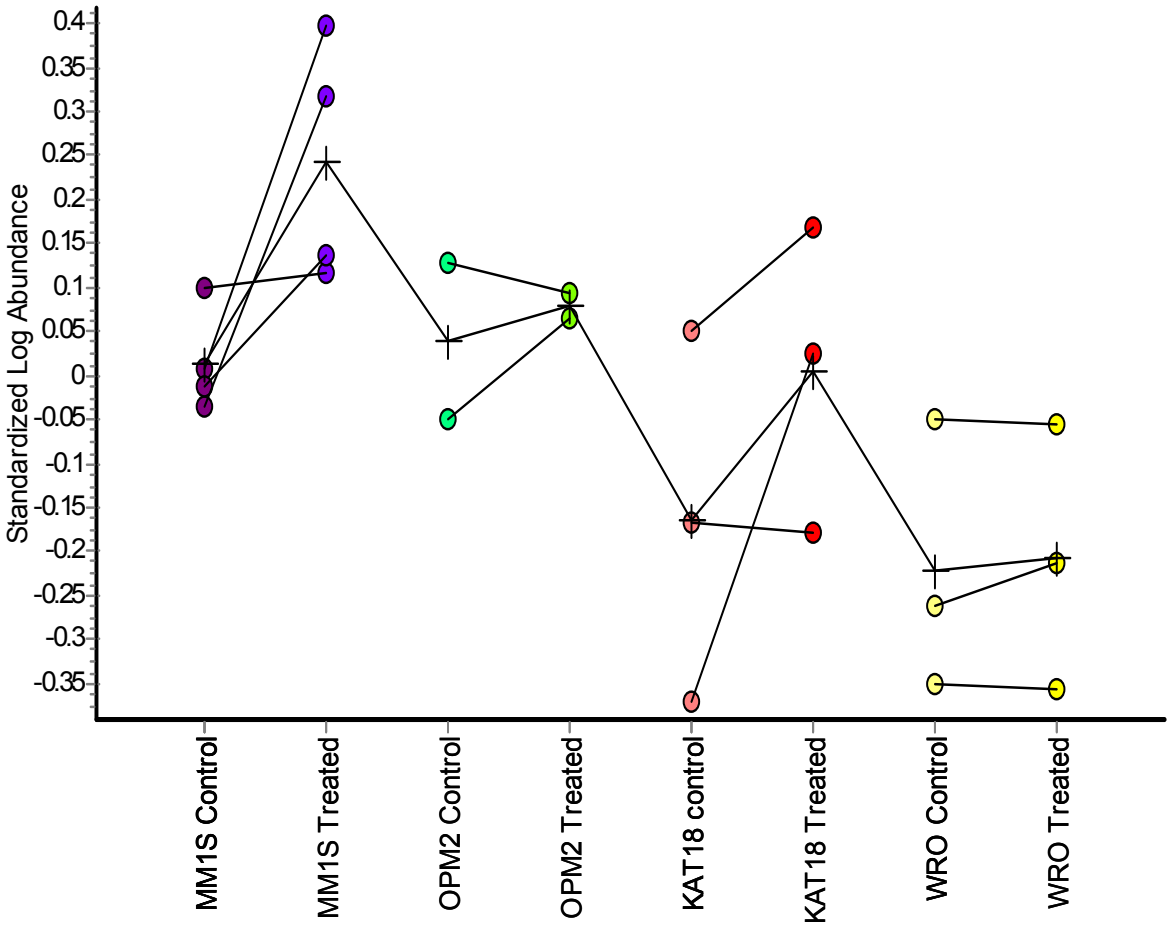

Fig 3.4.3.1 Trend of change in Heat shock protein 70kD

There was an increase in Hsp70 in sensitive cell lines (MM1.S and KAT18) and no change in resistant cell lines (OPM2 and WRO). The abundance of the Hsp70 protein for each cell line shown was calculated based on the intensity of the spot on the 2D-DIGE gel

3.4.3.2. Caspase-3 protein

Another protein identified was caspase-3. This protein was downregulated in the sensitive cells that were treated with bortezomib and there was no change in the resistant cell lines (Fig. 3.4.3.2). We validated this result in the bortezomib sensitive cell line MM1.S by Western blot (Fig. 3.4.3.3) showing a decrease in total caspase-3 and formation of cleaved products after treatment with bortezomib.

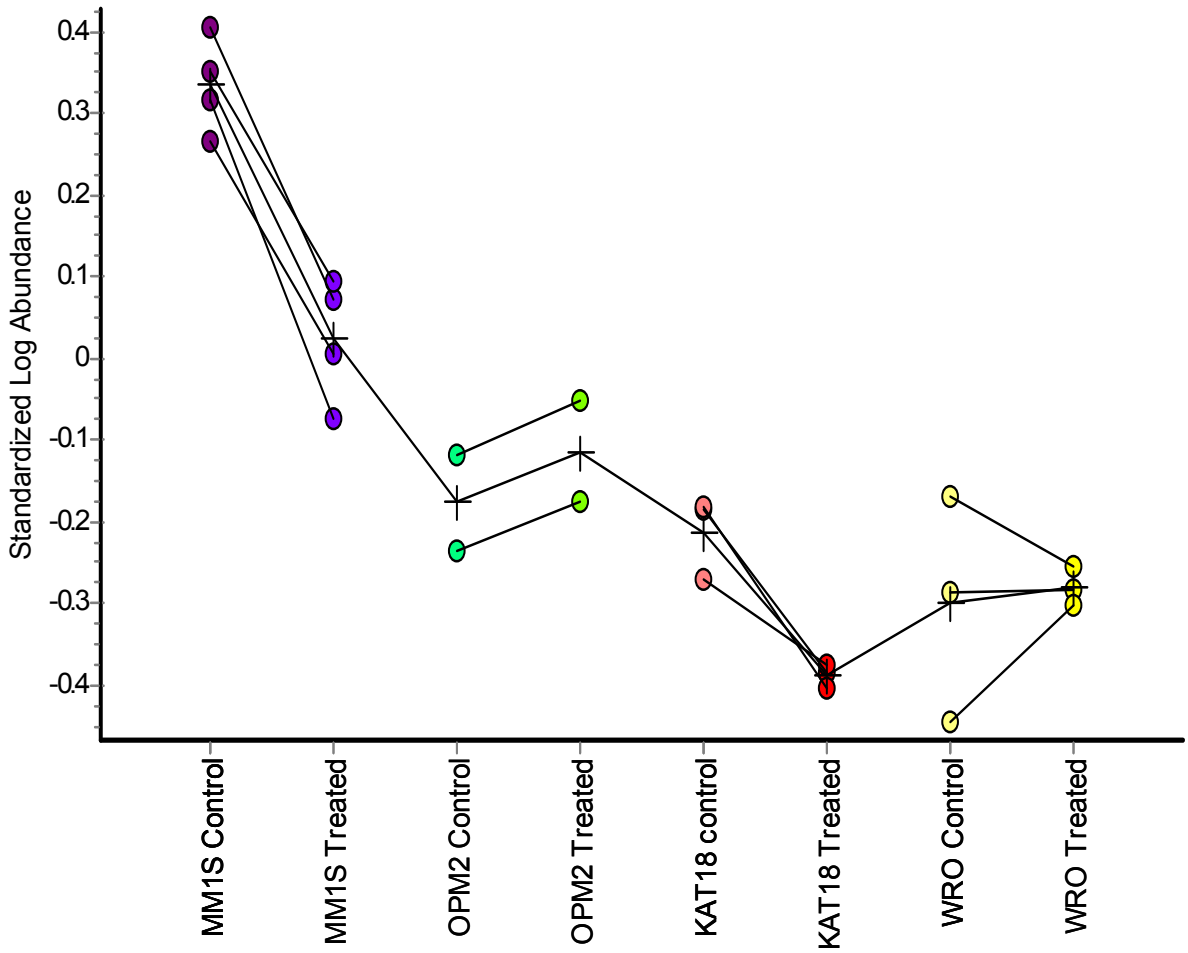

Fig 3.4.3.2 Trend of change in caspase-3 protein

There was a decrease in total caspase-3 in sensitive cell lines (MM1.S and KAT18) and no change in resistant cell lines (OPM2 and WRO). The abundance of the caspase-3 protein for each cell line shown was calculated based on the intensity of the spot on the 2D-DIGE gel

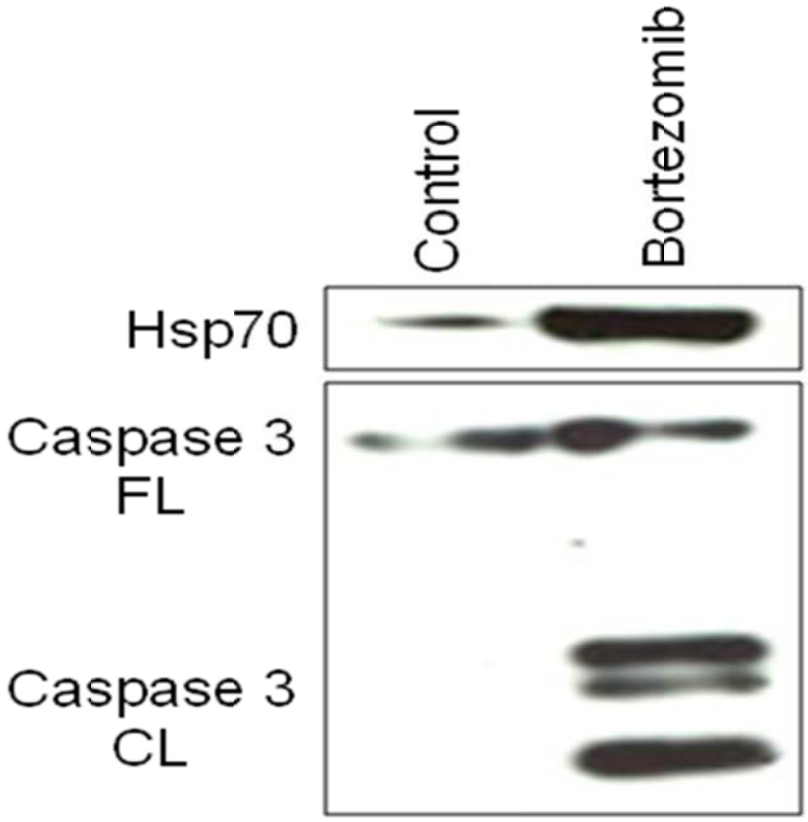

Fig. 3.4.3.3 Western blot analysis of the sensitive cell line MM1.S validating the results of proteins identified.

Western blot analysis demonstrating an increase in Hsp70 and a decrease in total caspase-3. The decrease in caspase-3 is secondary to cleavage products being generated due to bortezomib treatment.

3.4.4. Novel proteins identified

Proteins shown in Table 3.4.4.1 were proteins with no previously known association with myeloma or bortezomib treatment. These proteins were identified (from Table 3.4.2.2) showing a significant trend with the treatment and we plan to validate these proteins and further identify how bortezomib treatment affects or changes them. Heterogeneous nuclear ribonucleoprotein A2/B1 isoform B1 and KHSRP protein were picked from Table 3.4.4.1 to highlight the details of the Mascot software on obtaining the protein identification (Appendix A).

2D-DIGE analysis was used to identify the proteins in this experiment. To validate the proteins in Table 3.4.4.1, Western blotting was done. Fig. 3.4.4 demonstrated that Western blotting revealed the same trend of change as our results with 2D-DIGE (Table 3.4.4.1). Table 3.4.4.2 showed the densitometry readings analysed using Image J, of the protein bands in Fig. 3.4.4.

3 proteins that were also identified as having a significant trend were 26S protease (S4) regulatory subunit (protein ID 675), proteasome 26S subunit, ATPase 2 (protein ID 914) and proteasome 26S subunit, ATPase 2 (protein ID 1088). These proteins were not further studied as bortezomib is a proteasome inhibitor and would be expected to affect proteins such as these.

Protein ID	Protein Name	Sensitive - MM1.S		Resistant - OPM2		1 way ANOVA	Mascot Score
		Fold change		Fold change			
222	KHSRP protein	-1.59	↓	-1.06	⟷	0.016	149
443	FBP 1	-2.07	↓	1.06	⟷	3.20E-08	112
457	FSCN1 protein	1.7	↑	-1.08	⟷	0.048	63
605	HnRNP K	-1.61	↓	1.08	⟷	0.00036	142
1265	Annexin A2, isoform 2	1.73	↑	1.06	⟷	4.60E-05	116
1306	HnRNP A2/B1 isoform B1	-1.08	↓	1.16	⟷	0.022	370
1351	A+U-rich element RNA binding factor	-1.31	↓	1.03	⟷	9.40E-06	114
1436	HnRNP A1	-1.45	↓	1	⟷	0.00027	114
1669	ERp 29	1.24	↑	1.02	⟷	0.0032	134
1932	Ferritin, light polypeptide	13.06	↑↑	1.31	↑	0.0046	98

Table 3.4.4.1 Proteins identified for further analysis

These proteins identified from the generated list have no previously known association with myeloma or bortezomib treatment. They have been identified with other cancer types. All proteins have a 1 way ANOVA of <0.05.

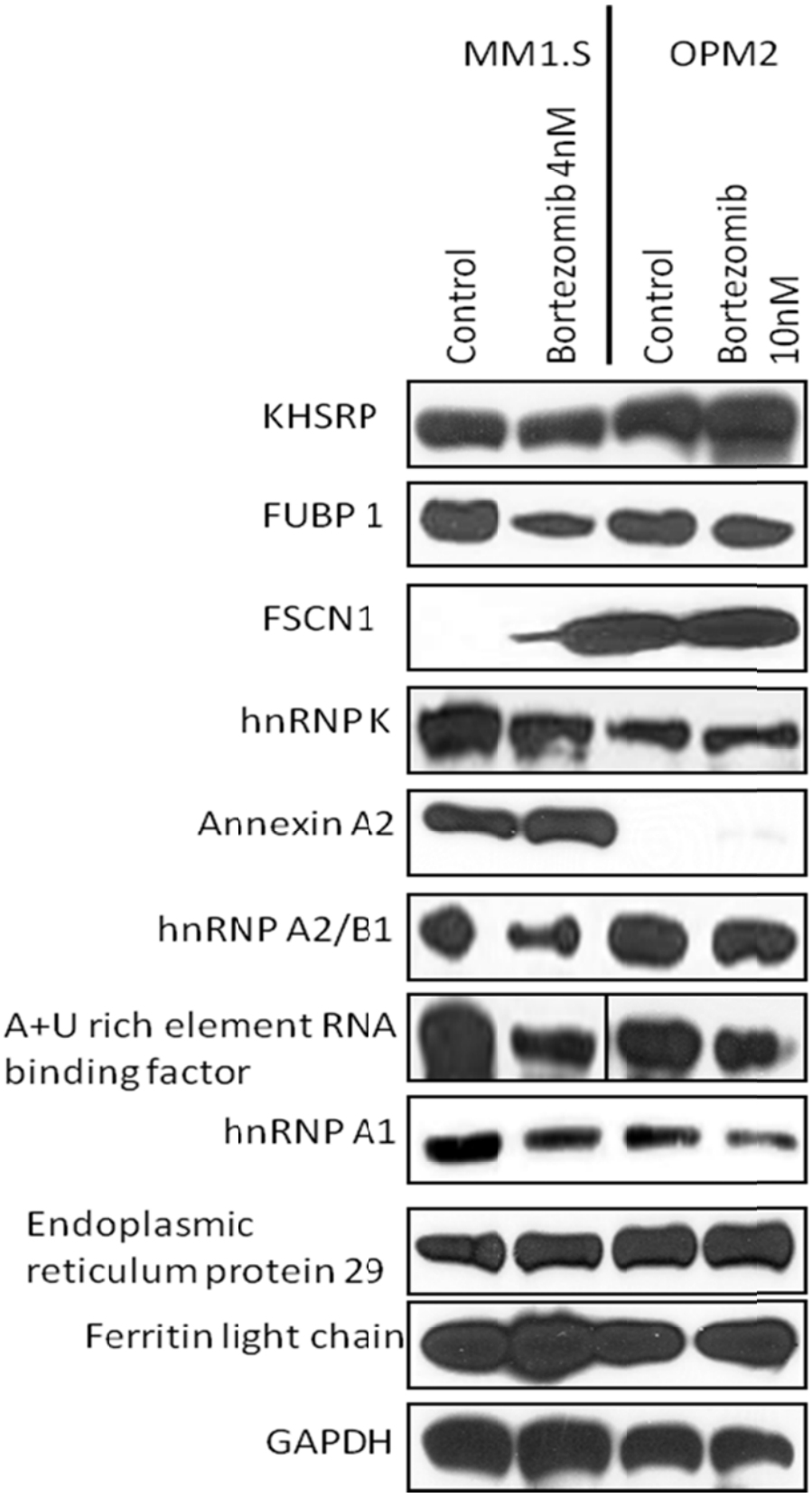

Figure 3.4.4 Western blot analysis of the proteins identified in Table 3.4.4.1

Immunoblotting validates the trend of change seen in our 2D-DIGE analysis. GAPDH was used as a loading control.

	MM1.S		OPM2	
	Control	Bortezomib 4nM	Control	Bortezomib 10nM
KHSRP	1.0	0.7	1.0	1.0
FUBP1	1.0	0.4	1.0	1.0
FSCN1	1.0	20.7	1.0	1.0
HnRNP K	1.0	0.5	1.0	1.0
Annexin A2	1.0	1.4	NA	NA
HnRNP A2/B1	1.0	0.7	1.0	1.0
A + U rich element RNA binding factor	1.0	0.5	1.0	1.0
HnRNP A1	1.0	0.6	1.0	1.0
ERp 29	1.0	1.2	1.0	1.0
Ferritin	1.0	1.4	1.0	1.1
GAPDH	1.0	1.0	1.0	1.0

Table 3.4.4.2 Densitometry readings of the Western blot analysis in Fig. 3.4.4

Chapter 4
Discussion

4. Investigation of the intrinsic mechanism of resistance

With the advent of novel therapies, patients with MM are enjoying a longer survival. With more patients surviving longer, genetic mutations that were rarely seen in MM, such as p53 mutation/deletion are now more commonplace. P-gp expression is also another resistance mechanism that has the potential to increase in relapse/refractory MM. Although bortezomib is an effective drug, more and more patients are relapsing when treated as a single therapy. The trend is to combine bortezomib with other conventional agents, such as dexamethasone, doxorubicin and melphalan and novel agents, such as lenalidomide. There are other clinical trials looking at the combination of bortezomib with other investigational agents such as perifosine and histone deacetylase inhibitors. The reason that bortezomib is used in so many different combinations is that it is a very effective agent in MM. Thus, being able to prolong its use in relapse/refractory patients is imperative. The aim of this thesis was to investigate resistant mechanisms in MM with regard to bortezomib treatment. Development of resistance to bortezomib via the overexpression of p-gp or through perturbations of the p53 pathway is overcome by using a p-gp modulator or Mdm2 inhibitor respectively. Using AMPK activators, we can overcome bortezomib-resistant MM by activating an alternative pathway to killing MM cells. Finally, using 2D-DIGE analysis, we have identified proteins that are potential targets in causing bortezomib resistance.

4.1 MDR associated protein expression as a mechanism of resistance

4.1.1. The relationship between Multiple Myeloma and MDR proteins

MM is an incurable plasma cell disorder which generally responds to treatment but inevitably relapses, even with the advent of newer more targeted therapies. As mentioned in the introduction, there exist primary (intrinsic) resistance where the drug insensitivity is present from first diagnosis and unresponsive to first line chemotherapy or secondary (acquired) resistance where tumour cells develop resistance during chemotherapy. One of the underlying causes of drug resistance is the acquisition of multidrug transporters in the cancer cells; these transporters are energy-dependent transmembrane proteins which can efflux a broad range of anticancer drugs, and thereby play a role in resistance to the actions of substrate agents. P-glycoprotein (P-gp; MDR-1; ABCB1), multidrug resistant protein-1 (MRP-1; ABCC1) and breast cancer resistance protein (BCRP; MXR; ABCG2) are thought

to play the most important roles in transporter-mediated resistance. That is the reason that these three MDR proteins were chosen to be studied in this thesis.

The incidence of MDR proteins in MM is not well characterised. P-gp does not seem to be overexpressed *de novo* in MM cells obtained from patients before they receive chemotherapy. In most P-gp related studies of MM, the collection and analysis of P-gp expression and function was limited due to technical difficulties. A study by Schwarzenbach [292] demonstrates the incidence of the three genes associated with multidrug resistance (MDR) in multiple myeloma in relation to treatment status. MDR1 mRNA/Pgp (P-glycoprotein) expression was detected in 41% of 93 myeloma samples. Generally, the incidence of MDR1/Pgp expression was higher in pretreated samples, and treatments with doxorubicin and/or vincristine were more effective in inducing MDR1/Pgp expression than with alkylating agents. Two other studies [146, 293] showed that P-gp expression does increase in approximately 75% of patients treated with vincristine, doxorubicin and dexamethasone (VAD). The likelihood of P-gp expression in MM correlated with the cumulative dose of doxorubicin and vincristine the patient received. As most previous and current MM regimens contain one or both of these drugs, MM patients who have been previously treated may have developed P-gp related resistance.

The same study by Schwarzenbach [292] showed that taking MRP mRNA and protein expression together, MRP was detected in 20.5% of 88 myeloma samples. LRP (lung-resistance protein) protein expression by immunohistochemistry was observed in 12.5% of 72 myeloma samples. MRP and LRP expression was similar in samples with and without prior therapy.

BCRP is a more recently identified multidrug resistance protein. Similar to the other members of the ATP-binding cassette family of membrane transporters, such as P-gp and MRP1, BCRP is expressed in a variety of malignancies, where it may produce resistance to chemotherapeutic agents [294]. Cell lines that express high levels of BCRP are fibrosarcoma, ovarian cancer, breast cancer, and myeloma cell lines [295]. Haematological malignancies such as acute myeloid leukaemia [296] and acute lymphoblastic leukemia [297] have been shown to express BCRP as a resistance mechanism. It has also been found to be expressed in the mitoxantrone-selected human MM cell line 8226[295]; however, the clinical relevance of this transporter in MM patients remains to be validated.

In the mid-1990s, there was a lot of interest in P-gp-mediated resistance and using P-gp inhibitors to overcome drug resistance in an attempt to improve treatment outcome of patients with MM. A phase I/II study was conducted using the MDR modulator verapamil, in combination with VAD, to treat patients with refractory MM [298]. An approximately 50% partial response was found in the study, but this combined therapeutic strategy resulted in significant cardiac toxicity. An attempt to minimise this side effect by using lower doses of verapamil in combination with VAD to treat patients with MM in a randomized phase III trial yielded no therapeutic benefit as a result of the suboptimal dose of verapamil[148]. Quinine was another P-gp modulator that was utilised in combination with VAD and prednisone in a phase III Southwestern Oncology Group trial [299]. Progression-free and OS rates were similar between the two arms. Sonneveld *et al*. [147] used cyclosporine, another MDR modulator, has been used with the VAD regimen in treating refractory or progressive MM patients. They reported more toxicity in the treatment arm containing cyclosporine with similar overall response rate, progression-free and OS rates in the two arms. Valspdar (also called PSC833) is an oral form of a cyclosporine D derivative and is approximately five-fold more potent than cyclosporine in inhibiting P-gp. Unlike the early generation of MDR modulators that are the substrates and competitive inhibitors of P-gp, valspodar is a non-competitive inhibitor of P-gp. There is a strong interaction between valspodar and other P-gp substrates. Valspodar can inhibit P-gp in the liver and kidneys, which is required for serum drug excretion. Concomitant use of valspodar was shown to increase the therapeutic efficacy of doxorubicin and reduce the total dose needed by 50% to 75%.In MM, valspodar had been tested in 22 patients with refractory MM in a phase I trial in which oral valspodar was used with VAD [300]. It seems to be less toxic than cyclosporine, however, recent data from phase III trials of other haematological malignancies, including AML, have failed to demonstrate the benefit of adding valspodar to the chemotherapy regiment in treating relapsed disease [301]. A phase III trial conducted by the Cancer and Leukemia Group B showed excessive toxicity and death from valspodar treatment in previously untreated elderly patients with AML, resulting in the premature closure of the study [302].

Newer generation P-gp modulators include GF120918 (also called elacridar), LY335979 (also called zosuquidar) and VX-710 (also called biricodar). Elacridar, a substituted isoquinolinyl acridonecarboxamide, is a multispecific third-generation MDR modulator [139]. *In vitro* studies indicate that elacridar fully reversed resistance to etoposide, doxorubicin, vinblastine, docetaxel, and paclitaxel in MDR

sarcoma cells [303] and enhanced doxorubicin tumour cell kill in Pgp–mediated resistant leukeamia and myeloma cells [304]. Recent publications also demonstrate complete reversal of mitoxantrone resistance due to the ATP-binding cassette half-transporter, BRCP, with the use of elacridar [305, 306]. Unlike valspodar, elacridar appears to have minimal interactions with MDR substrates. Clinical phase I trial combining elacridar with doxorubicin indicate that unlike valspodar, doxorubicin pharmacokinetics were not affected by the modulator [307]. Another phase I trial examining the above combination in solid tumours demonstrated that the doxorubicin dose was marginally influenced by elacridar but only at the highest dose levels. These patients however, had significant increase in the area under the curve of doxorucibin especially in later cycles, resulting in neutropenia [308].

Zosuquidar, a difluorocyclopropyl dibenzosuberane, is one of the most potent, highly selective P-gp modulators to date [140]. As such, it has been combined with various chemotherapy regimens in different malignancies. Zosuquidar has a high affinity to, but is not a substrate of, P-gp. Preclinical studies demonstrated that this compound sensitizes various MDR cell lines and enhances survival of nude mice engrafted with the Pgp–expressing leukaemia cell line, P388/ADR. A number of phase I trials combining oral zosuquidar with docetaxel in metastatic breast cancer and other solid tumours have been performed. An earlier trial [309] reported a minimal increase in docetaxel peak plasma concentration and area under the curve whereas a later trial [310] deemed the combination safe. The evidence on whether the pharmacokinetics of doxorubicin is similarly affected is controversial. One phase I trial [311] reported that zosuquidar at doses that exceed 500mg generated a modest decrease in doxorubicin clearance with haematological toxicity whereas another phase I/II trial [312] stated that the pharmacokinetics of doxorubicin was not affected. Zosuquidar also affects the pharmacokinetics of vincristine and vinorelbine [312, 313]..

Biricodar, an amido-keto-pipecolinate derivative, is a potent modulator of P-gp and also inhibits MRP1-related drug transport, thus overcoming two of the most prevalent resistance phenotypes [314]. biricodar reversed resistance to doxorubicin, etoposide, and vincristine in both Pgp– and MRP-expressing MDR cell lines. Rowinsky *et al*. [315] reported minimal toxicity when biricodar was used alone in patients with solid malignancies.

Thus far, the clinical trials using first and second generation P-gp modulators did not show clinical benefit or there was unacceptable toxicity. The newer modulators show some toxicity with but it was minimal compared to the older P-gp modulators. However, there was no clinical benefit seen when P-gp modulators were added to chemotherapeutics in metastatic breast cancer or elderly acute myeloid leukaemia [310, 316]. At the present time, clinical trial evidence indicates that P-gp modulation in combination with chemotherapeutics is still not a feasible strategy for improving overall treatment efficacy.

4.1.2. The rationale for proteasome inhibition as an anticancer therapy

As part of the ubiquitin–proteasome pathway, the proteasome is the final common endpoint of the vast majority of regulated intracellular proteolysis. Proteins destined for destruction and turnover are tagged with polyubiquitin chains by the ubiquitin conjugation system. In the first reaction, the E1 ubiquitin enzyme activates ubiquitin and attaches it to the ubiquitin-conjugating enzyme E2 in an ATP-dependent manner. The E3 ubiquitin ligase then links the ubiquitin molecule to the target protein and which is shuttled to the 20S and 26S proteasomes for digestion and turnover [317, 318]. By inhibiting proteasome activity, bortezomib affects this proteolytic process leading to an accumulation of intracellular ubiquitinated proteins.

NF-κB is composed of a family of homo- and heterodimeric transcription factors that bind to a common sequence motif called the κB site. Inhibition of κB (IκB) protein contain an N-terminal regulatory domain followed by multiple ankyrin repeats that interact with the Rel homology domain of NF-κB through protein-protein interaction. The various IκBs bind to NF-κB proteins, covering the nuclear localisation signal of NF-κB proteins, and thereby preventing their translocation from the cytoplasm to the nucleus.

NF-κB-I-κB complexes are mostly located in the cytoplasm and remain transcriptionally inactive until the cells receive extracellular stimuli, such as proinflammatory cytokines TNF-α and IL-1 [136]. In response to these stimuli, the IκB kinase complex (IKK) is activated and it phosphorylates NF-κB-bound IκB proteins on two conserved serine residues within the NH_2-terminal regulatory domain. Phosphorylated IκB proteins are then recognised by the TrCP-containing Skp1/Cullin/F-box protein ubiquitin ligase complex, resulting in its ubiquitination followed by proteolytic degradation through the function of 26S proteasome.

Removal of IκB proteins by proteasome-dependent degradation unmasks the nuclear localisation signals of NF-κB causing an activation of gene transcription that leads to the expression of anti-apoptotic proteins.

NF-κB has been to shown to promote myelomagenesis by inducing growth and angiogenesis factors such as interleukin-6 and vascular endothelial growth factor, by activating important cell-cycle regulators such as c-Myc and cyclin-D1, by promoting an antiapoptotic state through intermediates such as Bcl-2 and Bcl-x_L, and by enhancing myeloma cell adherence to the surrounding stroma, such as through effects on fibronectin and vascular cell adhesion molecule-1 [27]. Activation of apoptosis in cancer cells resulting from NF-κB inhibition is the basis that NF-κB inhibition could be used as a mechanism to treat cancers. Bortezomib is a drug that was specifically developed to block the signal transduction pathways activated by NF-κB [38]. The destruction of IκBα proteins after their phosphorylation by IKK and subsequent ubiquination is primarily mediated by proteasome degradation. Bortezomib suppresses NF-κB activity by inhibiting this degradation and stabilising IκBα, which binds NF-κB and prevents its nuclear translocation; thereby downregulating levels of its targets and producing a potent antimyeloma effect [27].

A number of studies have shown the inhibitory effect of proteasome inhibitors on tumour cell growth and proliferation [27, 44, 278, 319]. Hideshima *et al.* [27] have demonstrated *in vitro* that bortezomib can inhibit proliferation through induction of apoptosis of several human MM cell lines, as well as MM cells isolated from patients. In animal studies, bortezomib has been shown to have a therapeutic role by inhibiting tumour growth in mice treated with the drug [320]. On the basis of positive preclinical studies, several human trials with bortezomib were conducted. After phase I trials demonstrated the safety of bortezomib among patients with a variety of advanced malignancies [321], phase II trials (SUMMIT) and (CREST) were conducted to treat patients with relapsed of refractory MM. There was a response rate of 35% to 38% and a median survival of 16 months (SUMMIT) [40, 41]. These results were confirmed in the international, multicenter phase III Assessment of Proteasome Inhibition for EXtending remissions (APEX) trial, in the response rate among individuals in the bortezomib group was 38%, with a CR rate of 6%, whereas the OR and CR rates in the dexamethasone group were 18% and 1%, respectively. Superior median time to progression (TTP) (6.22 versus 3.49 months) and 1-year survival (80 versus 66%) were observed in the bortezomib as compared with dexamethasone-treated patients [42]. In an updated analysis, the OR and CR rates in the bortezomib arm were 43 and 9%, respectively [43].

However, patients who have been previously treated with bortezomib are now demonstrating resistance to proteasome inhibition.

4.1.3. Bortezomib's relationship with MDR ptoteins

As described earlier, bortezomib is a novel treatment for MM. Resistance to this drug is multifactorial and there is now emerging evidence that proteasome inhibitors interact with MDR proteins. Of all the MDR proteins, P-gp appears to be the most studied in relation to bortezomib but the nature of interactions between this agent and this efflux protein is controversial. There are indications that overexpression of this pump may contribute to resistance to bortezomib. Rumpold *et al* .[150] showed that knockdown of P-gp resensitises P-gp-expressing cells to proteasome inhibitors. The authors also showed that bortezomib was a P-gp substrate. In Ewing's sarcoma, Nakamura *et al.* [322] demonstrated that P-gp and MRP-1-expressing clones of Ewing's tumours, which have shown resistance to substrates of P-gp and MRP-1 (e.g. adriamycin, vincristine, etoposide, and actinomycin D), also possess a cross resistance to bortezomib. This suggests that bortezomib is not only a P-gp substrate but also a MRP-1 substrate. The authors proceeded to show that combination treatment with bortezomib and a P-gp or MRP-1 inhibitor reduced the resistance seen with single agent bortezomib treatment. This finding is further supported by Iijima *et al.* [323] who showed that the proteasome inhibitor class of agents are substrates of P-gp. With MDR-interacting agents, substrates are not necessarily inhibitors and vice versa and other studies have demonstrated that proteasome inhibitors are also P-gp inhibitors [324]. Finally, there are some studies which have demonstrated that bortezomib is not an MDR substrate at all. Such studies points to the fact that there is little cross resistance to bortezomib in cells that are known to be P-gp or MRP-1-overexpressors [325, 326]. Thus far, there is no conclusive evidence one way or the other about the interaction of bortezomib with MDR proteins.

In our findings, we wanted to clarify the interaction of bortezomib with MDR proteins. In the present study, we characterized the interaction of bortezomib with multidrug transporters; P-gp, BCRP and MRP1 and explored the potential for this interaction to play a role in resistance. To establish if bortezomib interacts with the MDR protein P-gp, we utilised cell lines that have different and defined levels of overexpression of P-gp; DLKP-A, RPMI-Dox40, A549-taxol and NCI-Adr/res (Table

3.3.1.) All but one of the cells lines that were used to determine MDR expression and function were different isogenic lines that were developed in the NICB, Dublin. It was important to use an isogenic line (i.e. to compare parent and resistant daughter line) to ensure that any comparison between the cell lines would be related to the MDR proteins and not a cell line-specific effect. In these lines, P-gp overexpression ranges from low (A549-taxol) to high (DLKP-A) (Fig. 3.1.5). This was necessary to be able to study the mechanism of bortezomib interaction with P-gp in detail.

Elacridar, a P-gp inhibitor was combined with bortezomib in a series of experiments. We first determined a dose of bortezomib for each cell line used that gave an $IC_{70\text{-}90.}$. Elacridar was also tested on the cell lines and it was non- toxic in all cell lines at the concentrations employed (Fig 3.1.2.5). Nonetheless, the dose used in the experiments was the lowest possible dose that still yielded an adequate P-gp inhibition (Fig. 3.1.2.6)

Using the DLKP-A cell line, we compared the response of bortezomib to its parental line, DLKP. There was a marked increase in resistance in the DLKP-A cell line (Fig.3.1.2.5). This suggests that P-gp is responsible for resistance to bortezomib but to better examine this hypothesis, bortezomib was combined with the P-gp inhibitor, elacridar and there was marked toxicological synergy in this combination (Fig. 3.1.2.1 and 3.1.2.2.) The synergy was most obvious when the two drugs were allowed to interact for a longer period of time. This means that not only cell death is involved but cell proliferation was inhibited by this combination as well.

To see if this synergistic cytotoxicity was maintained across different cancer types, we tested the bortezomib and elacridar combination in several different P-gp-overexpressing cancer cell lines; DLKP-A (lung cancer) NCI-Adr/res (ovarian cancer) and RPMI-Dox40 (MM), results of which confirmed that there was synergistic cytotoxicity when elacridar and bortezomib were combined (Fig. 3.1.6). These experiments demonstrate that bortezomib is a substrate of P-gp as it was able to reverse the resistance seen when P-gp was inhibited by elacridar. This finding that bortezomib is a P-gp substrate confirms the results of other recent studies [150, 322, 323].

In the literature, there is a study on a breast cancer cell line that suggested bortezomib is a P-gp inhibitor [324]. Two other studies undertaken using leukemia cell lines suggested that bortezomib is not an inhibitor as it does not synergise with

daunorubicin (an anthracycline) [327, 328]. In our data, we tested the P-gp overexpressing cell line DLKP-A and concluded that bortezomib is at best a weak inhibitor. When doxorubin, a P-gp substrate, was combined with bortezomib, we found only an additive effect except at the highest dose of bortezomib tested, where there was mild synergistic killing (Fig. 3.1.2.3). Collectively, these inconsistent reports suggest that findings with regard to interactions between bortezomib and anthracyclines might depend on the choice of drug used in combination, the cell line studied and the method used to assess the drug interactions.

Another reason that bortezomib synergises with doxorubicin may be related to other apoptotic mechanisms and is not P-gp related. In the treatment of MM, Mitsiades *et al.* investigated the mechanism of the chemosensitising activity of bortezomib with oligonucleotide gene microarray analysis [44]. The authors demonstrated that bortezomib could downregulate the transcripts for several effectors of the protective cellular response to genotoxic stress: topoisomerase II beta, which relaxes DNA torsion on replication, transcription, and cell division and is inhibited by doxorubicin. They concluded that this was the reason for synergy between bortezomib and doxorucibin. In support of this, we demonstrated that bortezomib and doxorubicin mildly synergises in a P-gp negative cell line (Fig. 3.1.2.4) implying that P-gp status has no bearing on bortezomib and doxorubicin synergy and consistent with the findings of Mitsiades *et al.*.[44]

Although P-gp is not usually overexpressed in early MM disease, with exposure to natural products such as anthracyclines and vinca alkaloids, and a longer disease period, there is increased expression of the transporter [146, 292]. Previous clinicals trial carried out with the premise that inhibition of overexpressed P-gp would lead to increased anti-cancer activity have failed to show a survival or progression free benefit in the P-gp positive patients [147-149]. One of the reasons for the failure of these trials was the increased general toxicity from anthracyclines. P-gp expression in normal body tissues, especially the liver, is important for eliminating such agents from the body, thereby abrogating the toxic actions of anthracyclines (and other P-gp substrate chemotherapeutics) and hence body-wide P-gp inhibition increases the incidence and severity of side effects. In our current study, we have shown that bortezomib is a good P-gp substrate and a weak inhibitor. The cross resistance to bortezomib seen in P-gp-overexpressing cells may be overcome by combining a P-gp inhibitor, such as elacridar, to bortezomib. Bortezomib is a very efficacious agent in MM, if we can extend the life of this agent in patients who have developed resistance to the drug by adding in a P-gp inhibitor,

we expect to see efficacy of this drug in the P-gp positive patient population. MM cells are exquisitely sensitive to bortezomib and if a P-gp inhibitor is functioning to increase the intracellular dose of bortezomib, it seems likely that we can use standard or even a lower dose of bortezomib to treat P-gp-induced resistance in MM patients. Thus we may be able to overcome toxicity issues associated with having to use elevated doses of bortezomib in such patients.

MRP overexpression is not a common phenomenon in MM. It was only detected in about 20.5% of 88 myeloma samples [292], with overexpression being more common in other haematological malignancies such as acute myeloid leukaemia [329]. However, MRP-1 is a known multidrug resistance protein and we wanted to investigate its interaction with bortezomib.

We used the DLKP cell line. DLKP is known to have MRP-1 overexpression. While the level of overexpression of this transporter is small, it still contributes to this cell line being resistant to MRP-1 substrate agents and inhibition of MRP-1 increases the efficacy of MRP-1 substrate drugs [272]. We combined bortezomib with sulindac sulphide, a MRP-1 inhibitor and failed to demonstrate any synergy (Fig. 3.1.3). Even though MRP-1 is only expressed in a small majority of MM resistance, our findings suggest that there is little evidence that MRP-1 resistance would affect bortezomib treatment although we have not specifically shown this in MM cells. This has also been seen in an MRP-1 overexpressing leukaemia cell line where there was no cross resistance to bortezomib [328].

BCRP is a relatively newly identified multidrug resistant protein. Similar to the other members of the ATP-binding cassette family of membrane transporters, such as MDR1 and MRP1, BCRP is expressed in a variety of malignancies, where it may produce resistance to chemotherapeutic agents [294]. Turner *et al.* [294] reported that BCRP mRNA and protein expression in myeloma cell lines increased after exposure to topotecan and doxorubicin, and was greater in log growth phase cells when compared with quiescent cells. Therefore, as with P-gp, BCRP can be induced in MM after exposure to chemotherapeutics.

We wanted to further characterise the role of BCRP in bortezomib resistance in MM. Treatment of DLKP-SQ/Mitox (which overexpresses BCRP) [279] did not show any synergistic cytotoxicity when bortezomib was combined with elacridar (which can also act as a BCRP inhibitor) (Fig. 3.1.4.1). We wanted to investigate this further and treated DLKP and DLKP-SQ/Mitox with bortezomib. The two cell lines

responded to bortezomib in a similar fashion without any resistance seen in the BCRP-overexpressing cell line (Fig. 3.1.4.2). This is unlike Fig. 3.1.2.5A where the P-gp expressing cell line DLKP-A, demonstrated significant resistance to bortezomib. This finding suggests that bortezomib is not a substrate for BCRP. The interaction of bortezomib with BCRP was further analysed. SN38 is an irinotecan metabolite which is a known substrate for BCRP. Bortezomib was combined with SN38 and DLKP-SQ/Mitox cells were treated with this combination. There was no synergistic killing evident demonstrating that bortezomib is not a BCRP inhibitor (Fig 3.1.4.3). These findings are in agreement with another study using leukaemia cells which also demonstrated that bortezomib is not a BCRP substrate [328].

4.1.4. P-gp expression correlates to bortezomib's efficacy as a substrate

As mentioned in section 4.1.1, clinical trials that used a combination of VAD with P-gp inhibitors such as cyclosporine [147], verapamil [148] or PS-833 [149] showed no clinical benefit in terms of increased OS or progression-free survival in the arm with VAD + P-gp inhibitor. Poor inhibition of tumour P-gp function by the P-gp inhibitors and requisite dose reduction of chemotherapeutics as a result of increased general toxicity are some of the postulated reasons for failure. Another potential reason is that patients in these trials were not stratified by tumour P-gp overexpression, so any potential benefit that may be seen in inhibition of tumour P-gp function was not taken into account. In all these trials [146-149], there was a slight benefit in the P-gp positive patients to VAD + P-gp inhibitors, but the numbers of patients that was evaluated was too small to show any statistical significance. The quantity of the P-gp expression was also not evaluated in these trials and we can show in our study that it has a bearing on how efficacious bortezomib is able to act as a P-gp substrate.

In our study, we first quantified the P-gp expression in different cell lines by densitometry (Fig. 3.1.5). Fig. 3.1.2.5. suggested that P-gp expression levels play a part in bortezomib resistance. We showed that a cell line with a higher level of P-gp overexpression (DLKP-A) demonstrated reduced sensitivity to bortezomib compared to its parental cell line but A549-taxol, which overexpresses a much lower P-gp level, had minimal attenuation of bortezomib activity. This suggested that the level of P-gp overexpression plays a part in bortezomib resistance. We then demonstrated that a cell's P-gp expression correlates with how effective bortezomib

is able to function as a substrate for P-gp (Fig. 3.1.6.1). DLKP-A which expresses the highest level of P-gp demonstrated the most synergy in the bortezomib and elacridar combination, whereas A549-taxol which had the lowest level of P-gp had mainly additive effect. In the clinical trials with P-gp inhibitor, the expression level of P-gp was not quantified. There is a possibility that doxorubicin has a similar effect as bortezomib in that the expression levels of P-gp will dictate the ability of doxorubicin to synergise with P-gp inhibitors. There are currently no studies addressing this specific question in the literature.

It was important to determine if this synergy correlation definitely related to P-gp levels and was not a tumour origin or cell line specific event. To address this, we examined RPMI-Dox40, a MM cell line which overexpresses P-gp. Its P-gp expression arose from *in vitro* selection by doxorubicin from the parental line RPMI8226. To maintain the P-gp expression, a low dose doxorubicin has to be in the culture medium to maintain the selection pressure. In our laboratory, we had a variant of this cell line RPMI-Dox40 LP that has not been cultured in doxorubicin, therefore, the P-gp expression was reduced (Fig. 3.1.6.3A). The RPMI-Dox40 which have been cultured in doxorubicin (RPMI-Dox40 HP) was more resistant to both doxorubicin and bortezomib (Fig. 3.1.6.2) and had a higher level of synergy with bortezomib and elacridar compared to RPMI-Dox40 LP (Fig. 3.1.6.3). This result suggests that the better synergy between bortezomib and elacridar is dependent upon P-gp and not the origin of the cancer or the cell line employed. For patients who subsequently develop P-gp expression or an increase in P-gp expression, we have shown that by combining a P-gp inhibitor and bortezomib, we should be able to overcome any P-gp-related resistance to bortezomib.

All the clinical studies conducted to date have a common weakness (where such data has even been analysed) that is the small numbers of P-gp positive patients enrolled. These studies were done in the era before the advent of novel treatments and thus the patient population was relatively early in their disease, despite there being cases of relapse patients. With the advent of novel therapies, MM patients are enjoying a longer survival. However, this increased survival benefit comes with a price. These patients would have been exposed to more lines of treatment including vinca alkaloids or anthracyclines and have lived with the disease longer for any potential P-gp resistance to emerge or be selected for. Therefore, P-gp-mediated resistance may yet be a potential resistance mechanism and impact treatment options for MM patients. It is also unclear if bortezomib-refractory patients

will give rise to P-gp expression such as seen with patients treated with vinca alkaloids and anthracyclines. If P-gp-mediated resistance were to arise in this treatment group, continuing with bortezomib treatment would be a viable treatment option if a P-gp inhibitor were included in the regime as a P-gp inhibitor could negate the effect of this form of resistance. Our findings indicate that the higher the manifested P-gp expression, the better the synergy seen when bortezomib is combined with a P-gp inhibitor. Thus, we have the ability to continue treating patients with a valuable drug for longer periods of time.

In line with the clinical theme of this thesis, we wanted to examine if the bone marrow microenvironment might affect the synergistic cytotoxicity seen with elacridar and bortezomib. Fig. 3.1.7.2 demonstrated that although there was a slight attenuation of the combination in the presence of BMSCs, the synergy seen in the absence of BMSCs persists. This indicates that the increased activity of bortezomib in combination with elacridar that might be seen in resistant MM would not be abrogated by the presence of other accessory stromal cells.

4.1.5. Bortezomib can affect P-gp expression and function

Previous studies have demonstrated that MDR1 overexpression occurs through NF-κB activation that requires a NF-κB binding site located distal to the MDR1 promoter [330, 331]. Further publications have implicated NF-kB in upregulation of P-gp expression, which controls drug efflux in cancer cells [332]. Therefore, it is likely that increased P-gp expression participates in NF-kB-related cancer cell resistance to treatment. As bortezomib inhibits NF-kB, we wanted to investigate if bortezomib is able to affect the expression and function of P-gp.

In this study, we demonstrated that in RPMI-Dox40 and DLKP-A cells, P-gp expression levels were downregulated with bortezomib treatment (Fig. 3.1.8.1). These results were also reported by Fujita and colleagues [324] who demonstrated that proteasome inhibitors decreased the expression of mdr1 at both mRNA and protein levels in the breast cancer cell line MCF7. Similar findings were reported using MG132 in gastric cancer by Zhang *et al*. [333].

Although interesting to note that bortezomib can affect the expression of P-gp, what we wanted to probe further as to whether the P-gp function was also similarly affected by bortezomib treatment (since P-gp expression may not correlate with

function/resistance). To demonstrate P-gp function, we utilised the Rh-123 efflux assay. Rhodamine 123 is a P-gp substrate and is pumped out in cells containing P-gp. The rate of efflux is dependent on the amount of P-gp present in the plasma membrane of the cell tested. We have demonstrated that bortezomib treatment of RPMI-Dox40 cells caused a reduction in P-gp function by showing an accumulation of Rh-123 in bortezomib-treated cells (Fig. 3.1.8.3). This reduction in function was seen at all doses of bortezomib tested and maximal inhibition of function was seen at 2 h.

As mentioned, NF-kB activation is thought to upregulate P-gp. When NF-kB is downregulated by proteasome inhibitors, P-gp expression may be downregulated as well. NF-kB activation is attributed to various signalling pathways, including drug resistance and anti-apoptosis [334]. Bentires-Alj *et al.* [335] showed a role for NF-kB in the regulation of the *mdr1* gene expression in cancer cells and drug resistance by demonstrating that inhibition of NF-kB, through transfection of a plasmid coding for a mutated IkBα inhibitor, increased cellular daunomycin uptake and reduced *mdr1* mRNA and P-gp expression in P-gp-overexpressing colon cancer cells. As outlined in section 4.1.2., one of the main mechanisms of action of bortezomib is to block the proteasomal degradation of IκB proteins which then prevents the activation of NF-κB. Therefore, inhibiting the NF-kB pathway with bortezomib might be expected to downregulate MDR1activation and P-gp expression.

The ubiquitination-proteasome system is known to be involved in the degradation of short-lived, mutant or misfolded proteins. P-gp is a relatively stable protein with a half-life of 14 to 17 h [336]. It has been shown that inhibition of *N*-glycosylation increases the ubiquitination, decreases the stability and reduces the function of P-gp [336]. Immature, core-glycosylated P-gp has a shorter half-life of approximately 3 h [151]. In addition, Loo and Clarke [337] demonstrated that mutant forms of P-gp which are unable to fold into the mature forms are rapidly degraded. Schinkel *et al*.[338] proposed that N-glycosylation contributes to proper routing or stability of P-gp. Furthermore, inhibiting *N*-glycosylation of P-gp has been shown to decrease drug resistance in cancer cells overexpressing the transporter [339]. These data suggest that the core-glycosylated, immature or glycosylation-deficient P-gp are the targets of ubiquitination-proteasome system. As mentioned in section 4.1.2, bortezomib is able to increase ubiquitination of cellular proteins by preventing their

proteasomal degradation. Thus, by increasing ubiquitination and proteasome mediated degradation, bortezomib is able to decrease P-gp expression.

Another explanation for the downregulation of P-gp expression with bortezomib treatment may be a block in the maturation of the P-gp protein by bortezomib. Loo and Clarke [151] have demonstrated that MG-132, a proteasome inhibitor is able to inhibit the maturation of P-gp by preventing P-gp from reaching the cell surface after synthesis in the endoplasmic reticulum. Whether this is caused by NF-kB inhibition is as yet unknown. Thus, the proteasome could play a dual role in the folding of ABC transporter; it could promote folding of the proteins as well as mediate degradation of incorrectly folded proteins, inhibition of this function would therefore reduce the activity of the protein.

4.1.6. P-gp transference between cancer and its microenvironment

It is well established that MM-induced disruption of the BM homeostasis between the highly organized cellular and extracellular compartments supports MM cell proliferation, survival, migration and drug resistance through activation of various signalling pathways. Conventional chemotherapeutics such as dexamethasone and doxorubicin have been shown to be attenuated in the presence of BMSCs [62-64, 280]. We know that growth factors such as cytokines and chemokines are responsible for MM proliferation and resistance to conventional chemotherapeutics. The other BM accessory cells also play a role in promoting MM growth and survival [61, 72]. Thus far, the literature has few clues as to whether P-gp plays a role in mediating resistance to chemotherapeutics in this setting. We had hypothesized that P-gp expression in MM cells would be upregulated when co-cultured with BMSCs. In fact, a recent paper by Perez *et al.* [340] showed that stroma-released factor(s) induced NF-kB activation. If NF-kB is able to upregulate P-gp [332, 335, 341], then coculture with stroma should induce P-gp expression in MM cells. We investigated the expression of P-gp when MM cells were cocultured with BMSCs and the findings were contrary to such a hypothesis. We found that P-gp expression was downregulated when RPMI-Dox40 cells were coculture with BMSCs (Fig. 3.1.9.1). This finding may be explained by transference of P-gp protein to the BMSCs so when the P-gp expression of the MM cells was measured, there was less measurable P-gp in the MM cells. It has been reported that intercellular transfer of functional P-gp from P-gp-positive to P-gp-negative cells *in vitro* and *in vivo* can occur and causes increased drug resistance in the recipient cells [281].

Most importantly, such transfer-acquired resistance permits tumour cells to survive potentially toxic drug concentrations long enough to develop intrinsic P-gp-mediated resistance. P-gp transfer also occurs to putative components of tumour stroma, such as fibroblasts, raising the possibility that multidrug resistance could be conferred by resistant tumour cells to critical stromal elements within the tumour mass [281].

In this present study, we demonstrated that BMSCs cocultured with MM cells acquired P-gp from them. As far as we know, this is the first study to evaluate this phenomenon in MM. Whether this observation of P-gp transference is the explanation that the activity of anthracyclines against MM is reduced in the presence of the BMSCs requires further study. P-gp transference has also been suggested to occur in solid tumours where it was observed that an increase in the proportion of cells expressing P-gp is evident after exposure to a combination chemotherapy program containing drugs known to select for P-gp expression *in vitro*. It is a common observation that there is an increase in P-gp expression in the endothelial cells within the tumour mass at these sites. The observation of increased immunoreactive endothelial cells suggests transactivation of the MDR1 in these cells and subsequent drug resistance [342]. Although bortezomib is also a substrate of P-gp, the reason that its activity is not attenuated by BMSCs is most likely because bortezomib works via a different mechanism from anthracyclines.

What is yet unknown, is whether this downregulation or upregulation of P-gp expression in both MM and stromal cells in a coculture is correlated with changes in P-gp function. In this present study, we showed that in MM cells a downregulation of P-gp expression was associated with a reduction in P-gp function (Fig. 3.1.9.4). At each time point time tested, there was an increase in median fluorescence intensity of Rh-123 in the MM cells that were cocultured with BMSCs compared to the MM cells that were not cocultured. However, the transferred P-gp (from RPMI-Dox40 to BMSCs) was shown to be non-functional (Fig. 3.1.9.7). When the stromal fraction of the coculture was analysed, the transferred P-gp was not functional as evidenced by the lack of Rh-123 extrusion in the absence of verapamil. This finding is different from that reported by Levchenko *et al.* [281]. Using P-gp labelling and dye extrusion assays, these authors demonstrated cell co-incubation results in a functional P-gp transfer from P-gp-positive to P-gp-negative cells.

The reason for the difference seen between our findings and Levchenko's is unclear. It may be that the P-gp transfer to BMSCs seen in our coculture system

was minimal whereas there was a much greater transfer of P-gp in their study. This could be related to the longer co-incubation time used in Levchenko's study (8 days vs. 3 days). The P-gp that was transferred may be detectable but not of a quantity to be able to confer a phenotype in the stromal cells. It may also be related to different cell lines used in the study, Levchenko's study utilised neuroblastoma cells and its P-gp positive derivative whereas we used two different cell lines (RPMI-Dox40 and BMSCs, HS-5), one malignant and one non-malignant. Further experiments will have to be done to investigate this further.

4.2 Investigation of p53 signalling perturbations in Multiple Myeloma resistance

4.2.1. The relationship between Mdm2 and p53

p53 activity in transcription, translation and protein stability is tightly controlled. The main stimuli of p53 expression include DNA damage (caused by UV, ionizing radiation, or genotoxic drugs), oxidative stress, osmotic shock, ribonucleotide depletion, and deregulated oncogene activation. Genotoxic stress activates PI3 kinase-like-kinases including DNA-PKc, Atm, and Atr at the DNA break sites, which in turn phosphorylate p53, Mdm2 and other proteins, leading to p53 stabilization/activation [343].

In normal unstressed cells, p53 activity is maintained at a low level through a combination of p53 degradation and direct transcriptional repression, principally mediated by Mdm2 and Mdm4 (also known as MDMX in humans) [164]. p53 and Mdm2 interact with each other through an autoregulatory feedback loop. When p53 is activated, it transcribes the Mdm2 gene and in turn, the Mdm2 protein inhibits p53 activity by binding to the p53 transactivation domain and inhibiting its transcriptional activity [165]. Mdm2 also ubiquitinates p53 in the nucleus and is responsible for exporting p53 out of the nucleus, promoting its degradation via the ubiquitin/proteasome pathway [166] and rendering it inaccessible to the target genes (Fig. 4.2.2). On the other hand, Mdm2 is a direct target of p53. Therefore, elevation of p53 upregulates Mdm2, which in turn downregulates p53 [164]. The significance of this regulatory loop is manifested by the genetic studies of Mdm2–/– and Mdm2–/–p53–/– mice. Knockout mice of Mdm2 show embryonic lethality, accompanied by an elevation of p53. Deletion of p53 in Mdm2–/– mice rescued the embryonic lethality phenotype, suggesting that p53 mediates the effects of Mdm2 deficiency on mouse development and survival [167, 168].

Mdm2 negatively regulates the stability of p53. Ubiquitination by Mdm2 is necessary for p53 nuclear export and degradation. The ubiquitination is dependent on the association between these two proteins [344]. Mdm2 binding-deficient p53 mutant could not be ubiquitinated by Mdm2 [345]. Furthermore, ubiquitination depends on p53 oligomerization as Mdm2 could not target oligomerization-deficient p53 for ubiquitination [346]. Ubiquitinated p53 exists in two forms, monoubiquitination, which might elicit nuclear export of p53, and polyubiquitination, which promotes proteasomal degradation of p53 [347]. In addition, it is reported that

phosphorylation of p53 at Ser46 renders p53 resistant to Mdm2-mediated ubiquitination [348].

Besides mediating p53 turnover, Mdm2 could also affect the activity of p53 through various mechanisms. First, Mdm2 binds to the transactivation domain of p53 and inhibits its transcriptional activity possibly through blocking its access to target genes [165]. Secondly, Mdm2 inhibits the translation of p53 by targeting ribosomal protein L26 (RPL26) that would otherwise enhance p53 mRNA translation [349].

4.2.2. The role of p53 in apoptosis

Apoptosis occurs through either one of two major pathways described as either the intrinsic mitochondrial or extrinsic death receptor pathway (Fig. 4.2.2). In the intrinsic pathway, nuclear p53 induces Puma expression, which in turn releases cytosolic p53 held inactive in the cytoplasm through binding to Bcl-X_L. Then, cytosolic p53 induces Bax oligomerization and mitochondrial translocation. Accumulation of p53 in the cytosol as a consequence of normal intracellular transport or stable monoubiquitination is the major source for mitochondrial p53. In the mitochondria, p53 induces Bax and Bak oligomerization, antagonizes the Bcl-2 and Bcl-X_L antiapoptotic effect, and forms a complex with cyclophilin D in the mitochondrial inner membrane. These changes result in marked disruption of mitochondrial membranes and subsequent release of both soluble and insoluble apoptogenic factors ultimately leading to caspase activation and apoptosis.

Cells committed to die via p53-dependent apoptosis typically follow the mitochondrial pathway, although p53 can also modulate cell death through death receptors. Furthermore, most evidence suggests that the key contribution of p53 to apoptosis is primarily dependent on transcriptional activity. p53 has the ability to activate transcription of various proapoptotic genes, including those encoding members of the Bcl-2 family, such as the BH-3 only proteins Bax, Noxa, and Puma. Alternatively, p53 can also trigger apoptosis by repression of antiapoptotic genes, such as *survivin,* thus promoting caspase activation [350].

Acting on the death receptor pathway of apoptosis, p53 overexpression enhances cell surface levels of Fas by promoting its trafficking from Golgi complex [351]. In addition, p53 activates DR5, the death domain-containing receptor for TRAIL; DR5 is induced in response to DNA damage and in turn, promotes cell death through caspase-8 [352]. Genes for proapoptotic proteins that may link apoptotic pathways,

such as *bid* and the p53-induced protein with a death domain (*PIDD)*, were also described as transcriptional targets of p53. Importantly, p53 is also involved in the activation of the apoptosome via induction of Apaf-1 expression [353].

p53 apoptotic function is not limited to transcriptional dependent activities, there is now emerging evidence that the proapoptotic functions of p53 are transcription-independent. Activation of p53 in enucleated cytoplasts is sufficient to directly or indirectly trigger apoptosis by inducing proapoptotic Bcl-2 family members [354]. A stress-stabilized cytoplasmic pool of p53 is probably the major source for p53 mitochondrial translocation; however, it is still a matter of debate on how the pool is generated. Some authors contend that unstressed cytoplasm contains a mixture of unstable polyubiquitinated p53 that is almost immediately targeted for proteasomal degradation, and functional monoubiquitinated p53 that serves as a source for p53 translocation to mitochondria. In the mitochondrion, p53 induces Bax and Bak oligomerization, physically interacts with protective Bcl-X_L and Bcl-2, antagonizing their antiapoptotic effects, and also forms a complex with cyclophilin D leading to disruption of mitochondrial structure [355].

In addition to mitochondrial-targeted p53 actions, an alternative cytosolic p53 death pathway was recently reported that directly activates cytosolic Bax in UV-treated transformed mouse embryonic fibroblasts [356]. After stress, nuclear p53 induces transcription of *puma*, which in turn, liberates p53 from an inactive pre-existing soluble p53-Bcl-X_L complex, via binding to Bcl-X_L. The cytosolic p53 then induces homo-oligomerization of Bax, followed by Bax mitochondrial translocation. Cytosolic p53 may also modulate other mechanisms apart from apoptosis. As an example, cytosolic p53 operates at the mitochondria to repress autophagy [357].

p53 driven apoptosis is very complex and we are only now starting to understand all facets of this interesting protein.

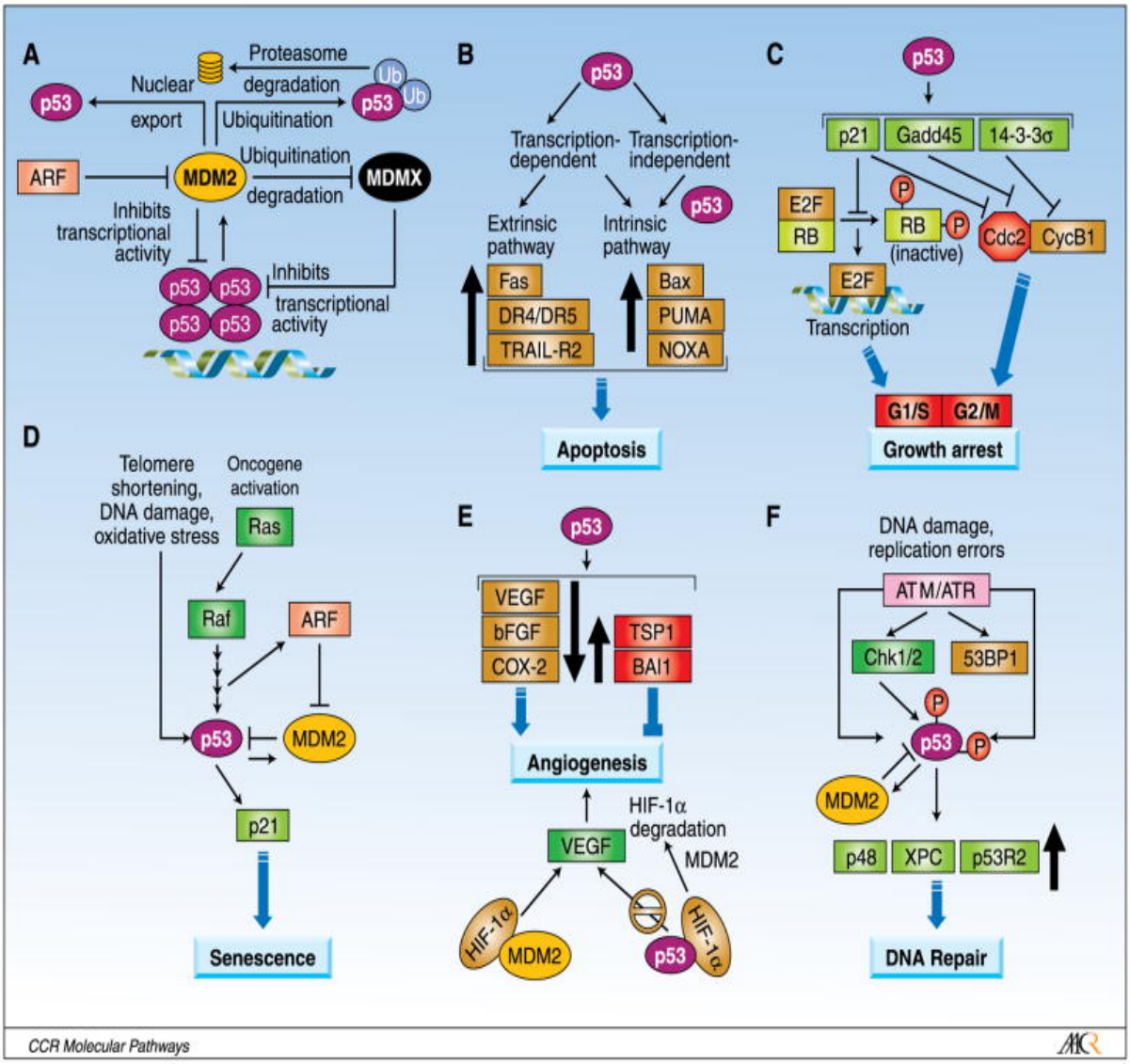

Figure 4.2.2 Regulation of p53 and Mdm2 and the outcomes of p53 activation.

(A) Mdm2 inhibits p53 through an autoregulatory loop. Mdm2 directly binds to the transactivation domain of p53 and inhibits its transcriptional activity, causes the ubiquitination and proteasomal degradation of p53, and exports p53 out of the nucleus which promotes p53 degradation and inhibits its activity. MDMX, a homologue of Mdm2, also directly binds to the transactivation domain of p53 and inhibits p53 activity, but does not induce p53 degradation. ARF binds to Mdm2 and sequesters Mdm2 into the nucleolus, leading to the stabilization of p53.

(B) Activation of p53 can also lead to induction of apoptosis via intrinsic (mitochondrial) and extrinsic (death receptor) apoptosis pathways. Apoptosis can be transcriptional-dependent or -independent because p53 itself can participate in

mitochondrial mediated apoptosis through interaction with proapoptotic and antiapoptotic members of the Bcl-2 family.

(C) Activation of p53 can halt cell cycle progression in the G1-S and G2-M boundaries of cell cycle through the up-regulation of the p21, Gadd45, and 14-3-3-j proteins. Transition into the S-phase requires cyclin-dependent kinases (CDK), such as CDK2, which phosphorylates and inactivates Rb, rendering E2F free and transcriptionally active, leading to cell cycle progression. However, p53 activation induces the CDK inhibitor p21, which leads to cell cycle arrest. Furthermore, Cdc2/cyclinE activity is essential for entry into mitosis, and this activity can be inhibited by p21, Gadd45, and 14-3-3-j, resulting in G2-M phase arrest.

(D) Senescence is a potent tumour suppressor mechanism of p53. Telomere erosion, DNA damage, and oxidative stress or oncogenic stress can signal p53 activation, triggering senescence response via the p21-Rb-E2F signaling pathway. Oncogenic Ras can activate MAP kinase pathway that phosphorylates and activates p53 and also induces the expression of ARF, which in turn binds to and inhibits Mdm2, leading to the up-regulation of p53 and the induction of senescence.

(E) p53 can suppress angiogenesis through the down-regulation of proangiogenic proteins

and up-regulation of antiangiogenic proteins. In addition, p53 can bind to HIF-1a, a promoter of angiogenesis during hypoxia, and target it for degradation by Mdm2. In a p53-independent manner, HIF-1a interacts with the p53-binding domain of Mdm2, and transcriptionally up-regulates the vascular endothelial growth factor (VEGF) promoting angiogenesis.

(F) p53 plays a critical role in DNA damage repair. DNA damage and replication errors can activate ataxia telangiectasia mutated (ATM) and ataxia telangiectasia and Rad-related (ATR) kinases, which trigger several cellular responses, including DNA repair. ATM and ATR can phosphorylate DNA repair protein 53BP1 as well as induce the accumulation of p53 through phosphorylation directly or via CHK1and CHK2 kinases. p53 participates in DNA repair in a transactivation-dependent manner through the up-regulation of proteins such as p53R2 (p53-inducible small subunit of ribonucleotide reductase), p48 (gene product of DDB2 gene), and XPC (xeroderma pigmentosum group C protein), and in an independent manner through interaction with other DNA repair proteins, such as 53BP1.

(Figure from [358])

4.2.3. The current role that bortezomib has in Multiple Myeloma and solid tumours

The proteasome inhibitor bortezomib represents a significant advance in the therapeutic armamentarium against MM. However, resistance to bortezomib, *de novo* or acquired, is an important obstacle to achieving better clinical results. Furthermore, bortezomib has not been shown to be active against most solid tumours. Research is therefore trying to identify clinically applicable approaches that would allow us to extend bortezomib activity against a broader spectrum of tumours. In that context, we compared responses to bortezomib in MM versus solid tumour models to delineate mechanisms of differential bortezomib responsiveness.

Bortezomib induces phosphorylation of p53 at serine 15 and induction of p53 phosphorylation is associated with s increased p53 mRNA and protein levels [278]. It is unclear whether phosphorylation of p53 causes the dissociation of p53 from the p53/Mdm2 complex. Some studies have demonstrated that it does but others have shown that phosphorylated p53 is still associated with Mdm2 [278]. p53 and Mdm2 interact with each other through an autoregulatory feedback loop. When p53 is activated, it transcribes the Mdm2 gene and in turn, the Mdm2 protein inhibits p53 activity by binding to the p53 transactivation domain and inhibiting its transcriptional activity [165]. Mdm2 is also responsible for exporting p53 out of the nucleus, promoting its degradation via the ubiquitin/proteasome pathway [166] and rendering it inaccessible to the target genes. We hypothesized that inhibition of Mdm2, the E3 ubiquitin ligase that ubiquitinates p53 and promotes its proteasomal degradation, could enhance p53 stabilization in bortezomib-treated MM cells, with a resultant synergistic effect on apoptosis induction.

4.2.4. The role of single agent Nutlin-3 in Multiple Myeloma and epithelial carcinomas

Many of the currently used cytotoxic drugs owe their antineoplastic effects to induction of apoptotic pathways. However, their therapeutic activity is a trade-off between efficacy and adverse effects, resulting in unspecific genotoxic collateral damage, which may induce genetic instability, selection of drug-resistant tumour subclones, and secondary malignancies. In contrast to the short-term side effects of genotoxic therapy, such as nausea, vomiting, mucositis, myelosuppression, and

infection, which are reversible and manageable, these long-term side effects are irreversible and cannot be managed clinically. Non-genotoxic activation of the p53 pathway would therefore be an attractive therapeutic strategy for cancers with intact p53-dependent signalling. That was the basis of development of Mdm2 inhibitors such as nutlins.

In our study, MM cell lines and epithelial tumours were sensitive to nutlin-3, although epithelial tumours were affected to a lesser extent than MM cells (Fig. 3.2.2). This is in agreement with other studies in the literature [172, 179, 186, 188, 359]. As an Mdm2 inhibitor, nutlin-3 is able to upregulate expression of several p53-dependent targets including Bax, PUMA, Noxa, p21, and Mdm2 itself amongst others (Table 3.2.3). As in this thesis, the nutlin-3 used is a racemic mixture and not a pure solution of the active enantiomer, the doses used to affect cytotoxicity either as a single agent or in combination with bortezomib are in the mid-micromolar range rather than low micromolar range that would be common for small molecule inhibitors.

The cellular response to genotoxic stress that damages DNA includes cell cycle arrest, activation of DNA repair, and in the event of irreparable damage, induction of apoptosis. When cells encounter genotoxic stress, certain sensors for DNA lesions eventually stabilize and activate p53. Caspase-3 cleavage was seen with nutlin-3 treatment even though nutlins are a non-genotoxic drug. This is caused by p53 activation of the apoptotic pathway (Fig. 3.2.3A). However, the pro-apoptotic effect of nutlin-3 was partially attenuated by the pan-caspase inhibitor, ZVAD-FMK (Fig. 3.2.3B), suggesting that caspase activity is not the sole mechanism of nutlin-3 induced cellular death.

We have shown that nutlin-3 has anticancer activity on its own at low micromolar range for MM cells and at a mid micromolar range for epithelial tumours. We hypothesised that this activity and the potency of the drug could be increased by combination with bortezomib.

4.2.5. The combined role of Mdm2 inhibitor and bortezomib

We found that the combination of the Mdm2 inhibitor, nutlin-3, with bortezomib demonstrated lack of synergistic cytotoxicity against bortezomib-sensitive MM cell lines MM.1S, MM.1R, and NCI-H929 (Fig. 3.2.4.1). The calculated combination

index using Calcusyn software was >1. Of all the MM cell lines tested, KMS-11 was the only one that demonstrated synergistic cytotoxicity with the combination of nutlin-3 and bortezomib. It should be noted that KMS-11 is less sensitive to single agent nutlin-3 compared to the other MM cell lines tested. Its response to nutlin-3 single agent was comparable to epithelial cancers.

This combination however, demonstrated synergistic activity against epithelial cancer cell lines including thyroid, breast and prostate carcinomas (Fig. 3.2.4.2). The calculated combination index for all the epithelial cancer cell lines was <1. In the MM1.S and MM1.R cell lines, which were the most sensitive cell lines to nutlin-3, the IC_{50} was 2μM. In the epithelial cancer cell lines, the IC_{50} was > 30μM.

Direct inhibition of the E3 ubiquitin ligase, Mdm2, stabilizes p53 and activates the p53 apoptotic pathway in a non-genotoxic manner and, therefore, represents a promising approach for the treatment of cancer [177]. Treatment of MM cells with nutlin-3, which interrupts the p53-Mdm2 interaction, increases protein levels of p53, thereby inducing p53 targets and apoptotic cell death [179]. The differential response of MM versus epithelial malignancies to the combination of bortezomib with nutlin-3 sheds light on the role of p53 in bortezomib-induced apoptosis and suggests a complex, tissue-dependent, interaction between the MDM2/p53 and proteasome pathways. It is possible that p53 is more important for bortezomib-induced apoptosis in epithelial malignancies than in MM. Mutations in p53 are very common in epithelial malignancies, whereas in MM, they have been historically considered to be present in only late stage disease (e.g., plasma cell leukaemia/extramedullary MM). However, their prevalence may increase in the future, because patients with advanced MM survive longer due to the therapeutic efficacy of novel agents including thalidomide, bortezomib, and lenalidomide. It is also possible that epithelial cancers that are bortezomib refractory may have more potential for sensitization upon Mdm2 inhibition than MM cells, which are more responsive to single-agent bortezomib and nutlin-3. We have also found that in KMS-11 MM cell line where the single agent nutlin-3 activity is more on par with epithelial cancer cell lines tested, the combination of nutlin-3 and bortezomib was synergistic (Fig. 3.2.4.1). Importantly, however, in advanced MM with p53 pathway lesions and bortezomib-resistance/refractoriness, concurrent Mdm2 inhibition may restore bortezomib sensitivity.

Ubiquitinated p53, in particular Mdm2-ubiquitinated p53, is, in general, transcriptionally inactive [360]. Ubiquitination targets p53 not only for proteasomal

degradation, but also for nuclear export and cytosolic localization, thus eliminating the opportunity for binding to DNA [360]. Also, many of the same sites that are ubiquitinated by Mdm2 can also be acetylated by p300/CBP to promote p53 activation. Acetylation of p53 is essential for the binding of p53 to p53-binding elements promoting transcription of various apoptosis or cell cycle arrest genes, including p21, PUMA, BAX, and Noxa [360]. However, when Mdm2 ubiquitinates p53, the latter cannot be acetylated by p300/CBP and becomes transcriptionally inactive, even in the absence of proteasome-mediated degradation [360]. This could explain why p53 does not seem to play a major role as a mediator of the effects of bortezomib monotherapy, because, although its total levels are increased in the presence of bortezomib [278], it is still ubiquitinated and functionally inactivated by Mdm2 [360]. Also, it provides another mechanism to explain the synergistic activity of bortezomib together with nutlin-3, which we describe in this study: the addition of Mdm2 inhibition to proteasome inhibition not only further stabilizes p53 and increases its protein levels, but also blocks its ubiquitination and transcriptional inactivation, thus making it more functional.

4.2.6. The combination of Nutlin-3 and bortezomib enhances the activation of the p53 apoptotic pathway

We next investigated the mechanism for the differential sensitivity of MM vs. epithelial cell lines to the combination of bortezomib with nutlin-3. Western blot analysis of MM cells treated with this combination demonstrated no evidence of synergistic activation of the p53 pathway and apoptosis mediators (Fig. 3.2.5), consistent with the lack of enhanced killing effect. In contrast, there was synergistic activation of the p53 pathway and apoptosis, associated with upregulation in p53, Mdm2, Noxa, and PUMA expression, as well as enhanced cleavage of PARP and caspase-3 (Fig. 3.2.5) when the epithelial carcinoma cell line was treated with this drug combination. These results were consistent with the lack of synergy seen in MM (Fig. 3.2.4.1) and synergistic activity seen in epithelial carcinoma (Fig. 3.2.4.2).

This upregulation in p53 and its downstream markers explains the synergy seen when bortezomib is combined with nutlin-3. Enhanced cleavage of PARP and caspase-3 suggests that the p53 apoptotic pathway is activated.

4.2.7. Nutlin-3 may counteract molecular pathways associated with decreased responsiveness to bortezomib

We had a hypothesis that cancers that are bortezomib refractory may have more potential for sensitization upon Mdm2 inhibition as outlined in Section 4.2.3... To probe this hypothesis, we next evaluated whether the transcriptional signature of tumour cell response to nutlin-3 treatment was enriched in genes which may correlate with clinical outcome.

Bortezomib-treated MM patients enrolled in phase II SUMMIT and phase III APEX trials were divided into cohorts with high vs. low expression of nutlin-3-suppressed genes. A transcriptional index of tumour cell response to nutlin-3 was identified, based on previously published studies of transcripts selectively downregulated by nutlin-3 treatment [180]. Bortezomib-treated patients who had, at baseline, high expression of nutlin-3-suppressed genes had significantly shorter progression-free (panel A, p=0.001, log-rank test) and OS (panel B, p=0.002, log-rank test) compared to those with low expression levels (Fig 3.2.8). This observation suggests that if patients tumours responded to nutlin-3 in the same way as the cellular models employed, treatment with nutlin-3 might counteract molecular pathways associated with decreased responsiveness to bortezomib and thereby overcome clinical bortezomib resistance.

4.2.8. Nutlin-3 activity in the presence of bone marrow stroma cells

As mentioned, the BM microenvironment plays an important role in MM growth, proliferation, survival and drug resistance (Chapter 1.3). Interactions of MM cells with normal cells of the bone marrow milieu can attenuate the antitumour activity of conventional therapies, such as glucocorticoids, standard cytotoxic agents, such as alkylators, and novel targeted therapies, such as bortezomib [27]. In our opinion, all new treatments for MM and combination treatments should be tested in the presence of stroma to ensure that there is no attenuation of activity.

In this study, we found that co-culture with BMSCs partially attenuated the response of MM cells to nutlin-3 (Fig.3.2.6.2). This is consistent with evidence that interaction with BMSCs suppresses p53 activity in highly bortezomib-responsive MM cells, MM1.S (Fig. 3.2.6.1). Quantitative RT-PCR of MM1S cells co-cultured with BMSCs demonstrated decreased expression of p53 and gene transcripts known to be

induced by p53 including Mdm2 [284], Bax [285], Noxa [286], PUMA [287], BTG1, DAPK1 [288], GADD45B, ID2, Jun, Plk1, and Plk2 [289]. These results suggest that co-culture with BMSCs triggers downregulation of the p53 pathway in MM cells, which can contribute to resistance to apoptosis, leading to attenuation of activity in the presence of BMSCs. We next wanted to assess if the downstream effectors of p53 would be upregulated upon nutlin-3 treatment in the presence of stroma, since its activity was attenuated. Importantly, however, treatment with nutlin-3 was able to induce the expression of Mdm2 (Fig. 3.2.6.3A), PUMA (Fig. 3.2.6.3B), Noxa, Bax and GADD45B, even in the presence of BMSCs. This implies that the drug is still having an effect although somewhat blunted by the presence of BMSCs.

As noted above, the combination of nutlin-3 with bortezomib mediates additive cytotoxicity against MM cells, but triggers synergistic cytotoxicity against epithelial carcinoma cell lines. We investigated whether this latter effect persists in the presence of BMSC. This is important to evaluate as other cancer types also metastasise to the BM. We evaluated the impact of BSMCs on the effect of the combination of nutlin-3 with bortezomib on MDA-MB-231 met-luc-neo cells. This is a breast cancer cell line that was generated from bony metastasis, making this a relevant clinical model. We demonstrated that co-culture with BSMCs did not protect against the synergistic pro-apoptotic effect of the combination of nutlin-3 with bortezomib in this epithelial carcinoma model (Fig. 3.2.7). These data suggest that the enhanced activity of nutlin-3 combined with bortezomib against epithelial models of cancer is unlikely to be inhibited by microenvironmental interactions. Thus, the combination of Mdm2 inhibitors and proteasome inhibitors promises to have good anticancer activity clinically.

Clinically relevant preclinical models can help identify drug combinations with enhanced anticancer activity. We have previously reported that DNA-damaging chemotherapeutics including doxorubicin and melphalan induce synergistic MM cytotoxicity when combined with bortezomib [44]. This approach has been validated clinically [46, 190], and the combination of bortezomib with pegylated liposomal doxorubicin or with melphalan plus prednisone are now Food and Drug Administration–approved anti-MM combination regimens. We now report that non-genotoxic activation of the p53 pathway using nutlin-3 can sensitize epithelial carcinoma cells to bortezomib in a manner that is not suppressed by microenvironmental interactions. These observations suggest that concurrent Mdm2 inhibition with nutlin-3 may extend the spectrum of bortezomib activity to

solid tumours, and also overcome bortezomib resistance in advanced MM. Our studies further provide the framework for derived combination clinical trials to improve outcome in patients with solid tumour and hematologic malignancies.

4.2.9. Mdm2/p53 interaction independent of p53

It is always thought that Mdm2 regulates tumourigenesis only when p53 is present. However, there is evidence that Mdm2 can mediate tumourigenesis independent of p53 [361]. For example, studies of human sarcomas and bladder cancers showed that a subset of these tumours overexpressed Mdm2 in addition to having mutated p53, and those patients whose tumours had both abnormalities had decreased survival compared with patients with tumours possessing either abnormality alone [362, 363]. Furthermore, one third of lymphomas that emerged in EA-myc transgenic mice that have mutated or deleted p53 also overexpressed Mdm2 [364]. For a tumour to overexpress Mdm2 and inactivate p53 would seem redundant, unless Mdm2 has other functions besides the regulation of p53. Alt *et al.*[365] have identified the Mre11/Rad50/Nbs1 (M/R/N) DNA repair complex in immunoprecipitations of endogenous Mdm2 from cells lacking functional p53. The M/R/N complex contributes to the preservation of genome stability by participating in DNA double-strand break repair, cell cycle check point control, and telomere maintenance [366]. The M/R/N complex functions in signalling the presence of DNA breaks, as well as the initial enzymatic processing of the broken DNA [366]. Mdm2 was shown to associate with the M/R/N DNA repair complex by specifically binding to Nbs1, a protein critical for genome stability [365]. Maintaining genome integrity is essential for the prevention of transformation, and several reports provide evidence that altered Mdm2 levels affect genome stability. *In vitro* experiments showed that expression of Mdm2 at levels 2- to 4-fold higher than endogenous levels led to centrosome amplification and chromosome instability [367]. This increase in genomic instability caused by Mdm2 overexpression promoted the transformation of p53-null MEFs, and an intact Nbs1-binding domain in Mdm2 was required for the increased transformation potential of Mdm2 [368]. These studies showed that elevated levels of Mdm2 compromise genomic stability, leading to transformation independent of p53 and dependent on interaction with Nbs1.

Nutlins have been shown to have activity in p53-deleted or p53-mutated cells, Nutlins are able to activate alternative transcription factors, in particular E2F1 [181, 182]. E2F1 can induce proliferation or apoptosis depending on the cell context and depending on the simultaneous activation of the Akt-prosurvival pathway [183]. Another study has demonstrated that Nutlins are able to induce apoptosis in p53-null cells through activation of p73 [184]. p73 is a homolog of p53 and is able to transactivate proapoptotic genes and induce cell death. It is also regulated by Mdm2. These two targets make Nutlin a viable therapeutic option even when p53 is deleted or mutated.

We hypothesised that we would continue to see synergy in p53 deleted/mutated cell lines with bortezomib and nutlin-3 combination. This investigation is important as most cancers are p53 mutated. Although MM in general, has little p53 mutation in early stage disease, there is mounting evidence that p53 deletion is a poor prognostic indicator [369]. There is also evidence that bortezomib therapy is unable to overcome the poor prognosis of chromosome 17p deletion [173].

To demonstrate if the synergy between bortezomib and nutlin-3 persist in a p53 independent situation, we utilised two p53 mutated cell lines; OPM2 and ANBL6. Fig. 3.2.9.1 showed that in both these cell lines, there was synergistic cytotoxicity in the combination. Synergy was calculated using Calcusyn (Table 3.2.9). Of note, these two cell lines are MM cell lines. In Fig. 3.2.4.1, we had shown that the combination of bortezomib and nutlin-3 did not yield synergy All the cell lines used then are p53 wild type. The p53 mutated cell lines appear to be less sensitive to single agent nutlin-3, requiring higher doses compared to p53 intact cell lines. For example, MM1.S a sensitive p53 intact MM cell line had an IC_{50} of 2μM whereas ANBL6, a p53 mutated MM cell line had an IC_{50} of 30μM nutlin-3. However, the combination of nutlin-3 and bortezomib appears to be more potent as, in the p53 mutated cell lines, we showed synergy when we did not demonstrate that in p53 intact cell lines. As we had mentioned before (Section 4.2.5), the exquisite sensitivity of p53 intact MM cell lines to single agent nutlin-3 may render the combination less potent as there is major cytotoxicity with single agent alone.

We then wanted to study if the activity of bortezomib and nutlin-3 would persist in a bortezomib resistant cell line. Using the subline of ANBL6 which developed bortezomib resistance *in vitro* with repeated exposure to bortezomib 5nM; ANBL6-VR5 (courtesy of Dr Robert Orlowski, MD Anderson Cancer Center); we showed

that the combination of bortezomib and nutlin-3 continued to effect synergy (Fig. 3.2.9.2A).

Tabe *et al* recently reported that Nutlin-3 and bortezomib had synergistic anti-proliferative effects in both p53 mutant- and p53 wild type-bearing mantle cell lymphoma cells .[359]. On a follow up to that study, it was demonstrated that the combination of nutlin-3 with bortezomib mainly induced synergistic cytotoxicity by apoptotic cell death [370]. The authors found that the nutlin-3 and bortezomib combination enhanced NOXA protein expression in p53 mutant-cells but not in wild type mantle cell lymphoma cells. They concluded that the combination of sublethal concentrations of nutlin-3 and bortezomib lead to an accumulation of NOXA protein by transcription-independent mechanisms as there was no increase of NOXA mRNA levels in the study.

This result is different from our study which found that there the combination of the two drugs demonstrated an increase in NOXA protein expression in wild type p53 cells that exhibited synergistic cytotoxicity i.e., the epithelial cancer cells. This difference between the two studies could be a cell specific effect or it is more likely related to the fact that NOXA upregulation is a result of bortezomib and nutlin-3 combination.

4.3 Activation of AMP-kinase pathway as an alternative to overcome drug resistance in Multiple Myeloma

4.3.1. AMPK pathway in Multiple Myeloma

AMP-activated protein kinase (AMPK) is a serine/threonine protein kinase and serves as an energy sensor in all eukaryotic cells. AMPK is activated under conditions that deplete cellular ATP and elevate AMP levels such as glucose deprivation, hypoxia, ischaemia and heat shock which are associated with an increased AMP/ATP ratio [192]. As a result of the activation, AMP binds to the γ subunit causing phosphorylation of threonine 172 in the activation loop of the α catalytic subunit by upstream kinases such as LKB1 and CaMKK.

LKB1 is a serine/threonine protein kinase and is the product of the gene *lkb1.* In patients with Peutz-Jeghers syndrome (PJS), this gene is mutated. Mutations in PJS patients were shown to be loss of function mutations of LKB1 ([193, 194]. PJS is characterized by mucocutaneous melanin pigmentation, gastrointestinal polyposis and markedly increased risk of cancer. LKB1 mutants that are inactive failed to suppress cell growth indicating that LKB1 has antiproliferative function and hence anti-tumour effect. LKB1 also induced p53 and p21 upregulation resulting in cell cycle arrest in melanoma cells [195] providing further evidence that it can function as a tumour suppressor. Several studies from different groups have shown a clear connection between LKB1 and AMPK-induced cell cycle arrest [196, 197].

Several groups have reported that activation of AMPK suppresses mTOR signalling by growth factors and amino acids [198-200]. When AMPK is activated, TSC2 is phosphorylated at Thr-1227 and Ser-1345 and increases the activity of TSC1–TSC2 complex to inhibit mTOR [201]. In addition, AMPK reportedly phosphorylates mTOR at Thr-2446 to reduce S6K1 phosphorylation by insulin, suggesting the inhibition of mTOR action [202]. Thus, AMPK directly and indirectly (via TSC2) suppresses mTOR activity to limit protein synthesis through the inhibition of translation elongation factor 2 (EF2). Therefore, AMPK activation regulates cellular proliferation in response to energy status or nutrient availability by limiting cell growth and proliferation when there is a lack thereof.

The mammalian target of rapamycin (mTOR) is an evolutionarily conserved serine/threonine kinase and a key regulator of protein translation/synthesis and cell growth [203, 204]. The mTOR pathway is activated by amino acids and by growth factors (e.g. PDGF, epidermal growth factor (EGF) and insulin. This stimulates protein synthesis, cell growth and proliferation. mTOR increases translation

initiation of 5′-terminal oligopyrimidine tract-containing mRNAs, which encode components of the protein synthesis machinery. The downstream effectors of mTOR ribosomal protein S6 kinase 1 ($p70^{S6K1}$ or S6K1) and the eukaryotic translation initiation factor 4E (eIF4E)-binding protein 1 (4E-BP1) stimulates the initiation step of translation [205].

The PI3K-Akt-mTOR pathway is a crucial signalling pathway for cancer pathophysiology. Somatic activating mutations and/or gene amplification of the *PIK3CA* gene (which encodes the p110α catalytic subunit of PI3K), the *PIK3R1* gene (that encodes for the p85α subunit of PI3K), and the *AKT* genes or somatic inactivating mutations, deletions and gene silencing of the *PTEN* gene (that encodes for a phosphatidylinositol-3,4,5-trisphosphate 3'-phosphatase that turns off the PI3K pathway), as well as numerous upstream receptor tyrosine kinases can activate the PI3K-Akt-mTOR pathway in cancer cells [371, 372]. Targeting mTOR signalling with small molecule inhibitors, e.g. temsirolimus, have some positive response in the clinic for breast cancer, renal cell carcinoma and non-Hodgkin lymphoma [373-375].

AMPK activation is a feasible therapeutic strategy for these cancers since AMPK inhibits mTOR signalling downstream of Akt, and inhibition of mTOR pathway has been reported to inhibit tumour growth and metastasis in experimental animal models as well as in cultured cells. Activation of AMPK by metformin, AICAR or thiazolidinediones or expression of constitutively active mutants have been shown to cause apoptosis or cell cycle arrest of various cancer cells. On the other hand, activation of this pathway has been shown to be protective on non-neoplastic tissues such as injured cells in cardiac ischemia and reperfusion injury models [215, 216]. AMPK activation protects human umbilical vein endothelial cells from hyperglycaemia by inhibition of caspase 3 and Akt activation [217] and by a similar mechanism in thymocytes [218]. These and other studies have suggested that AMPK activation confers protection against cell death. The underlying mechanism for these apparently opposing effects of AMPK activation is unknown at this time, but it can be postulated that in actively dividing cancer cells, the inhibition of ATP-consuming processes by AMPK may be less compatible with their survival, whereas in non-dividing (non-neoplastic) cells, where the protective effects of AMPK have been observed under acute stress, the shutdown of ATP-consuming pathways may not alter the balance for survival and may be beneficial [219].

It is known that a proportion of patients with MGUS and smouldering MM will progress on to full blown disease. There has been speculation that additional acquired genetic mutations are to blame for this progression, but no conclusive evidence. Thus far, there have been no therapies to prevent this transformation. Human epidemiologic evidence suggests that metformin, the most frequently used antidiabetic agent in the world, has anticancer activity [220, 221]. Both indirect effects of metformin on the endocrine and metabolic milieu, such as improvement of hyperinsulinemia, suppression of systemic IGF-I levels, and amelioration of the adipokine profile, and direct mechanisms [225-228, 230, 376-378] have been proposed to explain this effect. In the present study, we investigated the direct anticancer effects triggered by metformin and AICAR in multiple myeloma and solid tumour cell lines *in vitro*.

4.3.2. Metformin and AICAR have activity in Multiple Myeloma cells

We demonstrated that metformin is active in a panel of MM cell lines and solid tumour cell lines. The MM cells were generally more sensitive to metformin than solid tumour cell lines with an IC_{50} of 1-5mM in the MM cells and IC_{50} of ≥2mM in the solid tumour cell lines (Fig. 3.3.2.1). The doses used in our study was comparable to the other published studies in the literature [227, 228, 377], In our study, as well as others [227, 228, 377], such a direct effect may be mediated via increased phosphorylation of AMPK and decreased mTOR downstream effectors such as p70S6K and S6 ribosomal as well as their phosphorylated proteins (Fig 3.3.2.3). Decreased mTOR and p70S6K activation by metformin can suppress translation initiation and global protein synthesis [230, 376].

5-aminoimidazole-4-carboxamide ribonucleoside (AICAR) has similar metabolic effects as metformin and is a cell permeable activator of AMP-activated protein kinase (AMPK). Like metformin, AMPK activation by AICAR has also been recently reported to inhibit proliferation of various cancer cell lines *in vitro* and *in vivo*. AICAR has also been shown to have an anti-tumour role in myeloma, prostate cancer, gastric cancer, pancreatic cancer and liver cancer [235-239]. Similar to metformin, AICAR has anticancer activity in a panel of multiple myeloma cell lines as well as in epithelial carcinomas. Again as with metformin, the MM cell lines were more sensitive than for epithelial carcinomas. The IC_{50} of the most sensitive MM cell line, OCI-My5, was 20μM but the average IC_{50} was 200μM . This is in contrast

to the IC_{50} obtained for the solid tumour cell lines which averaged 1000μM (Fig. 3.3.3.1). Our data on the activity of AICAR was comparable to the studies listed above. The molecular signalling after treatment with AICAR is similar to that seen in metformin. There was increased phosphorylation of AMPK and a decrease in downstream effectors of mTOR such as phosphorylated (Thr389) and total p70S6K and phosphorylated (Ser235/236) and total S6 ribosomal (Fig. 3.3.3.3). GSK3 α/β and phosphorylated GSK3 α/β (Ser21/9) was also downregulated by AICAR treatment (Fig. 3.3.3.3).

Contrary to the direct AMPK-activating capacity of AICAR, metformin is an indirect AMPK activator [379]. The primary site of its action is currently considered to be a direct inhibitory effect on complex 1 of the respiratory chain 35. The resulting high cellular ratio of AMP:ATP functions as an allosteric signal that sensitizes AMPK to phosphorylation at Thr172 by LKB1 35. This raises the question whether the anticancer activity of metformin is mediated via AMPK. We found that the AMPK inhibitor Compound C could not attenuate the anticancer activity of metformin in myeloma or thyroid carcinoma cell lines, suggesting that the growth-suppressive effect of metformin in these cells is not exclusively dependent on AMPK (Fig. 3.3.6.1). In agreement, in a prostate carcinoma model, metformin induced phosphorylation of AMPK, yet siRNA-mediated depletion of AMPK did not prevent the antiproliferative effect of metformin [225]. Similar results were recently reported in chronic lymphocytic leukemia (CLL) cells [380]. In another study, metformin was found to inhibit mTOR signalling in an AMPK-independent, rag GTPase-dependent manner [381]. On the contrary, the inhibitory effect of metformin on growth and translation initiation in breast carcinoma cells was attenuated by siRNA against AMPK and the AMPK inhibitor compound C [230, 376], suggesting that the effects of metformin in that particular model are AMPK-dependent. The difference between our findings and the findings in these other studies may be due to a cell specific effect.

For both of these AMPK activators, studies have demonstrated their involvement in cell cycle inhibition at G0/G1 via a reduction in cyclin D1 [225, 232, 382, 383]. We have also demonstrated that AICAR and metformin affect cell cycle proteins in particular cyclin D1, cdk4 (or cdk6), cyclin B1 and cdc2 (Fig. 3.3.2.3 and Fig. 3.3.3.3). There was a decrease noted in these cell cycle proteins with AICAR and metformin except for cyclin B1 where there was little change before a late increase was noted with AICAR treatment. Cyclin D1 and cdk4/6 is associated with G1

progression and cyclin B1 and cdc2 wtih G2-M progression. Most of the reported literature has associated metformin and AICAR with G0/G1 arrest. Our findings reflect this with an early reduction in cyclin D1 and cdk4/6 seen. Cyclin B1 and cdc2 reduction was only seen much later in metformin. In AICAR treated cells, cdc2 reduction was seen only after cyclin D1 was reduced. Cyclin B1 in AICAR treated cells increased at the late time points after a reduction in cyclin D1 and cdk6 was noted. This may be a rebound phenomenon to the G0/G1 cell cycle arrest.

4.3.3. Metformin and AICAR are able to overcome the protective effect of the BM microenvironmental

The BM milieu consists of two parts; organized cellular and non-cellular components which include the liquid component. The cellular component of the BM is composed BMSCs and OCs amongst other cellular components. The non-cellular component comprises extracellular matrix (ECM) proteins (fibronectin, collagen, laminin and osteopontin) and the liquid component consists of growth factors and cytokines. It is now well established that MM-induced disruption of the bone marrow (BM) homeostasis between the highly organized cellular and extracellular compartments supports MM cell proliferation, survival, migration and drug resistance through activation of various signalling pathways (as reviewed in [60, 61]). For instance, it has been demonstrated that the response of MM to conventional therapies, such as glucocorticoids or cytotoxic chemotherapeutics is attenuated by the presence of bone marrow stromal cells (BMSCs) [27, 62-64]. This leads to decreased anticancer therapeutic activity, making the local microenvironment an important mechanism of treatment failure. As such, any new anticancer agent should be tested to see if its activity is attenuated in the presence of the local microenvironment.

Using our CS-BLI assay, we studied the impact of stromal cells and osteoclasts on tumour cell sensitivity to metformin and AICAR. It is encouraging that the anticancer activity of both agents was not suppressed in the presence of stromal cells or osteoclasts (Fig 3.3.2.2 and Fig. 3.3.3.2). The fact that, in some cases, their anti-tumour activity was enhanced in the presence of stromal cells or osteoclasts suggests that the signalling cascades [380] induced by these accessory cells interact in a synthetically lethal fashion with AMPK activation.

McMillin *et al*. [384] reported that the tumour stroma promotes in cancer cells a gene expression signature that is associated with stimulated Akt signalling (the upstream activator of mTOR signalling) and with self-renewal. In this study, we found that cells with constitutively active Akt (transfection of myristoylated Akt) are sensitized to acadesine, which may partially explain the sensitizing effect of the microenvironment (Fig 3.3.8.1). Collectively, these findings suggest that tumours with activated Akt/mTOR pathway (either constitutively due to somatic mutations in this pathway or due to tumour-stroma interactions in the context of the local microenvironment) may be even more sensitive to AMPK activators. Furthermore, there is emerging evidence that metformin suppresses self-renewal and proliferation of breast cancer stem/progenitor cell populations [385, 386].

4.3.4. AICAR has more antimyeloma activity compared to Metformin

Although both metformin and AICAR suppressed mTOR signalling and growth in our study, their anticancer effects were not identical. Between the two agents studied, it was obvious that AICAR was the more effective antimyeloma agent compared to metformin. In the treatment of CD 138 MM cells purified from BM aspirates from MM patients, AICAR was able to demonstrate better activity compared to Metformin (Fig. 3.3.4).When these patient tumour cells were treated with AICAR, 3 / 4 MM patients responded to the drug with IC50 values <500 μM whereas only 1 / 3 MM patient showed a response to metformin, and then only at much higher drug concentrations.

The anticancer activity of AICAR was further documented in a subcutaneous xenograft model (NOD.CB17 SCID mice). These mice are homozygous for the severe combined immune deficiency spontaneous mutation *Prkd*^{scid} and are characterised by an absence of functional T cells and B cells, lymphopaenia, hypogammaglobulinaemia but with a normal haematopoietic microenvironment. This characteristic of the NOD.CB17 SCID makes them an ideal model for cancer research as they will allow for the engraftment of xenograft cells. There were 7 mice in the control group and 8 mice in the treatment group. AICAR treatment significantly decreased tumour burden compared to controls (Fig. 3.3.9.1; P=0.005; unpaired one-tailed T-test). In addition, the survival of the treated mice was statistically significant compared to controls (Fig. 3.3.9.2; P=0.003; log-rank test) on Kaplan-Meier method. Furthermore, there was no significant change in the weights

of treated mice (Fig. 3.3.9.3) indicating that the mice tolerated the treatment well. There were also no potential toxicities observed during the course of treatment with AICAR. It is of interest that, in haematological malignancies, AICAR so far has demonstrated interesting preclinical activity against B-cell neoplasms (B-cell CLL [387] and B-cell lymphomas [388]), which is in agreement with our present results in MM.

AICAR-treated mice responded to the treatment in a rapid fashion. Due to the rapid disappearance of the tumours, there was development of ulcers in the central portion of the tumour. These ulcers did not discomfort the mice and were showing signs of healing as treatment with AICAR progressed. Unfortunately, as per the protocol in the handling of mice in the Animal Care and Use Committee of the Dana-Farber Cancer Institute, any ulcer formation in the mice regardless of healing status or shrinking tumour load, required the mice to be sacrificed. As a result, we had to censor the groups to get an accurate Kaplan-Meier calculation.

Although we showed that AICAR had more activity in MM patient cancer cells, the patient samples used when testing the activity of the two drugs were not the same. Differences in tumoural response may explain the difference in response seen between the two drugs. We are aware that the patient samples used in this study are small but there was difficulty in obtaining enough patient samples that had a high tumour load as most patients who attended Dana Farber Cancer Institute had been previously treated in their local institute. However, the finding that AICAR is more active an anti-MM agent is still valid as we have shown that AICAR has activity in a xenograft model and the mechanism of cell death is cytotoxic rather than cytostatic.

Further examination of apoptosis-related activity, contrary to the findings with metformin, AICAR also induced mitochondrial membrane depolarisation and cell apoptosis (Fig 3.3.7.4 and Fig. 3.3.7.5). The mitochondria is an intrinsic part of cell death control that plays a role in apoptosis [389]. Apoptosis is finely regulated at the molecular level with formation of a proteinaceous pore at sites of contact between the inner and outer mitochondrial membranes [389]. This is accompanied by a decrease in mitochondrial membrane potential and heralds a transition in the permeability of the mitochondria. The phenomenon culminates in the release of sequestered molecules such as cytochrome c and apoptosis inducing factor (AIF) that are involved in downstream control and formation of the apoptotic phenomenon [390]. We have demonstrated that Metformin causes a calculated cell death of 54%

on MTT testing (Fig. 3.3.7.4) but little apoptosis or even necrosis seen in Annexin V/PI staining (26%) (Fig. 3.3.7.3). The MTT test primarily measures cell viability whereas Annexin V/PI measures cell death. Therefore, as there is a greater reduction in viability of RPMI-8226 cells after treatment with metformin using MTT compared to actual cell death as demonstrated by Annexin V/PI staining, we can postulate that the main mechanism of metformin's antimyeloma activity is growth inhibition rather than apoptotic cell death. Thus, the fact that AICAR is able to induce apoptosis and growth inhibition rather than just growth inhibition as for metformin, makes AICAR a more attractive therapeutic option in treating MM cells.

The pro-apoptotic activity of AICAR was attenuated by overexpression of Bcl-2, an anti-apoptotic molecule that stabilizes the mitochondrial membrane potential (Fig. 3.3.8.1). Bcl-2 did not attenuate the anticancer activity of metformin, which is in agreement with the fact that metformin did not induce significant apoptosis in our models (Fig.3.3.8.1).

4.3.5. AMPK activators synergise with glycolysis inhibitors

Under aerobic conditions, mammalian cells can generate ATP through two metabolic pathways: glycolysis in the cytosol and oxidative phosphorylation in the mitochondria (aerobic respiration). ATP generation through mitochondrial respiration is more energy efficient (one glucose yields 36 ATP) than glycolysis (one glucose yields 2 ATP), and thus is a preferred pathway for the normal cells to generate energy supply.

Plasma glucose is regulated by complex endocrine systems in mammals. AMPK is activated in mammalian cells by a variety of physiological and pathological stresses that increase the intracellular AMP: ATP ratio, either by increasing ATP consumption (e.g. muscle contraction) or by decreasing ATP production (e.g., ischaemia or hypoxia). Once activated, AMPK acts to restore cellular energy homeostasis by promoting ATP generating pathways such as fatty acid oxidation, while simultaneously inhibiting ATP utilizing pathways, such as fatty acid synthesis and gluconeogenesis. By decreasing the amount of available glucose for cancer cells to utilise, the proliferation rate will be decreased. Otto Warburg first described that cancer cells have an increased rate of glucose uptake and glycolysis even under normoxic conditions ("Warburg effect") , but moderate rates of mitochondrial respiration [391]. A recent review by Lopez-Lazaro [290] highlighted the importance of glycolysis in cancer cell development. Activation of glycolysis protects cells from

H_2O_2- induced cell death, causes hypoxia-inducible factor 1 (HIF-1) activation and provides carbon skeletons for biosynthesis. HIF-1 activation plays a key role in the transcription of genes that code for glucose transporters and glycolytic enzymes [290]. A reduction of the glycolytic capacity of tumour cells would restrict their ability to proliferate, invade adjacent tissues and migrate to distant organs. Because AICAR caused mitochondrial membrane potential depolarization, we hypothesized that concurrent activation of AMPK and inhibition of glycolysis could severely impact cancer cell energy metabolism and result in enhanced death of malignant cells, sparing normal cells that do not exhibit the Warburg effect. We found that the pyruvate analog 3-bromopyruvate (3-BrPA), which is a hexokinase inhibitor, and the glucose analog 2-deoxyglucose (2-DG), a competitive inhibitor of glucose metabolism, enhanced the anticancer activity of AICAR, suggesting that targeting AMPK may expose the cancer cell's addiction to glycolysis [290].

Since the AMPK pathway plays an important role in promoting cellular nutrient uptake, cell growth and cell survival, a combination of AMPK activation and blockage of glycolysis seems to be a mechanism-based strategy to severely impact cancer cell energy metabolism and effectively kill the malignant cells. It was hypothesized that if glucose availability was reduced and the ability of cancer cells to generate ATP was inhibited by glycolysis inhibitors, that this combination would synergise and cause increased cancer cell death. There is also evidence that rapamycin, an mTOR inhibitor, can compromise the ability of cells to uptake glucose [392]. We demonstrated that the combination of AICAR and metformin with either 3-BrPA or 2-DG showed synergistic cytotoxicity even in cell lines such as MM1.S and FRO which are not very sensitive to single agent AICAR or metformin (Fig. 3.3.10.2 and Fig. 3.3.10.3). As far as we know, this is the first time that this combination has been examined for activity in MM and thyroid cancer cells. The mechanism of this synergy is not well understood. The combination would affect ATP generation and ATP depletion would certainly cause cell death. Pradelli *et al.* [393]. identified the signalling pathway initiated by glycolysis inhibition either by removal of glucose or the use of nonmetabolizable form of glucose (2-deoxyglucose), that resulted in sensitisation to death receptor-induced apoptosis by Fas or tumour necrosis factor-related apoptosis-inducing ligand (TRAIL). The authors reported that AMPK is activated upon glycolysis block. This study further supports the use of AMPK activators and glycolysis inhibitors in the treatment of human cancers.

4.3.6. The safety profile of metformin and AICAR

With any new anticancer agents, the therapeutic index and its safety profile is a major concern. Metformin is a biguanide developed from galegine, a guanidine derivative found in Galega officinalis (French lilac). Metformin is an antidiabetic medicine that is commonly used in the treatment of non-insulin dependent diabetes mellitus (NIDDM) since 1957 in Europe and other countries, and in the US from 1995. Metformin causes suppression of liver gluconeogenesis; decreased expression of lipogenic enzymes; increased fatty acid oxidation; and stimulation of glucose plasma membrane transport in skeletal muscle. Chemically, it is a hydrophilic base which exists at physiological pH as the cationic species (>99.9%). As a consequence, its passive diffusion through cell membranes is limited [394]. Studies with Caco-2 cells demonstrate a low rate of transport of metformin [395]. The oral bioavailability of metformin is 40-60% [394, 396]. It is absorbed predominately from the small intestine and gastrointestinal absorption is complete within 6 hours of ingestion. Metformin is rapidly distributed following absorption and does not bind to plasma proteins. No metabolites or conjugates of metformin have been identified. The absence of liver metabolism clearly differentiates the pharmacokinetics of metformin from that of other biguanides, such as phenformin. Metformin undergoes renal excretion and has a mean plasma elimination half-life after oral administration of between 4.0 and 8.7 hours. This elimination is prolonged in patients with renal impairment and correlates with creatinine clearance.

It has an excellent safety profile when used as labelled [397]. The maximum dosage for adults is 2550mg/day. A study by Sambol *et al*. [398] showed no significant differences in metformin kinetics in patients with NIDDM and healthy subjects, in men compared with women, or during multiple-dose treatment versus single-dose treatment. In patients with NIDDM, single doses of 1,700-mg or higher of metformin significantly decreased postprandial, but not preprandial, glucose concentrations and did not influence insulin concentrations. With multiple doses, both preprandial and postprandial glucose concentrations and preprandial insulin concentrations were significantly lower than with placebo. In healthy subjects, single and multiple doses of metformin showed no effect on plasma glucose, but significantly attenuated the rise in immediate postprandial insulin levels. This study reassures us that metformin can likely be safely given to non-diabetic patients without undue worry about high rates of drug-induced hypoglycaemia. With the limited diffusion into cells and the lack of active transport into cells via plasma protein binding, dosing of metformin has to be of a high enough dose to ensure

enough therapeutic activity. That is the reason for the high dose levels used in the *in vitro* studies in this thesis and in other published studies.

Nevertheless, our data should not be interpreted as support for the use of metformin in MM patients outside the context of a well-designed clinical trial. Physicians' perception of the potential risks of metformin use is influenced by the withdrawal of the related biguanide phenformin from the US market in 1976 because of probable association with lactic acidosis [397]. The latter is a much more lipophilic drug due to its phenyl and ethyl groups (N1,N1-phenylethylbiguanide) which can permeate biological membranes readily, and is a more potent respiratory chain inhibitor, while metformin is positively charged and accumulates (~1000 fold) within the mitochondrial matrix in a slow, membrane-potential driven fashion, that is also self-limiting because progressive inhibition of the respiratory chain leads to a drop in membrane potential, which will prevent further accumulation of the drug [399]. This may explain why lactic acidosis is extremely rare with metformin, in contrast to phenformin [397, 400, 401]. In a recent metaanalysis, pooled data from 347 comparative trials and cohort studies revealed no cases of fatal or non-fatal lactic acidosis in 70,490 patient-years of metformin use [402]. The upper limit for the true incidence of lactic acidosis per 100,000 patient years was calculated as 4.3 cases in metformin users and 5.4 cases in non-metformin users [402]. The authors concluded that there is no evidence from prospective comparative trials or from observational cohort studies that metformin is associated with an increased risk of lactic acidosis, compared to other anti-hyperglycemic treatments [402]. Still, it would be prudent to limit metformin use to patients with adequate renal function, as metformin is renally cleared [403, 404]. Relevant guidelines have been proposed [405], including using metformin with caution if serum creatinine>130 micromol/l or eGFR <45 ml/minute/1.73 m^2, and discontinuing metformin if serum creatinine >150 micromol/l or eGFR <30 ml/minute/1.73 m^2. For the same reason, the concurrent use of metformin and iodinated intravenous radiographic contrast or other nephrotoxins should be avoided.

Existing MM treatment, such as glucocorticoids, can have the side effect of hyperglycaemia, concurrent metformin administration would have an added benefit of controlling their glucose levels whilst having anticancer properties. IGF-1R inhibitors have been shown in preclinical studies to have anti-myeloma properties [82]. When the trials for IGF-1R inhibitors were carried out, hyperglycaemia was an

unexpected complication that was not seen in mouse models [82]. Most studies [406-408] reported grade I-II toxicity with the exception of a trial reported by Hidalgo *et al.* [409] which reported grade III toxicity. Metformin was one of the agents used to normalise the patients' blood glucose. It was demonstrated that IGF-1R inhibitor-induced hyperglycaemia was treateable with metformin.

More importantly, the clinical development of other AMPK activators, such as AICAR, holds promise of anticancer activity without concern, real or perceived, for lactic acidosis. AICAR was originally developed as an exercise mimicker by stimulating the uptake of glucose into skeletal muscle. The experimental doses of AICAR employed in this thesis may prompt some concern as to human extrapolations. There is little data on the literature about the optimal dose and few studies on the pharmacokinetics of this drug. Dixon *et al.* [410] reported a study of AICAR on treatment of ischemic heart disease. In a placebo-controlled, double-blind study in healthy men, the safety and kinetics of the drug after oral and IV administration of 10, 25, 50, and 100 mg/kg doses were evaluated. The authors reported that the drug was well tolerated at all dose levels. The post-infusion plasma concentrations of AICA-riboside declined rapidly in a biphasic fashion, and the terminal elimination phase had a harmonic mean t1/2 beta of 1.4 hours. The drug was not protein bound, and there was rapid uptake and phosphorylation in red blood cells to its 5'-monophosphate nucleotide. AICAR was renally cleared and and only 8% of the IV dose was excreted in the urine as intact AICAR. The highest intravenous dose of AICAR used, 100mg/kg converts to 267μM (see Appendix B for calculation). This dose level is within the doses used in the *in vitro* experiments in this thesis and in other studies. In the synergistic experiments with glycolysis inhibitors, we had utilised a higher dose (up to 600 μM) to exaggerate any potential synergistic action but we were assured that the lower dose of 200 μM also yielded a synergistic cytotoxicity with the glycolysis inhibitors.

To futher research on AICAR's therapeutic potential, we had undertaken several studies to examine the actions of this agent. We demonstrated that the majority of MM cell lines are much more sensitive than non-neoplastic tissues to the cytotoxic effects of AICAR. The BMSC line HS-5 and the immortalized hepatocyte cell line THLE-3 were shown to be insensitive to AICAR with calculated EC_{50} values >1000μM (Fig. 3.3.5.1). Treatment of normal PBMCs, at doses of AICAR that induced killing of both MM cell lines and patient samples *in vitro* had minimal effect on these normal cells (Fig. 3.3.5.2). Our *in vivo* study also demonstrated that the

mice suffered no toxicities and had a steady weight throughout the study (Fig. 3.3.9.3). This data suggest a favourable therapeutic index for AICAR. Recently, AICAR has received particular clinical attention as an agent that might prevent complications following coronary artery bypass graft surgery [411, 412]. As an anticancer agent, it is currently in Phase I testing in B-cell CLL using a dose of 50mg/g [413] and the findings of this research may provide useful evidence for conducting MM-specific clinical research with the agent.

4.4 Proteomic analysis to examine bortezomib resistance

4.4.1. Investigating bortezomib resistance mechanisms in Multiple Myeloma using proteomics

Proteomics provide an advantage to genomics investigations of disease as it allows protein-protein interaction to be studied. Recent advances in the use of proteomic technologies (specifically the comparative proteomic approach) provide a robust approach to study multiple signalling pathways simultaneously and mechanisms of resistance to anticancer therapy. We are interested in the mechanisms of resistance developed by MM cells to bortezomib therapy. In this study, we used MM cell lines that are sensitive and of intermediate resistance, MM1.S and OPM2 respectively, that were treated with bortezomib to IC_{50}. As a resistant cell line to bortezomib is difficult to generate in MM cells, we had to use non-isogenic cell lines. We wanted to make the finding more robust by including a solid tumour cell line that has sensitive and resistant counterparts to bortezomib. We choose to use the thyroid carcinoma cell line, KAT18 (sensitive) and WRO (resistant). These cells lines were also treated to IC_{50} with bortezomib. The rationale for adding on a solid tumour counterpart was to account for any potential artefact that may arise due to differences in the cell lines themselves rather than due to bortezomib-induced changes.

4.4.2. Generation of protein list

Four lists of differentially expressed proteins were established. These compared control and treated MM1.S (list 1), control and treated KAT18 (list 2), control and treated OPM2 (list 3) and control and treated WRO (list 4). The generated protein list was analysed and the trend of change in the cell lines before (control) and after (24h) treatment with bortezomib was noted. Therefore, in order to further determine the significance of these differentially changed proteins, the design analysis was planned to specifically identify proteins that were altered in the same trend in both of the sensitive lines (MM1S, KAT18) vs. the resistant lines (OPM2, WRO), e.g. protein x upregulated in sensitive lines and downregulated or unchanged in resistant lines. The proteins of interest were determined (Table 3.4.2.1).

4.4.3. Identified proteins on proteomic analysis

From the generated protein list, 50 spots containing proteins of interest were identified (Table 3.4.2.1) and 39 of those proteins were picked from the preparative-scale gels which provided sufficient sample for identification studies on the mass spec. The other 11 spots contained proteins that were of too low abundance to be identified from the preparative gel. The picked spots were identified after trypsin digestion and mass spectrometry analysis. The MASCOT software was able to identify 14 of these 39 (Table 3.4.2). The reason that the other 25 spots containing proteins of interest were unable to be identified was because the low abundance of the proteins present even in a preparative-scale gel. In the case of these spots, too few peptides were identified in the post-trypsin digestion to generate a confident identification.

Hsp70 and caspase-3 were two proteins that our proteomic analysis of bortezomib treatment in sensitive and resistant cells identified. This is an encouraging finding as these two proteins were already known in the literature as being associated with bortezomib treatment [278, 414]. As outlined below, the trend of the proteins seen in sensitive vs. resistant lines were consistent with what is known about them post bortezomib exposure. This finding validates the model and the technique that we used in this analysis.

Proteasome 26S proteins were also identified in our analysis with a protein ID of 675 (26S protease (S4) regulatory subunit), 914 (Proteasome 26S subunit, ATPase 2) and 1088 (Proteasome 26S subunit, ATPase 2). It is not surprising to find these proteins as bortezomib is a proteasome inhibitor. Protein 675 and 914 were consistent with each other showing no change in the sensitive cell lines and an increase in the resistant cell lines. This can be explained by the fact that as the cells were exposed to bortezomib, the sensitive cells were rapidly killed whereas the resistant cells were able to mount a response to the bortezomib exposure by inducing proteasome synthesis. What is unclear is why protein 1088 did not behave as the others and had an opposite response (an increase in sensitive cells and a decrease in resistant cells). We would need to further investigate this phenomenon.

The other proteins identified are discussed below with a review of what is known about their functions.

4.4.3.1. Heat shock protein 70kDa

Our analysis showed that Hsp70 was upregulated in the sensitive cell lines vs. no change in the resistant cell lines (Fig. 3.4.3.1). This result was validated using Western blot and showed that Hsp70 was induced by bortezomib treatment in the sensitive cell line MM1.S resulting in an increase in Hsp70 levels (Fig. 3.4.3.3).

Heat shock proteins (HSPs) or stress response proteins (SRPs) are synthesized in variety of environmental and pathophysiological stressful conditions. Many HSPs are involved in processes such as protein denaturation-renaturation, folding-unfolding, transport-translocation, activation-inactivation, and secretion. HSP70 has been shown to be involved in protective roles against thermal stress, cytotoxic drugs, and other damaging conditions leading to association with drug resistance.

Hsp70 is known to be upregulated post bortezomib treatment [319, 415, 416]. NPI-0052 have been shown to induce Hsp70 as well although to a lesser extent than bortezomib [415]. The presence of misfolded proteins in the cytosol may partially explain why proteasome inhibitors induce the expression of not only Hsp70 but also Hsp27 and Hsp90 [416]. In fact, there is evidence that inhibition of Hsp90 synergises with bortezomib [53] and there is currently a clinical trial investigating this combination.

4.4.3.2. Caspase-3

The caspase family of cysteine proteases play a key role in apoptosis. Caspase 3 (also known as CPP32, YAMA and apopain) is synthesized as an inactive pro enzyme that is processed in cells undergoing apoptosis by self proteolysis and/or cleavage by other upstream proteases (e.g. Caspases 8, 9 and 10). The cleaved form of Caspase 3 consists of large (17kD) and small (12kD) subunits which associate to form an active enzyme. Caspase 3 is cleaved at Asp28 - Ser29 and Asp175 - Ser176. The active Caspase 3 proteolytically cleaves and activates other caspases (e.g. Caspases 6, 7 and 9), as well as relevant targets in the cells (e.g. PARP).

Our analysis showed that caspase-3 was downregulated in the sensitive cell lines vs. no change in the resistant cell lines (Fig. 3.4.3.2). This result was validated using

Western blot and showed that total caspase-3 was cleaved by bortezomib treatment in the sensitive cell line MM1.S resulting in a reduction in total caspase-3 (Fig. 3.4.3.3).

Bortezomib has been shown to activate caspase-3 cleavage in several studies [278, 415, 417]. Hideshima *et al.* [278] demonstrated that bortezomib activates caspase-3 through caspase-8 activation as pan caspase inhibitors and caspase-8 inhibitors completely abrogate bortezomib–induced caspase-8/caspase-3 activation. The authors also showed that JNK inhibition was able to block bortezomib-induced cell death by the abrogation of caspase-3 cleavage. NPI-0052, another proteasome inhibitor is also able to activate caspse-3 cleavage [418] showing that this mechanism of apoptotic cell death is a class response and not specific to bortezomib.

4.4.3.3. Far upstream element binding protein

Overexpression of far upstream element binding protein 1 (FBP-1) and 2 (also known as KHSRP protein or FBP-2) has been shown to be associated with poor patient survival in >70% of human hepatocellular carcinoma [419]. *In vitro*, FBP-1 over expression predominantly induced tumour cell proliferation, while FBP-2 primarily supported migration in different HCC cell lines [419]. FBP-1, an activator of transcription of the proto-oncogene c-myc, demonstrated strong overexpression in human hepatocellular carcinoma (HCC) [420]. Rabenhorst *et al.,* showed that knockdown of the protein in HCC cells resulted in increased sensitivity to apoptotic stimuli, reduced cell proliferation and impaired tumour formation in a mouse xenograft transplantation model [420]. The authors identified p21 as a direct target gene repressed by FBP1, and expression levels of the proapoptotic genes tumour necrosis factor alpha, tumour necrosis factor-related apoptosis- inducing ligand, Noxa and Bik were elevated in the absence of FBP1. Bortezomib treatment is known to cause induction of proapoptotic proteins such as Noxa [417].

The two FBP proteins identified in our analysis were downregulated in the sensitive cell lines after bortezomib treatment. This suggests that bortezomib is able to overcome the c-myc activation and induce cytotoxicity. Deregulated or elevated expression of c-myc occurs in ~30% of human cancers, including breast, colon, cervical, small cell lung cancer, osteosarcoma, glioblastoma, melanoma, and myeloid leukemias.[421]. C-myc facilitates tumour cell growth via angiogenesis involving upregulation of HIF1 [421]. It

has been reported that bortezomib is able to downregulate HIF1 and inhibit angiogenesis and tumourigenesis [421].

4.4.3.4. Fascin

Human fascin is a highly conserved actin-bundling protein and is thought to be involved in the formation of microfilament bundles. It is now thought that fascin is involved in filopodia assembly and cancer invasion and metastasis of multiple epithelial cancer types. Gastric cancer [422], prostate cancer [423] and colon cancer [424] have shown upregulation of fascin and an increase in cell invasiveness and metastasis. Li *et al.* [425] elegantly demonstrated that fascin is an integral component of invadopodia and is implicated in invasive migration into collagen I-Matrigel gels. It is unclear why fascin was found to be upregulated in the sensitive cell lines after bortezomib treatment.

4.4.3.5. Heterogeneous nuclear ribonucleoprotein

Heterogeneous nuclear ribonucleoprotein (hnRNP) family consists of several members including hnRNP A2/B1 isoform B1, hnRNP K, hnRNP D and hnRNP A1. The hnRNP family has several different cellular roles including transcription, mRNA shuttling, RNA editing and translation. Several reports implicate hnRNP K having a role in tumourigenesis, for instance hnRNP K increases transcription of the oncogene c-myc and hnRNP K expression is regulated by the p53/MDM 2 pathway [426]. In the mouse myeloma cell line, GS-NS0, there is an up-regulation of proteins triggered by a cellular response to external stress stimuli, revealing induction of different proteins including hnRNP K [427]. Recently, a loss of function screen done on a derivative pool of cells with loss of migration phenotype demonstrated the involvement of hnRNP K in metastasis [428]. HnRNP K was also implicated as being overexpressed in colon cancer and the authors showed that hnRNP K had an aberrant subcellular localisation in cancer cells [426]. Finally, overexpression of hnRNP K in breast cancer cells significantly increased target c-myc promoter activity and c-Myc protein and enhanced breast cancer cell proliferation and growth in an anchorage dependent manner. The

authors suggested that the activity of human EGF receptor family members regulates hnRNP K expression [429].

There is less known about the other hnRNP family members. There is reports in the literature that HnRNP A2/B1 was shown to be upregulated in HepG2 [430], endometrial adenocarcinoma [431] and pancreatic epithelial cells (via EGF) [432]. Meanwhile, HnRNP D overexpression was shown in oral squamous cell cancer [433]. Thus far, the only member of this family to be reported to be involved in MM. HnRNP A1 was found to be a mediator of the IL-6 effect in MM. It does this by binding to the myc internal ribosome entry site (IRES) *in vivo* in myeloma cell lines as well as patient samples [434]. The authors then showed that knock down of hnRNP A1 prevented an IL-6 increase in myc protein expression, myc IRES activity, and cell growth pointing to hnRNP A1 as a critical regulator of c-myc translation and a potential therapeutic target in MM [434].

In our analysis, all the members of the hnRNP protein family were downregulated after treatment with bortezomib in sensitive cells. This suggests that bortezomib treatment may be able to overcome this bad prognostic marker that has been found to be overexpressed in multiple cancer types.

4.4.3.6. Annexin A2

The Annexins are a family of structurally similar proteins. Annexins bind to phospholipids and may be involved in regulation of membrane transport, membrane channel activity, and interaction of the cell membrane with the extracellular matrix. Annexin II is a calcium-regulated membrane-binding protein whose affinity for calcium is greatly enhanced by anionic phospholipids. This protein functions as an autocrine factor which heightens osteoclast formation and bone resorption.

2DE-based proteomic analysis of oesophageal squamous cell cancer compared to an immortal cell line, identified downregulation of annexin A2 and upregulation of heat shock 70 kDa protein amongst other proteins that are correlated to malignant transformation [435]. This result compares to our analysis where heat shock 70 kDa protein was upregulated by bortezomib treatment in sensitive cells. However, our result

showed an upregulation of annexin A2 in sensitive cells and was unchanged in the resistant cells. It is unclear how annexin interacts with bortezomib and this difference between our results and the what is known in the literature may be a drug related process.

4.4.3.7. Endoplasmic reticulum protein 29

Endoplasmic reticulum protein 29 (ERp29) is a novel endoplasmic reticulum (ER) secretion factor that facilitates the transport of secretory proteins in the early secretory pathway. Overexpression of ERp29 resulted in G0/G1 arrest leading to inhibition of cell proliferation in breast cancer cells, decreased cell migration/invasion and reduced cell transformation [436]. Unsurprisingly, we demonstrated that ERp29 is upregulated in the sensitive cell lines post bortezomib treatment. We know that bortezomib causes cell cycle arrest although in the reported literature the arrest was at G2/M [437-439] rather than at G0/G1. There may be others proteins involved in bortezomib treatment that can cause cell cycle arrest and ERp29 could be just one of the many proteins upregulated by bortezomib treatment.

Conditions that disrupt protein folding in the ER, such as a chemical insult or nutrient deprivation, activate a stress signalling pathway known as the unfolded protein response (UPR) [416]. UPR induction results in both an initial decrease in general protein synthesis, to reduce the influx of nascent proteins into the ER and increased transcription of ER resident chaperones, folding enzymes and components of the protein degradative machinery to prevent the aggregation of the accumulating misfolded proteins. These misfolded proteins are recognized by ER quality control systems and retained in the ER, preventing them from proceeding further through the protein maturation process [416]. Proteins that cannot be properly refolded are then targeted for ER-associated protein degradation (ERAD), which involves the retrograde translocation or dislocation of the misfolded proteins out of the ER and subsequent degradation by cytosolic 26S proteasomes [416]. Therefore, bortezomib induces ER stress as it prevents degradation of misfolded proteins. This may explain the induction of ERp29.

4.4.3.8. Ferritin light chain

Ferritin is a ubiquitous and highly conserved protein which plays a major role in iron homeostasis by sequestering and storing iron in a non-toxic and soluble form. It forms a holoenzyme of ~450 kDa, consisting of 24 subunits of two types, H (heavy; 21 kDa) and L (light; 19 kDa), and is capable of storing up to 4,500 atoms of ferric iron. Depending on the tissue type and physiological status of the cell, the ratio of H to L subunits in ferritin can vary widely. Ferritin is found in the liver, spleen, kidney and heart, with smaller amounts being found in blood. Serum ferritin levels serve as an indicator of the amount of iron stored in the body and is a sensitive test for anaemia. As ferritin is an acute-phase reactant, levels are often elevated during infection. Studies have shown the association of elevated serum ferritin and poor prognosis in MM [440, 441] ,and lymphoma [442]. However, these studies looked at secreted ferritin and we are still unsure of the function of the light and heavy chain of the ferritin protein in tumourigenesis and drug resistance. A recent study found that cells transformed with oncogenic RAS have increased iron content relative to their normal cell counterparts through upregulation of transferrin receptor 1 and downregulation of ferritin heavy chain 1 and ferritin light chain [443]. Another study in breast cancer associated high levels of cytosolic ubiquitin and/or low levels of ferritin light chain were associated with a good prognosis in breast cancer [444]. In our proteomic analysis, the levels of ferritin light chain were upregulated by bortezomib treatment in both sensitive and resistant cell lines, although markedly in the sensitive cell lines. It is unclear why there should be an increase in the sensitive cell line to bortezomib treatment as upregulation of this protein is usually associated with poor prognosis. It could be that as ferritin is an acute phase reactant, it is a cellular inflammatory response to cell death caused by bortezomib.

Chapter 5
Summary and Conclusion

5.1. MDR associated protein expression as a mechanism of resistance in Multiple Myeloma

- Bortezomib was shown to likely be a P-gp substrate and a weak inhibitor. The combination of P-gp inhibitor, elacridar with bortezomib showed synergistic cytotoxicity. There was also cross resistance seen in P-gp expressing cell line DLKP-A. This suggests that P-gp overexpression could cause resistance to Bortezomib therapy.

- Clinically, the combination of a P-gp inhibitor and bortezomib in P-gp positive myeloma patient should have a therapeutic effect.

- Bortezomib was not shown to be a MRP-1 substrate.

- Bortezomib was not demonstrated to be a BCRP substrate or inhibitor. There was no synergy when bortezomib was combined with a BCRP substrate (SN38) or inhibitor (elacridar). There was also no cross resistance seen in BCRP expressing cell line DLKP-SQ/Mitox.

- P-gp expression levels correlated to bortezomib's ability to function as a P-gp substrate. Cell lines that have a higher expression of P-gp were intrinsically more resistant to the actions of the drug and showed more synergy when bortezomib was combined with elacridar.

- Bortezomib downregulated P-gp expression levels and function.

- P-gp expression and function was downregulated when MM cells are co-cultured with BMSCs.

- There was transference of P-gp from the P-gp-positive MM cell line to the P-gp-negative stromal cells when the two cell lines were co-cultured together.

5.2. Investigation of p53 signaling perturbations in Multiple Myeloma resistance

- Nutlin-3, a Mdm2 inhibitor showed antimyeloma activity and anticancer activity.

- Nutlin-3 upregulated the expression of p53-dependent targets such as Bak, Bax, PUMA, Noxa, p21, Hdm2, Hsp90 and VEGF. Nutlin-3 was also able to induce caspase-3 cleavage but this effect was only partially abrogated by a pan-caspase inhibitor suggesting that caspase activation was not the only mechanism of cell death.

- Nutlin-3 combined with bortezomib was able to induce additive cytotoxicity in MM cells and synergistic activity in epithelial tumour cells. This is because MM cells were very sensitive to single agent bortezomib and nutlin-3, leaving little room for the synergistic action of when both drugs were combined. This effect was demonstrated by Western blot which demonstrated that the p53 apoptotic pathway was enhanced in the epithelial tumours but not in MM cells by the combination.

- Nutlin-3 was not able to overcome the protective effect of BMSCs. However, the drug was still able to induce expression of p53 downstream effectors in the presence of BMSCs but to a lesser degree compared to in the absence of BMSCs.

- The synergistic cytotoxicity seen with bortezomib in epithelial tumours was not affected by the presence of BMSCs.

- The synergy between bortezomib and nutlin-3 was shown to be p53 independent in certain cell lines.

- Bortezomib-treated patients who had, at baseline, high expression of nutlin-3-suppressed genes had significantly shorter progression-free survival ($p=0.001$, log-rank test) and OS ($p=0.002$, log-rank test) compared to those with low expression levels.

5.3. Activation of AMPK pathway as an alternative to overcome drug resistance in Multiple Myeloma

- Metformin and AICAR were shown to have activity in MM cells and other epithelial cancer cell lines.
- Both drugs were able to overcome the protective effect of BMSCs and OCs.
- Both drugs activated AMPK and inhibited the downstream effectors of mTOR. The cell cycle proteins, cyclin D1 and cdk4/6 were also downregulated by metformin and AICAR.
- As compound C, an AMPK inhibitor, did not reverse the antitumour activity of metformin completely, there is a suggestion that the anticancer activity of metformin also acts via an indirect AMPK pathway.
- Both of the AMPK activators have a good safety profile. Metformin has been used as an antidiabetic agents for many years and AICAR was shown to have little effect on non-neoplastic cells. The mice also tolerated AICAR with no overt toxicity.
- AICAR is the more potent of the two AMPK activators as it had more activity in the patient sample and was able to induce apoptosis and mitochondrial membrane depolarisation.
- We were able to demonstrate a statistically significant results in a subcutaneous xenograft mouse model with reduction in tumour burden and statistically significant survival .
- AICAR and Metformin synergised with glycolysis inhibitors, 2DG and 3BrPA and caused apoptosis with PARP and caspase 3 cleavage.
- AMPK activation is promising as an anticancer pathway and there is a possibility that it can prevent cancer.

5.4. Proteomic analysis to examine bortezomib resistance

- Proteomic comparative analysis of sensitive cell lines (MM1.S and KAT18) vs. resistant cell lines (OPM2 and WRO) pre- and post-bortezomib treatment for 24hrs generated lists of differentially expressed proteins.

- The distinctive design analysis of overlapping the four generated proteins lists to specifically identify proteins that had a trend of change that was unique to the sensitive cell lines vs. the resistant cell lines lead to the identification of these proteins:-

    - Heat shock protein 70kDa
    - Caspase-3
    - Far upstream element binding protein
    - Fascin
    - Heterogeneous nuclear ribonucleoprotein
    - Annexin A2
    - Endoplasmic reticulum protein
    - Ferritin, light polypeptide

- Heat shock protein 70kDa and caspase-3 protein are known in the literature to be associated with bortezomib treatment. Our findings confirmed the data published and demonstrated the validity of using this technique to identify proteins that were affected by bortezomib treatment.

The focus of this thesis was to evaluate the mechanisms whereby myeloma cells develop intrinsic resistance with a focus on resistance in the context of bortezomib treatment. We believe that there is interplay between different mechanistic elements that gives rise to drug resistance and the most effective treatment regime will consist of well researched combinations of drugs individualised to the biology of the patient rather than a single super-agent.

In our study, bortezomib cytotoxicity is reduced in P-gp overexpression, but the other MDR proteins; MRP-1 and BCRP are unlikely to contribute to the resistance seen to bortezomib. This makes bortezomib combination therapy with an P-gp modulator, i.e. elacridar, clinically relevant in surmounting bortezomib resistance caused by P-gp overexpression. We have further proved that this combination is clinically feasible as the combination activity is still synergistic even in the presence of the local tumour microenvironment. Bortezomib has a further role in modulating P-gp resistance by downregulating P-gp expression and function. We demonstrated that there is a transference of P-gp between MM cells and the local microenvironment that may contribute to the resistance seen to P-gp substrates such as doxorubicin and daunorubicin.

We then tested the combination of bortezomib with an Mdm2 inhibitor, nutlin-3. In p53-wild type (WT) cells, nutlin-3 affects the p53 apoptotic pathway. In p53-mutated cells, nutlin-3 also had activity but the dose levels used were much higher than for the p53 wild type. Recent studies showed that nutlin-3's cytotoxic activity in p53-negative and p53-mutant human tumour cells is via E2F1 binding to Mdm2 [181, 182]. In cell ines that require a higher dose of nutlin-3 as a single agent to have cytotoxic activity, the combination with bortezomib yielded synergy. This comprises p53-mutated MM cell lines and epithelial cell lines (p53-WT or p53-null or mutated). We postulate that the reason that the combination of bortezomib and nutlin-3 in p53-WT MM cells did not show synergy is because MM cells were very sensitive to single agent bortezomib and nutlin-3, leaving little room for the synergistic action of both drugs combined. Although nutlin-3 was not able to overcome the protective effect of BMSCs, it still has a clinical role as the drug was still able to induce expression of p53 downstream effectors in the presence of BMSCs but to a lesser degree compared to in the absence of BMSCs. The clinical relevance of the drug is further proven by the synergistic cytotoxicity seen with bortezomib in epithelial tumours in the presence of BMSCs.

The AMPK pathway is of interest in MM as activation of AMPK will inhibit mTOR, which is involved in cell proliferation and growth. Metformin and AICAR, both AMPK activators, were studied in the thesis and have clinical relevance as not only do they have anticancer activity *in vitro but* both of these drugs can overcome the protective (pro-cancer) effect of the local microenvironment. Although the dose levels used in this study appears to be higher than the normal practice, it is consistent with the reported levels used in other studies. Metformin is positively charged and accumulates (~1000 fold) within the mitochondrial matrix in a slow, membrane-potential-driven fashion, that is also self-limiting because progressive inhibition of the respiratory chain leads to a drop in membrane potential, which will prevent further accumulation of the drug [399]. Furthermore, as a hydrophilic base, metformin's passive diffusion through cell membranes is limited [394]. Clinically, metformin has been in use since the 1950s and has an excellent safety profile when used as labelled [397]. As with metformin, the AICAR doses used are higher than the normal practice. The thesis findings showed that AICAR is non-toxic to non-neoplastic cells at the cytotoxic doses used for cancer cells and the *in vivo* study showed no toxicity to the animals. Furthermore, a study by Dixon *et al.* [410] reported the pharmacokinetics of AICAR and the doses used in this study are within the range of doses used for our *in vitro* experiments. Between the two AMPK activators, AICAR has more antimyeloma activity and a clinical trial of this agent should be pursued.

Proteomic comparative analysis of MM cells to mechanism of bortezomib resistance revealed novel proteins that are not known to be associated with MM. These proteins have been associated with other cancer types in the literature. This technique is a sensitive tool to examine bortezomib resistance.

Recent studies published that both nutlin and metformin are P-gp substrates and they affect P-gp expression and function [445, 446]. Nutlin was shown to affect MRP-1 as well [446]. These two studies further connect the different anti-MM agents studied.

Chapter 6
Future Work

6.1. MDR protein resistance in Multiple Myeloma

1. To confirm whether bortezomib is truly a P-gp substrate, we would like to look at the extrusion of bortezomib from a P-gp overexpressing cell, using either a radio-labelled or fluorescent-labelled bortezomib.

2. We have showed that bortezomib is able to change the levels of P-gp protein expression and function, therefore investigation of the impacts of bortezomib treatment on other resistance proteins, i.e. BCRP and MRP-1 should be done.

3. As recent studies have showed that nutlin-3 and metformin can affect P-gp function and expression, investigation into combination of these agents with bortezomib on the impact of P-gp expression is warranted.

4. As it has been seen with other chemotherapeutic agents that are P-gp substrates, such as doxorubicin, we want to clinically correlate the P-gp expression in BM samples of bortezomib responsive and bortezomib refractory patients to see if exposure to bortezomib can select for P-gp expression.

6.2. p53 signalling perturbations in Multiple Myeloma

1. As p53-null or p53-mutated cell lines showed synergy with nutlin-3 and bortezomib, examination into the mechanism of cell death caused by this combination should be undertaken.

6.3 APMK activation as an alternative pathway to overcome resistance to conventional treatment in Multiple Myeloma

1. The combination of glycolysis inhibitors and AMPK activators yielded synergy and investigation into the mechanism of the combination should be undertaken.

6.4. Proteomic analysis of bortezomib resistance in Multiple Myeloma

1. The proteins identified in this thesis were novel proteins that are not known to be associated with MM or bortezomib treatment. Investigation of potential targets for resistance mechanism to bortezomib treatment by using siRNA to

generate a knockdown or upregulation of the target proteins. Alternatively, if there are small molecule inhibitors available, to use them to inhibit or activate the target proteins.

Abbreviations

ABBREVIATIONS

2-DE - Two-dimensional gel electrophoresis

2-DIGE - Two-dimensional differential in gel electrophoresis

AICAR - 5-aminoimidazole-4-carboxamide ribonucleoside

AMPK - AMP-activated protein kinase

ASCT - Autologous stem cell transplant

BAFF - B-cell activating factor

BCRP - Breast cancer resistance protein

BM - Bone marrow

BMECs - Bone marrow endothelial cells

BMSCs - Bone marrow stromal cells

DKK1 - Dickkopf 1

ECM - Extracellular matrix

ERp - Endoplasmic reticulum protein

FBP protein) - Far upstream element binding protein (also known as FUSE binding

FGFs - Fibroblast growth factors (FGFs)

FISH - Fluorescent in-situ hybridization

FLC - Free light chain

HCC - Hepatocellular carcinoma

HDAC - Histone deacytelase

HGF - Hepatocyte growth factor

HIF-1 - Hypoxia-inducible factor 1

HnRNP - Heterogeneous nuclear ribonucleoprotein

HSP - Heat shock protein

HRD - Hyperdiploid

IGF-1 - Insulin-like growth factor-1

IGHR	- Immunoglobulin heavy chain variable region
IL	- Interleukin
MDR-1	- Multidrug resistance -1
MGUS	- Monoclonal gammopathy of unknown significance
MIP	- Macrophage inflammatory protein
MM	- Multiple Myeloma
MMP	- Matrix metalloproteinases
MP	- Melphalan and Prednisolone
MS	- Mass spectometry
mTOR	- Mammalian target of rapamycin
MVD	- Microvascular density
NF-κB	- Nuclear factor-kappaB
NHRD	- Nonhyperdiploid
OB	- Osteoblasts
OC	- Osteoclasts
p38 MAPK	- p38 mitogen-activated protein kinase
P-gp	- P-glycoprotein
PI3k	- Phosphotidylinositidol-3-phosphate-kinase
PMF	- Peptide mass fingerprint
RANKL	- Receptor activator of NF-κB ligand
SDF-1a	- Stromal cell–derived factor –1a
TGF	- Transforming growth factor
TNF-α	- Tumour necrosis factor-α
VAD	- Vincristine, doxorubicin, and dexamethasone
VEGF	- Vascular endothelial growth factor

References

1. Knudson, A.G., *Two genetic hits (more or less) to cancer.* Nat Rev Cancer, 2001. **1**(2): p. 157-62.

2. Landgren, O., et al., *Monoclonal gammopathy of undetermined significance (MGUS) consistently precedes multiple myeloma: a prospective study.* Blood, 2009. **113**(22): p. 5412-7.
3. Rajkumar, S.V., et al., *Serum free light chain ratio is an independent risk factor for progression in monoclonal gammopathy of undetermined significance.* Blood, 2005. **106**(3): p. 812-7.
4. Kyle, R.A., et al., *A long-term study of prognosis in monoclonal gammopathy of undetermined significance.* N Engl J Med, 2002. **346**(8): p. 564-9.
5. Ries, L., et al., *SEER Cancer Statistics Review, 1975-2001*. 2004, Bethesda, MD, National Cancer Institute.
6. Malpas, J., et al., *Multiple myeloma: biology and management.* . 1998, Oxford: Oxford University Press.
7. Cohen, H., et al., *Racial differences in the prevalence of monoclonal gammopathy in a community-based sample of the elderly.* Am J Med, 1998(104): p. 439–44.
8. Munshi, N.C., *Plasma cell disorders: an historical perspective.* Hematology Am Soc Hematol Educ Program, 2008: p. 297.
9. Laubach, J.P., et al., *Novel therapies in the treatment of multiple myeloma.* J Natl Compr Canc Netw, 2009. **7**(9): p. 947-60.
10. Avet-Loiseau, H., et al., *Genetic abnormalities and survival in multiple myeloma: the experience of the Intergroupe Francophone du Myelome.* Blood, 2007. **109**(8): p. 3489-95.
11. Stewart, A.K., et al., *Diagnostic evaluation of t(4;14) in multiple myeloma and evidence for clonal evolution.* Leukemia, 2007. **21**(11): p. 2358-9.
12. Chng, W.J., et al., *Genetic events in the pathogenesis of multiple myeloma.* Best Pract Res Clin Haematol, 2007. **20**(4): p. 571-96.
13. Fonseca, R., et al., *Genetics and cytogenetics of multiple myeloma: a workshop report.* Cancer Res, 2004. **64**(4): p. 1546-58.
14. Bergsagel, D.E., et al., *Evaluation of new chemotherapeutic agents in the treatment of multiple myeloma. IV. L-Phenylalanine mustard (NSC-8806).* Cancer Chemother Rep, 1962. **21**: p. 87-99.
15. Mass, R.E., *A comparison of the effect of prednisone and a placebo in the treatment of multiple myeloma.* Cancer Chemother Rep, 1962. **16**: p. 257-9.
16. Alexanian, R., et al., *Treatment for multiple myeloma. Combination chemotherapy with different melphalan dose regimens.* JAMA, 1969. **208**(9): p. 1680-5.
17. Alexanian, R., B. Barlogie, and S. Tucker, *VAD-based regimens as primary treatment for multiple myeloma.* Am J Hematol, 1990. **33**(2): p. 86-9.
18. Barlogie, B., L. Smith, and R. Alexanian, *Effective treatment of advanced multiple myeloma refractory to alkylating agents.* N Engl J Med, 1984. **310**(21): p. 1353-6.
19. Barlogie, B., et al., *High-dose chemoradiotherapy and autologous bone marrow transplantation for resistant multiple myeloma.* Blood, 1987. **70**(3): p. 869-72.
20. Attal, M., et al., *A prospective, randomized trial of autologous bone marrow transplantation and chemotherapy in multiple myeloma. Intergroupe Francais du Myelome.* N Engl J Med, 1996. **335**(2): p. 91-7.
21. Attal, M., et al., *Single versus double autologous stem-cell transplantation for multiple myeloma.* N Engl J Med, 2003. **349**(26): p. 2495-502.
22. Barlogie, B., et al., *Total therapy with tandem transplants for newly diagnosed multiple myeloma.* Blood, 1999. **93**(1): p. 55-65.

23. Tricot, G., et al., *Graft-versus-myeloma effect: proof of principle.* Blood, 1996. **87**(3): p. 1196-8.
24. Verdonck, L.F., et al., *Graft-versus-myeloma effect in two cases.* Lancet, 1996. **347**(9004): p. 800-1.
25. Aschan, J., et al., *Graft-versus-myeloma effect.* Lancet, 1996. **348**(9023): p. 346.
26. Crawley, C., et al., *Reduced-intensity conditioning for myeloma: lower nonrelapse mortality but higher relapse rates compared with myeloablative conditioning.* Blood, 2007. **109**(8): p. 3588-94.
27. Hideshima, T., et al., *The proteasome inhibitor PS-341 inhibits growth, induces apoptosis, and overcomes drug resistance in human multiple myeloma cells.* Cancer Res, 2001. **61**(7): p. 3071-6.
28. Singhal, S., et al., *Antitumor activity of thalidomide in refractory multiple myeloma.* N Engl J Med, 1999. **341**(21): p. 1565-71.
29. Richardson, P.G., et al., *Immunomodulatory drug CC-5013 overcomes drug resistance and is well tolerated in patients with relapsed multiple myeloma.* Blood, 2002. **100**(9): p. 3063-7.
30. D'Amato, R.J., et al., *Thalidomide is an inhibitor of angiogenesis.* Proc Natl Acad Sci U S A, 1994. **91**(9): p. 4082-5.
31. Vacca, A., et al., *Bone marrow angiogenesis and progression in multiple myeloma.* Br J Haematol, 1994. **87**(3): p. 503-8.
32. Vacca, A., et al., *Bone marrow of patients with active multiple myeloma: angiogenesis and plasma cell adhesion molecules LFA-1, VLA-4, LAM-1, and CD44.* Am J Hematol, 1995. **50**(1): p. 9-14.
33. Barlogie, B., et al., *Extended survival in advanced and refractory multiple myeloma after single-agent thalidomide: identification of prognostic factors in a phase 2 study of 169 patients.* Blood, 2001. **98**(2): p. 492-4.
34. van Rhee, F., et al., *First thalidomide clinical trial in multiple myeloma: a decade.* Blood, 2008. **112**(4): p. 1035-8.
35. Dimopoulos, M.A., et al., *Thalidomide and dexamethasone combination for refractory multiple myeloma.* Ann Oncol, 2001. **12**(7): p. 991-5.
36. Lee, C.K., et al., *DTPACE: an effective, novel combination chemotherapy with thalidomide for previously treated patients with myeloma.* J Clin Oncol, 2003. **21**(14): p. 2732-9.
37. Offidani, M., et al., *Low-dose thalidomide with pegylated liposomal doxorubicin and high-dose dexamethasone for relapsed/refractory multiple myeloma: a prospective, multicenter, phase II study.* Haematologica, 2006. **91**(1): p. 133-6.
38. Adams, J., et al., *Proteasome inhibitors: a novel class of potent and effective antitumor agents.* Cancer Res, 1999. **59**(11): p. 2615-22.
39. Orlowski, R.Z., et al., *Tumor growth inhibition induced in a murine model of human Burkitt's lymphoma by a proteasome inhibitor.* Cancer Res, 1998. **58**(19): p. 4342-8.
40. Richardson, P.G., et al., *A phase 2 study of bortezomib in relapsed, refractory myeloma.* N Engl J Med, 2003. **348**(26): p. 2609-17.
41. Jagannath, S., et al., *A phase 2 study of two doses of bortezomib in relapsed or refractory myeloma.* Br J Haematol, 2004. **127**(2): p. 165-72.
42. Richardson, P.G., et al., *Bortezomib or high-dose dexamethasone for relapsed multiple myeloma.* N Engl J Med, 2005. **352**(24): p. 2487-98.
43. Richardson, P.G., et al., *Extended follow-up of a phase 3 trial in relapsed multiple myeloma: final time-to-event results of the APEX trial.* Blood, 2007. **110**(10): p. 3557-60.

44. Mitsiades, N., et al., *The proteasome inhibitor PS-341 potentiates sensitivity of multiple myeloma cells to conventional chemotherapeutic agents: therapeutic applications.* Blood, 2003. **101**(6): p. 2377-80.
45. Orlowski, R.Z., et al., *Phase 1 trial of the proteasome inhibitor bortezomib and pegylated liposomal doxorubicin in patients with advanced hematologic malignancies.* Blood, 2005. **105**(8): p. 3058-65.
46. Orlowski, R.Z., et al., *Randomized phase III study of pegylated liposomal doxorubicin plus bortezomib compared with bortezomib alone in relapsed or refractory multiple myeloma: combination therapy improves time to progression.* J Clin Oncol, 2007. **25**(25): p. 3892-901.
47. Palumbo, A., et al., *Bortezomib, doxorubicin and dexamethasone in advanced multiple myeloma.* Ann Oncol, 2008. **19**(6): p. 1160-5.
48. Weber, D.M., et al., *Lenalidomide plus dexamethasone for relapsed multiple myeloma in North America.* N Engl J Med, 2007. **357**(21): p. 2133-42.
49. Dimopoulos, M., et al., *Lenalidomide plus dexamethasone for relapsed or refractory multiple myeloma.* N Engl J Med, 2007. **357**(21): p. 2123-32.
50. Knop, S., et al., *Lenalidomide, adriamycin, and dexamethasone (RAD) in patients with relapsed and refractory multiple myeloma: a report from the German Myeloma Study Group DSMM (Deutsche Studiengruppe Multiples Myelom).* Blood, 2009. **113**(18): p. 4137-43.
51. Hideshima, T., et al., *Inhibition of Akt induces significant downregulation of survivin and cytotoxicity in human multiple myeloma cells.* Br J Haematol, 2007. **138**(6): p. 783-91.
52. Mitsiades, C.S., et al., *From the bench to the bedside: emerging new treatments in multiple myeloma.* Best Pract Res Clin Haematol, 2007. **20**(4): p. 797-816.
53. Mitsiades, C.S., et al., *Antimyeloma activity of heat shock protein-90 inhibition.* Blood, 2006. **107**(3): p. 1092-100.
54. Mitsiades, C.S., et al., *Transcriptional signature of histone deacetylase inhibition in multiple myeloma: biological and clinical implications.* Proc Natl Acad Sci U S A, 2004. **101**(2): p. 540-5.
55. Catley, L., et al., *Aggresome induction by proteasome inhibitor bortezomib and alpha-tubulin hyperacetylation by tubulin deacetylase (TDAC) inhibitor LBH589 are synergistic in myeloma cells.* Blood, 2006. **108**(10): p. 3441-9.
56. Richardson, P., et al., *Phase I trial of oral vorinostat (suberoylanilide hydroxamic acid, SAHA) in patients with advanced multiple myeloma.* Leuk Lymphoma, 2008. **49**(3): p. 502-7.
57. Mitsiades, C.S. and M. Koutsilieris, *Molecular biology and cellular physiology of refractoriness to androgen ablation therapy in advanced prostate cancer.* Expert Opin Investig Drugs, 2001. **10**(6): p. 1099-115.
58. van Kempen, L.C., et al., *The tumor microenvironment: a critical determinant of neoplastic evolution.* Eur J Cell Biol, 2003. **82**(11): p. 539-48.
59. Zhou, J., et al., *The role of the tumor microenvironment in hematological malignancies and implication for therapy.* Front Biosci, 2005. **10**: p. 1581-96.
60. Mitsiades, C.S., et al., *The role of the bone marrow microenvironment in the pathophysiology of myeloma and its significance in the development of more effective therapies.* Hematol Oncol Clin North Am, 2007. **21**(6): p. 1007-34, vii-viii.
61. Podar, K., D. Chauhan, and K.C. Anderson, *Bone marrow microenvironment and the identification of new targets for myeloma therapy.* Leukemia, 2009. **23**(1): p. 10-24.

62. Chauhan, D., et al., *Multiple myeloma cell adhesion-induced interleukin-6 expression in bone marrow stromal cells involves activation of NF-kappa B.* Blood, 1996. **87**(3): p. 1104-12.
63. Chauhan, D., et al., *Regulation of interleukin 6 in multiple myeloma and bone marrow stromal cells.* Stem Cells, 1995. **13 Suppl 2**: p. 35-9.
64. Uchiyama, H., et al., *Adhesion of human myeloma-derived cell lines to bone marrow stromal cells stimulates interleukin-6 secretion.* Blood, 1993. **82**(12): p. 3712-20.
65. Giuliani, N., V. Rizzoli, and G.D. Roodman, *Multiple myeloma bone disease: Pathophysiology of osteoblast inhibition.* Blood, 2006. **108**(13): p. 3992-6.
66. Chauhan, D., et al., *Identification of genes regulated by 2-methoxyestradiol (2ME2) in multiple myeloma cells using oligonucleotide arrays.* Blood, 2003. **101**(9): p. 3606-14.
67. Reimold, A.M., et al., *Plasma cell differentiation requires the transcription factor XBP-1.* Nature, 2001. **412**(6844): p. 300-7.
68. Carrasco, D.R., et al., *The differentiation and stress response factor XBP-1 drives multiple myeloma pathogenesis.* Cancer Cell, 2007. **11**(4): p. 349-60.
69. Le Gouill, S., et al., *Mcl-1 regulation and its role in multiple myeloma.* Cell Cycle, 2004. **3**(10): p. 1259-62.
70. Hideshima, T., et al., *Biologic sequelae of interleukin-6 induced PI3-K/Akt signaling in multiple myeloma.* Oncogene, 2001. **20**(42): p. 5991-6000.
71. Berger, L.C., et al., *Tyrosine phosphorylation of JAK-TYK kinases in malignant plasma cell lines growth-stimulated by interleukins 6 and 11.* Biochem Biophys Res Commun, 1994. **202**(1): p. 596-605.
72. Hideshima, T., et al., *Characterization of signaling cascades triggered by human interleukin-6 versus Kaposi's sarcoma-associated herpes virus-encoded viral interleukin 6.* Clin Cancer Res, 2000. **6**(3): p. 1180-9.
73. Lowik, C.W., et al., *Parathyroid hormone (PTH) and PTH-like protein (PLP) stimulate interleukin-6 production by osteogenic cells: a possible role of interleukin-6 in osteoclastogenesis.* Biochem Biophys Res Commun, 1989. **162**(3): p. 1546-52.
74. Bataille, R., et al., *Biologic effects of anti-interleukin-6 murine monoclonal antibody in advanced multiple myeloma.* Blood, 1995. **86**(2): p. 685-91.
75. Klein, B., et al., *Murine anti-interleukin-6 monoclonal antibody therapy for a patient with plasma cell leukemia.* Blood, 1991. **78**(5): p. 1198-204.
76. Lu, Z.Y., et al., *Measurement of whole body interleukin-6 (IL-6) production: prediction of the efficacy of anti-IL-6 treatments.* Blood, 1995. **86**(8): p. 3123-31.
77. Montero-Julian, F.A., et al., *Pharmacokinetic study of anti-interleukin-6 (IL-6) therapy with monoclonal antibodies: enhancement of IL-6 clearance by cocktails of anti-IL-6 antibodies.* Blood, 1995. **85**(4): p. 917-24.
78. Hankinson, S.E., et al., *Circulating concentrations of insulin-like growth factor-I and risk of breast cancer.* Lancet, 1998. **351**(9113): p. 1393-6.
79. Chan, J.M., et al., *Plasma insulin-like growth factor-I and prostate cancer risk: a prospective study.* Science, 1998. **279**(5350): p. 563-6.
80. LeRoith, D. and C.T. Roberts, Jr., *The insulin-like growth factor system and cancer.* Cancer Lett, 2003. **195**(2): p. 127-37.
81. Mitsiades, C.S. and N. Mitsiades, *Treatment of hematologic malignancies and solid tumors by inhibiting IGF receptor signaling.* Expert Rev Anticancer Ther, 2005. **5**(3): p. 487-99.

82. Garcia-Echeverria, C., et al., *In vivo antitumor activity of NVP-AEW541-A novel, potent, and selective inhibitor of the IGF-IR kinase.* Cancer Cell, 2004. **5**(3): p. 231-9.
83. Rajkumar, S.V. and R.A. Kyle, *Angiogenesis in multiple myeloma.* Semin Oncol, 2001. **28**(6): p. 560-4.
84. Podar, K. and K.C. Anderson, *The pathophysiologic role of VEGF in hematologic malignancies: therapeutic implications.* Blood, 2005. **105**(4): p. 1383-95.
85. Jakob, C., et al., *Angiogenesis in multiple myeloma.* Eur J Cancer, 2006. **42**(11): p. 1581-90.
86. Podar, K. and K.C. Anderson, *Inhibition of VEGF signaling pathways in multiple myeloma and other malignancies.* Cell Cycle, 2007. **6**(5): p. 538-42.
87. Tai, Y.T., et al., *Human anti-CD40 antagonist antibody triggers significant antitumor activity against human multiple myeloma.* Cancer Res, 2005. **65**(13): p. 5898-906.
88. Tai, Y.T., et al., *Mechanisms by which SGN-40, a humanized anti-CD40 antibody, induces cytotoxicity in human multiple myeloma cells: clinical implications.* Cancer Res, 2004. **64**(8): p. 2846-52.
89. Tai, Y.T., et al., *Immunomodulatory drug lenalidomide (CC-5013, IMiD3) augments anti-CD40 SGN-40-induced cytotoxicity in human multiple myeloma: clinical implications.* Cancer Res, 2005. **65**(24): p. 11712-20.
90. Silvestris, F., et al., *Impaired osteoblastogenesis in myeloma bone disease: role of upregulated apoptosis by cytokines and malignant plasma cells.* Br J Haematol, 2004. **126**(4): p. 475-86.
91. Hideshima, T., et al., *The role of tumor necrosis factor alpha in the pathophysiology of human multiple myeloma: therapeutic applications.* Oncogene, 2001. **20**(33): p. 4519-27.
92. Landowski, T.H., et al., *Cell adhesion-mediated drug resistance (CAM-DR) is associated with activation of NF-kappa B (RelB/p50) in myeloma cells.* Oncogene, 2003. **22**(16): p. 2417-21.
93. Moreaux, J., et al., *BAFF and APRIL protect myeloma cells from apoptosis induced by interleukin 6 deprivation and dexamethasone.* Blood, 2004. **103**(8): p. 3148-57.
94. Moreaux, J., et al., *TACI expression is associated with a mature bone marrow plasma cell signature and C-MAF overexpression in human myeloma cell lines.* Haematologica, 2007. **92**(6): p. 803-11.
95. Hideshima, T., et al., *The biological sequelae of stromal cell-derived factor-1alpha in multiple myeloma.* Mol Cancer Ther, 2002. **1**(7): p. 539-44.
96. Podar, K., et al., *GW654652, the pan-inhibitor of VEGF receptors, blocks the growth and migration of multiple myeloma cells in the bone marrow microenvironment.* Blood, 2004. **103**(9): p. 3474-9.
97. Hov, H., et al., *A selective c-met inhibitor blocks an autocrine hepatocyte growth factor growth loop in ANBL-6 cells and prevents migration and adhesion of myeloma cells.* Clin Cancer Res, 2004. **10**(19): p. 6686-94.
98. Asosingh, K., et al., *In vivo homing and differentiation characteristics of mature (CD45-) and immature (CD45+) 5T multiple myeloma cells.* Exp Hematol, 2001. **29**(1): p. 77-84.
99. Tai, Y.T., et al., *Insulin-like growth factor-1 induces adhesion and migration in human multiple myeloma cells via activation of beta1-integrin and phosphatidylinositol 3'-kinase/AKT signaling.* Cancer Res, 2003. **63**(18): p. 5850-8.

100. Hazlehurst, L.A., et al., *Adhesion to fibronectin via beta1 integrins regulates p27kip1 levels and contributes to cell adhesion mediated drug resistance (CAM-DR).* Oncogene, 2000. **19**(38): p. 4319-27.
101. Hazlehurst, L.A., et al., *Genotypic and phenotypic comparisons of de novo and acquired melphalan resistance in an isogenic multiple myeloma cell line model.* Cancer Res, 2003. **63**(22): p. 7900-6.
102. Barille, S., et al., *Metalloproteinases in multiple myeloma: production of matrix metalloproteinase-9 (MMP-9), activation of proMMP-2, and induction of MMP-1 by myeloma cells.* Blood, 1997. **90**(4): p. 1649-55.
103. Flomenberg, N., J. DiPersio, and G. Calandra, *Role of CXCR4 chemokine receptor blockade using AMD3100 for mobilization of autologous hematopoietic progenitor cells.* Acta Haematol, 2005. **114**(4): p. 198-205.
104. Werts, E.D., et al., *Characterization of marrow stromal (fibroblastoid) cells and their association with erythropoiesis.* Exp Hematol, 1980. **8**(4): p. 423-33.
105. Urashima, M., et al., *Transforming growth factor-beta1: differential effects on multiple myeloma versus normal B cells.* Blood, 1996. **87**(5): p. 1928-38.
106. Urashima, M., et al., *CD40 ligand triggered interleukin-6 secretion in multiple myeloma.* Blood, 1995. **85**(7): p. 1903-12.
107. Nefedova, Y., et al., *Involvement of Notch-1 signaling in bone marrow stroma-mediated de novo drug resistance of myeloma and other malignant lymphoid cell lines.* Blood, 2004. **103**(9): p. 3503-10.
108. Houde, C., et al., *Overexpression of the NOTCH ligand JAG2 in malignant plasma cells from multiple myeloma patients and cell lines.* Blood, 2004. **104**(12): p. 3697-704.
109. Jundt, F., et al., *Jagged1-induced Notch signaling drives proliferation of multiple myeloma cells.* Blood, 2004. **103**(9): p. 3511-5.
110. Gan, Z.H. and Y. Chen, *[Notch signaling pathway and multiple myeloma.].* Zhongguo Shi Yan Xue Ye Xue Za Zhi, 2009. **17**(5): p. 1380-3.
111. Zdzisinska, B., A. Walter-Croneck, and M. Kandefer-Szerszen, *Matrix metalloproteinases-1 and -2, and tissue inhibitor of metalloproteinase-2 production is abnormal in bone marrow stromal cells of multiple myeloma patients.* Leuk Res, 2008. **32**(11): p. 1763-9.
112. Kline, M., et al., *Cytokine and chemokine profiles in multiple myeloma; significance of stromal interaction and correlation of IL-8 production with disease progression.* Leuk Res, 2007. **31**(5): p. 591-8.
113. Vacca, A., et al., *Thalidomide downregulates angiogenic genes in bone marrow endothelial cells of patients with active multiple myeloma.* J Clin Oncol, 2005. **23**(23): p. 5334-46.
114. Roccaro, A.M., et al., *Bortezomib mediates antiangiogenesis in multiple myeloma via direct and indirect effects on endothelial cells.* Cancer Res, 2006. **66**(1): p. 184-91.
115. Bataille, R., et al., *Mechanisms of bone destruction in multiple myeloma: the importance of an unbalanced process in determining the severity of lytic bone disease.* J Clin Oncol, 1989. **7**(12): p. 1909-14.
116. Esteve, F.R. and G.D. Roodman, *Pathophysiology of myeloma bone disease.* Best Pract Res Clin Haematol, 2007. **20**(4): p. 613-24.
117. Terpos, E., et al., *Myeloma bone disease and proteasome inhibition therapies.* Blood, 2007. **110**(4): p. 1098-104.
118. Hofbauer, L.C. and M. Schoppet, *Clinical implications of the osteoprotegerin/RANKL/RANK system for bone and vascular diseases.* JAMA, 2004. **292**(4): p. 490-5.

119. Choi, S.J., et al., *Antisense inhibition of macrophage inflammatory protein 1-alpha blocks bone destruction in a model of myeloma bone disease.* J Clin Invest, 2001. **108**(12): p. 1833-41.
120. Choi, S.J., et al., *Macrophage inflammatory protein 1-alpha is a potential osteoclast stimulatory factor in multiple myeloma.* Blood, 2000. **96**(2): p. 671-5.
121. Oba, Y., et al., *MIP-1alpha utilizes both CCR1 and CCR5 to induce osteoclast formation and increase adhesion of myeloma cells to marrow stromal cells.* Exp Hematol, 2005. **33**(3): p. 272-8.
122. Franchimont, N., S. Rydziel, and E. Canalis, *Transforming growth factor-beta increases interleukin-6 transcripts in osteoblasts.* Bone, 2000. **26**(3): p. 249-53.
123. Nguyen, A.N., et al., *Normalizing the bone marrow microenvironment with p38 inhibitor reduces multiple myeloma cell proliferation and adhesion and suppresses osteoclast formation.* Exp Cell Res, 2006. **312**(10): p. 1909-23.
124. Breitkreutz, I., et al., *Lenalidomide inhibits osteoclastogenesis, survival factors and bone-remodeling markers in multiple myeloma.* Leukemia, 2008. **22**(10): p. 1925-32.
125. Breitkreutz, I., et al., *Targeting MEK1/2 blocks osteoclast differentiation, function and cytokine secretion in multiple myeloma.* Br J Haematol, 2007. **139**(1): p. 55-63.
126. Vallet, S., et al., *MLN3897, a novel CCR1 inhibitor, impairs osteoclastogenesis and inhibits the interaction of multiple myeloma cells and osteoclasts.* Blood, 2007. **110**(10): p. 3744-52.
127. Feng, R., et al., *The histone deacetylase inhibitor, PXD101, potentiates bortezomib-induced anti-multiple myeloma effect by induction of oxidative stress and DNA damage.* Br J Haematol, 2007. **139**(3): p. 385-97.
128. Boissy, P., et al., *Resveratrol inhibits myeloma cell growth, prevents osteoclast formation, and promotes osteoblast differentiation.* Cancer Res, 2005. **65**(21): p. 9943-52.
129. Feng, R., et al., *SDX-308, a nonsteroidal anti-inflammatory agent, inhibits NF-kappaB activity, resulting in strong inhibition of osteoclast formation/activity and multiple myeloma cell growth.* Blood, 2007. **109**(5): p. 2130-8.
130. Karsenty, G., et al., *Cbfa1 as a regulator of osteoblast differentiation and function.* Bone, 1999. **25**(1): p. 107-8.
131. Tian, E., et al., *The role of the Wnt-signaling antagonist DKK1 in the development of osteolytic lesions in multiple myeloma.* N Engl J Med, 2003. **349**(26): p. 2483-94.
132. Oshima, T., et al., *Myeloma cells suppress bone formation by secreting a soluble Wnt inhibitor, sFRP-2.* Blood, 2005. **106**(9): p. 3160-5.
133. Fujita, K. and S. Janz, *Attenuation of WNT signaling by DKK-1 and -2 regulates BMP2-induced osteoblast differentiation and expression of OPG, RANKL and M-CSF.* Mol Cancer, 2007. **6**: p. 71.
134. Ehrlich, L.A., et al., *IL-3 is a potential inhibitor of osteoblast differentiation in multiple myeloma.* Blood, 2005. **106**(4): p. 1407-14.
135. Standal, T., et al., *HGF inhibits BMP-induced osteoblastogenesis: possible implications for the bone disease of multiple myeloma.* Blood, 2007. **109**(7): p. 3024-30.
136. Yang, H.H., et al., *Overcoming drug resistance in multiple myeloma: the emergence of therapeutic approaches to induce apoptosis.* J Clin Oncol, 2003. **21**(22): p. 4239-47.
137. Sharom, F.J., *ABC multidrug transporters: structure, function and role in chemoresistance.* Pharmacogenomics, 2008. **9**(1): p. 105-27.

138. Krishna, R. and L.D. Mayer, *Multidrug resistance (MDR) in cancer. Mechanisms, reversal using modulators of MDR and the role of MDR modulators in influencing the pharmacokinetics of anticancer drugs.* Eur J Pharm Sci, 2000. **11**(4): p. 265-83.
139. Hyafil, F., et al., *In vitro and in vivo reversal of multidrug resistance by GF120918, an acridonecarboxamide derivative.* Cancer Res, 1993. **53**(19): p. 4595-602.
140. Dantzig, A.H., et al., *Reversal of P-glycoprotein-mediated multidrug resistance by a potent cyclopropyldibenzosuberane modulator, LY335979.* Cancer Res, 1996. **56**(18): p. 4171-9.
141. Dale, I.L., et al., *Reversal of P-glycoprotein-mediated multidrug resistance by XR9051, a novel diketopiperazine derivative.* Br J Cancer, 1998. **78**(7): p. 885-92.
142. Newman, M.J., et al., *Discovery and characterization of OC144-093, a novel inhibitor of P-glycoprotein-mediated multidrug resistance.* Cancer Res, 2000. **60**(11): p. 2964-72.
143. Pusztai, L., et al., *Phase II study of tariquidar, a selective P-glycoprotein inhibitor, in patients with chemotherapy-resistant, advanced breast carcinoma.* Cancer, 2005. **104**(4): p. 682-91.
144. Fromm, M.F., *Importance of P-glycoprotein at blood-tissue barriers.* Trends Pharmacol Sci, 2004. **25**(8): p. 423-9.
145. van Tellingen, O., et al., *P-glycoprotein and Mrp1 collectively protect the bone marrow from vincristine-induced toxicity in vivo.* Br J Cancer, 2003. **89**(9): p. 1776-82.
146. Grogan, T.M., et al., *P-glycoprotein expression in human plasma cell myeloma: correlation with prior chemotherapy.* Blood, 1993. **81**(2): p. 490-5.
147. Sonneveld, P., et al., *Cyclosporin A combined with vincristine, doxorubicin and dexamethasone (VAD) compared with VAD alone in patients with advanced refractory multiple myeloma: an EORTC-HOVON randomized phase III study (06914).* Br J Haematol, 2001. **115**(4): p. 895-902.
148. Dalton, W.S., et al., *A phase III randomized study of oral verapamil as a chemosensitizer to reverse drug resistance in patients with refractory myeloma. A Southwest Oncology Group study.* Cancer, 1995. **75**(3): p. 815-20.
149. Friedenberg, W.R., et al., *Phase III study of PSC-833 (valspodar) in combination with vincristine, doxorubicin, and dexamethasone (valspodar/VAD) versus VAD alone in patients with recurring or refractory multiple myeloma (E1A95): a trial of the Eastern Cooperative Oncology Group.* Cancer, 2006. **106**(4): p. 830-8.
150. Rumpold, H., et al., *Knockdown of PgP resensitizes leukemic cells to proteasome inhibitors.* Biochem Biophys Res Commun, 2007. **361**(2): p. 549-54.
151. Loo, T.W. and D.M. Clarke, *The human multidrug resistance P-glycoprotein is inactive when its maturation is inhibited: potential for a role in cancer chemotherapy.* FASEB J, 1999. **13**(13): p. 1724-32.
152. Fardel, O., et al., *Physiological, pharmacological and clinical features of the multidrug resistance protein 2.* Biomed Pharmacother, 2005. **59**(3): p. 104-14.
153. Leslie, E.M., R.G. Deeley, and S.P. Cole, *Multidrug resistance proteins: role of P-glycoprotein, MRP1, MRP2, and BCRP (ABCG2) in tissue defense.* Toxicol Appl Pharmacol, 2005. **204**(3): p. 216-37.
154. Hipfner, D.R., R.G. Deeley, and S.P. Cole, *Structural, mechanistic and clinical aspects of MRP1.* Biochim Biophys Acta, 1999. **1461**(2): p. 359-76.

155. Boumendjel, A., et al., *Anticancer multidrug resistance mediated by MRP1: recent advances in the discovery of reversal agents.* Med Res Rev, 2005. **25**(4): p. 453-72.
156. Doyle, L.A., et al., *A multidrug resistance transporter from human MCF-7 breast cancer cells.* Proc Natl Acad Sci U S A, 1998. **95**(26): p. 15665-70.
157. Allikmets, R., et al., *A human placenta-specific ATP-binding cassette gene (ABCP) on chromosome 4q22 that is involved in multidrug resistance.* Cancer Res, 1998. **58**(23): p. 5337-9.
158. Staud, F. and P. Pavek, *Breast cancer resistance protein (BCRP/ABCG2).* Int J Biochem Cell Biol, 2005. **37**(4): p. 720-5.
159. Diestra, J.E., et al., *Frequent expression of the multi-drug resistance-associated protein BCRP/MXR/ABCP/ABCG2 in human tumours detected by the BXP-21 monoclonal antibody in paraffin-embedded material.* J Pathol, 2002. **198**(2): p. 213-9.
160. Steinbach, D. and O. Legrand, *ABC transporters and drug resistance in leukemia: was P-gp nothing but the first head of the Hydra?* Leukemia, 2007. **21**(6): p. 1172-6.
161. Sugimoto, Y., et al., *Breast cancer resistance protein: molecular target for anticancer drug resistance and pharmacokinetics/pharmacodynamics.* Cancer Sci, 2005. **96**(8): p. 457-65.
162. Koshland, D.E., Jr., *Molecule of the year.* Science, 1993. **262**(5142): p. 1953.
163. Junttila, M.R. and G.I. Evan, *p53--a Jack of all trades but master of none.* Nat Rev Cancer, 2009. **9**(11): p. 821-9.
164. Iwakuma, T. and G. Lozano, *MDM2, an introduction.* Mol Cancer Res, 2003. **1**(14): p. 993-1000.
165. Momand, J., et al., *The mdm-2 oncogene product forms a complex with the p53 protein and inhibits p53-mediated transactivation.* Cell, 1992. **69**(7): p. 1237-45.
166. Vogelstein, B. and K.W. Kinzler, *Cancer genes and the pathways they control.* Nat Med, 2004. **10**(8): p. 789-99.
167. Jones, S.N., et al., *Rescue of embryonic lethality in Mdm2-deficient mice by absence of p53.* Nature, 1995. **378**(6553): p. 206-8.
168. Montes de Oca Luna, R., D.S. Wagner, and G. Lozano, *Rescue of early embryonic lethality in mdm2-deficient mice by deletion of p53.* Nature, 1995. **378**(6553): p. 203-6.
169. Francoz, S., et al., *Mdm4 and Mdm2 cooperate to inhibit p53 activity in proliferating and quiescent cells in vivo.* Proc Natl Acad Sci U S A, 2006. **103**(9): p. 3232-7.
170. Marine, J.C., et al., *Keeping p53 in check: essential and synergistic functions of Mdm2 and Mdm4.* Cell Death Differ, 2006. **13**(6): p. 927-34.
171. Hainaut, P. and M. Hollstein, *p53 and human cancer: the first ten thousand mutations.* Adv Cancer Res, 2000. **77**: p. 81-137.
172. Secchiero, P., et al., *The MDM2 inhibitor Nutlins as an innovative therapeutic tool for the treatment of haematological malignancies.* Curr Pharm Des, 2008. **14**(21): p. 2100-10.
173. Loiseau, H.A., et al., *Induction with Velcade®/Dexamethasone Partially Overcomes the Poor Prognosis of t(4;14), but Not That of Del(17p), in Young Patients with Multiple Myeloma.* Blood, 2009. **114**(22).
174. Song, H., M. Hollstein, and Y. Xu, *p53 gain-of-function cancer mutants induce genetic instability by inactivating ATM.* Nat Cell Biol, 2007. **9**(5): p. 573-80.
175. Xu, Y., *Induction of genetic instability by gain-of-function p53 cancer mutants.* Oncogene, 2008. **27**(25): p. 3501-7.

176. Fakharzadeh, S.S., S.P. Trusko, and D.L. George, *Tumorigenic potential associated with enhanced expression of a gene that is amplified in a mouse tumor cell line.* EMBO J, 1991. **10**(6): p. 1565-9.
177. Vassilev, L.T., et al., *In vivo activation of the p53 pathway by small-molecule antagonists of MDM2.* Science, 2004. **303**(5659): p. 844-8.
178. Kojima, K., et al., *Mdm2 inhibitor Nutlin-3a induces p53-mediated apoptosis by transcription-dependent and transcription-independent mechanisms and may overcome Atm-mediated resistance to fludarabine in chronic lymphocytic leukemia.* Blood, 2006. **108**(3): p. 993-1000.
179. Stuhmer, T., et al., *Nongenotoxic activation of the p53 pathway as a therapeutic strategy for multiple myeloma.* Blood, 2005. **106**(10): p. 3609-17.
180. Tovar, C., et al., *Small-molecule MDM2 antagonists reveal aberrant p53 signaling in cancer: implications for therapy.* Proc Natl Acad Sci U S A, 2006. **103**(6): p. 1888-93.
181. Ambrosini, G., et al., *Mouse double minute antagonist Nutlin-3a enhances chemotherapy-induced apoptosis in cancer cells with mutant p53 by activating E2F1.* Oncogene, 2007. **26**(24): p. 3473-81.
182. Secchiero, P., et al., *The MDM-2 antagonist nutlin-3 promotes the maturation of acute myeloid leukemic blasts.* Neoplasia, 2007. **9**(10): p. 853-61.
183. Hallstrom, T.C., S. Mori, and J.R. Nevins, *An E2F1-dependent gene expression program that determines the balance between proliferation and cell death.* Cancer Cell, 2008. **13**(1): p. 11-22.
184. Lau, L.M., et al., *HDM2 antagonist Nutlin-3 disrupts p73-HDM2 binding and enhances p73 function.* Oncogene, 2008. **27**(7): p. 997-1003.
185. Secchiero, P., et al., *Functional integrity of the p53-mediated apoptotic pathway induced by the nongenotoxic agent nutlin-3 in B-cell chronic lymphocytic leukemia (B-CLL).* Blood, 2006. **107**(10): p. 4122-9.
186. Coll-Mulet, L., et al., *MDM2 antagonists activate p53 and synergize with genotoxic drugs in B-cell chronic lymphocytic leukemia cells.* Blood, 2006. **107**(10): p. 4109-14.
187. Secchiero, P., et al., *Synergistic cytotoxic activity of recombinant TRAIL plus the non-genotoxic activator of the p53 pathway nutlin-3 in acute myeloid leukemia cells.* Curr Drug Metab, 2007. **8**(4): p. 395-403.
188. Kojima, K., et al., *MDM2 antagonists induce p53-dependent apoptosis in AML: implications for leukemia therapy.* Blood, 2005. **106**(9): p. 3150-9.
189. Drakos, E., et al., *Inhibition of p53-murine double minute 2 interaction by nutlin-3A stabilizes p53 and induces cell cycle arrest and apoptosis in Hodgkin lymphoma.* Clin Cancer Res, 2007. **13**(11): p. 3380-7.
190. San Miguel, J.F., et al., *Bortezomib plus melphalan and prednisone for initial treatment of multiple myeloma.* N Engl J Med, 2008. **359**(9): p. 906-17.
191. Hardie, D.G., *Minireview: the AMP-activated protein kinase cascade: the key sensor of cellular energy status.* Endocrinology, 2003. **144**(12): p. 5179-83.
192. Kemp, B.E., et al., *AMP-activated protein kinase, super metabolic regulator.* Biochem Soc Trans, 2003. **31**(Pt 1): p. 162-8.
193. Mehenni, H., et al., *Loss of LKB1 kinase activity in Peutz-Jeghers syndrome, and evidence for allelic and locus heterogeneity.* Am J Hum Genet, 1998. **63**(6): p. 1641-50.
194. Ylikorkala, A., et al., *Mutations and impaired function of LKB1 in familial and non-familial Peutz-Jeghers syndrome and a sporadic testicular cancer.* Hum Mol Genet, 1999. **8**(1): p. 45-51.

195. Tiainen, M., et al., *Growth arrest by the LKB1 tumor suppressor: induction of p21(WAF1/CIP1).* Hum Mol Genet, 2002. **11**(13): p. 1497-504.
196. Kyriakis, J.M., *At the crossroads: AMP-activated kinase and the LKB1 tumor suppressor link cell proliferation to metabolic regulation.* J Biol, 2003. **2**(4): p. 26.
197. Hardie, D.G., *The AMP-activated protein kinase pathway--new players upstream and downstream.* J Cell Sci, 2004. **117**(Pt 23): p. 5479-87.
198. Bolster, D.R., et al., *AMP-activated protein kinase suppresses protein synthesis in rat skeletal muscle through down-regulated mammalian target of rapamycin (mTOR) signaling.* J Biol Chem, 2002. **277**(27): p. 23977-80.
199. Kimura, N., et al., *A possible linkage between AMP-activated protein kinase (AMPK) and mammalian target of rapamycin (mTOR) signalling pathway.* Genes Cells, 2003. **8**(1): p. 65-79.
200. Krause, U., L. Bertrand, and L. Hue, *Control of p70 ribosomal protein S6 kinase and acetyl-CoA carboxylase by AMP-activated protein kinase and protein phosphatases in isolated hepatocytes.* Eur J Biochem, 2002. **269**(15): p. 3751-9.
201. Inoki, K., T. Zhu, and K.L. Guan, *TSC2 mediates cellular energy response to control cell growth and survival.* Cell, 2003. **115**(5): p. 577-90.
202. Cheng, S.W., et al., *Thr2446 is a novel mammalian target of rapamycin (mTOR) phosphorylation site regulated by nutrient status.* J Biol Chem, 2004. **279**(16): p. 15719-22.
203. Fingar, D.C., et al., *Mammalian cell size is controlled by mTOR and its downstream targets S6K1 and 4EBP1/eIF4E.* Genes Dev, 2002. **16**(12): p. 1472-87.
204. Schmelzle, T. and M.N. Hall, *TOR, a central controller of cell growth.* Cell, 2000. **103**(2): p. 253-62.
205. Carrera, A.C., *TOR signaling in mammals.* J Cell Sci, 2004. **117**(Pt 20): p. 4615-6.
206. Hideshima, T., et al., *Cytokines and signal transduction.* Best Pract Res Clin Haematol, 2005. **18**(4): p. 509-24.
207. Descamps, G., et al., *The magnitude of Akt/phosphatidylinositol 3'-kinase proliferating signaling is related to CD45 expression in human myeloma cells.* J Immunol, 2004. **173**(8): p. 4953-9.
208. Lu, Y., H. Wang, and G.B. Mills, *Targeting PI3K-AKT pathway for cancer therapy.* Rev Clin Exp Hematol, 2003. **7**(2): p. 205-28.
209. Toker, A. and M. Yoeli-Lerner, *Akt signaling and cancer: surviving but not moving on.* Cancer Res, 2006. **66**(8): p. 3963-6.
210. Martelli, A.M., et al., *Phosphoinositide 3-kinase/Akt signaling pathway and its therapeutical implications for human acute myeloid leukemia.* Leukemia, 2006. **20**(6): p. 911-28.
211. Hideshima, T., et al., *Perifosine, an oral bioactive novel alkylphospholipid, inhibits Akt and induces in vitro and in vivo cytotoxicity in human multiple myeloma cells.* Blood, 2006. **107**(10): p. 4053-62.
212. McMillin, D.W., et al., *Antimyeloma activity of the orally bioavailable dual phosphatidylinositol 3-kinase/mammalian target of rapamycin inhibitor NVP-BEZ235.* Cancer Res, 2009. **69**(14): p. 5835-42.
213. Baumann, P., et al., *The novel orally bioavailable inhibitor of phosphoinositol-3-kinase and mammalian target of rapamycin, NVP-BEZ235, inhibits growth and proliferation in multiple myeloma.* Exp Cell Res, 2009. **315**(3): p. 485-97.

214. Pene, F., et al., *Role of the phosphatidylinositol 3-kinase/Akt and mTOR/P70S6-kinase pathways in the proliferation and apoptosis in multiple myeloma.* Oncogene, 2002. **21**(43): p. 6587-97.
215. Kristiansen, S.B., et al., *5-Aminoimidazole-4-carboxamide-1-beta-D-ribofuranoside increases myocardial glucose uptake during reperfusion and induces late pre-conditioning: potential role of AMP-activated protein kinase.* Basic Clin Pharmacol Toxicol, 2009. **105**(1): p. 10-6.
216. Russell, R.R., 3rd, et al., *AMP-activated protein kinase mediates ischemic glucose uptake and prevents postischemic cardiac dysfunction, apoptosis, and injury.* J Clin Invest, 2004. **114**(4): p. 495-503.
217. Ido, Y., D. Carling, and N. Ruderman, *Hyperglycemia-induced apoptosis in human umbilical vein endothelial cells: inhibition by the AMP-activated protein kinase activation.* Diabetes, 2002. **51**(1): p. 159-67.
218. Stefanelli, C., et al., *Inhibition of glucocorticoid-induced apoptosis with 5-aminoimidazole-4-carboxamide ribonucleoside, a cell-permeable activator of AMP-activated protein kinase.* Biochem Biophys Res Commun, 1998. **243**(3): p. 821-6.
219. Rattan, R., et al., *5-Aminoimidazole-4-carboxamide-1-beta-D-ribofuranoside inhibits cancer cell proliferation in vitro and in vivo via AMP-activated protein kinase.* J Biol Chem, 2005. **280**(47): p. 39582-93.
220. Evans, J.M., et al., *Metformin and reduced risk of cancer in diabetic patients.* BMJ, 2005. **330**(7503): p. 1304-5.
221. Bowker, S.L., et al., *Increased cancer-related mortality for patients with type 2 diabetes who use sulfonylureas or insulin.* Diabetes Care, 2006. **29**(2): p. 254-8.
222. Wright, J.L. and J.L. Stanford, *Metformin use and prostate cancer in Caucasian men: results from a population-based case-control study.* Cancer Causes Control, 2009. **20**(9): p. 1617-22.
223. Bodmer, M., et al., *Long-term metformin use is associated with decreased risk of breast cancer.* Diabetes Care. **33**(6): p. 1304-8.
224. Jiralerspong, S., et al., *Metformin and pathologic complete responses to neoadjuvant chemotherapy in diabetic patients with breast cancer.* J Clin Oncol, 2009. **27**(20): p. 3297-302.
225. Ben Sahra, I., et al., *The antidiabetic drug metformin exerts an antitumoral effect in vitro and in vivo through a decrease of cyclin D1 level.* Oncogene, 2008. **27**(25): p. 3576-86.
226. Buzzai, M., et al., *Systemic treatment with the antidiabetic drug metformin selectively impairs p53-deficient tumor cell growth.* Cancer Res, 2007. **67**(14): p. 6745-52.
227. Cantrell, L.A., et al., *Metformin is a potent inhibitor of endometrial cancer cell proliferation-implications for a novel treatment strategy.* Gynecol Oncol, 2009.
228. Rattan, R., et al., *Metformin attenuates ovarian cancer cell growth in an AMP-kinase dispensable manner.* J Cell Mol Med, 2009.
229. Wang, L.W., et al., *Metformin induces apoptosis of pancreatic cancer cells.* World J Gastroenterol, 2008. **14**(47): p. 7192-8.
230. Zakikhani, M., et al., *Metformin is an AMP kinase-dependent growth inhibitor for breast cancer cells.* Cancer Res, 2006. **66**(21): p. 10269-73.
231. Corton, J.M., et al., *5-aminoimidazole-4-carboxamide ribonucleoside. A specific method for activating AMP-activated protein kinase in intact cells?* Eur J Biochem, 1995. **229**(2): p. 558-65.

232. Imamura, K., et al., *Cell cycle regulation via p53 phosphorylation by a 5'-AMP activated protein kinase activator, 5-aminoimidazole- 4-carboxamide-1-beta-D-ribofuranoside, in a human hepatocellular carcinoma cell line.* Biochem Biophys Res Commun, 2001. **287**(2): p. 562-7.
233. Jones, R.G., et al., *AMP-activated protein kinase induces a p53-dependent metabolic checkpoint.* Mol Cell, 2005. **18**(3): p. 283-93.
234. Igata, M., et al., *Adenosine monophosphate-activated protein kinase suppresses vascular smooth muscle cell proliferation through the inhibition of cell cycle progression.* Circ Res, 2005. **97**(8): p. 837-44.
235. Baumann, P., et al., *Activation of adenosine monophosphate activated protein kinase inhibits growth of multiple myeloma cells.* Exp Cell Res, 2007. **313**(16): p. 3592-603.
236. Xiang, X., et al., *AMP-activated protein kinase activators can inhibit the growth of prostate cancer cells by multiple mechanisms.* Biochem Biophys Res Commun, 2004. **321**(1): p. 161-7.
237. Saitoh, M., et al., *Adenosine induces apoptosis in the human gastric cancer cells via an intrinsic pathway relevant to activation of AMP-activated protein kinase.* Biochem Pharmacol, 2004. **67**(10): p. 2005-11.
238. Kefas, B.A., et al., *AICA-riboside induces apoptosis of pancreatic beta cells through stimulation of AMP-activated protein kinase.* Diabetologia, 2003. **46**(2): p. 250-4.
239. Meisse, D., et al., *Sustained activation of AMP-activated protein kinase induces c-Jun N-terminal kinase activation and apoptosis in liver cells.* FEBS Lett, 2002. **526**(1-3): p. 38-42.
240. Jung, J.E., et al., *5-Aminoimidazole-4-carboxamide-ribonucleoside enhances oxidative stress-induced apoptosis through activation of nuclear factor-kappaB in mouse Neuro 2a neuroblastoma cells.* Neurosci Lett, 2004. **354**(3): p. 197-200.
241. Meri, S. and M. Baumann, *Proteomics: posttranslational modifications, immune responses and current analytical tools.* Biomol Eng, 2001. **18**(5): p. 213-20.
242. Poly, W.J., *Nongenetic variation, genetic-environmental interactions and altered gene expression. III. Posttranslational modifications.* Comp Biochem Physiol A Physiol, 1997. **118**(3): p. 551-72.
243. Graves, P.R. and T.A. Haystead, *Molecular biologist's guide to proteomics.* Microbiol Mol Biol Rev, 2002. **66**(1): p. 39-63; table of contents.
244. Yates, J.R., 3rd, *Mass spectrometry. From genomics to proteomics.* Trends Genet, 2000. **16**(1): p. 5-8.
245. Blackstock, W.P. and M.P. Weir, *Proteomics: quantitative and physical mapping of cellular proteins.* Trends Biotechnol, 1999. **17**(3): p. 121-7.
246. Deng, M., et al., *Mapping Gene Ontology to proteins based on protein-protein interaction data.* Bioinformatics, 2004. **20**(6): p. 895-902.
247. Shen, D.W., et al., *Multiple drug-resistant human KB carcinoma cells independently selected for high-level resistance to colchicine, adriamycin, or vinblastine show changes in expression of specific proteins.* J Biol Chem, 1986. **261**(17): p. 7762-70.
248. Sinha, P., et al., *Increased expression of annexin I and thioredoxin detected by two-dimensional gel electrophoresis of drug resistant human stomach cancer cells.* J Biochem Biophys Methods, 1998. **37**(3): p. 105-16.
249. Wang, Y., et al., *Proteomic approach to study the cytotoxicity of dioscin (saponin).* Proteomics, 2006. **6**(8): p. 2422-32.

250. Wang, Y., J.F. Chiu, and Q.Y. He, *Proteomics approach to illustrate drug action mechanisms.* Curr Drug Discov Technol, 2006. **3**(3): p. 199-209.
251. Wang, Y., et al., *Modulation of gold(III) porphyrin 1a-induced apoptosis by mitogen-activated protein kinase signaling pathways.* Biochem Pharmacol, 2008. **75**(6): p. 1282-91.
252. Ge, F., et al., *Proteomic and functional analyses reveal a dual molecular mechanism underlying arsenic-induced apoptosis in human multiple myeloma cells.* J Proteome Res, 2009. **8**(6): p. 3006-19.
253. Rees-Unwin, K.S., et al., *Proteomic evaluation of pathways associated with dexamethasone-mediated apoptosis and resistance in multiple myeloma.* Br J Haematol, 2007. **139**(4): p. 559-67.
254. Pratt, W.B. and D.O. Toft, *Steroid receptor interactions with heat shock protein and immunophilin chaperones.* Endocr Rev, 1997. **18**(3): p. 306-60.
255. Weinkauf, M., et al., *2-D PAGE-based comparison of proteasome inhibitor bortezomib in sensitive and resistant mantle cell lymphoma.* Electrophoresis, 2009. **30**(6): p. 974-86.
256. Loeffler-Ragg, J., et al., *Proteomic identification of aldo-keto reductase AKR1B10 induction after treatment of colorectal cancer cells with the proteasome inhibitor bortezomib.* Mol Cancer Ther, 2009. **8**(7): p. 1995-2006.
257. Sinha, P., et al., *Increased expression of epidermal fatty acid binding protein, cofilin, and 14-3-3-sigma (stratifin) detected by two-dimensional gel electrophoresis, mass spectrometry and microsequencing of drug-resistant human adenocarcinoma of the pancreas.* Electrophoresis, 1999. **20**(14): p. 2952-60.
258. Sinha, P., et al., *Search for novel proteins involved in the development of chemoresistance in colorectal cancer and fibrosarcoma cells in vitro using two-dimensional electrophoresis, mass spectrometry and microsequencing.* Electrophoresis, 1999. **20**(14): p. 2961-9.
259. Yoo, B.C., et al., *Metabotropic glutamate receptor 4-mediated 5-Fluorouracil resistance in a human colon cancer cell line.* Clin Cancer Res, 2004. **10**(12 Pt 1): p. 4176-84.
260. Shin, Y.K., et al., *Down-regulation of mitochondrial F1F0-ATP synthase in human colon cancer cells with induced 5-fluorouracil resistance.* Cancer Res, 2005. **65**(8): p. 3162-70.
261. Sinha, P., et al., *Identification of novel proteins associated with the development of chemoresistance in malignant melanoma using two-dimensional electrophoresis.* Electrophoresis, 2000. **21**(14): p. 3048-57.
262. Urbani, A., et al., *A proteomic investigation into etoposide chemo-resistance of neuroblastoma cell lines.* Proteomics, 2005. **5**(3): p. 796-804.
263. Yoo, B.C., et al., *Decreased pyruvate kinase M2 activity linked to cisplatin resistance in human gastric carcinoma cell lines.* Int J Cancer, 2004. **108**(4): p. 532-9.
264. Hathout, Y., et al., *Differential protein expression in the cytosol fraction of an MCF-7 breast cancer cell line selected for resistance toward melphalan.* J Proteome Res, 2002. **1**(5): p. 435-42.
265. Gehrmann, M.L., C. Fenselau, and Y. Hathout, *Highly altered protein expression profile in the adriamycin resistant MCF-7 cell line.* J Proteome Res, 2004. **3**(3): p. 403-9.
266. Smith, L., et al., *Cancer proteomics and its application to discovery of therapy response markers in human cancer.* Cancer, 2006. **107**(2): p. 232-41.

267. Martin, A. and M. Clynes, *Acid phosphatase: endpoint for in vitro toxicity tests.* In Vitro Cell Dev Biol, 1991. **27A**(3 Pt 1): p. 183-4.
268. Jakubikova, J., Y. Bao, and J. Sedlak, *Isothiocyanates induce cell cycle arrest, apoptosis and mitochondrial potential depolarization in HL-60 and multidrug-resistant cell lines.* Anticancer Res, 2005. **25**(5): p. 3375-86.
269. Mulligan, G., et al., *Gene expression profiling and correlation with outcome in clinical trials of the proteasome inhibitor bortezomib.* Blood, 2007. **109**(8): p. 3177-88.
270. Chou, T.C. and P. Talalay, *Trends in Pharmacological Sciences*. Vol. 4. 1983.
271. Chou, T.C. and P. Talalay, *Quantitative analysis of dose-effect relationships: the combined effects of multiple drugs or enzyme inhibitors.* Adv Enzyme Regul, 1984. **22**: p. 27-55.
272. Duffy, C.P., et al., *Enhancement of chemotherapeutic drug toxicity to human tumour cells in vitro by a subset of non-steroidal anti-inflammatory drugs (NSAIDs).* Eur J Cancer, 1998. **34**(8): p. 1250-9.
273. Clynes, M., et al., *Multiple drug-resistance in variant of a human non-small cell lung carcinoma cell line, DLKP-A.* Cytotechnology, 1992. **10**(1): p. 75-89.
274. Imai, Y., et al., *C421A polymorphism in the human breast cancer resistance protein gene is associated with low expression of Q141K protein and low-level drug resistance.* Mol Cancer Ther, 2002. **1**(8): p. 611-6.
275. Collins, D.M., et al., *Tyrosine kinase inhibitors potentiate the cytotoxicity of MDR-substrate anticancer agents independent of growth factor receptor status in lung cancer cell lines.* Invest New Drugs, 2009.
276. Roovers, D.J., et al., *Idarubicin overcomes P-glycoprotein-related multidrug resistance: comparison with doxorubicin and daunorubicin in human multiple myeloma cell lines.* Leuk Res, 1999. **23**(6): p. 539-48.
277. Sarver, J.G., et al., *Microplate screening of the differential effects of test agents on Hoechst 33342, rhodamine 123, and rhodamine 6G accumulation in breast cancer cells that overexpress P-glycoprotein.* J Biomol Screen, 2002. **7**(1): p. 29-34.
278. Hideshima, T., et al., *Molecular mechanisms mediating antimyeloma activity of proteasome inhibitor PS-341.* Blood, 2003. **101**(4): p. 1530-4.
279. Liang, Y., et al., *Enhanced in vitro invasiveness and drug resistance with altered gene expression patterns in a human lung carcinoma cell line after pulse selection with anticancer drugs.* Int J Cancer, 2004. **111**(4): p. 484-93.
280. Hideshima, T., et al., *Understanding multiple myeloma pathogenesis in the bone marrow to identify new therapeutic targets.* Nat Rev Cancer, 2007. **7**(8): p. 585-98.
281. Levchenko, A., et al., *Intercellular transfer of P-glycoprotein mediates acquired multidrug resistance in tumor cells.* Proc Natl Acad Sci U S A, 2005. **102**(6): p. 1933-8.
282. Brown, C.J., et al., *Awakening guardian angels: drugging the p53 pathway.* Nat Rev Cancer, 2009. **9**(12): p. 862-73.
283. Mitsiades, N., et al., *Molecular sequelae of proteasome inhibition in human multiple myeloma cells.* Proc Natl Acad Sci U S A, 2002. **99**(22): p. 14374-9.
284. Wu, X., et al., *The p53-mdm-2 autoregulatory feedback loop.* Genes Dev, 1993. **7**(7A): p. 1126-32.
285. Miyashita, T. and J.C. Reed, *Tumor suppressor p53 is a direct transcriptional activator of the human bax gene.* Cell, 1995. **80**(2): p. 293-9.

286. Tai, Y.T., et al., *Ku86 variant expression and function in multiple myeloma cells is associated with increased sensitivity to DNA damage.* J Immunol, 2000. **165**(11): p. 6347-55.
287. Yu, J., et al., *PUMA induces the rapid apoptosis of colorectal cancer cells.* Mol Cell, 2001. **7**(3): p. 673-82.
288. Martoriati, A., et al., *dapk1, encoding an activator of a p19ARF-p53-mediated apoptotic checkpoint, is a transcription target of p53.* Oncogene, 2005. **24**(8): p. 1461-6.
289. Burns, T.F., et al., *Silencing of the novel p53 target gene Snk/Plk2 leads to mitotic catastrophe in paclitaxel (taxol)-exposed cells.* Mol Cell Biol, 2003. **23**(16): p. 5556-71.
290. Lopez-Lazaro, M., *The warburg effect: why and how do cancer cells activate glycolysis in the presence of oxygen?* Anticancer Agents Med Chem, 2008. **8**(3): p. 305-12.
291. Ralser, M., et al., *A catabolic block does not sufficiently explain how 2-deoxy-D-glucose inhibits cell growth.* Proc Natl Acad Sci U S A, 2008. **105**(46): p. 17807-11.
292. Schwarzenbach, H., *Expression of MDR1/P-glycoprotein, the multidrug resistance protein MRP, and the lung-resistance protein LRP in multiple myeloma.* Med Oncol, 2002. **19**(2): p. 87-104.
293. Cornelissen, J.J., et al., *MDR-1 expression and response to vincristine, doxorubicin, and dexamethasone chemotherapy in multiple myeloma refractory to alkylating agents.* J Clin Oncol, 1994. **12**(1): p. 115-9.
294. Turner, J.G., et al., *ABCG2 expression, function, and promoter methylation in human multiple myeloma.* Blood, 2006. **108**(12): p. 3881-9.
295. Ross, D.D., et al., *Atypical multidrug resistance: breast cancer resistance protein messenger RNA expression in mitoxantrone-selected cell lines.* J Natl Cancer Inst, 1999. **91**(5): p. 429-33.
296. Ross, D.D., *Novel mechanisms of drug resistance in leukemia.* Leukemia, 2000. **14**(3): p. 467-73.
297. Sauerbrey, A., et al., *Expression of the BCRP gene (ABCG2/MXR/ABCP) in childhood acute lymphoblastic leukaemia.* Br J Haematol, 2002. **118**(1): p. 147-50.
298. Fisher, G.A., et al., *Pharmacological considerations in the modulation of multidrug resistance.* Eur J Cancer, 1996. **32A**(6): p. 1082-8.
299. Berenson, J.R., et al., *Maintenance therapy with alternate-day prednisone improves survival in multiple myeloma patients.* Blood, 2002. **99**(9): p. 3163-8.
300. Boote, D.J., et al., *Phase I study of etoposide with SDZ PSC 833 as a modulator of multidrug resistance in patients with cancer.* J Clin Oncol, 1996. **14**(2): p. 610-8.
301. Advani, R., et al., *Treatment of refractory and relapsed acute myelogenous leukemia with combination chemotherapy plus the multidrug resistance modulator PSC 833 (Valspodar).* Blood, 1999. **93**(3): p. 787-95.
302. Baer, M.R., et al., *Phase 3 study of the multidrug resistance modulator PSC-833 in previously untreated patients 60 years of age and older with acute myeloid leukemia: Cancer and Leukemia Group B Study 9720.* Blood, 2002. **100**(4): p. 1224-32.
303. Traunecker, H.C., et al., *The acridonecarboxamide GF120918 potently reverses P-glycoprotein-mediated resistance in human sarcoma MES-Dx5 cells.* Br J Cancer, 1999. **81**(6): p. 942-51.

304. den Ouden, D., et al., *In vitro effect of GF120918, a novel reversal agent of multidrug resistance, on acute leukemia and multiple myeloma cells.* Leukemia, 1996. **10**(12): p. 1930-6.
305. Allen, J.D., et al., *The mouse Bcrp1/Mxr/Abcp gene: amplification and overexpression in cell lines selected for resistance to topotecan, mitoxantrone, or doxorubicin.* Cancer Res, 1999. **59**(17): p. 4237-41.
306. de Bruin, M., et al., *Reversal of resistance by GF120918 in cell lines expressing the ABC half-transporter, MXR.* Cancer Lett, 1999. **146**(2): p. 117-26.
307. Sparreboom, A., et al., *Clinical pharmacokinetics of doxorubicin in combination with GF120918, a potent inhibitor of MDR1 P-glycoprotein.* Anticancer Drugs, 1999. **10**(8): p. 719-28.
308. Planting, A.S., et al., *A phase I and pharmacologic study of the MDR converter GF120918 in combination with doxorubicin in patients with advanced solid tumors.* Cancer Chemother Pharmacol, 2005. **55**(1): p. 91-9.
309. Fracasso, P.M., et al., *Phase I study of docetaxel in combination with the P-glycoprotein inhibitor, zosuquidar, in resistant malignancies.* Clin Cancer Res, 2004. **10**(21): p. 7220-8.
310. Ruff, P., et al., *A randomized, placebo-controlled, double-blind phase 2 study of docetaxel compared to docetaxel plus zosuquidar (LY335979) in women with metastatic or locally recurrent breast cancer who have received one prior chemotherapy regimen.* Cancer Chemother Pharmacol, 2009. **64**(4): p. 763-8.
311. Sandler, A., et al., *A Phase I trial of a potent P-glycoprotein inhibitor, zosuquidar trihydrochloride (LY335979), administered intravenously in combination with doxorubicin in patients with advanced malignancy.* Clin Cancer Res, 2004. **10**(10): p. 3265-72.
312. Morschhauser, F., et al., *Phase I/II trial of a P-glycoprotein inhibitor, Zosuquidar.3HCl trihydrochloride (LY335979), given orally in combination with the CHOP regimen in patients with non-Hodgkin's lymphoma.* Leuk Lymphoma, 2007. **48**(4): p. 708-15.
313. Le, L.H., et al., *Phase I study of the multidrug resistance inhibitor zosuquidar administered in combination with vinorelbine in patients with advanced solid tumours.* Cancer Chemother Pharmacol, 2005. **56**(2): p. 154-60.
314. Germann, U.A., et al., *Chemosensitization and drug accumulation effects of VX-710, verapamil, cyclosporin A, MS-209 and GF120918 in multidrug resistant HL60/ADR cells expressing the multidrug resistance-associated protein MRP.* Anticancer Drugs, 1997. **8**(2): p. 141-55.
315. Rowinsky, E.K., et al., *Phase I and pharmacokinetic study of paclitaxel in combination with biricodar, a novel agent that reverses multidrug resistance conferred by overexpression of both MDR1 and MRP.* J Clin Oncol, 1998. **16**(9): p. 2964-76.
316. Cripe, L.D., et al., *Zosuquidar, a novel modulator of P-glycoprotein, does not improve the outcome of older patients with newly diagnosed acute myeloid leukemia: a randomized, placebo-controlled trial of the Eastern Cooperative Oncology Group 3999.* Blood. **116**(20): p. 4077-85.
317. Orlowski, M. and S. Wilk, *Catalytic activities of the 20 S proteasome, a multicatalytic proteinase complex.* Arch Biochem Biophys, 2000. **383**(1): p. 1-16.
318. Rechsteiner, M.C., *Ubiquitin-mediated proteolysis: an ideal pathway for systems biology analysis.* Adv Exp Med Biol, 2004. **547**: p. 49-59.
319. Fribley, A., Q. Zeng, and C.Y. Wang, *Proteasome inhibitor PS-341 induces apoptosis through induction of endoplasmic reticulum stress-reactive oxygen*

species in head and neck squamous cell carcinoma cells. Mol Cell Biol, 2004. **24**(22): p. 9695-704.
320. LeBlanc, R., et al., *Proteasome inhibitor PS-341 inhibits human myeloma cell growth in vivo and prolongs survival in a murine model.* Cancer Res, 2002. **62**(17): p. 4996-5000.
321. Adams, J. and P.J. Elliott, *New agents in cancer clinical trials.* Oncogene, 2000. **19**(56): p. 6687-92.
322. Nakamura, T., et al., *The mechanism of cross-resistance to proteasome inhibitor bortezomib and overcoming resistance in Ewing's family tumor cells.* Int J Oncol, 2007. **31**(4): p. 803-11.
323. Iijima, M., I. Momose, and D. Ikeda, *Increased ABCB1 expression in TP-110-resistant RPMI-8226 cells.* Biosci Biotechnol Biochem. **74**(9): p. 1913-9.
324. Fujita, T., et al., *Proteasome inhibitors can alter the signaling pathways and attenuate the P-glycoprotein-mediated multidrug resistance.* Int J Cancer, 2005. **117**(4): p. 670-82.
325. Styczynski, J., et al., *Activity of bortezomib in glioblastoma.* Anticancer Res, 2006. **26**(6B): p. 4499-503.
326. Wiberg, K., et al., *In vitro activity of bortezomib in cultures of patient tumour cells--potential utility in haematological malignancies.* Med Oncol, 2009. **26**(2): p. 193-201.
327. Lu, S., et al., *The effects of proteasome inhibitor bortezomib on a P-gp positive leukemia cell line K562/A02.* Int J Lab Hematol, 2009.
328. Minderman, H., et al., *Bortezomib activity and in vitro interactions with anthracyclines and cytarabine in acute myeloid leukemia cells are independent of multidrug resistance mechanisms and p53 status.* Cancer Chemother Pharmacol, 2007. **60**(2): p. 245-55.
329. Sonneveld, P., *Multidrug resistance in haematological malignancies.* J Intern Med, 2000. **247**(5): p. 521-34.
330. Kuo, M.T., et al., *Induction of human MDR1 gene expression by 2-acetylaminofluorene is mediated by effectors of the phosphoinositide 3-kinase pathway that activate NF-kappaB signaling.* Oncogene, 2002. **21**(13): p. 1945-54.
331. Thevenod, F., et al., *Up-regulation of multidrug resistance P-glycoprotein via nuclear factor-kappaB activation protects kidney proximal tubule cells from cadmium- and reactive oxygen species-induced apoptosis.* J Biol Chem, 2000. **275**(3): p. 1887-96.
332. Ros, J.E., et al., *Induction of Mdr1b expression by tumor necrosis factor-alpha in rat liver cells is independent of p53 but requires NF-kappaB signaling.* Hepatology, 2001. **33**(6): p. 1425-31.
333. Zhang, Y., et al., *Proteasome inhibitor MG132 reverses multidrug resistance of gastric cancer through enhancing apoptosis and inhibiting P-gp.* Cancer Biol Ther, 2008. **7**(4): p. 540-6.
334. Mayo, M.W. and A.S. Baldwin, *The transcription factor NF-kappaB: control of oncogenesis and cancer therapy resistance.* Biochim Biophys Acta, 2000. **1470**(2): p. M55-62.
335. Bentires-Alj, M., et al., *NF-kappaB transcription factor induces drug resistance through MDR1 expression in cancer cells.* Oncogene, 2003. **22**(1): p. 90-7.
336. Zhang, Z., et al., *Regulation of the stability of P-glycoprotein by ubiquitination.* Mol Pharmacol, 2004. **66**(3): p. 395-403.

337. Loo, T.W. and D.M. Clarke, *Functional consequences of glycine mutations in the predicted cytoplasmic loops of P-glycoprotein.* J Biol Chem, 1994. **269**(10): p. 7243-8.
338. Schinkel, A.H., et al., *N-glycosylation and deletion mutants of the human MDR1 P-glycoprotein.* J Biol Chem, 1993. **268**(10): p. 7474-81.
339. Kramer, R., et al., *Inhibition of N-linked glycosylation of P-glycoprotein by tunicamycin results in a reduced multidrug resistance phenotype.* Br J Cancer, 1995. **71**(4): p. 670-5.
340. Perez, L.E., et al., *Bortezomib restores stroma-mediated APO2L/TRAIL apoptosis resistance in multiple myeloma.* Eur J Haematol, 2009.
341. Garcia, M.G., et al., *PI3K/Akt inhibition modulates multidrug resistance and activates NF-kappaB in murine lymphoma cell lines.* Leuk Res, 2009. **33**(2): p. 288-96.
342. Petrylak, D.P., et al., *P-glycoprotein expression in primary and metastatic transitional cell carcinoma of the bladder.* Ann Oncol, 1994. **5**(9): p. 835-40.
343. Zhou, X., et al., *Nitric oxide induces thymocyte apoptosis via a caspase-1-dependent mechanism.* J Immunol, 2000. **165**(3): p. 1252-8.
344. Fuchs, S.Y., et al., *Mdm2 association with p53 targets its ubiquitination.* Oncogene, 1998. **17**(19): p. 2543-7.
345. Inoue, T., et al., *Downregulation of MDM2 stabilizes p53 by inhibiting p53 ubiquitination in response to specific alkylating agents.* FEBS Lett, 2001. **490**(3): p. 196-201.
346. Maki, C.G., *Oligomerization is required for p53 to be efficiently ubiquitinated by MDM2.* J Biol Chem, 1999. **274**(23): p. 16531-5.
347. Li, M., et al., *Mono- versus polyubiquitination: differential control of p53 fate by Mdm2.* Science, 2003. **302**(5652): p. 1972-5.
348. Di Stefano, V., et al., *HIPK2 neutralizes MDM2 inhibition rescuing p53 transcriptional activity and apoptotic function.* Oncogene, 2004. **23**(30): p. 5185-92.
349. Ofir-Rosenfeld, Y., et al., *Mdm2 regulates p53 mRNA translation through inhibitory interactions with ribosomal protein L26.* Mol Cell, 2008. **32**(2): p. 180-9.
350. Hoffman, W.H., et al., *Transcriptional repression of the anti-apoptotic survivin gene by wild type p53.* J Biol Chem, 2002. **277**(5): p. 3247-57.
351. Bennett, M., et al., *Cell surface trafficking of Fas: a rapid mechanism of p53-mediated apoptosis.* Science, 1998. **282**(5387): p. 290-3.
352. Wu, G.S., et al., *KILLER/DR5 is a DNA damage-inducible p53-regulated death receptor gene.* Nat Genet, 1997. **17**(2): p. 141-3.
353. Moroni, M.C., et al., *Apaf-1 is a transcriptional target for E2F and p53.* Nat Cell Biol, 2001. **3**(6): p. 552-8.
354. Schuler, M., et al., *p53 induces apoptosis by caspase activation through mitochondrial cytochrome c release.* J Biol Chem, 2000. **275**(10): p. 7337-42.
355. Wolff, S., et al., *p53's mitochondrial translocation and MOMP action is independent of Puma and Bax and severely disrupts mitochondrial membrane integrity.* Cell Res, 2008. **18**(7): p. 733-44.
356. Chipuk, J.E. and D.R. Green, *Cytoplasmic p53: bax and forward.* Cell Cycle, 2004. **3**(4): p. 429-31.
357. Tasdemir, E., et al., *p53 represses autophagy in a cell cycle-dependent fashion.* Cell Cycle, 2008. **7**(19): p. 3006-11.
358. Shangary, S. and S. Wang, *Targeting the MDM2-p53 interaction for cancer therapy.* Clin Cancer Res, 2008. **14**(17): p. 5318-24.

359. Tabe, Y., et al., *MDM2 antagonist nutlin-3 displays antiproliferative and proapoptotic activity in mantle cell lymphoma.* Clin Cancer Res, 2009. **15**(3): p. 933-42.
360. Lee, J.T. and W. Gu, *The multiple levels of regulation by p53 ubiquitination.* Cell Death Differ. **17**(1): p. 86-92.
361. Ganguli, G. and B. Wasylyk, *p53-independent functions of MDM2.* Mol Cancer Res, 2003. **1**(14): p. 1027-35.
362. Cordon-Cardo, C., et al., *Molecular abnormalities of mdm2 and p53 genes in adult soft tissue sarcomas.* Cancer Res, 1994. **54**(3): p. 794-9.
363. Lu, M.L., et al., *Impact of alterations affecting the p53 pathway in bladder cancer on clinical outcome, assessed by conventional and array-based methods.* Clin Cancer Res, 2002. **8**(1): p. 171-9.
364. Alt, J.R., et al., *Mdm2 haplo-insufficiency profoundly inhibits Myc-induced lymphomagenesis.* EMBO J, 2003. **22**(6): p. 1442-50.
365. Alt, J.R., et al., *Mdm2 binds to Nbs1 at sites of DNA damage and regulates double strand break repair.* J Biol Chem, 2005. **280**(19): p. 18771-81.
366. Stracker, T.H., et al., *The Mre11 complex and the metabolism of chromosome breaks: the importance of communicating and holding things together.* DNA Repair (Amst), 2004. **3**(8-9): p. 845-54.
367. Carroll, P.E., et al., *Centrosome hyperamplification in human cancer: chromosome instability induced by p53 mutation and/or Mdm2 overexpression.* Oncogene, 1999. **18**(11): p. 1935-44.
368. Bouska, A., et al., *Mdm2 promotes genetic instability and transformation independent of p53.* Mol Cell Biol, 2008. **28**(15): p. 4862-74.
369. Drach, J., et al., *Presence of a p53 gene deletion in patients with multiple myeloma predicts for short survival after conventional-dose chemotherapy.* Blood, 1998. **92**(3): p. 802-9.
370. Jin, L., et al., *MDM2 antagonist Nutlin-3 enhances bortezomib-mediated mitochondrial apoptosis in TP53-mutated mantle cell lymphoma.* Cancer Lett. **299**(2): p. 161-70.
371. Engelman, J.A., *Targeting PI3K signalling in cancer: opportunities, challenges and limitations.* Nat Rev Cancer, 2009. **9**(8): p. 550-62.
372. Engelman, J.A., J. Luo, and L.C. Cantley, *The evolution of phosphatidylinositol 3-kinases as regulators of growth and metabolism.* Nat Rev Genet, 2006. **7**(8): p. 606-19.
373. Hess, G., et al., *Phase III study to evaluate temsirolimus compared with investigator's choice therapy for the treatment of relapsed or refractory mantle cell lymphoma.* J Clin Oncol, 2009. **27**(23): p. 3822-9.
374. Chan, S., et al., *Phase II study of temsirolimus (CCI-779), a novel inhibitor of mTOR, in heavily pretreated patients with locally advanced or metastatic breast cancer.* J Clin Oncol, 2005. **23**(23): p. 5314-22.
375. Kapoor, A. and R.A. Figlin, *Targeted inhibition of mammalian target of rapamycin for the treatment of advanced renal cell carcinoma.* Cancer, 2009. **115**(16): p. 3618-30.
376. Dowling, R.J., et al., *Metformin inhibits mammalian target of rapamycin-dependent translation initiation in breast cancer cells.* Cancer Res, 2007. **67**(22): p. 10804-12.
377. Gotlieb, W.H., et al., *In vitro metformin anti-neoplastic activity in epithelial ovarian cancer.* Gynecol Oncol, 2008. **110**(2): p. 246-50.
378. Pu, X.Y., et al., *Insulin-like growth factor-1 restores erectile function in aged rats: modulation the integrity of smooth muscle and nitric oxide-cyclic*

guanosine monophosphate signaling activity. J Sex Med, 2008. **5**(6): p. 1345-54.
379. Ben Sahra, I., et al., *Metformin in cancer therapy: a new perspective for an old antidiabetic drug?* Mol Cancer Ther, 2010. **9**(5): p. 1092-9.
380. Santidrian, A.F., et al., *AICAR induces apoptosis independently of AMPK and p53 through upregulation of the BH3-only proteins BIM and NOXA in chronic lymphocytic leukemia cells.* Blood, 2010: p. blood-2010-05-283960.
381. Kalender, A., et al., *Metformin, independent of AMPK, inhibits mTORC1 in a rag GTPase-dependent manner.* Cell Metab, 2010. **11**(5): p. 390-401.
382. Zhuang, Y. and W.K. Miskimins, *Cell cycle arrest in Metformin treated breast cancer cells involves activation of AMPK, downregulation of cyclin D1, and requires p27Kip1 or p21Cip1.* J Mol Signal, 2008. **3**: p. 18.
383. Alimova, I.N., et al., *Metformin inhibits breast cancer cell growth, colony formation and induces cell cycle arrest in vitro.* Cell Cycle, 2009. **8**(6): p. 909-15.
384. McMillin, D.W., et al., *Tumor cell-specific bioluminescence platform to identify stroma-induced changes to anticancer drug activity.* Nat Med. **16**(4): p. 483-9.
385. Hirsch, H.A., et al., *Metformin selectively targets cancer stem cells, and acts together with chemotherapy to block tumor growth and prolong remission.* Cancer Res, 2009. **69**(19): p. 7507-11.
386. Vazquez-Martin, A., et al., *The anti-diabetic drug metformin suppresses self-renewal and proliferation of trastuzumab-resistant tumor-initiating breast cancer stem cells.* Breast Cancer Res Treat, 2010.
387. Campas, C., et al., *Acadesine activates AMPK and induces apoptosis in B-cell chronic lymphocytic leukemia cells but not in T lymphocytes.* Blood, 2003. **101**(9): p. 3674-80.
388. Campas, C., et al., *Acadesine induces apoptosis in B cells from mantle cell lymphoma and splenic marginal zone lymphoma.* Leukemia, 2005. **19**(2): p. 292-4.
389. Green, D.R. and G.P. Amarante-Mendes, *The point of no return: mitochondria, caspases, and the commitment to cell death.* Results Probl Cell Differ, 1998. **24**: p. 45-61.
390. Susin, S.A., N. Zamzami, and G. Kroemer, *Mitochondria as regulators of apoptosis: doubt no more.* Biochim Biophys Acta, 1998. **1366**(1-2): p. 151-65.
391. Warburg, O., *On the origin of cancer cells.* Science, 1956. **123**(3191): p. 309-14.
392. Xu, R.H., et al., *Synergistic effect of targeting mTOR by rapamycin and depleting ATP by inhibition of glycolysis in lymphoma and leukemia cells.* Leukemia, 2005. **19**(12): p. 2153-8.
393. Pradelli, L.A., et al., *Glycolysis inhibition sensitizes tumor cells to death receptors-induced apoptosis by AMP kinase activation leading to Mcl-1 block in translation.* Oncogene, 2009.
394. Graham, G.G., et al., *Clinical pharmacokinetics of metformin.* Clin Pharmacokinet. **50**(2): p. 81-98.
395. Dimitrijevic, D., A.J. Shaw, and A.T. Florence, *Effects of some non-ionic surfactants on transepithelial permeability in Caco-2 cells.* J Pharm Pharmacol, 2000. **52**(2): p. 157-62.
396. Scheen, A.J., *Clinical pharmacokinetics of metformin.* Clin Pharmacokinet, 1996. **30**(5): p. 359-71.
397. Misbin, R.I., *The phantom of lactic acidosis due to metformin in patients with diabetes.* Diabetes Care, 2004. **27**(7): p. 1791-3.

398. Sambol, N.C., et al., *Pharmacokinetics and pharmacodynamics of metformin in healthy subjects and patients with noninsulin-dependent diabetes mellitus.* J Clin Pharmacol, 1996. **36**(11): p. 1012-21.
399. Owen, M.R., E. Doran, and A.P. Halestrap, *Evidence that metformin exerts its anti-diabetic effects through inhibition of complex 1 of the mitochondrial respiratory chain.* Biochem J, 2000. **348 Pt 3**: p. 607-14.
400. Bailey, C.J. and R.C. Turner, *Metformin.* N Engl J Med, 1996. **334**(9): p. 574-9.
401. Gan, S.C., et al., *Biguanide-associated lactic acidosis. Case report and review of the literature.* Arch Intern Med, 1992. **152**(11): p. 2333-6.
402. Salpeter, S.R., et al., *Risk of fatal and nonfatal lactic acidosis with metformin use in type 2 diabetes mellitus.* Cochrane Database Syst Rev, 2010(1): p. CD002967.
403. Bailey, C.J., *Biguanides and NIDDM.* Diabetes Care, 1992. **15**(6): p. 755-72.
404. Hermann, L.S., *Metformin: a review of its pharmacological properties and therapeutic use.* Diabete Metab, 1979. **5**(3): p. 233-45.
405. *National Collaborating Centre for Chronic Conditions. Type 2 diabetes: national clinical guideline for management in primary and secondary care (update).* London: Royal College of Physicians, 2008.
406. Atzori, F., *A phase I, pharmacokinetic (PK) and pharmacodynamic (PD) study of weekly (qW) MK-0646, an insulin-like growth factor-1 receptor (IGF1R) monoclonal antibody (MAb) in patients (pts) with advanced solid tumors* ASCO Meeting Abstracts 2008. **26**: p. 3519.
407. Lacy, M.Q., et al., *Phase I, pharmacokinetic and pharmacodynamic study of the anti-insulinlike growth factor type 1 Receptor monoclonal antibody CP-751,871 in patients with multiple myeloma.* J Clin Oncol, 2008. **26**(19): p. 3196-203.
408. Sarantopoulos, J. *A phase IB study of AMG 479, a type 1 insulin-like growth factor receptor (IGF1R) antibody, in combination with panitumumab (P) or gemcitabine (G)*. in *ASCO*. 2008.
409. Hidalgo, M., *A phase I study of MK-0646, a humanized monoclonal antibody against the insulin-like growth factor receptor type 1 (IGF1R) in advanced solid tumor patients in a q2 wk schedule.* ASCO Meeting Abstracts 2008. **26**: p. 3520.
410. Dixon, R., et al., *AICA-riboside: safety, tolerance, and pharmacokinetics of a novel adenosine-regulating agent.* J Clin Pharmacol, 1991. **31**(4): p. 342-7.
411. Mangano, D.T., et al., *Post-reperfusion myocardial infarction: long-term survival improvement using adenosine regulation with acadesine.* J Am Coll Cardiol, 2006. **48**(1): p. 206-14.
412. Mangano, D.T., *Effects of acadesine on myocardial infarction, stroke, and death following surgery. A meta-analysis of the 5 international randomized trials. The Multicenter Study of Perioperative Ischemia (McSPI) Research Group.* JAMA, 1997. **277**(4): p. 325-32.
413. Van Den Neste, E., G. Van den Berghe, and F. Bontemps, *AICA-riboside (acadesine), an activator of AMP-activated protein kinase with potential for application in hematologic malignancies.* Expert Opin Investig Drugs, 2010. **19**(4): p. 571-8.
414. Spisek, R., et al., *Bortezomib enhances dendritic cell (DC)-mediated induction of immunity to human myeloma via exposure of cell surface heat shock protein 90 on dying tumor cells: therapeutic implications.* Blood, 2007. **109**(11): p. 4839-45.

415. Chauhan, D., et al., *Combination of proteasome inhibitors bortezomib and NPI-0052 trigger in vivo synergistic cytotoxicity in multiple myeloma.* Blood, 2008. **111**(3): p. 1654-64.
416. Obeng, E.A., et al., *Proteasome inhibitors induce a terminal unfolded protein response in multiple myeloma cells.* Blood, 2006. **107**(12): p. 4907-16.
417. Ooi, M.G., et al., *Interactions of the Hdm2/p53 and Proteasome Pathways May Enhance the Antitumor Activity of Bortezomib.* Clin Cancer Res, 2009.
418. Chauhan, D., T. Hideshima, and K.C. Anderson, *A novel proteasome inhibitor NPI-0052 as an anticancer therapy.* Br J Cancer, 2006. **95**(8): p. 961-5.
419. Malz, M., et al., *Overexpression of far upstream element binding proteins: a mechanism regulating proliferation and migration in liver cancer cells.* Hepatology, 2009. **50**(4): p. 1130-9.
420. Rabenhorst, U., et al., *Overexpression of the far upstream element binding protein 1 in hepatocellular carcinoma is required for tumor growth.* Hepatology, 2009. **50**(4): p. 1121-9.
421. Zhang, J., et al., *Targeting angiogenesis via a c-Myc/hypoxia-inducible factor-1alpha-dependent pathway in multiple myeloma.* Cancer Res, 2009. **69**(12): p. 5082-90.
422. Kim, S.J., et al., *Galectin-3 Increases Gastric Cancer Cell Motility by Up-Regulating Fascin-1 Expression.* Gastroenterology, 2009.
423. Darnel, A.D., et al., *Fascin regulates prostate cancer cell invasion and is associated with metastasis and biochemical failure in prostate cancer.* Clin Cancer Res, 2009. **15**(4): p. 1376-83.
424. Qualtrough, D., et al., *The actin-bundling protein fascin is overexpressed in colorectal adenomas and promotes motility in adenoma cells in vitro.* Br J Cancer, 2009. **101**(7): p. 1124-9.
425. Li, A., et al., *The Actin-Bundling Protein Fascin Stabilizes Actin in Invadopodia and Potentiates Protrusive Invasion.* Curr Biol.
426. Carpenter, B., et al., *Heterogeneous nuclear ribonucleoprotein K is over expressed, aberrantly localised and is associated with poor prognosis in colorectal cancer.* Br J Cancer, 2006. **95**(7): p. 921-7.
427. Krampe, B., H. Swiderek, and M. Al-Rubeai, *Transcriptome and proteome analysis of antibody-producing mouse myeloma NS0 cells cultivated at different cell densities in perfusion culture.* Biotechnol Appl Biochem, 2008. **50**(Pt 3): p. 133-41.
428. Inoue, A., et al., *Loss-of-function screening by randomized intracellular antibodies: identification of hnRNP-K as a potential target for metastasis.* Proc Natl Acad Sci U S A, 2007. **104**(21): p. 8983-8.
429. Mandal, M., et al., *Growth factors regulate heterogeneous nuclear ribonucleoprotein K expression and function.* J Biol Chem, 2001. **276**(13): p. 9699-704.
430. Ma, K.W., S.W. Au, and M.M. Waye, *Over-expression of SUMO-1 induces the up-regulation of heterogeneous nuclear ribonucleoprotein A2/B1 isoform B1 (hnRNP A2/B1 isoform B1) and uracil DNA glycosylase (UDG) in hepG2 cells.* Cell Biochem Funct, 2009. **27**(4): p. 228-37.
431. Byrjalsen, I., et al., *Two-dimensional gel analysis of human endometrial proteins: characterization of proteins with increased expression in hyperplasia and adenocarcinoma.* Mol Hum Reprod, 1999. **5**(8): p. 748-56.
432. Hong, O.K., et al., *Proteomic analysis of differential protein expression in response to epidermal growth factor in neonatal porcine pancreatic cell monolayers.* J Cell Biochem, 2005. **95**(4): p. 769-81.

433. Kang, X., et al., *Regulation of the hTERT promoter activity by MSH2, the hnRNPs K and D, and GRHL2 in human oral squamous cell carcinoma cells.* Oncogene, 2009. **28**(4): p. 565-74.
434. Shi, Y., et al., *IL-6-induced stimulation of c-myc translation in multiple myeloma cells is mediated by myc internal ribosome entry site function and the RNA-binding protein, hnRNP A1.* Cancer Res, 2008. **68**(24): p. 10215-22.
435. Qi, Y.J., et al., *Proteomic identification of malignant transformation-related proteins in esophageal squamous cell carcinoma.* J Cell Biochem, 2008. **104**(5): p. 1625-35.
436. Bambang, I.F., et al., *Overexpression of endoplasmic reticulum protein 29 regulates mesenchymal-epithelial transition and suppresses xenograft tumor growth of invasive breast cancer cells.* Lab Invest, 2009. **89**(11): p. 1229-42.
437. Russo, A., et al., *Bortezomib: A New Pro-apoptotic Agent in Cancer Treatment.* Curr Cancer Drug Targets.
438. Wang, Y., et al., *Targeted proteasome inhibition by Velcade induces apoptosis in human mesothelioma and breast cancer cell lines.* Cancer Chemother Pharmacol, 2009.
439. Pitts, T.M., et al., *Vorinostat and bortezomib exert synergistic antiproliferative and proapoptotic effects in colon cancer cell models.* Mol Cancer Ther, 2009. **8**(2): p. 342-9.
440. Song, M.K., et al., *Elevation of serum ferritin is associated with the outcome of patients with newly diagnosed multiple myeloma.* Korean J Intern Med, 2009. **24**(4): p. 368-73.
441. Linkesch, W. and H. Ludwig, *Serum ferritin and beta 2-microglobulin in patients with multiple myeloma.* Cancer Detect Prev, 1983. **6**(1-2): p. 297-301.
442. Ohnishi, K., et al., *Quantification of ferritin-secreting cells in patients with non-Hodgkin's lymphoma.* Acta Haematol, 1985. **73**(3): p. 145-9.
443. Yang, W.S. and B.R. Stockwell, *Synthetic lethal screening identifies compounds activating iron-dependent, nonapoptotic cell death in oncogenic-RAS-harboring cancer cells.* Chem Biol, 2008. **15**(3): p. 234-45.
444. Ricolleau, G., et al., *Surface-enhanced laser desorption/ionization time of flight mass spectrometry protein profiling identifies ubiquitin and ferritin light chain as prognostic biomarkers in node-negative breast cancer tumors.* Proteomics, 2006. **6**(6): p. 1963-75.
445. Kim, H.G., et al., *Metformin inhibits P-glycoprotein expression via the NF-kappaB pathway and CRE transcriptional activity through AMPK activation.* Br J Pharmacol. **162**(5): p. 1096-108.
446. Michaelis, M., et al., *Reversal of P-glycoprotein-mediated multidrug resistance by the murine double minute 2 antagonist nutlin-3.* Cancer Res, 2009. **69**(2): p. 416-21.

Appendix

APPENDIX A

Details of the Mascot software identification

(a) KHSRP protein

Ascension - gi|54648253

Mass - 73307

Mascot score - 149

Expect - 1.6e-010

Peptide match - 22

Fixed modifications: Carbamidomethyl (C)
Variable modifications: Oxidation (M)
Cleavage by Trypsin: cuts C-term side of KR unless next residue is P
Sequence Coverage: **26%**
Matched peptides shown in **Bold Red**

1 MSDYSTGGPP PGPPPPAGGG GGAGGAGGGP PPGPPGAGDR GGGPGGGGP
51 GGGSAGGPSQ PPGGGGPGIR K**DAFADAVQR** ARQIAAKIGG DAATTVNNST
101 PDFGFGGQKR QLEDGDQPES KKLASQGDSI SSQLGPIHPP PR**TSMTEEYR**
151 **VPDGMVGLII GR**GGEQINKI QQDSGCK**VQI SPDSGGLPER SVSLTGAPES**
201 **VQKAK**MMLDD IVSRGRGGPP GQFHDNANGG QNGTVQEIMI PAGKAGLVIG
251 KGGETIKQLQ ERAGVK**MILI QDGSQNTNVD KPLRIIGDPY K**VQQACEMVM
301 DILR**ERDQGG FGDR**NEYGSR **IGGGIDVPVP RHSVGVVIGR** SGEMIK**KIQN**
351 **DAGVR**IQFKQ DDGTGPEK**IA HIMGPPDR**CE HAAR**IINDLL QSLR**SGPPGP
401 PGGPGMPPGG RGRGRGQGNW GPPGGEMTFS IPTHKCGLVI GRGGENVK**AI**
451 **NQQTGAFVEI SR**QLPPNGDP NFKLFIIRGS PQQIDHAKQL IEEKIEGPLC
501 PVGPGPGGPG PAGPMGPFNP GPFNQGPPGA PPHAGGPPPH YPPQGWGNT
551 YPQWQPPAPH DPSKAAAAAA DPNAAWAAYY SHYYQQPPGP VPGPAPAPAA
601 PPAQGEPPQP PPTGQSDYTK **AWEEYYK**K**IG QQPQQPGAPP QQDYTKAWEE**
651 **YYK**KQAQVAT GGGPGAPPGF LAPPTVFQPL LSSALAQLPR PRPSPLPGLV
701 CCLFICSRGD

Observed	Mr(expt)	Mr(calc)	Delta	Start	End	Miss	Ions	Peptide
805.4341	804.4268	804.4381	-0.0113	285	291	0	---	R.IIGDPYK.V
851.3661	850.3588	850.3569	0.0019	307	314	0	---	R.DQGGFGDR.N
872.4899	871.4826	871.4511	0.0315	348	355	0	---	K.IQNDAGVR.I
923.5353	922.5280	922.5348	-0.0068	332	340	0	---	R.HSVGVVIGR.S
988.4399	987.4326	987.4338	-0.0011	621	627	0	28	K.AWEEYYK.K
988.4399	987.4326	987.4338	-0.0011	647	653	0	---	K.AWEEYYK.K
992.4481	991.4408	991.4723	-0.0315	72	80	0	---	K.DAFADAVQR.A
1000.5678	999.5605	999.5461	0.0144	347	355	1	---	K.KIQNDAGVR.I
1016.4730	1015.4657	1015.4280	0.0377	143	150	0	---	R.TSMTEEYR.V
1079.6150	1078.6077	1078.6134	-0.0057	321	331	0	17	R.IGGGIDVPVPR.H
1079.6150	1078.6077	1078.6134	-0.0057	321	331	0	---	R.IGGGIDVPVPR.H
1122.5692	1121.5619	1121.5651	-0.0032	369	378	0	---	K.IAHIMGPPDR.C + Oxidation (M)
1122.5692	1121.5619	1121.5651	-0.0032	369	378	0	---	K.IAHIMGPPDR.C + Oxidation (M)
1136.5399	1135.5326	1135.5006	0.0320	305	314	1	---	R.ERDQGGFGDR.N
1184.6915	1183.6842	1183.6924	-0.0082	385	394	0	---	R.IINDLLQSLR.S
1242.6794	1241.6721	1241.6801	-0.0080	151	162	0	---	R.VPDGMVGLIIGR.G + Oxidation (M)
1354.6958	1353.6885	1353.6888	-0.0003	178	190	0	---	K.VQISPDSGGLPER.S
1501.7175	1500.7102	1500.8147	-0.1045	191	205	1	---	R.SVSLTGAPESVQKAK.M
1533.8008	1532.7935	1532.7946	-0.0011	449	462	0	5	K.AINQQTGAFVEISR.Q
1533.8008	1532.7935	1532.7946	-0.0011	449	462	0	---	K.AINQQTGAFVEISR.Q
1980.9694	1979.9621	1979.9701	-0.0080	629	646	0	---	K.IGQQPQQPGAPPQQDYTK.A
2058.0652	2057.0579	2057.0575	0.0004	267	284	0	---	K.MILIQDGSQNTNVDKPLR.I + Oxidation (M)

Table 1A Peptides matched to KHSRP protein

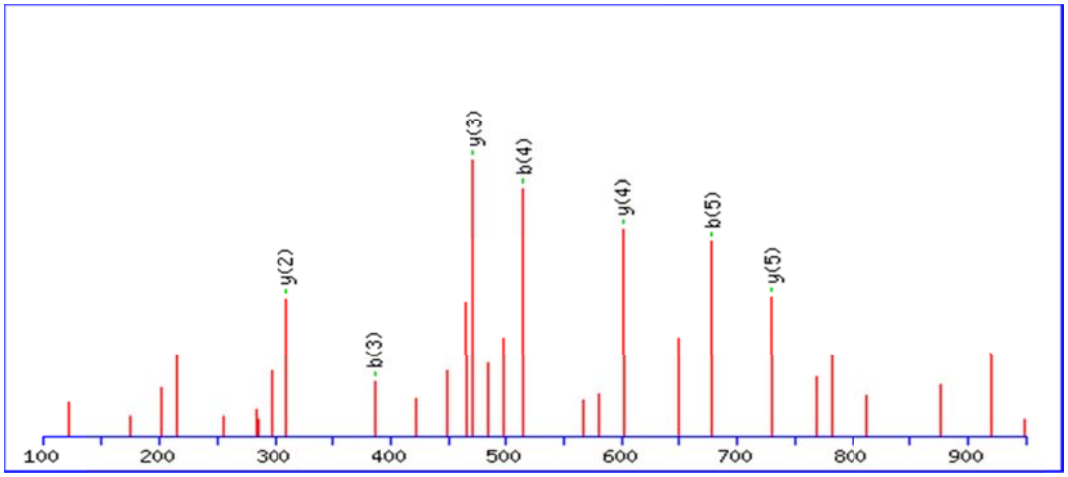

Fig. 1A Ion match to peptide AWEEYYK

Monoisotopic mass of neutral peptide Mr(calc): 987.4338
Fixed Modifications : Carbamidomethyl (C)
Ions Score: 28 Expect: 0.17
Matches (Bold Red): 7/60 fragment ions using 12 most intense peaks

#	Immon.	A	a^0	b	b^0	Seq.	y	y*	y^0	#
1	44.0495	44.0495		72.0444		A				7
2	159.0917	230.1288		258.1237		W	917.404	900.3774	899.3934	6
3	102.055	359.1714	341.1608	**387.1663**	369.1557	E	**731.3246**	714.2981	713.3141	5
4	102.055	488.214	470.2034	**516.2089**	498.1983	E	**602.2821**	585.2555	584.2715	4
5	136.0757	651.2773	633.2667	**679.2722**	661.2616	Y	**473.2395**	456.2129		3
6	136.0757	814.3406	796.3301	842.3355	824.325	Y	**310.1761**	293.1496		2
7	101.1073					K	147.1128	130.0863		1

Table 1B Ions match

(b) Heterogeneous nuclear ribonucleoprotein A2/B1 isoform B

Ascension - gi|14043072

Mass - 37464

Mascot score - 370

Expect - 1.3e-032

Peptide match - 24

Fixed modifications: Carbamidomethyl (C)
Variable modifications: Oxidation (M)
Cleavage by Trypsin: cuts C-term side of KR unless next residue is P
Sequence Coverage: **50%**

Matched peptides shown in **Bold Red**

1 MEK**TLETVPL ER**KKR**EKEQF R**K**LFIGGLSF ETTEESLRNY YEQWGKLTDC**
51 **VVMR**DPASKR SRGFGFVTFS SMAEVDAAMA ARPHSIDGRV VEPKRAVARE
101 ESGKPGAHVT VK**KLFVGGIK EDTEEHHLRD YFEEYGKIDT IEIITDR**QSG
151 KKR**GFGFVTF DDHDPVDK**IV LQK**YHTINGH NAEVRK**ALSR **QEMQEVQSSR**
201 SGR**GGNFGFG DSRGGGGNFG PGPGSNFRGG SDGYGSGR**GF GDGYNGYGGG
251 PGGGNFGGSP GYGGGRGGYG GGGPGYGNQG GGYGGGYDNY GGGNYGSGNY
301 NDFGNYNQQP SNYGPMKSGN FGGSR**NMGGP YGGGNYGPGG SGGSGGYGGR**
351 SRY

Observed	Mr(expt)	Mr(calc)	Delta	Start		End	Miss	Ions	Peptide
836.4279	835.4206	835.4188	0.0018	16	-	21	1	14	R.EKEQFR.K
836.4279	835.4206	835.4188	0.0018	16	-	21	1	---	R.EKEQFR.K
861.5499	860.5426	860.5483	-0.0057	113	-	120	1	---	K.KLFVGGIK.E
912.3812	911.3739	911.3733	0.0007	229	-	238	0	---	R.GGSDGYGSGR.G
1009.4787	1008.4714	1008.4732	-0.0018	47	-	54	0	---	K.LTDCVVMR.D + Oxidation (M)
1013.4435	1012.4362	1012.4362	0.0000	204	-	213	0	29	R.GGNFGFGDSR.G
1013.4435	1012.4362	1012.4362	0.0000	204	-	213	0	---	R.GGNFGFGDSR.G
1050.4384	1049.4311	1049.4341	-0.0030	130	-	137	0	30	R.DYFEEYGK.I
1050.4384	1049.4311	1049.4341	-0.0030	130	-	137	0	---	R.DYFEEYGK.I
1057.5878	1056.5805	1056.5815	-0.0010	4	-	12	0	---	K.TLETVPLER.K
1087.4813	1086.4740	1086.4770	-0.0030	39	-	46	0	53	R.NYYEQWGK.L
1087.4813	1086.4740	1086.4770	-0.0030	39	-	46	0	---	R.NYYEQWGK.L
1165.5220	1164.5147	1164.5159	-0.0012	121	-	129	0	4	K.EDTEEHHLR.D
1165.5220	1164.5147	1164.5159	-0.0012	121	-	129	0	---	K.EDTEEHHLR.D
1188.6450	1187.6377	1187.6398	-0.0020	138	-	147	0	56	K.IDTIEIITDR.Q
1188.6450	1187.6377	1187.6398	-0.0020	138	-	147	0	---	K.IDTIEIITDR.Q
1237.5436	1236.5363	1236.5404	-0.0041	191	-	200	0	---	R.QEMQEVQSSR.S + Oxidation (M)
1377.6301	1376.6228	1376.6221	0.0008	214	-	228	0	42	R.GGGGNFGPGPGSNFR.G
1377.6301	1376.6228	1376.6221	0.0008	214	-	228	0	---	R.GGGGNFGPGPGSNFR.G
1538.7664	1537.7591	1537.7749	-0.0158	174	-	186	1	---	K.YHTINGHNAEVRK.A
1695.7605	1694.7532	1694.7576	-0.0044	154	-	168	0	49	R.GFGFVTFDDHDPVDK.I
1695.7605	1694.7532	1694.7576	-0.0044	154	-	168	0	---	R.GFGFVTFDDHDPVDK.I
1798.9182	1797.9109	1797.9148	-0.0039	23	-	38	0	---	K.LFIGGLSFETTEESLR.N
2205.9026	2204.8953	2204.8928	0.0025	326	-	350	0	---	R.NMGGPYGGGNYGPGGSGGSGGYGGR.S + Oxidation (M)

Table 2A Peptides matched to HnRNP A2/B1 isoform B protein

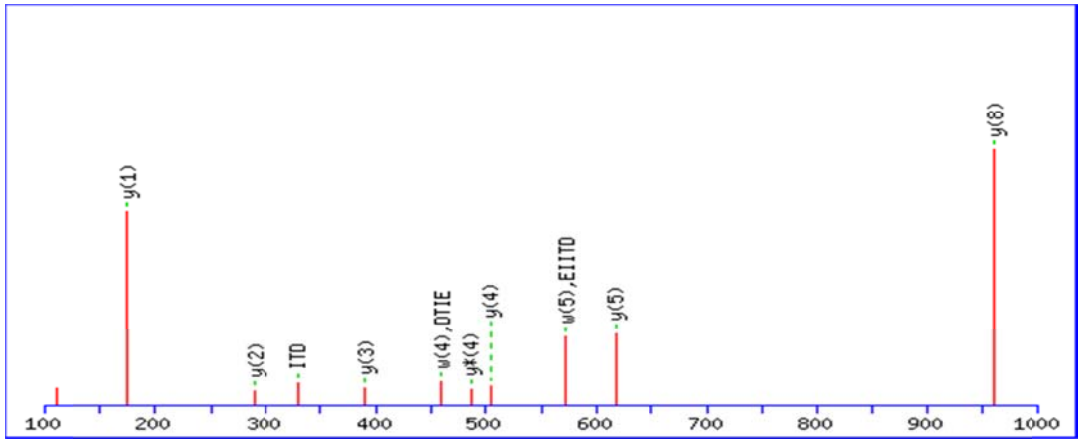

Fig. 2A Ions matched to IDTIEIITDR

MONOISOTOPIC mass of neutral peptide Mr(calc): 1187.6398
Fixed modifications: Carbamidomethyl (C)
Ions Score: 56 **Expect:** 0.00067
Matches (Bold Red): 16/143 fragment ions using 11 most intense peaks

#	Immon.	a	a^0	b	b^0	Seq.	v	w	w'	y	y^0	#
1	86.0964	86.0964		114.0913		I						10
2	88.0393	201.1234	183.1128	229.1183	211.1077	D	1015.542	1014.547		1075.563	1057.552	9
3	74.06	302.171	284.1605	**330.166**	312.1554	T	914.4942	927.5146	929.4938	**960.536**	942.5255	8
4	86.0964	415.2551	397.2445	443.25	425.2395	I	801.4101	814.4305	828.4461	859.4883	841.4778	7
5	102.055	544.2977	526.2871	**572.2926**	554.282	E	672.3675	671.3723		746.4043	728.3937	6
6	86.0964	657.3818	639.3712	685.3767	667.3661	I	559.2834	**572.3038**	586.3195	**617.3617**	599.3511	5
7	86.0964	770.4658	752.4552	798.4607	780.4502	I	446.1994	**459.2198**	473.2354	**504.2776**	486.2671	4
8	74.06	871.5135	853.5029	899.5084	881.4978	T	345.1517	358.1721	360.1514	**391.1936**	373.183	3
9	88.0393	986.5404	968.5299	1014.535	996.5248	D	230.1248	229.1295		**290.1459**	272.1353	2
10	129.1135					R	74.0237	73.0284		**175.119**		1

Table 2B Ions match

APPENDIX B

Calculation of AICAR dose

100mg/kg of AICAR in 200ml of normal saline administered to a 70kg man. The molecular weight of AICAR is 258.2. The C_{max} of AICAR of this administered dose was 68.9 µg/mL.

Using the formula,

Molecular weight = g/moles and Molar = moles/L

1 M = 258.2 mg/mL

1mM = 258.2 µg/mL

1 µg/mL = 1/258.2 mM
= 0.003873 mM
= 3.873 µM

68.9 µg/mL = 266.8497 µM

APPENDIX C

Scientific work published or presented

Manuscript

1. **Ooi MG**, Hayden PJ, Kotoula V, McMillin DW, Charalambous E, Daskalaki E, Raje NS, Munshi NC, Chauhan D, Hideshima T, Buon L, Clynes M, O'Gorman P, Richardson PG, Mitsiades CS, Anderson KC, Mitsiades N. Interactions of the Hdm2/p53 and proteasome pathways may enhance the antitumor activity of bortezomib. Clin Cancer Res. 2009 Dec 1;15(23):7153-60. Epub 2009 Nov 24.

Presentations to Learned Societies

1. **Ooi MG**, O'Connor R, Jakubikova J, Meiller, J, Klippel S, Delmore J, Kastritis E, McMillin DW, Clynes M, Richardson PG, Mitsiades CS, O'Gorman P, Anderson KC. The Interaction of Bortezomib with P-Gp, MRP-1 and BCRP Drug Transporters: Implications for Therapeutic Applications of Bortezomib in Advanced Multiple Myeloma and Other Neoplasias. Poster Presentation, American Society of Haematology, Dec 2009

2. **Ooi MG**, Dowling P, Richardson PG, Mitsiades CS, Clynes M, Anderson KC, O'Gorman P. Proteomics as a Functional Tool in Evaluating Bortezomib Treatment and Drug Resistance Mechanism. Poster Presentation, American Society of Haematology, Dec 2009

3. **Ooi M, ,** Kotoula V, Charalambous E, Daskalaki E, Mitsiades CS, Mitsiades N. The Antidiabetic Biguanide Metformin Induces Growth Arrest in Thyroid Carcinoma Cells *In Vitro.* Poster Presentation, The Endocrine Society's Annual Meeting, June 2009

4. **Ooi MG**, Hayden PJ, McMillin DW, Negri JM, Delmore J, Raje NS, Munshi NC, Chauhan D, Hideshima T, Richardson PG, Mitsiades CS, Anderson KC, Mitsiades N. Interactions of the Mdm2/p53 and Proteasome Pathways: Implications for Combination Strategies to Enhance the Anti-Myeloma Activity of Bortezomib. Poster Presentation, American Society of Haematology, Dec 2008

5. **Ooi MG**, McMillin DW, Negri JM, Delmore J, Munshi NC, Chauhan D, Hideshima T, Richardson PG, Mitsiades CS, Anderson KC, Mitsiades N. The Antidiabetic Biguanide Metformin Induces Growth Arrest in Multiple Myeloma Cells in Vitro, overcoming the Effect of Stromal Cells. Poster Presentation, American Society of Haematology, Dec 2008